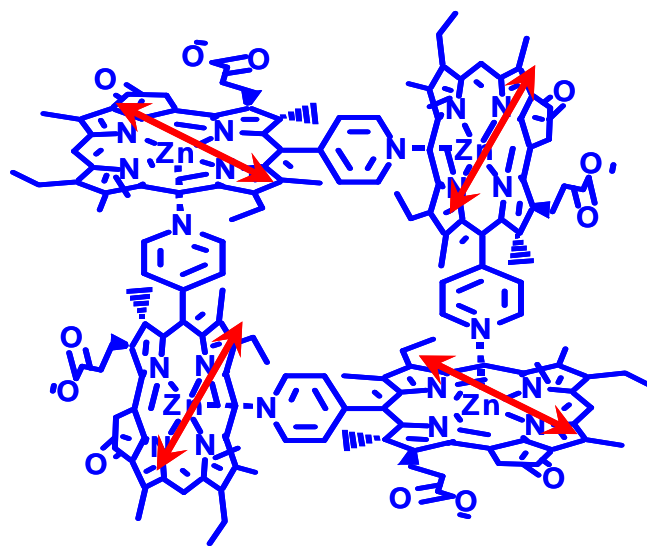
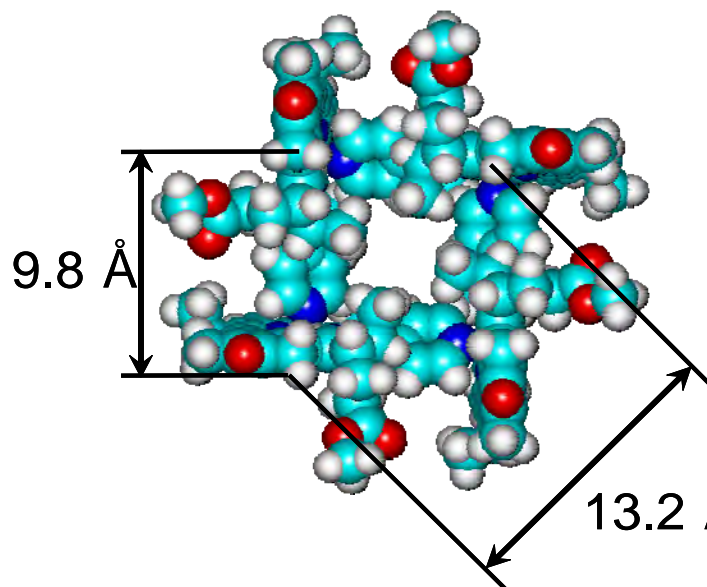


Wintergreen Resort
Wintergreen, VA
June 1-4, 2008

Proceedings of the
Thirtieth
DOE Solar Photochemistry
Research Conference



Sponsored by:

Chemical Sciences, Geosciences, and Biosciences Division
U.S. Department of Energy

Cover Graphics

Biomimetic chromophore rings have been prepared which offer insights into the photophysics of energy collection and transfer in photosynthetic proteins. A zinc chlorophyll derivative is shown that self-assembles into a cyclic tetramer and exhibits intramolecular energy transfer rates comparable to those observed for covalent ring structures. The structure of this self-assembled light-harvesting cyclic chlorophyll array was determined using SAXS in solution at the APS. The larger transition dipole moment for the lowest energy electronic transition of zinc chlorophylls compared to that of porphyrins increases the rate of Förster (through-space) energy transfer between the chlorophylls.

(Michael Wasielewski, Northwestern University)

FOREWORD

The 30th Department of Energy Solar Photochemistry Research Conference, sponsored by the Chemical Sciences, Geosciences, and Biosciences Division of the Office of Basic Energy Sciences, is being held June 1-4, 2008 at the Wintergreen Resort in Wintergreen, Virginia. These proceedings include the meeting agenda, abstracts of the formal presentations and posters of the conference, and an address list for the participants.

This Conference represents the gathering of grantees and contractors who do research in solar photochemical energy conversion with the support of the Chemical Sciences, Geosciences, and Biosciences Division. The purpose of the meeting is to foster collaboration, cooperation, and the exchange of new information and ideas among these researchers. The synergy that results constitutes a major strength of this Program and fosters the standards of excellence in research which has sustained this program over the years. The Program benefits this year from new funding resulting from the DOE workshop on Basic Research Needs in Solar Energy Utilization. As a result of the solicitation following that workshop, there will be fourteen new grantees in solar photoconversion attending this research conference this year.

The Solar Photochemistry Research Conference will have as its guests this year a number of researchers from the Photosynthetic Systems Program, which is a sibling Program in the newly formed Photo- and Biochemistry Team within the Division. They will present posters on their exploration of photochemistry in photosynthesis, which has long served as a model for energy transduction schemes in the Solar Photochemistry Program. One of their members will serve as the special guest lecturer for this conference, Professor Robert Blankenship of Washington University, who will present his research on photosynthetic structures for energy and electron transfer that are distinctly different from those normally seen at a Solar Photochemistry Conference. The conference sessions that follow will feature presentations on the homogeneous catalysis of water splitting, photoinduced electron transfer in molecular constructs, charge separation in heterogeneous systems, and energy transduction in photosynthetic systems and in quantum dots and nanostructures.

I would like to express my appreciation to Sophia Kitts and Margaret Lyday of the Oak Ridge Institute for Science and Education for assistance with the preparation of this volume. I am also grateful to all of the participants in this meeting, the speakers and poster presenters, who, with their energy, enthusiasm and spirit of scientific inquiry, have contributed so much to the success of this program.

Mark T. Spittler
Chemical Sciences, Geosciences,
and Biosciences Division
Office of Basic Energy Sciences

Solar Photochemistry Research Conference Overview

Time	Sunday, June 1	Monday, June 2	Tuesday, June 3	Wednesday, June 4
7:00		Continental Breakfast Skyline	Continental Breakfast Skyline	Continental Breakfast Skyline
8:00				
8:30		Opening Remarks		
8:45				
9:00		Session I <i>Plenary Speaker</i>	Session VI	Session IX
9:30				
9:45		Break		
10:00				Break
10:15			Break	
10:30		Session II		Session X
11:00			Session VII	
11:30				
11:50				Lunch Skyline
12:15		Lunch Skyline	Lunch Skyline	
12:30			Free Afternoon	
12:45				
1:00				
1:30		Session III		Session XI
2:00				
2:30		Break		
2:45				Closing Remarks
3:00				
3:30	Registration	Session IV		
4:00	Mountain Inn Lobby (3:00 - 6:00 P.M.)			
4:30		Break		
5:00				
5:30	No Host Reception	Session V		
6:00	Edge Restaurant Bar		Session VIII	
6:30				
7:00	Dinner Buffet Skyline	Dinner Blue Ridge Terrace	Social Hour Dinner Blue Ridge Terrace	
7:30				
8:00				
8:30		Posters (even numbers)	Posters (odd numbers)	
9:00	Reception (cont.)	Commonwealth	Commonwealth	
9:30	Edge Restaurant Bar	Ballroom Refreshments	Ballroom Refreshments	

Table of Contents

Table of Contents

Foreword.....	i
Overview.....	ii
Program.....	xv

Abstracts of Oral Presentations

Session I – Plenary Session

Photosynthetic Complexes as Natural Nanoscale Bioenergy Conversion Systems Robert Blankenship , Washington University.....	1
--------------------------------------------------------------------------------------------------------------------------------------	---

Session II – Mechanistic Aspects of Homogeneous Solar Photochemistry

Mechanisms of Water Oxidation Catalyzed by Ruthenium Diimine Complexes J. L. Cape, S. Das, and James K. Hurst , Washington State University.....	5
Hydride Ion Transfer Reactions in Water Carol Creutz , Brookhaven National Laboratory.....	8
Proton-Coupled Electron Transfer – The Engine that Drives Water Splitting Daniel G. Nocera , Massachusetts Institute of Technology.....	11

Session III – Photoinduced Electron Transfer

Dynamics of Photoinduced Electron Transfer in DNA Frederick D. Lewis , Northwestern University.....	17
Luminescent Platinum Complexes for Hydrogen Generation and Photo-induced Charge Separation P. Du, J. Schneider, P. Jarosz, J. Zhang, T. Lazarides, J. Thall, K. Knowles and Richard Eisenberg , University of Rochester.....	20
Theoretical Studies of Photoactive Molecular Systems: Electron Transfer, Energy Transport, and Optical Spectroscopy Richard A. Friesner , Columbia University.....	23

Session IV - Heterogeneous Systems for Solar Photoconversion I

Quantum Dot Solar Cells: Modulation of Photoresponse with Particle Size and 1-D Support Architecture A. Kongkanand, K. Tvrdy, P. Brown, I. Robel, and Prashant Kamat , Notre Dame Radiation Laboratory.....	27
Vertically Oriented TiO ₂ and Ternary Nanotube Arrays and Their Use in Water Photoelectrolysis Craig A. Grimes , Pennsylvania State University	32
Photoactive Inorganic Membranes for Charge Transport Prabir Dutta, Henk Verweij, and Bern Kohler , Ohio State University.....	36

Session V - Structures of Excited States

Tracking Electrons and Atoms in Photoexcited Molecules with X-Ray Transient Absorption Spectroscopy X. Zhang, E.C. Wasinger, J.V. Lockard, K. Attenkofer, G. Jennings, A.Z. Muresan, J.S. Lindsey and Lin X. Chen , Argonne National Laboratory and Northwestern University	41
Visualizing Geometry Changes on Photoexcitation: From Microsecond to Picosecond Time Resolution M. Gembicky, M. Pitak, S.-L. Zheng, M. Messerschmidt and Phillip Coppens , State University of New York, Buffalo.....	45

Session VI - Heterogeneous Systems for Solar Photoconversion II

Electron Transfer Dynamics in Efficient Molecular Solar Cells A. Staniscewski, A. Morris, and Gerald J. Meyer , Johns Hopkins University.....	49
Metal-to-Ligand Charge Transfer Excited States on Surfaces and in Rigid Media: Application to Energy Conversion J.M. Papanikolas and Thomas J. Meyer , University of North Carolina.....	52
Conjugated Polyelectrolytes: Disrupted Interactions, Self-Assembled Structures, and Hybrid Polymer Solar Photoconversion Kirk S. Schanze, Valeria D. Kleiman, and John R. Reynolds , University of Florida.....	55

Session VII - Dye Sensitized Semiconductors

Fundamental Investigations of Dye/Semiconductor Interfaces Y. Lu, M.T. Spitler, D. Choi, B. Jäckel, R. Herrick and Bruce Parkinson , Colorado State University.....	61
----------------------------------------------------------------------------------------------------------------------------------------------------------------------------------	----

Model Dyes for Study of Molecule/Metal Oxide Interfaces and Electron Transfer Processes Elena Galoppini , Rutgers University, Newark.....	64
Interfacial Photochemical Processes in Sensitized Nanostructured Electrodes N. Kopidakis, N.R. Neale, J. van de Lagemaat, K. Zhu, and Arthur J. Frank , National Renewable Energy Laboratory	67
<u>Session VIII - Photosynthetic Systems I</u>	
Magnetic Resonance and Proton Loss Studies of Carotenoid Radical Cations A. L. Focsan, T.A. Konovalova, J. Lawrence, M.K. Bowman, D.A. Dixon, P. Molnar, J. Deli and Lowell D. Kispert , University of Alabama.....	73
Photosynthetic Light Harvesting and its Regulation K.K. Niyogi, E. Read, T. Calhoun, G. Schlau-Cohen, N. Ginsberg, T. Ahn, R. Bassi and Graham Fleming , University of California, Berkeley.....	77
<u>Session IX – Molecular Complexes for Energy and Charge Transfer</u>	
Energy and Charge Transport in Self-Assembled Systems for Artificial Photosynthesis Michael R. Wasielewski , Northwestern University.....	83
Fundamental Studies of Charge Migration and Delocalization Relevant to Solar Energy Conversion Michael J. Therien , Duke University.....	87
Potential of Molecular Wires for Solar Photovoltaics A. Cook, P. Sreearunothai, S. Asaoka, N. Takeda, S. McIlroy, J.M. Keller and K. Schanze and John R. Miller , Brookhaven National Laboratory	90
<u>Session X – Photosynthetic Systems II</u>	
Regulation of the Electron Transfer Pathways in Natural Photosynthesis L.M. Utschig, D.M. Tiede, and Oleg G. Poluektov , Argonne National Laboratory.....	95
Photoactivity and Electron Transfer Extremes in Macromolecular Biosystems N. Ponomarenko, O. Poluektov, P. Hasjim, A. Marino, A. Wang, A. Block, E. Gasyna, Z. Gasyna, and James Norris , University of Chicago.....	99
<u>Session XI – Quantum Particles for Solar Photoconversion</u>	
Femtosecond Kerr-Gated Fluorescence Microscopy L. Gundlach, L. Schneemeyer, M. Myahkostupov and Piotr Piotrowiak , Rutgers University, Newark.....	105

Multiple Exciton Generation: Silicon QDs, QD arrays, QD Solar Cells, and Controversy M.C. Beard, R.J. Ellingson, M. Law, J.M. Luther, J.C. Johnson, Q. Song, M.C. Hanna, J.E. Murphy and Arthur J. Nozik , Renewable Energy Laboratory.....	108
Photophysics of Individual Single-Walled Carbon Nanotubes L.J. Carlson, L. Huang, H. Pedrosa and Todd D. Krauss , Rochester University.....	112
Photovoltage and Hot Electrons in Silver Nanocrystals P. Redmond, X. Wu, H. Liu and Louis Brus , Columbia University.....	115
Poster Abstracts (by Poster Number)	
1. “Electrochemically Wired” Semiconductor Nanoparticles: Toward Vectoral Electron Transport in Hybrid Materials <u>N.R. Armstrong</u> , J. Pyun, S. Saavedra	121
2. Are the Electronic Properties of Polymers Deformable? J. Bolinger, L. Fradkin, K.-J. Lee, R.E. Palacios, and <u>P.F. Barbara</u>	122
3. Improving the Efficiency of Dye Sensitized Solar Cells for Hybrid Cell/Silicon Concentrator Systems <u>G. D. Barber</u> , A. Lee, T. E. Mallouk.....	123
4. Design of Molecular Rectifiers for Solar Photocatalytic Cells R. Snoeberger, C.A Schmuttenmaer., RH Crabtree, GW Brudvig, <u>VS Batista</u>	124
5. Multiple Exciton Generation and Charge Carrier Dynamics in Electronically Coupled Films of PbSe Nanocrystals <u>Matthew C. Beard</u> , M. Law, J.M. Luther, Q. Song, R.J. Ellingson, Sukgeun Choi, M. Hanna, and A. J. Nozik.....	125
6. Photophysics of Thiophene-based Light Harvesters A. Huss, N. Wells, K. Mann, W. Gladfelter, and <u>D.Blank</u>	126
7. Hole Transfer in Tetrapyrrolic Dyads: $^2A_{1U}$ versus $^2A_{2U}$ Ground States J. R. Diers, P. Thamyongkit, A. Muresan, M. Taniguchi, D. Holten, J.S. Lindsey, and <u>D. F. Bocian</u>	127
8. Photoinitiated Electron Collection in Mixed-Metal Supramolecular Complexes: Development of Photocatalysts for Hydrogen Production <u>K.J. Brewer</u> , S. Arachchige, R. Miao, J. Brown, and D. Zigler.....	128
9. Formation of Carotenoid Neutral Radicals in Photosystem II Y. Gao, K.E. Shinopoulos, C. A. Tracewell, A. L. Focsan, L. D. Kispert and <u>G.W. Brudvig</u>	129
10. Light Energy Transduction in Green Sulfur Bacteria	

<u>D. A. Bryant, J. A. Maresca, A. Gomez Maqueo Chew, Z. Liu, A. M. Garcia Costas, and F. Shen</u>	130
11. Enhancement of Photoelectrochemical Properties via Electrochemical Morphology Control of Photoelectrodes <u>K.-S. Choi</u>	131
12. Acetylacetonate as a Robust Anchor and Electron Conduit for Solar Cell Dyes W. McNamara, C. Cady, R. Snoeberger, C. A. Schmuttenmaer, G.W. Brudvig, V.S. Batista, R.H. <u>Crabtree</u>	132
13. Tools for Elucidating Mechanism Following Adaptive Control and Progress Towards Control of Multiple Exciton Generation <u>N.H. Damrauer, M.A. Montgomery, E.M. Grumstrup</u>	133
14. CW- and Time-resolved Photoluminescence Studies of Semiconductor Nanocrystals and Nanocrystal Arrays for Efficient Solar Energy Conversion <u>R.J. Ellingson, M. Law, J. Luther, Q. Song, J.C. Johnson, B. Hughes, K.A. Gerth, A. Midgett, O. Semonin, M.C. Beard, and A.J. Nozik</u>	134
15. Mass Transfer of Polypyridyl Cobalt Complexes within Mesoporous TiO ₂ Dye-Sensitized Solar Cell Photoanodes <u>J.J. Nelson, T.J. Amick, and C. M. Elliott</u>	135
16. Optical and Electrochemical Properties of Shell-Core Dendrimers: Ruthenium Coordination Complexes Capped with Sized Phenothiazine-Substituted Bipyridines <u>M.A. Fox, J.K. Whitesell, and L. Zhu</u>	136
17. Binuclear TiOCr Charge-Transfer Chromophore Driven by Visible Light Water Oxidation at Ir Oxide Nanoclusters <u>H. Han and H. Frei</u>	137
18. Water Oxidation by a Ruthenium Complex with Non-Innocent Quinone Ligands <u>E. Fujita, J.T. Muckerman, M.-K. Tsai, D.E. Polyansky, T. Wadu, and K. Tanaka</u>	138
19. Protein-Protein Interactions in the Heliobacterial Reaction Center <u>J. H. Golbeck</u>	139
20. Solvatochromism Measures of Energetic Disorder in Polymer Charge-Transport Systems <u>B. Deason, I.R. Gould and D. Matyushov</u>	140
21. Charged Defects in π -conjugated Polymers <u>B.A. Gregg, D. Wang, N. Kopidakis, X. Ai, and M.O. Rose</u>	141
22. Mechanistic Investigations of the Photocatalytic Reduction of CO ₂ in Supercritical CO ₂ <u>D.C. Grills, E. Fujita, and M.D. Doherty</u>	142

23. A Bioinspired Construct that Mimics the Proton-Coupled Electron Transfer between P680 ^{•+} and the TyrZ-His190 Pair of Photosystem II G.F. Moore, M. Hambourger, M. Gervaldo, A. Keirstad, G. Kodi, O.G. Poluektov, T. Rajh, D. Gust, T. Moore, and A.L. Moore.....	143
24. Photochemical Properties of Single-Walled Carbon Nanotubes: Precisely Tuned Chirality Mixtures and SWNT-Hydrogenase Complexes J.L. Blackburn, M.C. Beard, T.M. Barnes, D. Svedruzic, P.W. King, and M.J. Heben.....	144
25. Photoactivities of n-Doped Rutile and Anatase Surfaces T. Ohsawa, S.H. Cheung, M.A. Henderson, S.A. Chambers.....	145
26. A Stable Molecular Catalyst for Oxygen Evolution from Water Y.V. Geletii, Z. Huang, Y. Hu, A. Kuznetsov, T. Lian, J. Musaev, and C.L. Hill.....	146
27. Determination of the Rates of Ground-State Hole Transfer in One-Electron Oxidized Tetrapyrrole Arrays via Time-Resolved Optical Spectroscopy H. Song, C. Kirmaier, M. Taniguchi, J.R. Diers, D.F. Bocian, J.S. Lindsey, and D. Holten.....	147
28. Excited-State and Proton-Coupled Electron Transfer Properties of Tungsten Alkylidyne Chromophores and Assemblies B.W. Cohen, M.I. Newsom, B. Lovaasen, and M.D. Hopkins.....	148
29. Fundamental Studies of Light-Induced Charge Transfer, Energy Transfer, and Energy Conversion with Supramolecular Systems J. Hupp.....	149
30. Covalent and Non-Covalent Coupling of Novel Chromophores for High Single Fission Yields J.C. Johnson, A. Akdag, X. Chen, J. Michl, and A.J. Nozik.....	150
31. Towards Multidimensional Spectroscopy of Quantum Dots B. Cho, W.K. Peters, R.J. Hill, and D.M. Jonas.....	151
32. Exciton Dynamics in GaSe Quantum Dot Aggregates D. F. Kelley.....	152
33. Snapshots of Biological Proton-Coupled Electron Transfer: Pulsed Electron Paramagnetic Resonance Spectroscopy of Tyrosine Intermediates in Photosystem II O. Poluektov, S. Lee, S. Chand, A. Wagner, and K.V. Lakshmi.....	153
34. Chemical Control over the Electrical Properties of GaAs and Zn ₃ P ₂ Semiconductor Surfaces and Photoelectrodes G.M. Kimball, M.C. Traub, and N.S. Lewis.....	154
35. Semiconductor Dependence of Interfacial Electron Transfer J. Huang, D. Stockwell, C. Anfuso, B. Wu, and T. Lian.....	155

36. Accessing the Near-Infrared Spectral Region with Stable, Synthetic Wavelength-Tunable Bacteriochlorins M. Taniguchi, D.L. Cramer, A.D. Bhise, H.L. Kee, D.F. Bocian, D. Holten, and <u>J.S. Lindsey</u>	156
37. Conjugated Ionomers for Photovoltaic Applications: Electric Field Driven Charge Separation at Organic Junctions F. Lin, E. Walker, D. Stay, Y. Wang, and <u>M. Lonergan</u>	157
38. Molecular Level Organization of Heterometallic Oxides/Organics for Photocatalysis <u>P.A. Maggard</u>	158
39. Semiconductor-Sensitizer-Catalyst Systems for Overall Water Splitting Using Visible Light W. J. Youngblood, S.-H. A. Lee, D. Lentz, H. Hata, R. Ma, P.G. Hoetz, T. A. Moore, A.L. Moore, D. Gust, and <u>T.E. Mallouk</u>	159
40. Zinc Oxide Nanocrystals – Transition Metal Dye Dyads R. Chitta, K. Schwartz, D. Blank, W.L. Gladfelter, and <u>K.R. Mann</u>	160
41. Charge Transfer in Crystal Violet Lactone: Conventional Solvents and Ionic Liquids <u>M. Maroncelli</u> and X. Li.....	161
42. Energetics of Natural Photosynthesis and Mechanisms of Reduction of Reduction of Charge Recombination D. N. LeBard and <u>D. V. Matyushov</u>	162
43. Control of Ultrafast Charge Transfer-State Deactivation in First-Row Transition Metal Chromophores A. Brown, Lindsey, and <u>J.K. McCusker</u>	163
44. Stages in Photochemical Solar Conversion: Catalytic H ₂ Evolution as the Particles See It G. Merga, L.C. Cass, D.M. Chipman, and <u>D. Meisel</u>	164
45. Photochemical Generation of a Hydride Donor and its Reactions <u>J. T. Muckerman</u> , D. E. Polyansky, D. Cabelli, P. Achord, K. Tanaka, and E.Fujita.....	165
46. Theoretical/Computational Probes of Inter- and Intramolecular Electron Transfer: Electronic Structure and Energetics <u>M.D. Newton</u>	166
47. Two-Color Two-Dimensional Fourier Transform Electronic Spectroscopy with a Pulse-Shaper J.A. Myers, K.L.M. Lewis, P.F. Tekavic, and <u>J.P. Ogilvie</u>	167
48. Photochemical Dynamics of the Nanoscale: Time-Domain <i>ab initio</i> Studies of Quantum Dots and Molecule-Semiconductor Interfaces <u>O.V. Prezhdo</u>	168

49. Combustion Synthesis and Characterization of Nanocrystalline Tungsten Oxide W.Morales, N. de Tacconi, and <u>K. Rajeshwar</u>	169
50. Microwave Conductivity Studies of Photoinduced Carriers in Single-Walled Nanotubes <u>G. Rumbles</u> , N. Kopidakis, A. Ferguson, J. Blackburn, M. Heben.....	170
51. Quenching of Triplet Excitons in Conjugated Polyelectrolytes H. Jiang, J.R. Miller, and <u>K.S. Schanze</u>	171
52. Excited State Energetics and Photoredox Reactions of Pt(II) Terpyridyl Complexes K. Shankar, H. Hester, D. Kumaresan, K. Lebkowski, and <u>R. Schmehl</u>	172
53. Characterization of Charge Injection and Charge Separation in Functionalized TiO ₂ for Use in Solar Hydrogen Production C.W. Cady, J.M. Schleicher, G.Li, W.R. McNamara, R. C. Snoeberger, V.S. Batista, R.H. Crabtree, G.W. Brudvig, and <u>C.A. Schmittenmaer</u>	173
54. Investigation of Ruthenium-Based Water Oxidation Catalysts R. Zong, H.-W. Tseng, Z. Deng, D. Wang, B. Wang, and <u>R. Thummel</u>	174
55. Conformational Analysis of a Supramolecular Porphyrin Array Using Molecular Dynamics Modeling and X-ray Scattering <u>D.M. Tiede</u> , K.L. Mardis, X. Zuo, and J.S. Lindsey.....	175
56. Discovery of Native Metal Ion Sites on the Ferredoxin Docking Side of Photosystem I <u>L.M. Utschig</u> , L.X. Chen, J.V. Lockhard, D.M. Tiede, and O.G. Polutektov.....	176
57. Plasmon Resonance Imaging M.J. Romero, G. Rumbles, M. Al-Jassim, and <u>J. van de Lagemaat</u>	177
58. Structural Changes in the Oxygen Evolving Complex of Photosystem II Detected Using X-Ray Spectroscopy J. Yano, U. Pushkar, A. Boussac, U. Bergmann, K. Sauer, and <u>V. Yachandra</u>	178
List of participants	181
Author Index	192

Program

**30th DOE SOLAR PHOTOCHEMISTRY
RESEARCH CONFERENCE**

June 1-4, 2008

**Wintergreen Resort
Wintergreen, Virginia**

PROGRAM

Sunday, June 1

3:00 – 6:00 p.m. Registration (Mountain Inn Lobby)
6:30 – 8:00 p.m. Buffet Dinner, Skyline Room

Monday Morning, June 2

SESSION I

Plenary Session – Skyline Room

Mark T. Spitler, Chair

7:30 a.m. Continental Breakfast, Skyline Room

8:30 a.m. Opening Remarks
 Mark Spitler and Richard Greene, Department of Energy

8:45 a.m. **Plenary Lecture.**
 Photosynthetic Complexes as Natural Nanoscale Bioenergy Conversion Systems
 Robert Blankenship, Washington University

9:45 a.m. Coffee Break

SESSION II

Mechanistic Aspects of Homogeneous Solar Photochemistry

Etsuko Fujita, Chair

10:15 a.m. Mechanisms of Water Oxidation Catalyzed by Ruthenium Diimine Complexes
 James K. Hurst, Washington State University

10:45 a.m. Hydride Ion Transfer Reactions in Water
 Carol Creutz, Brookhaven National Laboratory

11:15 a.m. Proton-Coupled Electron Transfer – The Engine that Drives Water Splitting
 Daniel G. Nocera, Massachusetts Institute of Technology

11:50 a.m. Lunch, Dining Room

Monday Afternoon, June 2

SESSION III
Photoinduced Electron Transfer
Thomas Moore, Chair

- 1:00 p.m. Dynamics of Photoinduced Electron Transfer in DNA
Frederick D. Lewis, Northwestern University
- 1:30 p.m. Luminescent Platinum Complexes for Hydrogen Generation and Photo-induced Charge Separation
Richard Eisenberg, University of Rochester
- 2:00 p.m. Theoretical Studies of Photoactive Molecular Systems: Electron Transfer, Energy Transport, and Optical Spectroscopy
Richard A. Friesner, Columbia University
- 2:30 p.m. Coffee Break

SESSION IV
Heterogeneous Systems for Solar Photoconversion I
Krishnan Rajeshwar, Chair

- 3:00 p.m. Quantum Dot Solar Cells: Modulation of Photoresponse with Particle Size and 1-D Support Architecture
Prashant Kamat, Notre Dame Radiation Laboratory
- 3:30 p.m. Vertically Oriented TiO₂ and Ternary Nanotube Arrays and Their Use in Water Photoelectrolysis
Craig A. Grimes, Pennsylvania State University
- 4:00 p.m. Photoactive Inorganic Membranes for Charge Transport
Prabir Dutta, Henk Verweij, and Bern Kohler, Ohio State University
- 4:30 p.m. Break

SESSION V
Structures of Excited States
Mark Maroncelli, Chair

- 5:00 p.m. Tracking Electrons and Atoms in Photoexcited Molecules with X-ray Transient Absorption Spectroscopy
Lin X. Chen, Argonne National Laboratory and Northwestern University
- 5:30 p.m. Visualizing Geometry Changes on Photoexcitation: From Microsecond to Picosecond Time Resolution
Phillip Coppens, State University of New York, Buffalo
- 6:30 p.m.. Dinner, Blue Ridge Terrace

7:30 p.m. Posters (Odd numbers), Ball Room
Refreshments

Tuesday Morning, June 3

7:30 a.m. Continental Breakfast, Skyline Room

SESSION VI
Heterogeneous Systems for Solar Photoconversion II
Karen Brewer, Chair

8:30 a.m. Electron Transfer Dynamics in Efficient Molecular Solar Cells
Gerald J. Meyer, Johns Hopkins University

9:00 a.m. Metal-to-Ligand Charge Transfer Excited States on Surfaces and in Rigid Media:
Application to Energy Conversion
Thomas J. Meyer, University of North Carolina

9:30 a.m. Conjugated Polyelectrolytes: Disrupted Interactions, Self-Assembled Structures,
and Hybrid Polymer Solar Photoconversion
Kirk S. Schanze, Valeria D. Kleiman, and John R. Reynolds,
University of Florida

10:15 a.m. Coffee Break

SESSION VII
Dye Sensitized Semiconductors
Tianquan Lian, Chair

10:30 a.m. Fundamental Investigations of Dye/Semiconductor Interfaces
Bruce Parkinson, Colorado State University

11:00 a.m. Model Dyes for Study of Molecule/Metal Oxide Interfaces and Electron Transfer
Processes
Elena Galoppini, Rutgers University, Newark

11:30 a.m. Interfacial Photochemical Processes in Sensitized Nanostructured Electrodes
Arthur J. Frank, national Renewable Energy Laboratory

Tuesday Afternoon, June 3

12:15 p.m. Lunch, Skyline Room

Tuesday Evening, June 3

**SESSION VIII
Photosynthetic Systems I**

David Tiede, Chair

- 5:30 p.m. Magnetic Resonance and Proton Loss Studies of Carotenoid Radical Cations
Lowell D. Kispert, University of Alabama
- 6:00 p.m. Photosynthetic Light Harvesting and its Regulation
Graham Fleming, University of California, Berkeley
- 6:30 p.m. Social Hour
7:30 p.m. Dinner, Blue Ridge Terrace
- 8:30 p.m. Posters (Even numbers)
Refreshments

Wednesday Morning, June 13

- 7:30 a.m. Continental Breakfast, Skyline Dining Room

**Session IX
Molecular Complexes for Energy and Charge Transfer**

David Bocian, Chair

- 8:30 a.m. Energy and Charge Transport in Self-Assembled Systems for Artificial
Photosynthesis
Michael R. Wasielewski, Northwestern University
- 9:00 a.m. Fundamental Studies of Charge Migration and Delocalization Relevant to Solar
Energy Conversion
Michael J. Therien, Duke University
- 9:30 a.m. Potential of Molecular Wires for Solar Photovoltaics
John R. Miller, Brookhaven National Laboratory
- 10:00 a.m. Coffee Break

**Session X
Photosynthetic Systems II**

Dewey Holten, Chair

- 10:30 a.m. Regulation of the Electron transfer Pathways in Natural Photosynthesis
Oleg G. Poluektov, Argonne National Laboratory
- 11:00 a.m. Photoactivity and Electron Transfer Extremes in Macromolecular Biosystems
James Norris, University of Chicago

11:40 a.m. Lunch, Skyline Room

Session XI
Quantum Particles for Solar Photoconversion
David Kelley, Chair

12:45 p.m. Femtosecond Kerr-Gated Fluorescence Microscopy
Piotr Piotrowiak, Rutgers University, Newark

1:15 p.m. Multiple Exciton Generation: Silicon QDs, QD arrays, QD Solar Cells, and Controversy
Arthur J. Nozik, Renewable Energy Laboratory

1:45 p.m. Photophysics of Individual Single-Walled Carbon Nanotubes
Todd D. Krauss, Rochester University

2:15 p.m. Photovoltage and Hot Electrons in Silver Nanocrystals
Louis Brus, Columbia University

2:45 p.m. Closing Remarks
Mark Spitler and Richard Greene, U.S. Department of Energy

Session I

Plenary Session



PHOTOSYNTHETIC COMPLEXES AS NATURAL NANOSCALE BIOENERGY CONVERSION SYSTEMS

Robert E. Blankenship, Bradley L. Postier, Jianzhong Wen, Aaron M. Collins
Departments of Biology and Chemistry, Washington University, St. Louis, MO

Graham R. Fleming, Elizabeth L. Read
Department of Chemistry, University of California, Berkeley and Physical Biosciences Division,
Lawrence Berkeley National Laboratory, Berkeley CA

Gregory S Engel
Department of Chemistry, University of Chicago, Chicago, IL

Dale E. Tronrud, Leslie Gay
Howard Hughes Medical Institute, Institute of Molecular Biology, University of Oregon,
Eugene, OR 97403, USA

Pratim Biswas, Elijah Thimsen, Luis Modesto-Lopez
Department of Energy, Environmental and Chemical Engineering, Washington University, Saint
Louis, MO

Michael Gross, Hao Zhang
Department of Chemistry, Washington University, Saint Louis, MO

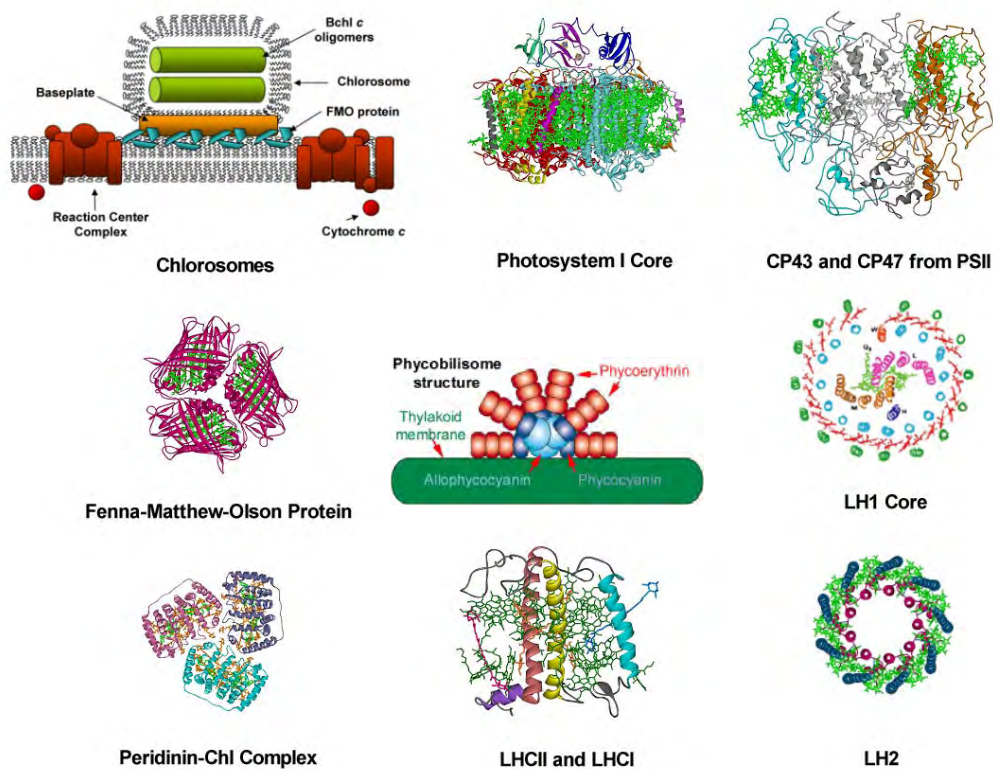
Photosynthetic membranes carry out solar energy storage using an integrated series of nanoscale complexes that collectively convert light into chemical energy. These natural systems include photosynthetic antenna complexes and reaction center complexes. These systems, while biological in origin, have many characteristics that can serve as design principles of artificial energy conversion systems (1). These features include self-assembly, self-repair and adaptability. The antenna systems that will be discussed in detail in this talk include the chlorosome and Fenna-Matthews-Olson (FMO) antenna complexes from green photosynthetic bacteria (2). The chlorosome is a unique antenna complex that features pigment self-assembly into large oligomeric structures and has minimal protein content. Preliminary steps toward using chlorosomes in biohybrid devices will be discussed. The FMO protein has been investigated using high-resolution X-ray structure determination, ultrafast 2D laser spectroscopy (3-6) and advanced techniques of mass spectroscopy.

Additional research will be reported on the unique cyanobacterium *Acaryochloris marina*, which uses chlorophyll *d* as its principal photopigment. Chl *d* extends the spectral range of light that can drive oxygenic photosynthesis by 30 nm further into the near infrared region of the solar spectrum (7,8).

References

1. Blankenship RE (2005) Natural Organic Photosynthetic Solar Energy Transduction. In: *Organic Photovoltaics: Mechanisms, Materials and Devices*, S-S Sun and S Sariciftci, Eds. CRC Press, Boca Raton, FL pps. 37-48.

2. Blankenship RE and Matsuura K (2003) Antenna Complexes from Green Photosynthetic Bacteria. In: *Light-Harvesting Antennas*, Green BR and Parson WW, eds. (Dordrecht: Kluwer), 195-217.
3. Brixner T, Stenger J, Vaswani HM, Cho M, Blankenship RE and Fleming GR (2005) Two-dimensional spectroscopy of electronic couplings in photosynthesis *Nature*, **434**: 625-629.
4. Engel GS, Calhoun TR, Read EL, Ahn TK, Mancal T, Cheng Y-C, Blankenship RE and Fleming GR (2007) Evidence for wavelike energy transfer through quantum coherence in photosynthetic systems. *Nature* **446**: 782-786.
5. Read EL, Engel GS, Calhoun TR, Mancal T, Ahn TK, Blankenship RE and Fleming GR (2007) Cross-Peak Specific Two Dimensional Electronic Spectroscopy. *Proc. Nat'l. Acad. Sci. USA* **104**: 14203-14208.
6. Read EL, Schlau-Cohen G, Engel GS, Wen J, Blankenship RE, Fleming GR (2008) Visualization of Excitonic Structure in the Fenna-Matthews-Olson Photosynthetic Complex by Polarization-Dependent Two-Dimensional Electronic Spectroscopy. *Biophysical Journal* In Press doi:10.1529/biophysj.107.128199.
7. Chen M, Telfer A, Lin S, Pascal A, Larkum AWD, Barber J and Blankenship RE (2005) The nature of the Photosystem II reaction centre in the chlorophyll *d* containing prokaryote, *Acaryochloris marina*. *Photochemical & Photobiological Sciences*, **4**: 1060-1064.
8. Swingley WD, Chen M, Cheung PC, Conrad AL, Dejesa LC, Hao J, Honchak BM, Karbach LE, Kurdoglu A, Lahiri S, Mastrian SD, Miyashita H, Page LE, Ramakrishna P, Satoh S, Sattley WM, Shimada Y, Taylor HL, Tomo T, Tsuchiya T, Wang ZT, Raymond J, Mimuro M, Blankenship RE and Touchman JW (2008) Niche adaptation and genome expansion in the chlorophyll *d*-producing cyanobacterium *Acaryochloris marina*. *Proc. Nat'l. Acad. Sci. USA* **105**: 2005-2010.



Session II

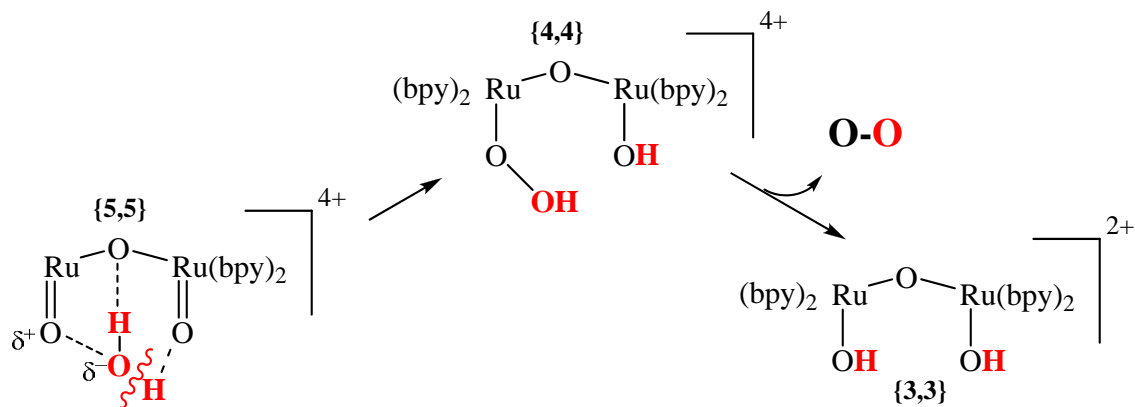
*Mechanistic Aspects
of Homogeneous Solar Photochemistry*

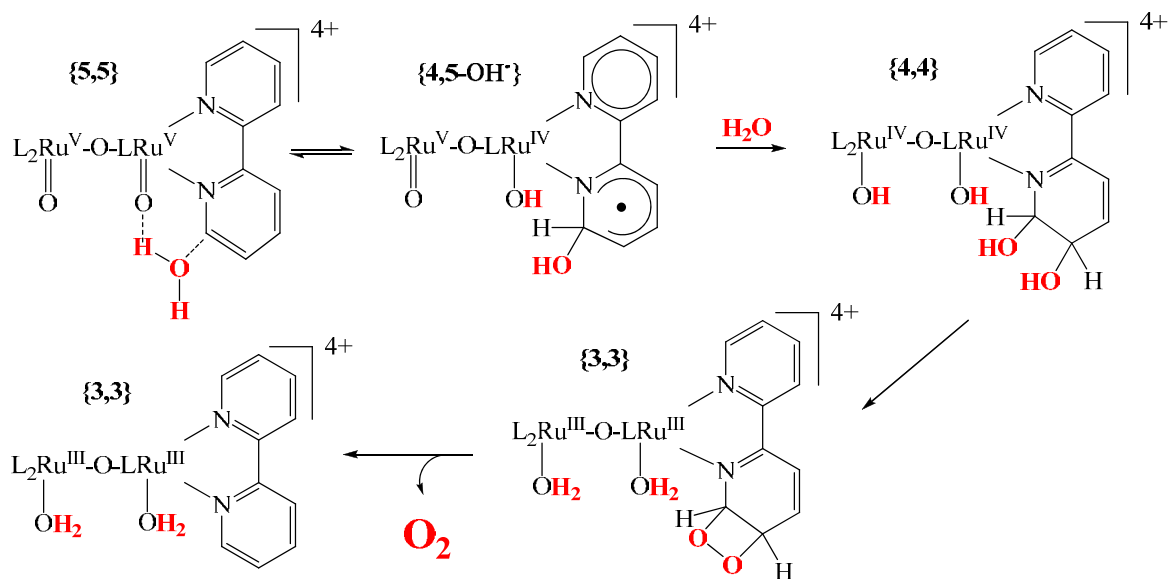
MECHANISMS OF WATER OXIDATION CATALYZED BY RUTHENIUM DIIMINE COMPLEXES

Jonathan L. Cape, Samir Das, and James K. Hurst
Department of Chemistry
Washington State University
Pullman, WA 99164-4630

This project has two main interrelated goals, namely (1) to develop vesicle-based assemblies containing electroneutral cyclic photoredox mediators that are capable of generating H₂, and (2) to develop catalysts that are capable of rapid, sustained water oxidation for use in place of sacrificial electron donors in integrated photochemical systems for water splitting. Emphasis within the current funded period has been placed upon the second goal, although very recently we have initiated studies to couple water oxidation to transmembrane reduction of acceptor molecules using pyrylium ions as combined photosensitizer/redox relays.

Our research in water oxidation has involved primarily reactions of the “blue” ruthenium μ -oxo dimer (i.e., [(Ru(bpy)₂OH₂)₂O]⁴⁺, denoted **{3,3}**), and related bipyridine ring-modified congeners. Our recent investigations have focused on two aspects of catalysis by these ions, specifically (a) an improved understanding of reaction mechanisms through characterization of reaction transients, and (b) determination of photochemically initiated reaction pathways in neutral media, as originally described by Grätzel and coworkers [Rotzinger, et al. *JACS* **1987**, *109*, 6619-26]. Impetus for these studies derives primarily from our single-turnover ¹⁸O-isotopic labeling studies [Yamada et al. *JACS* **2004**, *126*, 9786-9795], which clearly indicated that two reaction pathways exist for “blue dimer”-catalyzed water oxidation in acidic solutions. In one pathway, the O₂ formed obtains one O atom from solvent and the other O atom from a terminal ruthenyl oxo atom formed upon oxidation of the complex to the **{5,5}** state; in the other pathway, both O atoms are obtained from solvent. These studies also exclude from further consideration all previously proposed pathways involving O₂ formation by concerted reductive elimination of ruthenyl O atoms from the coordination spheres of the dimer. In seeking a self-consistent mechanism for the two pathways, we have suggested⁴ that the reaction is initiated by concerted addition of the elements of H₂O to **{5,5}**, as illustrated below:





Both pathways are consistent with current views of oxidation reactions catalyzed by monomeric ruthenyl ions, which may involve H-atom abstraction as reaction-initiating steps, and with energy constraints excluding formation of free OH^\bullet as a reaction intermediate. The first pathway, involving addition of templated H_2O across the two ruthenyl centers, has recently received theoretical support [Yang & Baik, *JACS* **2006**, *128*, 7476-85]; the second pathway, involving non-innocent participation of bipyridine ligands, has precedents in the well-described “covalent hydration” reactions of nitrogen heterocycles and the demonstrated propensity of OH^\bullet to add to aromatic rings; it is also consistent with the following experimental observations:⁴ *i*) relative contributions by the two pathways for bipyridine-substituted congeners parallel the expected ease of covalent adduct formation with water; *ii*) reactions of radiolytically-generated OH^\bullet with **{3,3}** and **{3,4}** give bipyridine ring adducts, rather than oxidized metal centers, as immediate products (as determined by the appearance of diagnostic NIR absorption bands); *iii*) formation of **{5,5}** is accompanied by the appearance of cryogenic EPR signals that could represent the ligand radical species, **{4,5-OH \cdot }**; *iv*) literature precedents exist for diol formation following OH^\bullet addition to the bipyridine ring (e.g., [Maliyackel, et al. *Inorg Chem* **1990**, *29*, 340-8]).

To study catalysis outside strongly acidic environments, we have been investigating dimer-catalyzed RuL_3^{2+} -photosensitized water oxidation by the $\text{S}_2\text{O}_8^{2-}$ ion. Our measurements indicate the following: optimized quantum yields for O_2 production are $\Phi \sim 0.2$ ($\Phi_{\text{theo}} = 0.25\text{-}0.50$), the O_2 evolution rate increases slowly with increasing alkalinity to pH 9, and the maximal turnover rate based upon total catalyst present is $k_{\text{cat}} \sim 2 \text{ s}^{-1}$. The catalytically active oxidation state also appears to be **{5,5}** under these conditions; this oxidation state does not accumulate to an appreciable extent under continuous photolysis conditions, suggesting that its actual catalytic activity are much higher than the apparent value estimated from measured O_2 evolution rates. Finally, rates of decay of NIR and EPR signals from transient state levels correlate with rates of O_2 evolution, indicating that these signal-generating species are kinetically competent to be bona

fide reaction intermediates.

Research in the coming year will be directed primarily at identifying the species giving rise to the unusual EPR signals in the {5,5} formal oxidation state. Preliminary results from Dr. Michael Bowman's laboratory (University of Alabama) indicate that ENDOR spectra can be obtained; complete structural analysis will be sought through recently established collaborations with him and Dr. David Britt (UC Davis). Additionally, we will investigate chemical coupling of water oxidation catalysts to photoinduced transmembrane redox reactions in vesicle assemblies that utilize pyrylium ions as combined photosensitizers/cyclic redox mediators [Khairutdinov & Hurst, *JACS* **2001**, *123*, 7352-9], the intent being to develop efficient systems for long-lived charge separation using water as the source of electrons. Several new tri- and tetranuclear clusters containing Ru and Ir metal centers that show water oxidizing catalytic function have been synthesized; the more active of these will also be characterized.

DOE Sponsored Publications 2006-2008

1. L. Zhu, R. F. Khairutdinov, J. L. Cape, & J. K. Hurst: "Photoregulated transmembrane charge separation by linked spiropyran-anthraquinone molecules". *J. Am. Chem. Soc.* **2006**, *128*, 825-835.
2. M.-Q. Zhu, J. J. Han, W. Wu, J. K. Hurst & A. D. Q. Li: "Spiropyran-based photochromic polymer nanoparticles with optically switchable luminescence." *J. Am. Chem. Soc.* **2006**, *128*, 4303-4309.
3. L. Zhu, W. Wu, M.-Q. Zhu, J. J. Han, J. K. Hurst & A. D. Q. Li: "Reversibly photoswitchable dual-color fluorescent nanoparticles as new tools for live cell imaging". *J. Am. Chem. Soc.* **2007**, *129*, 3524-3526.
4. J. K. Hurst, J. L. Cape, A. E. Clark, S. Das & C. Qin: "Mechanisms of water oxidation catalyzed by ruthenium diimine complexes". *Inorg. Chem.* **2008**, *47*, 1753-1764 (contribution to Forum entitled "Making Oxygen").
5. J. L. Cape & J. K. Hurst: "Detection and mechanistic relevance of transient ligand radicals formed during $[\text{Ru}(\text{bpy})_2(\text{OH}_2)]_2\text{O}^{4+}$ -catalyzed water oxidation". *J. Am. Chem. Soc.* **2008**, *130*, 827-829.

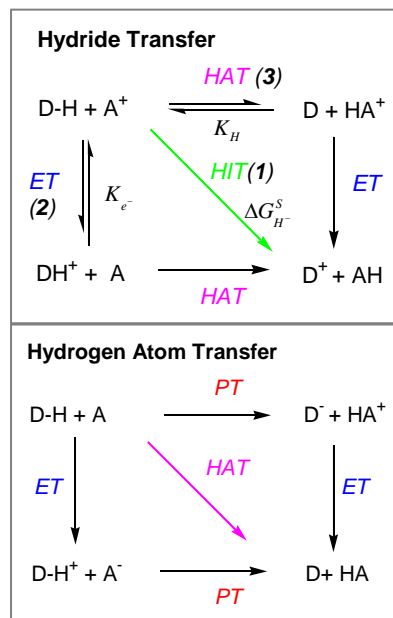
HYDRIDE ION TRANSFER REACTIONS IN WATER

Carol Creutz

Chemistry Department
Brookhaven National Laboratory
Upton, NY 11973-5000

Scope:

The photodriven generation of fuels from abundant materials such as water and carbon dioxide is inextricably tied to coupled proton and electron transfer reactions. The coupled processes may occur through concerted or stepwise mechanisms. A concerted hydride ion transfer reaction effects the transfer of two electrons and one proton. Net hydride transfer may be accomplished *via* several mechanistic pathways, depending upon the properties of the donor and acceptor. For carbon centers, two pathways are in evidence: (1) hydride ion transfer (HIT) and (2) electron transfer (ET), followed by H atom transfer (HAT) (or electron transfer, followed by H⁺ (PT) and electron transfer). These are illustrated in the upper square scheme at the right, where DH refers to the hydride donor and A⁺ to the hydride or electron acceptor and where hydrogen-atom transfers are horizontal, electron-transfer reactions are vertical and hydride ion transfer occurs on the diagonal. For metal hydrides, the low intrinsic barrier to H-atom transfer³⁹ leads to the additional consideration of initial H-atom transfer, followed by electron transfer (top horizontal, pathway 3). As shown at the lower right, the H-atom transfer may also be accomplished by different mechanistic pathways: initial proton (horizontal), electron (vertical), or H-atom (diagonal) transfer.

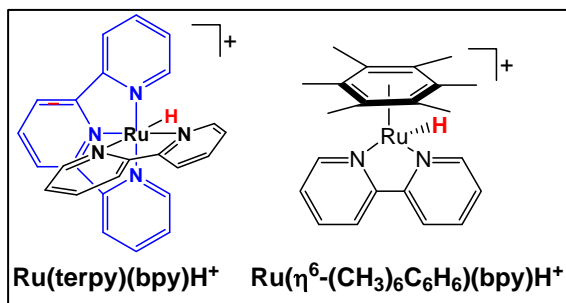


DuBois has advanced the concept of thermodynamic hydricity for metal hydrides. Hydricity is defined as the free energy change for dissociation of H⁻ in contrast with acidity and homolytic cleavage. For pathway (1), hydride transfer, the thermodynamic hydricity of the hydride might be expected to determine the rate of hydride transfer, whereas for pathway (2) the driving force for the first electron transfer should be critical. Pathway (3), hydrogen-atom transfer depends upon the homolytic bond free energy of the metal hydride ($\Delta G_{H\bullet}$).

Dissociation of H ⁻ :	D-H = D ⁺ + H ⁻	ΔG_{H^-}
Acidity	D-H = D ⁻ + H ⁺	$\Delta G_{H^+}, pK_a$
Homolysis	D-H = D + H \bullet	$\Delta G_{H\bullet}$

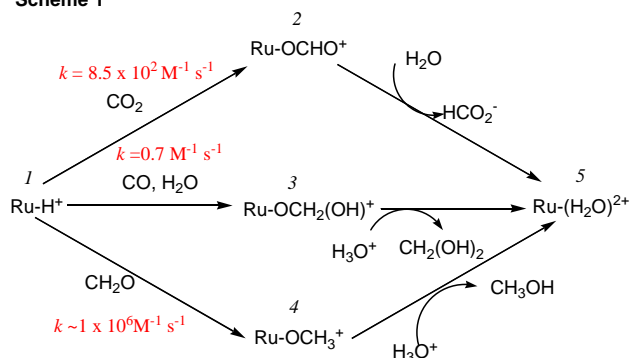
While the thermodynamics of a number of transition-metal and carbon based hydrides have been now been examined in several organic solvents, few have been studied in aqueous media—this despite the fact that water provides an ideal source of the hydrogen needed in environmentally sound photodriven generation of fuels. Consequently, we have embarked on an effort to characterize both the thermodynamics and kinetics of hydride ion transfer reactions in water specifically choosing metal hydride complexes that are capable of donating hydride ion to H₃O⁺ and CO₂ and are thus of potential interest as mediators in solar fuel generation.

Recent Results:



In aqueous media we are examining the reactivity of two hydride complexes, Ru(terpy)(bpy)H^+ and $\text{Ru}(\eta^6\text{-(CH}_3)_6\text{C}_6\text{H}_6\text{)(bpy)H}^+$. As summarized in Scheme 1, the complex Ru(terpy)(bpy)H^+ reacts rapidly with the C_1 species CO_2 , CO , and CH_2O to give O-bonded complexes of the two-electron reduction products (formate, formaldehyde, and methanol, respectively) which subsequently hydrolyze, releasing the C_1 product.

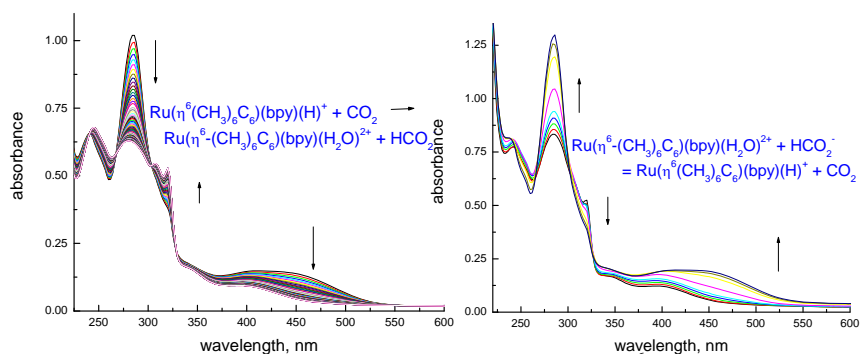
Scheme 1



On the basis of the observations on reaction 12, we estimated that K_{12} for the hydride transfer (from the ratio of forward and reverse constants) to be $\geq 10^4 \text{ M}^{-1}$ and $\Delta G^0 \leq -5 \text{ kcal/mol}$. Since the hydricity of formate in water is 23 kcal/mol (based on $\text{pK}_a(\text{H}_2) = 22$ rather than the commonly used, earlier value 31), the hydricity of Ru(terpy)(bpy)H^+ in water was estimated as $\leq 18 \text{ kcal/mol}$.

In recent work, we have found that we can

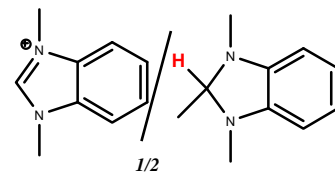
equilibrate the hydride complexes and CO_2 , starting from formate ion and the aqua complexes (reaction 51). From the absorbance changes registered at equilibrium, hydricity values of $\Delta G_{\text{H}}^0 = 18.5$ for Ru(terpy)(bpy)H^+ and 20.3 kcal/mol for $\text{Ru}(\eta^6\text{-(CH}_3)_6\text{C}_6\text{H}_6\text{)(bpy)H}^+$ in water ($\mu = 0.5 \text{ M}$) at 25 °C are obtained. The results of our kinetics and equilibrium studies will be presented.



Spectral changes following (left) reaction of $\text{Ru}(\eta^6\text{-(CH}_3)_6\text{C}_6\text{H}_6\text{)(bpy)H}^+$ with 3 mM CO_2 at pH 5.8 and (right) reaction of $\text{Ru}(\eta^6\text{-(CH}_3)_6\text{C}_6\text{H}_6\text{)(bpy)(H}_2\text{O)}_2^{2+}$ with 0.1 M HCO_2^- at pH 6.

Future Plans:

- Refine thermodynamic estimates of hydricity in water with expanded series of hydride donors/acceptors, e.g. the benzimidazole derivatives **1/2** at right. Make contact with data for organic solvents.
- Determine rates of hydride transfer as a function of hydricity difference as a beginning to systematic testing and modeling of mechanism.



DOE Sponsored Publications 2006-2008

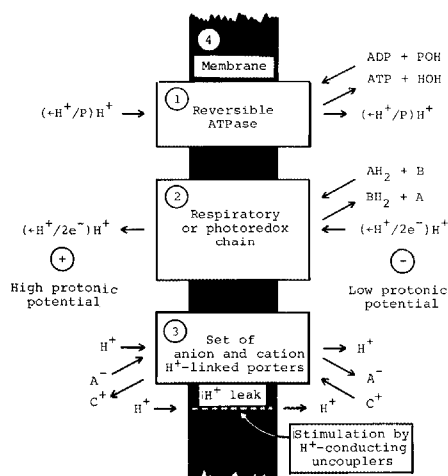
1. Creutz, C.; Brunschwig, B. S.; Sutin, N., Interfacial charge transfer absorption: Application to metal-molecule assemblies. *Chem. Phys.* **2006**, 324, 244-258.
2. Creutz, C.; Brunschwig, B. S.; Sutin, N., Interfacial charge transfer absorption: 3. Application to semiconductor-molecule assemblies. *J. Phys. Chem B* **2006**, 110, 25181-25190.
3. Creutz, C.; Ford, P. C.; Meyer, T. J., Henry Taube: Inorganic Chemist Extraordinaire. *Inorg. Chem.* **2006**, 45, (18), 7059 - 7068.
4. Fujita, E.; Brunschwig, B. S.; Creutz, C.; Muckerman, J. T.; Sutin, N.; Szalda, D.; van Eldik, R., Transition state characterization for the reversible binding of dihydrogen to bis(2,2'-bipyridine)rhodium(I) from temperature- and pressure-dependent experimental and theoretical studies. *Inorg. Chem.* **2006**, 45, (4), 1595-1603.
5. Creutz, C., Nonadiabatic, Intramolecular Electron Transfer from Ruthenium(II) to Cobalt(III) Complexes. *J. Phys. Chem B* **2007**, 111, 6713-6717.
6. Creutz, C.; Chou, M. H., Rapid Transfer of Hydride Ion from a Ruthenium Complex to C₁ Species in Water. *J. Am Chem. Soc.* **2007**, 129, (33), 10108 - 10109.
7. Creutz, C.; Chou, M. H., Binding of Catechols to Mononuclear Titanium(IV) and to 1- and 5-nm TiO₂ Nanoparticles. *Inorg. Chem.* **2008**, 47, ASAP Article; DOI: 10.1021/ic701687k
8. Petroski, J.; Chou, M.; Creutz, C., The Coordination Chemistry of Gold Surfaces: Formation and Far-Infrared Spectra of Alkanethiolate-Capped Gold Nanoparticles. submitted.
9. Creutz, C.; Chou, M. H., Doherty M., Hydride Ion Transfer from Ruthenium Hydride Complexes in Water: Kinetics and Equilibrium Measurements, submitted.

PROTON-COUPLED ELECTRON TRANSFER – THE ENGINE THAT DRIVES WATER-SPLITTING

Daniel G. Nocera

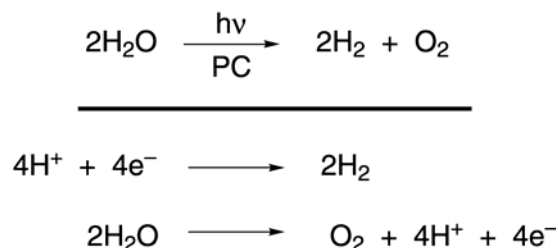
Department of Chemistry, 6-335
Massachusetts Institute of Technology
Cambridge, MA 02139-4307

Water splitting is inextricably linked to Mitchell's original proposal of the chemiosmotic principle. In his 1961 *Nature* paper, Peter Mitchell stated that the "coupling of phosphorylation to electron and hydrogen transfer by a chemiosmotic type of mechanism". In this simple statement, Mitchell succinctly related the coupling between the electron and proton to energy conversion. Since this Nobel Prize winning discovery, the coupling of electron and proton has become dogma in bioenergy conversion. However, this dogma is not restricted to bioenergy – it is also evident in the energy conversion schemes that are at the heart of this DOE program.



The original diagram postulating the chemiosmotic principle (Nature 1961, 191, 144).

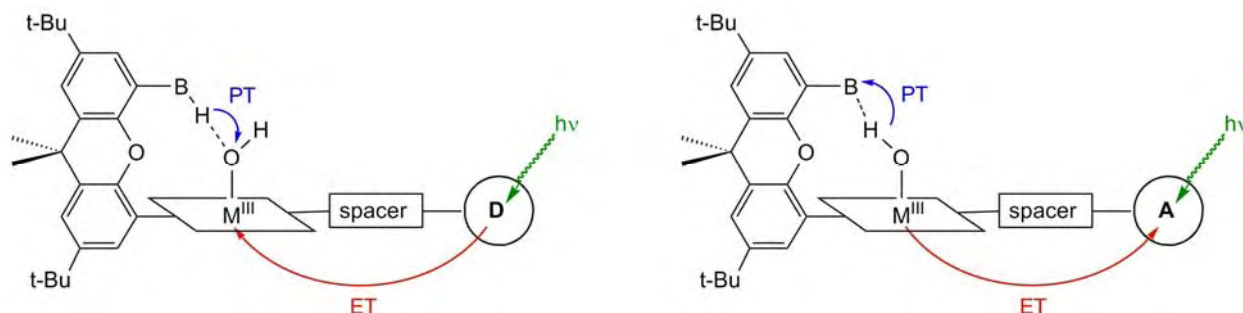
Four protons must couple to four electrons in the water splitting transformation:



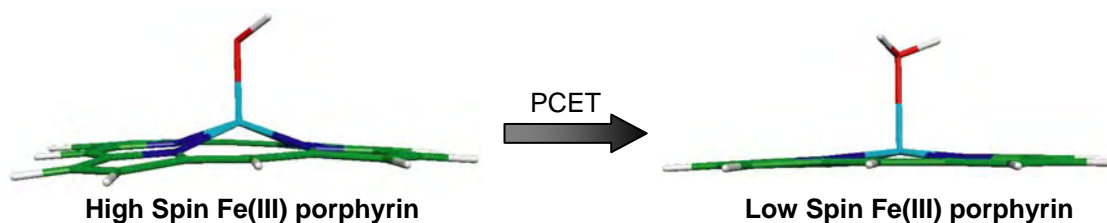
This is not a simple issue. The electron is quantum mechanical object. The proton is a classical object. But they both must tunnel in their coupling. This is an issue of kinetics. Work prior to our program treated proton-coupled electron transfer (PCET) on a thermodynamic basis (e.g., Pourbaix diagram). In this DOE program, we seek to elucidate the kinetics of PCET, especially as it pertains to the water-splitting reaction. The added complexity for water activation is that protons are coupled to *multielectron* transfers. Without control over PC-multi-ET, large overpotentials confront the water splitting transformation.

To investigate the PCET and oxygen atom activation, we have created the Hangman platform. In this construct, an acid-base functionality is poised over a redox active metal platform. The acid-base functionality is used to form a secondary coordination sphere that can assist proton movement to and from substrates bound to the redox center. At a mechanistic front, the

Hangman systems orthogonalize PCET systems and in doing so permit control of the proton transfer over short distances and the electron transfer over long distances. The activation of hydroxide to oxo or hydroxide to water by PCET may be examined by appending an acceptor or donor, respectively, to the redox platform of the Hangman scaffold:



Over twenty different Hangman systems have been synthesized that feature porphyrins, salens and metal polypyridyls as the redox platform. In each case, transient kinetics of the particular system has been elucidated. For porphyrins, we have uncovered a major problem in the literature. Despite literature claims dating back to the 1980's, Zn(II) porphyrins do not undergo electron transfer with Fe(III) porphyrins unless the porphyrin is axially coordinated by two strong field ligands. If the iron center is coordinated by two weak field ligands, strong and weak field ligands or five-coordinate, electron transfer is retarded owing to a large reorganizational energy associated with relaxation of a high spin Fe(III) center into the porphyrin core upon reduction to a low spin Fe(II) center:



The electron transfer rate is sufficiently slowed by this large reorganization that energy transfer always wins out over electron transfer. This discovery necessitated a redesign of the PCET approach pursued in this program. We have turned to metal polypyridyl Hangman systems. In these compounds, the PCET of oxygen activation may be examined. This work directly ties to the water oxidation reactions that are so often claimed for metal, especially ruthenium, polypyridyl complexes. The PCET kinetics of Hangman ruthenium polypyridyls will be presented along with parallel chemical studies aimed at promoting water oxidation.

DOE Sponsored Publications 2006-2008

1. "Hangman Salen Platforms Containing Two Xanthene Scaffolds" Jenny Y. Yang, Julien Bachmann and Daniel G. Nocera, *J. Org. Chem.* **2006**, *71*, 8706-14.
2. "Mechanistic Studies of Hangman Salophen-Mediated Activation of O—O Bonds"; Shih-

- Yuan Liu, Jake D. Soper, Jenny Y. Yang, Elena V. Rybak-Akimova and Daniel G. Nocera, *Inorg. Chem.* **2006**, *45*, 7572-4.
3. “A Simple and Versatile Method for Alkene Epoxidation using Aqueous Hydrogen Peroxide and Manganese Salophen Complexes as Catalysts”; Shih-Yuan Liu and Daniel G. Nocera, *Tetrahedron Lett.* **2006**, *47*, 1923-6.
 4. “The Relation between Hydrogen Atom Transfer and Proton-Coupled Electron Transfer in Model Systems”; Justin M. Hodgkiss, Joel Rosenthal and Daniel G. Nocera, In *Handbook of Hydrogen Transfer. Physical and Chemical Aspects of Hydrogen Transfer*; J. T. Hynes, J. P. Klinman, H.-H. Limbach, R. L. Schowen, Eds; Wiley-VCH: Weinheim, Germany, **2006**; Vol. II, Part IV, Ch. 17, pp 503-62.
 5. “Powering the Planet: Chemical Challenges in Solar Energy Utilization”; Nathan S. Lewis and Daniel G. Nocera, *Proc. Natl. Acad. Sci.* **2006**, *103*, 15729-35.
 6. “On the Future of Global Energy; Daniel G. Nocera, *Daedalus* **2006**, *135*, 112-15.
 7. “Proton-Directed Redox Control of O–O Bond Activation by Heme Hydroperoxidase Models”; Jake D. Soper, Sergey V. Kryatov, Elena V. Rybak-Akimova and Daniel G. Nocera, *J. Am. Chem. Soc.* **2007**, *129*, 5069-75.
 8. “Stereolectronic Control of H₂O₂ Dismutation by Hangman Porphyrins”; Joel Rosenthal, Leng Leng Chng, Stephen D. Fried, and Daniel G. Nocera, *Chem. Commun.* **2007**, 2642-4.
 9. “Catalase and Epoxidation Activity of Manganese Salen Complexes Bearing Two Xanthene Scaffolds”; Jenny Y. Yang and Daniel G. Nocera, *J. Am. Chem. Soc.* **2007**, *129*, 8192-8.
 10. “Excited State Dynamics of Hangman Dyads”; Justin Hodgkiss, Alex Krivokapic and Daniel G. Nocera, *J. Phys. Chem.* **2007**, *111*, 8258-68.
 11. “The Role of Proton-Coupled Electron Transfer in O—O Bond Activation”; Joel Rosenthal and Daniel G. Nocera, *Acc. Chem. Res.* **2007**, *40*, 543-53.
 12. “Oxygen Activation Chemistry of Pacman and Hangman Porphyrin Architectures Based on Xanthene and Dibenzofuran Spacers”; Joel Rosenthal and Daniel G. Nocera, *Prog. Inorg. Chem.* **2007**, *55*, 483-544.
 13. “A Ligand Field Chemistry of Oxygen Generation by the Oxygen Evolving Complex and Synthetic Active Sites”; Theodore A. Betley, Yogesh Surendranath, Montana V. Childress, Glen E. Alliger, Ross Fu, Christopher C. Cummins and Daniel G. Nocera, *Phil. Trans. Royal Soc. B* **2008**, *363*, 1293-303.
 14. “Metal Oxo Complexes for Oxygen-Oxygen Bond Formation”; Theodore A. Betley, Qin Wu, Troy Van Voorhis and Daniel G. Nocera, *Inorg. Chem.* **2008**, *47*, 1849-61.
 15. “Manganese Amido-Imine Bisphenol Hangman Complexes”; Jenny Y. Yang and Daniel G. Nocera, *Tetrahedron Lett.* **2008**, in press.
 16. “Hangman Salen Platforms Containing Two Dibenzofuran Scaffolds: Catalase Activity and Epoxidation of Unfunctionalized Olefins”; Jenny Y. Yang and Daniel G. Nocera, *ChemSusChem*. **2008**, submitted for publication.

Contributing Author to Reports 2006-2008

1. Grand Challenges Report, *Directing Matter and Energy: Five Challenges for Science and the Imagination*, U.S. Department of Energy, Washington, D.C. 2007.
2. Basic Research Needs Report, *Electrical Energy Storage*, U.S. Department of Energy, Washington, D.C. 2007.
3. Basic Research Needs Report, *Catalysis for Energy*, U.S. Department of Energy, Washington, D.C. 2007.
6. Sustaining America's Competitive Edge, National Science Foundation, National Institute of Standards and Technology, National Institutes of Health, Washington, D.C. 2007.
7. Bioinspired Chemistry for Energy, National Research Council, National Academies Press, Washington, D.C. 2008.

Session III

Photoinduced Electron Transfer

DYNAMICS OF PHOTOINDUCED ELECTRON TRANSFER IN DNA

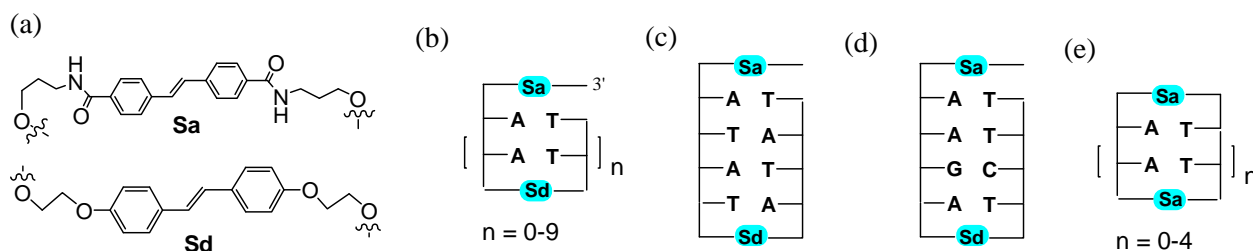
Frederick D. Lewis

Department of Chemistry, Northwestern University, Evanston, IL 60201

The principle objective of this project is to investigate the mechanism and dynamics of photoinduced charge separation processes in systems which possess an electron donor and electron acceptor separated by aromatic spacers having a face-to-face or π -stacked geometric relationship. The π -stacked base pairs in duplex DNA possess such a geometry and have been proposed to function as a “molecular wire.” Our approach to the study of electron transfer in DNA is based on the use of hairpin-forming bis(oligonucleotide) conjugates in which a stilbenedicarboxamide chromophore (Sa, Scheme 1a) serves both as a linker connecting two complementary oligonucleotide arms and as a photooxidant. Second generation capped hairpin and dumbbell systems contain a stilbene diether chromophore (Sd) at the opposite end of the duplex from the Sa chromophore.

Charge Separation Across A-Tracts. In our initial studies of photoinduced charge separation in capped hairpins, polymeric poly(A)-poly(T) base pair domains known as A-tracts were used to separate the Sa and Sd chromophores (Scheme 1b).^{1,2} Differences in the transient absorption spectra for $^1\text{Sa}^*$, Sa^- and Sd^+ make possible the temporal resolution of hole injection from $^1\text{Sa}^*$ to the A-tract and hole arrival at the Sd hole trap. Rate constants for hole injection are independent of the distance between chromophores. Rate constants for charge separation and charge recombination are more strongly distance dependent at short distances (1 to 4 base pairs) than at longer distances. For hairpins having three or more base pairs, hole injection is more rapid than hole arrival, consistent with a multistep hopping mechanism for charge separation. Single step superexchange competes with hopping only at short distances (one or two intervening base pairs). The distance dependent efficiency of charge separation (Φ_{cs}) parallels the dynamics. Superexchange charge transfer is observed for charge recombination across A-tracts and when the excited state chromophore is unable to inject a hole into the A-tract.³

Charge Separation Across Alternating AT Base Sequences. We have extended our studies of Sa/Sd capped hairpins to include alternating AT sequences (Scheme 1c).⁴ Rate constants for hole injection are somewhat smaller for AT sequences, plausibly reflecting greater stabilization of the $\text{Sa}^- \text{A}^+$ contact radical ion pair by an adjacent A vs. T. Rate constants for hole arrival at Sd are smaller for the AT vs. A hairpins for all values of n , the difference being most



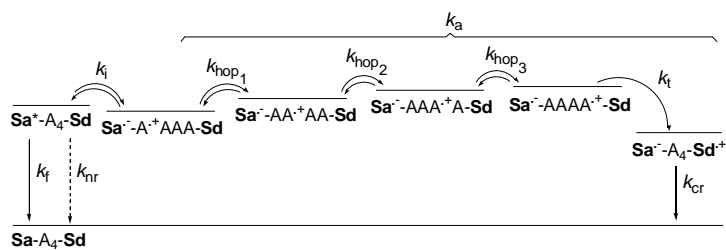
Scheme 1. Structures of (a) chromophores Sa and Sd, (b) capped A-tract hairpin, (c) hairpin with alternating ATAT base sequence, (d) hairpin with a single G-C base pair, and (e) dumbbells with Sa linkers.

pronounced for $n = 3$. Φ_{cs} values are also smaller for nAT vs. nA hairpins, the most pronounced difference being observed for $n = 3$. For larger values of n both k_a and Φ_{cs} are only weakly distance-dependent for both the nA and nAT hairpins. The higher energy for of A^+T vs. A^+A bridge-oxidized states can account for slower and less efficient hole transport via nAT vs. nA sequences.

Introduction of Guanine into the A-Tract. We have also investigated the effect of a single G-C base pair on the efficiency and dynamics of photoinduced charge separation in synthetic DNA capped hairpins in which a poly(A)-poly(T) base pair domain separates the electron acceptor Sa and electron donor Sd (Scheme 1d).^{5,6} The quantum yields for charge separation and the hole arrival times at Sd have been determined for all possible di- and trinucleotide sequences containing a single G. There is a marked decrease in Φ_{cs} when G is adjacent to Sa in sequences GA and GAA and a smaller decrease when G is located in the middle of the AGA sequence. The effect of a G:C base pair on the behavior of longer base pair sequences has been investigated for A_nGA sequences ($n = 0$ to 4). For some donor-acceptor distances, the rate constants for hole arrival are actually larger for the A_nGA series than for the A_n series, the largest advantage being observed for the penta-nucleotide A_3GA vs. A_5 . Values of Φ_{cs} increase with n for the A_nGA sequences for $n = 0$ to $n = 3$, reaching a maximum value of ca. 0.3 for the tetra- and pentanucleotides and then decrease for the longer polypurine sequences. To our knowledge the values of $\Phi_{cs} = 0.3 \pm 0.1$ for A_2GA and A_3GA are the largest reported to date for photoinduced charge separation over four or more base pairs, regardless of the acceptor and base sequence.

Symmetry-Breaking in Stilbene-linked Dumbbells. Excited state symmetry breaking occurs when the locally excited state of a symmetric bichromophoric molecule A^*-A is converted to the charge-separated state A^+-A^- . This process normally requires both high solvent polarity and strong through-bond coupling between chromophores, as is the case for 9,9'-bianthryl, the classic example of symmetry breaking. We have observed symmetry breaking between the Sa chromophores in Sa-linked dumbbells (Scheme 1e).⁷ The fs transient absorption spectra display changes in band shape indicative of the conversion of a locally excited $^1Sa^*$ state to the $Sa^-A_n-Sa^+$ charge-separated state. The occurrence of symmetry breaking in Sa- A_n -Sa dumbbells is a consequence of both the unique ability of A-tract DNA to mediate hole transport and the highly polar aqueous solvent.

The symmetry-breaking mechanism is outlined in Scheme 2. According to this mechanism, charge separation occurs via a multi-step process consisting of hole injection, hole transport against a Coulomb energy gradient, and hole trapping. Hole transport is the rate determining step for symmetry breaking in dumbbells possessing one or more A-T base pair. Charge recombination occurs by the reverse of this process; hole detrapping and hole return leading to $^1Sa^*$ delayed fluorescence.



Scheme 2. Kinetic scheme for fluorescence, non-radiative decay, hole injection, hole transport, hole trapping and charge recombination in a Sa/Sd capped hairpin.

DOE Sponsored Publications 2006-2008

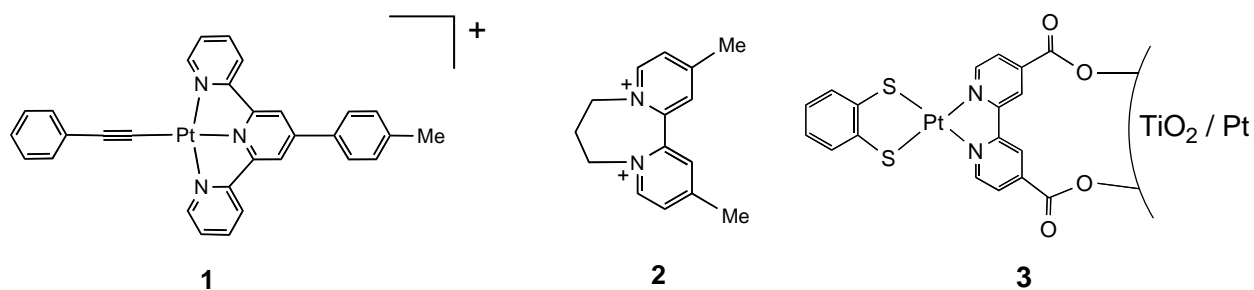
- (1) Lewis, F. D.; Zhu, H.; Daublain, P.; Fiebig, T.; Raytchev, M.; Wang, Q.; Shafirovich, V. Crossover from superexchange to hopping as the mechanism for photoinduced charge transfer in DNA hairpin conjugates. *J. Am. Chem. Soc.* **2006**, *128*, 791-800.
- (2) Lewis, F. D.; Zhu, H.; Daublain, P.; Cohen, B.; Wasielewski, M. R. Hole mobility in DNA A-tracts. *Angew. Chem. Int. Ed.* **2006**, *45*, 7982-7985.
- (3) Lewis, F. D.; Zhang, L.; Kelley, R. F.; McCamant, D.; Wasielewski, M. R. A perylenedicarboxamide linker for DNA hairpins. *Tetrahedron* **2007**, *63*, 3457-3464.
- (4) Lewis, F. D.; Daublain, P.; Cohen, B.; Vura-Weis, J.; Shafirovich, V.; Wasielewski, M. R. Dynamics and efficiency of DNA hole transport via alternating AT versus poly(A) sequences. *J. Am. Chem. Soc.* **2007**, *129*, 15130-15131.
- (5) Lewis, F. D.; Daublain, P.; Cohen, B.; Vura-Weis, J.; Wasielewski, M. R. The influence of guanine on DNA hole transport efficiency. *Angew. Chem. Int. Ed.* **2008**, in press.
- (6) Lewis, F. D.; Zhu, H.; Daublain, P.; Sigmund, K.; Fiebig, T.; Raytchev, M.; Wang, Q.; Shafirovich, V. Getting to guanine: Mechanism and dynamics of charge separation and charge recombination in DNA revisited. *Photochem. Photobiol. Sci.* **2008**, in press.
- (7) Lewis, F. D.; Daublain, P.; Zhang, L.; Cohen, B.; Vura-Weis, J.; Wasielewski, M. R.; Shafirovich, V.; Wang, Q.; Raytchev, M.; Fiebig, T. Reversible bridge-mediated excited state symmetry breaking in stilbene-linked DNA dumbbells. *J. Phys. Chem. B* **2008**, *112*, 3838-3843.
- (8) Lewis, F. D. DNA photonics. *Pure Appl. Chem.* **2006**, *78*, 2287-2295.
- (9) Zuo, X.; Cui, G.; Merz, K. M., Jr.; Zhang, L.; Lewis, F. D.; Tiede, D. M. X-ray diffraction "fingerprinting" of DNA structure in solution for quantitative evaluation of molecular dynamics simulation. *Proc. Nat. Acad. Sci. USA* **2006**, *103*, 3534-3539.

LUMINESCENT PLATINUM COMPLEXES FOR HYDROGEN GENERATION AND PHOTO-INDUCED CHARGE SEPARATION

Pingwu Du, Jacob Schneider, Paul Jarosz, Jie Zhang, Theodore Lazarides,
Jason Thall, Kathryn Knowles and Richard Eisenberg
Department of Chemistry
University of Rochester
Rochester, NY 14627-0216

Despite seminal work done more than three decades ago on the light-driven generation of hydrogen from water using visible light, the development of an efficient and robust system to accomplish this goal remains elusive. The research to be presented addresses two aspects of this challenge. The first deals with the photo-generation of H₂ employing a multiple component system consisting of platinum(II) chromophores, an electron relay, a sacrificial electron source and colloidal Pt as the actual H₂-generating catalyst, while the second concentrates on photoinduced charge separation (PICS) using a similar platinum(II) chromophore covalently connected to spatially specific electron donor and acceptor moieties. The latter has been studied by transient absorption (TA) spectroscopy in collaboration with Professor Russell Schmehl of Tulane University.

Photogeneration of Hydrogen. In 2006, we reported that complex **1** can promote the photochemical generation of H₂ in a system containing methyl viologen (MV²⁺) as the electron relay, triethanol amine (TEOA) as the sacrificial electron donor and colloidal Pt as the H₂-generating catalyst. Subsequent studies found that other Pt(II) complexes having bi- and terpyridyl ligands with similar ³MLCT excited states also drive this reaction with light of $\lambda > 410$ nm. Different diquats were used in place of MV²⁺ as the electron relay and compound **2** was found to be most effective with more than 800 turnovers of H₂ and a 67% yield of H₂ based on TEOA. Since **2** was the most difficult to reduce of the different diquats employed, we concluded that electron transfer from the reduced diquat to the colloid may be turnover limiting rather than the quenching step between the excited chromophore and the electron relay.

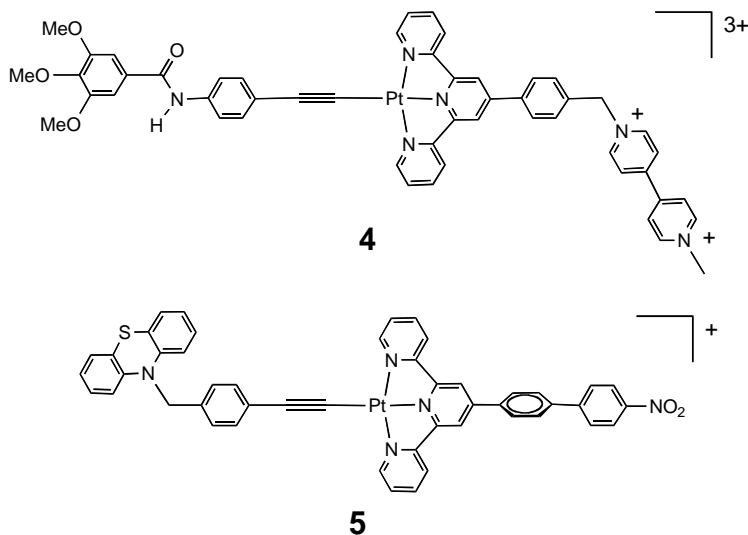


Two problematic aspects of these systems were the slow decomposition of the electron relay by hydrogenation and the radiation energy needed by **1** to effect the proton reduction to hydrogen. In order to address the first deficiency, TiO₂ was employed as the electron relay with platinization of the semiconductor nanoparticles providing catalytic sites for H₂ formation. The second problem stimulated a change in the Pt(II) chromophore away from acetylide complexes to corresponding dithiolate systems since these complexes were known from earlier work to have a lower energy ³CT state involving a mixed Pt(d)/S(p)/dithiolate HOMO and a π^* diimine

LUMO. Importantly, Pt(diimine)(dithiolate) complexes when attached to TiO₂ through carboxylate substituents were reported by Arakawa to generate photocurrent. The system shown as **3** was thus found to generate H₂ in the presence of TEOA. While the system efficiency was low, the system appeared to be photostable when irradiation was limited to $\lambda > 455$ nm.

Observations of photo-instability for Pt complexes when $\lambda > 410$ nm but not when $\lambda > 455$ nm led to an examination of Pt bi- and terpyridyl chloride complexes that had been suggested as possible molecular catalysts for H₂ production. A recent communication in collaboration with Professor Felix Castellano of Bowling Green State University addresses this matter on several levels. In particular, through the use of TEM images of TiO₂ before and after irradiation, corresponding EDAX data, the use of Hg to sequester or inhibit catalysis by colloids and variants of **3** with molecular complex catalysts in place of surface bound Pt islands, we have been able to show that catalysis of the photogeneration of H₂ is achieved by metallic Pt and that the purported Pt(II) molecular catalysts are simply serving as colloidal metal precursors.

Photoinduced Charge Separation in Platinum Chromophore Based Triads and Dyads. In a continuation of studies on PICS with Pt(II)-based multi-component systems such as triad **4** and its nicotinamide analog, together with the corresponding chromophore-acceptor dyads, have been synthesized, characterized and examined spectroscopically by transient absorption methods. The results reveal that **4** exhibits a long-lived transient characteristic of electron transfer to the viologen in contrast with analogous pyridinium and nicotinamide acceptors in which electron transfer was not observed. However, the charge separated transient in **4** is formed very inefficiently. An additional problem identified with the multi-component systems having pyridinium acceptors attached as in **4** is the sensitivity of the N-C(benzylic) bond to cleavage by OH⁻ which is formed in systems for H₂ generation from H₂O. This sensitivity to base had not been recognized in other studies employing this type of linkage. For comparison of PICS with other reported triads having phenothiazine(PTZ) donors and nitrobenzene (NB) acceptors, the triad shown as **5** was synthesized using Pd-catalyzed coupling chemistry. While the chromophore-acceptor link in this system is robust, electron transfer to NB does not occur because of poor coupling between chromophore and NB and lower driving force for the electron transfer.



Also to be presented are current and planned efforts at developing integrated systems for H₂ generation in which more effective chromophores and true molecular catalysts are employed.

DOE Sponsored Publications 2006-2008

1. Photocatalytic Generation of Hydrogen from Water Using a Platinum(II) Terpyridyl Acetylde Chromophore, Du, P.; Schneider, J.; Jarosz, P.; Eisenberg, R., *J. Am. Chem. Soc.* **2006**, *128*, 7726-7727.
2. Photoinduced Electron Transfer in Platinum(II) Terpyridyl Acetylde Chromophores: Reductive and Oxidative Quenching and Hydrogen Production, Du, P.; Schneider, J.; Jarosz, P.; Zhang, J.; Brennessel, W. W.; Eisenberg, R., *J. Phys. Chem. B* **2007**, *111*, 6887-6894.
4. Photogeneration of Hydrogen from Water Using an Integrated System Based on TiO₂ and Platinum(II) Diimine Dithiolate Sensitizers, Zhang, J.; Du, P.; Schneider, J.; Jarosz, P.; Eisenberg, R., *J. Am. Chem. Soc.* **2007**, *129*, 7726-7727.
5. The Synthesis and Structural Characterization of a New Vapochromic Pt(II) Complex Based on the 1-Terpyridyl-2,3,4,5,6-Pentaphenylphenyl (TPPPB) Ligand, Du, P.; Schneider, J.; Brennessel, W. W.; Eisenberg, R., *Inorg. Chem.* **2008**, *47*, 69-77.
6. Bi- and Terpyridyl Platinum(II) Chloro Complexes: Molecular Catalysts for the Photogeneration of Hydrogen from Water or Simply Precursors for Colloidal Platinum?, Du, P.; Schneider, J.; Castellano, F.; Eisenberg, R., *J. Am. Chem. Soc.* **2008**, *30*, 5056-5058.
7. Synthesis, Characterization, and Photophysical Properties of Platinum(II) Terpyridyl-based Molecular Assemblies, Jarosz, P.; Thall, J.; Schneider, J.; Kumaresan, D.; Schmehl, R. and Eisenberg, R. *Energy & Environmental Science*, submitted for publication.
8. Synthesis and Photophysical Properties of Pt(II)(bipy)(dithiolate) Complexes Containing a Dipyromethane-BF₂ Chromophore, Lazarides, T.; Eisenberg, R., manuscript in preparation.
9. Transient DC Photocurrent Measurements of a Charge Separated Platinum(II) Diimine Dyad, McGarrah, J. E.; Smirnov, S. N.; Hupp, J. T.; Eisenberg, R., manuscript in preparation.
10. Photoinduced Hydrogen Production Catalyzed by Cobalt Macrocyclic Complexes: A New Integrated System, Du, P.; Knowles, K.; Schneider, J.; Eisenberg, R., manuscript in preparation.
11. Sensitized Energy Upconversion by a Platinum(II) Terpyridyl Acetylde Complex, Du, P.; Eisenberg, R., manuscript in preparation.
12. Cyclometalated 6-Phenyl-2,2'-bipyridyl (CNN) Platinum(II) Acetylde Complexes as Potential Chromophores for the Photogeneration of Hydrogen from Water: Structure, Electrochemistry, Photophysics, and Electron Transfer Quenching Studies, Schneider, J.; Du, P.; Jarosz, P.; Lazarides, T.; Wang, X.; Brennessel, W. W.; Eisenberg, R., manuscript in preparation.
13. Synthesis, Electrochemistry, Photophysics and Solvatochromism in New Cyclometalated 6-Phenyl-4-(*p*-R-phenyl)-2,2'-bipyridyl (R = CH₃, COOCH₃, P(O)(OEt)₂) (C^NN) Platinum(II) Thiophenolate Chromophores, Schneider, J.; Du, P.; Brennessel, W. W.; Eisenberg, R. manuscript in preparation.
14. Platinum(II) Terpyridyl-Acetylde Dyads and Triads with Nitrophenyl Acceptors via a Convenient Synthesis of a Boronated Phenylterpyridine, Jarosz, P.; Lotito, K.; Schneider, J.; Kumaresan, D.; Schmehl, R. and Eisenberg, R., manuscript in preparation.

THEORETICAL STUDIES OF PHOTOACTIVE MOLECULAR SYSTEMS: ELECTRON TRANSFER, ENERGY TRANSPORT, AND OPTICAL SPECTROSCOPY

Richard A. Friesner
Department of Chemistry
Columbia University
New York, NY 10027

The present project has two principal long term goals. The first is to develop computational methodology that is capable of modeling charge separation, electron transport, energy transport, and optical spectroscopy in complex molecules and materials. The second objective is to apply these methods to systems of interest to the DOE solar photochemistry program.

We have made progress in both of these areas in the current granting period. In the methods development area, we have focused on an intensive examination of the accuracy and reliability of density functional theory (DFT) and have developed a highly promising, novel approach to improving the quality of DFT results. We have also implemented TDDFT excited state methods in Jaguar, in collaboration with Todd Martinez at the University of Illinois. In applications, we are investigating carbon nanotubes, conducting polymers, and TiO₂ nanostructures.

We have developed a new approach to density functional theory based on analyzing the errors in DFT as being attributable to inaccurate modeling of nondynamical electron correlation in localized electron pairs and unpaired electrons. These errors can be substantially reduced using simple empirical localized orbital corrections (DFT-LOC) for different types of bonds, lone pairs, and radicals, based on chemical structure, which are transferable from one molecule to another. There are also some corrections which take into account environmental effects. Using our correction scheme with the B3LYP functional (B3LYP-LOC), the average error in atomization energies for the G3 set of test cases developed by Pople and coworkers (222 molecules) is reduced from 4.8 kcal./mole to 0.8 kcal/mole, comparable to the errors observed using high level ab initio techniques such as coupled cluster theory. We have reduced the errors in ionization potentials and electron affinities by a factor of ~3.

More recently, we have studied atomic excitation energies, and bond dissociation energies, for a series of small first row transition metal containing species, and applied correction parameters similar to what was described in our previous report for second and third row elements, using the B3LYP density functional. The average error for 36 atomic excitation energies is reduced from 7.7 kcal/mole to 0.4 kcal/mole, while the average bond dissociation energy error is reduced from 5.3 kcal/mole to 1.7 kcal/mole, as compared to experimental data. Coupled cluster calculations were also carried out to check the results using very high level ab initio electronic structure methods, and in one case, a large error in the experimental data was identified. The agreement between the coupled cluster and B3LYP-LOC calculations is good in all cases.

We are in the process of investigating dispersion interactions, transition states, and other aspects of DFT calculations that display systematic errors. Based on these studies, we intend to construct a functional which consists of a "standard" DFT component (e.g. B3LYP or perhaps a newer functional such as M06-2X) and a molecular mechanics type of component which can incorporate the localized orbital corrections, dispersion corrections, and other types of

corrections. We believe that such a functional can at this point achieve quantitative accuracy for a wide range of complex chemical structures and materials.

In the applications area, work on carbon nanotubes was published last year. We are currently preparing papers on conducting polymers (oligothiophene series with various sidechains) and modeling of TiO₂ nanostructures. We will discuss the electronic structures of these systems. Once the new functional described above is ready to use, we will switch our focus to applying this functional in the various applications areas. The ability of investigate relevant systems and produce results with high accuracy and reliability should be greatly enhanced.

DOE Sponsored Publications 2006-2008

1. Friesner, Richard A., Eric H. Knoll, Yixiang Cao, A Localized Orbital Analysis of the Thermochemical Errors in Hybrid Density Functional Theory: Achieving Chemical Accuracy via a Simple Empirical Correction Scheme, *J. Chem. Phys.*, 125, 12, 124107 (2006).
2. Knoll, Eric H., and Richard A. Friesner, Localized Orbital Corrections for the Calculation of Ionization Potentials and Electron Affinities in Density Functional Theory, *J. Phys. Chem. B*, 110, 38, 18787-18802 (2006).
3. Chen, Yiing-Rei, Lei Zhang, Mark S. Hybertsen, Theoretical study of trends in conductance for molecular junctions formed with armchair carbon nanotube electrodes, *Phys. Rev. B*, 76, 11, 115408 (2007).
4. Ko, Chaehyuk, David K. Malick, Dale A. Braden, Richard A. Friesner, and Todd J. Martinez, Pseudospectral time-dependent density functional theory, *J. Chem. Phys.*, 128, 10, 104103 (2008).
5. Bochevarov, Artem D. and Richard A. Friesner, The densities produced by the density functional theory: Comparison to full configuration interaction, *J. Chem. Phys.*, 128, 3, 034102 (2008).
6. Rinaldo, David, Li Tian, Jeremy N. Harvey, and Richard A. Friesner, Density Functional Localized Orbital Corrections for Transition Metals, *J. Chem. Phys.*, submitted (2008).
7. Schneebeli, Severin T., Michelle Lynn Hall, Ronald Breslow, and Richard A. Friesner, Prediction of Enantioselectivities for a Large Dataset of Dioxirane-Catalysed Epoxidations Using Density Functional Theory, *J. Am. Chem. Soc.* submitted (2008).
8. Wang, Ting and Richard A. Friesner, Quantum Chemical Modeling of Oligothiophene Polymers, in preparation (2008).
9. Bochevarov, Artem D., Michelle Hall, Severin. Schneebeli and Richard A. Friesner, Modeling of Dispersion Interactions in the Context of Density Functional Theory, in preparation (2008).
10. Chen, Yiing-Rei, B. Blagojevic, M. L. Steigerwald, Louis Brus, and Richard A. Friesner, Ab Initio Electronic Structure Modeling of Titanium dioxide clusters and small molecules, in preparation (2008).

Session IV

Heterogeneous Systems for Solar Photoconversion I

QUANTUM DOT SOLAR CELLS. MODULATION OF PHOTO RESPONSE WITH PARTICLE SIZE AND 1-D SUPPORT ARCHITECTURE

Prashant V. Kamat, Anusorn Kongkanand, Kevin Tvrdy, Patrick Brown and Istvan Robel
Radiation Laboratory and Department of Chemistry and Biochemistry
University of Notre Dame, Notre Dame, IN 46556

New strategies are being considered to employ nanostructured semiconductors and molecular assemblies for harvesting visible and near IR photons. Semiconductor quantum dots such as CdSe with their tunable band edges offer new opportunities to harvest light energy in the entire visible region of the solar spectrum. They also offer the possibility of generating multiple charge carriers under high energy excitations. The challenge now is to capture these photogenerated electrons as quickly as they are generated and transport them to the electrode surface in an efficient manner. The focus of our current research is threefold: (i) To improve the photoconversion efficiency by facilitating the charge transport through 1-D architecture, (ii) to tune the photoelectrochemical response and photoconversion efficiency via size control of CdSe quantum dots and (iii) to obtain fundamental understanding of the interfacial charge transfer processes in semiconductor quantum dot systems.

Single wall carbon nanotube (SWCNT) and TiO₂ nanotube arrays have been used as support architecture to direct the flow of photogenerated charge carriers and improve the photocurrent generation in photoelectrochemical solar cells (Figure 1). Furthermore these nanotube scaffolds can be used as supports to anchor various semiconductor nanoparticles. By

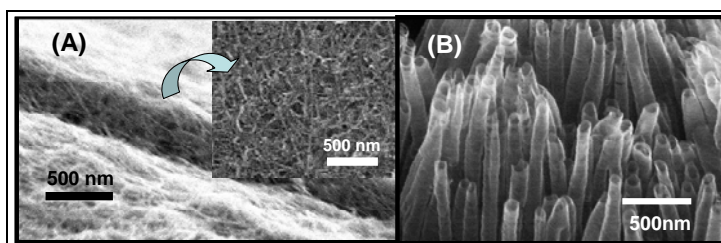


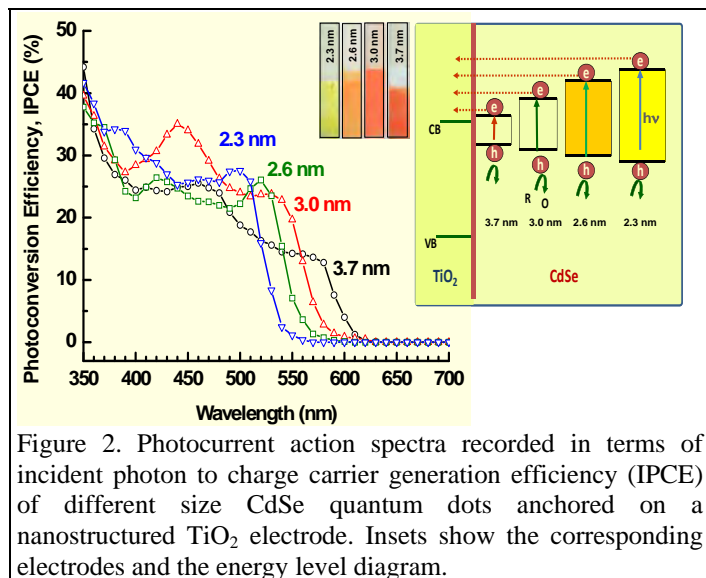
Figure 1. Scanning Electron Micrographs (SEM) of (A) SWCNT architecture on conducting glass electrode and (B) TiO₂ nanotubes anchored on Ti electrode. The nanotube network serves as scaffolds to anchor light harvesting assemblies and facilitate collection and transport of charge carriers.

employing this strategy, we were able to achieve twofold enhancement in the photocurrent generation in TiO₂ particulate films. A shift of ~100 mV in apparent Fermi level of the SWCNT-TiO₂ system as compared to the unsupported TiO₂ system is seen as the Fermi level of the two systems undergo charge equilibration. The interplay between the TiO₂ and SWCNT of attaining charge equilibration is an important factor for improving photoelectrochemical performance of nanostructured semiconductor based solar cells. The beneficial aspect of charge collection by SWCNT was further explored by sensitizing TiO₂ with Ru(II)polypyridyl complex. The dye-sensitized solar cells constructed using SWCNT scaffold show improvement in the photocurrent generation. However, this improvement is neutralized by the lower photovoltage as the apparent Fermi level of TiO₂ shifts unfavorably to less negative potentials as it equilibrates with SWCNT.

CdSe quantum dots of four different size (3.7, 3.0, 2.6 and 2.3 nm diameter) were anchored on nanostructured TiO₂ (particulate and tubular) films with the aid of a bifunctional surface modifier (HOOC-CH₂-CH₂-SH). Incident photon to charge conversion efficiency (IPCE) recorded with TiO₂-CdSe electrodes at the excitonic band was greater for the smaller particles (Figure 2). The ability to tune the photoresponse by varying the size of CdSe particles affords

modulation of the photoelectrochemical performance of quantum dot solar cells.

Femtosecond transient absorption studies indicate that the rate constant for electron transfer from the thermalized s-state increases with decreasing particle size.



value (45%) obtained with CdSe/TiO₂(nanotube) is greater than the IPCE (35%) of CdSe/TiO₂ (nanoparticle). Tubular TiO₂ architecture thus provides a better scaffold for the construction of quantum dot solar cells.

The overall performance of quantum dot solar cell is dictated by two opposing effects. Decrease in the particle size of CdSe increases photocurrent as the conduction band shifts to more negative potentials. On the other hand decreasing CdSe particle size lowers the photoresponse in the visible region. Efforts are underway to improve the light harvesting capability of quantum dot solar cells. One such approach under consideration is the construction of a *rainbow solar cell* which employs an ordered assembly of CdSe nanoparticles of different diameter. An example of TiO₂ nanotubes decorated with different sized CdSe nanoparticles is shown in Figure 3. As white light enters the cell, smaller size CdSe particles (larger bandgap) absorb the portion of the light with smaller wavelengths (blue region). Light with longer wavelengths (red region) which is transmitted through the initial layer is absorbed by subsequent layers, and so on. By creating an orderly gradient of quantum dots of different size, it should be possible to increase the effective capture of incident light. In addition we are also probing the interfacial electron transfer by capping the CdSe quantum dots with a shell of electron acceptor (e.g. C₆₀) and elucidating the factors controlling the fast capture of photogenerated electrons.

The energy gap between the two semiconductor systems acts as a driving force for the electron transfer in the normal Marcus region. An increase in the interparticle electron transfer rate constant by three orders of magnitude (from $\sim 10^7$ to 10^{10} s⁻¹) has been achieved by decreasing the CdSe particle diameter from 7.5 nm to 2.4 nm.

For quantum dot solar cells the difference in TiO₂ morphology has little effect on the charge injection rate, but influences the electron transport within the film.

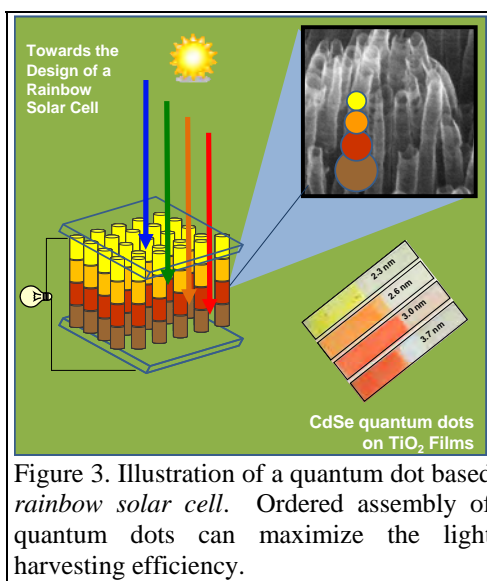


Figure 3. Illustration of a quantum dot based *rainbow solar cell*. Ordered assembly of quantum dots can maximize the light harvesting efficiency.

DOE Sponsored Publications 2006-2008

1. Hasobe, T.; Fukuzumi, S. and Kamat, P. V., *Stacked-Cup Carbon Nanotubes for Photoelectrochemical Solar Cells*. **Angew. Chem. (Int. Ed.)**, 2006, 45, 755-759.
2. Robel, I.; Subramanian, V.; Kuno, M. and Kamat, P. V., *Quantum Dot Solar Cells. Harvesting Light Energy with CdSe Nanocrystals Molecularly Linked to Mesoscopic TiO₂ Films*. **J. Am. Chem. Soc.**, 2006, 128, 2385-2393.
3. Hasobe, T.; Hattori, S.; Kamat, P. V. and Fukuzumi, S., *Supramolecular nanostructured assemblies of different types of porphyrins with fullerene using TiO₂ nanoparticles for light energy conversion*. **Tetrahedron**, 2006, 62, 1937-1946.
4. Kikuchi, H.; Kitano, M.; Takeuchi, M.; Matsuoka, M.; Anpo, M. and Kamat, P. V., *Extending the Photoresponse of TiO₂ to the Visible Light Region: Photoelectrochemical Behavior of TiO₂ Thin Films Prepared by RF-Magnetron Sputtering Deposition Method*. **J. Phys. Chem. B**, 2006, 110, 5537-5541.
5. Sudeep, P. K.; James, P. V.; Thomas, K. G. and Kamat, P. V., *Singlet and Triplet Excited State Interactions and Photochemical Reactivity of Phenyleneethynylene Oligomers*. **J. Phys. Chem. A**, 2006, 110, 5642-5649.
6. Kamat, P. V., *Carbon Nanomaterials: Building Blocks in Energy Conversion Devices*. **Interface**, 2006, 15, 45-47 (review article).
7. Robel, I.; Kamat, P. V. and Kuno, M. K., *Exciton Recombination in CdSe nanowires. Bimolecular to three-particle Auger Kinetics*. **Nano Lett.**, 2006, 6, 1344-1349.
8. Dintinger, J.; Robel, I.; Kamat, P. V.; Genet, C. and Ebbesen, T. W., *Terahertz All-Optical Molecule-Plasmon Modulation*. **Adv. Mater.**, 2006, 18, 1645-1648.
9. Lahiri, D.; Subramanian, V.; Bunker, B. A. and Kamat, P. V., *Probing photochemical transformations at TiO₂/Pt and TiO₂/Ir interfaces using x-ray absorption spectroscopy*. **J. Chem. Phys.**, 2006, 124, article 204720.
10. Takechi, K.; Sudeep, S. and Kamat, P. V., *Harvesting Infrared Photons with Tricarbocyanine Dye Clusters*. **J. Phys. Chem. B**, 2006, 110, 16169-16173.
11. Hasobe, T.; Fukuzumi, S. and Kamat, P. V., *Hierarchical Assembly of Porphyrins and Fullerenes for Solar Cells*. **Interface**, 2006, 15, 47-51 (review article).
12. Hasobe, T.; Fukuzumi, S. and Kamat, P. V., *Organized Assemblies of Single-Wall Carbon Nanotube (SWCNT) and Porphyrin for Photochemical Solar Cells. Charge Injection from Excited Porphyrin into SWCNT*. **J. Phys. Chem. B**, 2006, 110, 25477-25484.
13. Pramod, P.; Sudeep, P. K.; Thomas, K. G. and Kamat, P. V., *Photochemistry of Ruthenium trisbipyridine Functionalized on Gold Nanoparticles*. **J. Phys. Chem. B**, 2006, 110, 20737-20741.
14. Kamat, P. V., *Harvesting photons with carbon nanotubes*. **Nanotoday**, 2006, 1, 20-27 (review article).

15. Hasobe, T.; Fukuzumi, S. and Kamat, P. V., *Organized assemblies of single wall carbon nanotubes and porphyrin for photochemical solar cells: Charge injection from excited porphyrin into single-walled carbon nanotubes*. **J. Phys. Chem. B**, 2006, *110*, 25477-25484.
16. Sudeep, P. K.; Takechi, K. and Kamat, P. V., *Harvesting Photons in the Infrared. Electron Injection from Excited Tricarbocyanine dye (IR 125) into TiO₂ and Ag@TiO₂ core-shell nanoparticles*. **J. Phys. Chem. C**, 2007, *111*, 488-494.
17. Hasobe, T.; Saito, K.; Kamat, P. V.; Troiani, V.; Qiu, H.; Solladié, N.; Kim, K. S.; Park, J. K.; Kim, D.; D'Souza, F. and Fukuzumi, S., *Organic Solar Cells. Supramolecular Composites of Porphyrins and Fullerenes Organized by Polypeptide Structures as Light Harvesters*. **J. Mater. Chem.**, 2007, *17*, 4160-4170.
18. Arunkumar, E.; Sudeep, P. K.; Kamat, P. V.; Noll, B. C. and Smith, B. D., *Singlet Oxygen Generation Using Iodinated Squaraine and Squaraine-Rotaxane Dyes*. **New J. Chem.**, 2007, *31*, 677-683.
19. Kongkanand, A.; Domínguez, R. M. and Kamat, P. V., *Single Wall Carbon Nanotube Scaffolds for Photoelectrochemical Solar Cells. Capture and Transport of Photogenerated Electrons*. **Nano Lett.**, 2007, *7*, 676-680.
20. Hasobe, T.; Fukuzumi, S.; Hattori, S. and Kamat, P. V., *Shape- and Functionality-Controlled Organization of TiO₂-Porphyrin-C₆₀ Assembly for Improved Performance of Photochemical Solar Cells*. **Chemistry, Asian J.**, 2007, *2*, 265-272.
21. Kamat, P. V., *Meeting the Clean Energy Demand: Nanostructure Architectures for Solar Energy Conversion*. **J. Phys. Chem. C**, 2007, *111*, 2834-2860 (Feature article).
22. Vietmeyer, F.; Seger, B. and Kamat, P. V., *Anchoring ZnO Particles on Functionalized Single Wall Carbon Nanotubes. Excited State Interactions and Charge Collection*. **Adv. Mater.**, 2007, *19*, 2935-2940.
23. Seger, B.; Vinodgopal, K. and Kamat, P. V., *Proton activity in Nafion films. Probing exchangeable protons with methylene blue*. **Langmuir**, 2007, *23*, 5471-5476.
24. Hasobe, T.; Fukuzumi, S.; Kamat, P. V. and Murata, H., *Porphyrin based molecular architectures for light energy conversion*. **Mol. Cryst. Liq. Cryst.**, 2007, *471*, 39-51 (review article).
25. Robel, I.; Kuno, M. and Kamat, P. V., *Size-Dependent Electron Injection from Excited CdSe Quantum Dots into TiO₂ Nanoparticles*. **J. Am. Chem. Soc.**, 2007, *129*, 4136-4137.
26. Jebb, M.; Sudeep, P. K.; Pramod, P.; Thomas, K. G. and Kamat, P. V., *Ru(II)trisbipyridine Functionalized Gold Nanorods. Morphological Changes and Excited-State Interactions*. **J. Phys. Chem. B**, 2007, *111*, 6839-6844.
27. Kongkanand, A. and Kamat, P. V., *Interactions of Single Wall Carbon Nanotubes with Methyl Viologen Radicals. Quantitative Estimation of Stored Electrons*. **J. Phys. Chem. C**, 2007, *111*, 9012-9015.
28. Kongkanand, A. and Kamat, P. V., *Electron Storage in Single Wall Carbon Nanotubes. Fermi Level Equilibration in Semiconductor-SWCNT Suspensions*. **ACS Nano**, 2007, *1*, 13-21.

29. Hasobe, T. and Kamat, P. V., *Photoelectrochemistry of stacked cup carbon nanotube films. Tube-Length dependence and charge transfer with excited porphyrin*. **J. Phys. Chem. C**, 2007, *111*, 16626-16634.
30. Xu, T.; Kamat, P. V.; Joshi, S.; Mebe, A. M.; Cai, Y. and O'Shea, K. E., *Hydroxyl Radical Mediated Degradation of Phenylarsonic Acid*. **J. Phys. Chem. A**, 2007, *111*, 7819-7824.
31. Hasobe, T.; Fukuzumi, S.; Kamat, P. V. and Murata, H., *Fullerene-Based Supramolecular Nanoclusters with poly[2-methoxy-5-(2'-ethylhexyloxy)-p-phenylenevinylene] (MEH-PPV) for Light Energy Conversion*. **Jap. J. Appl. Phys.**, 2008, *47*, 1223-1229.
32. Takechi, K.; Kamat, P. V.; Avira, R. R.; Jyothi, K. and Ramaih, D., *Harvesting Infrared Photons with Croconate Dyes*. **Chem. Mater.**, 2008, *20*, 265-272.
33. Wan, J.; Ferreira, A.; Xia, W.; Chow, C. H.; Takechi, K.; Kamat, P. V.; Guilford Jones, I. and Vullev, V. I., *Solvent Dependence of the Charge-Transfer Properties of a Quaterthiophene-Anthraquinone Dyad*. **J. Photochem. A**, 2008, In Press.
34. Kongkanand, A.; Tvrdy, K.; Takechi, K.; Kuno, M. K. and Kamat, P. V., *Quantum Dot Solar Cells. Tuning Photoresponse through Size and Shape Control of CdSe-TiO₂ Architecture*. **J. Am. Chem. Soc.**, 2008, *130*, 4007-4015.
35. Brown, P. R.; Takechi, K. and Kamat, P. V., *Single-Walled Carbon Nanotube Scaffolds for Dye-Sensitized Solar Cells*. **J. Phys. Chem. C**, 2008, *112*, 4776-4782.
36. Muszynski, R.; Seger, B. and Kamat, P., *Decorating Graphene Sheets with Gold Nanoparticles*. **J. Phys. Chem. C**, 2008, *112*, 5263-5266.
37. Brown, P. and Kamat, P. V., *Quantum Dot Solar Cells. Electrophoretic Deposition of CdSe-C₆₀ Composite Films and Capture of Photogenerated Electrons with nC₆₀ Cluster Shell*. **J. Am. Chem. Soc.**, 2008, *130*, submitted.

VERTICALLY ORIENTED TiO₂ AND TERNARY NANOTUBE ARRAYS AND THEIR USE IN WATER PHOTOELECTROLYSIS

Craig A. Grimes

The Pennsylvania State University
University Park, PA 16802

Building upon our work in the development and water photoelectrolysis application of vertically oriented TiO₂ nanotube arrays, over the past two years we have investigated means to control the bandgap response of the nanotube arrays to enhance their visible spectrum properties, while maintaining their excellent charge transfer behavior, by in-situ doping of the titania during synthesis through cation incorporation from the anodization electrolyte. Further, we have extended our nanotube array architecture, an architecture that appears ideal for water photoelectrolysis, to n and p-type ternary oxides for fabrication of photocorrosion stable, visible light responding photoelectrochemical diodes [1].

It is well established that the TiO₂ nanotube array properties are dependent upon their specific architecture, including nanotube array length, wall thickness, pore diameter, and tube-to-tube spacing. Under program auspices we have determined fabrication routes by which self-aligned highly-ordered nanotube arrays up to 1 mm in length could be achieved by potentiostatic anodization of Ti foil. Depending upon the anodization voltage the inner pore diameters of the resulting nanotube arrays can be controlled from 10 nm to 150 nm. Nanotube-array samples $\approx 20 \mu\text{m}$ long, 550°C annealed, show IPCE values of 80% between 320 nm to 380 nm.

In 2007 we reported the synthesis, characterization and application to water photoelectrolysis of ternary Ti-Fe-O nanotube arrays [1]. The underlying premise of the work is to combine the light absorbing properties of hematite (2.2 eV bandgap) with the outstanding charge transfer properties of TiO₂ in the nanotube array architecture. Since the minority carrier diffusion length in iron oxide is small, $\approx 4 \text{ nm}$, critical to achieving high photoconversion efficiencies in the Fe-Ti-O nanotubes was the premise that we needed to, and could, control the wall thickness down to a comparable length scale, as we have been able to do in TiO₂. However for the work reported in [1] we were initially unable to control the wall thickness, in all cases achieving a wall thickness of approximately 22 nm. Starting from thin films of variable Fe:Ti content, made by sputter co-deposition onto FTO coated glass substrates, Fe-Ti-O nanotube arrays were synthesized using an ethylene glycol electrolyte and then characterized. Although the films were poorly crystallized, with a maximum length of $\approx 1 \mu\text{m}$, and had wall thicknesses of $\approx 23 \text{ nm}$ we still obtained over 2.0 mA/cm^2 under AM 1.5 illumination (second best photocurrent value ever reported from an iron oxide system). We now have determined how to control wall thickness, as well as optimize crystallization, hence we plan to return to the Fe-Ti-O work once films of suitable thickness can be achieved.

Building upon our initial ternary oxide efforts, we have fabricated vertically oriented p-type Cu-Ti-O nanotube array films by anodization of copper rich (60% to 74%) - Ti metal films, and n-type Cu-Ti-O nanotube array films by anodization of copper poor (24% to 11%) metal films, co-sputtered onto fluorine doped tin oxide (FTO) coated glass [2]. p-type Cu-Ti-O nanotube array films $1 \mu\text{m}$ thick exhibit external quantum efficiencies up to 11%, with a spectral photoresponse indicating that the complete visible spectrum, 380 nm to 950 nm, contributes significantly to the photocurrent generation. Water-splitting photoelectrochemical pn-junction

diodes have been fabricated using p-type Cu-Ti-O nanotube array films in combination with n-type TiO₂ nanotube array films [2]. With the glass substrates oriented back-to-back, light is incident upon the UV absorbing n-TiO₂ side, with the visible light passing to the p-Cu-Ti-O side. Photocatalytic reactions are powered only by the incident light to generate fuel with oxygen evolved from the n-TiO₂ side of the diode and hydrogen from the p-Cu-Ti-O side.

Figure 1 presents a schematic illustration of the n-TiO₂:p-Cu-Ti-O photoelectrochemical diode, with light incident upon the TiO₂ film. The photoresponse of a n-TiO₂:p-Cu-Ti-O coupled system, see **Figure 1**, under global AM 1.5 illumination is shown in **Figure 2**. The n-TiO₂ nanotube array film was made by sputtering a Ti film upon a FTO coated glass substrate, then performing an anodization to achieve a titania nanotube array structure approximately 600 nm long, 30 nm pore size, with wall thickness of about 7 nm; the initially amorphous sample was oxygen annealed at 450°C for one hour for crystallization. The p-Cu-Ti-O sample is that resulting from anodization of a 74:26 Cu-Ti metal film, 550°C vacuum annealed for 1 hr, nanotube array length 1 μm, pore size ≈ 65 nm, wall thickness ≈ 35 nm. The films, atop FTO coated glass substrates, were mounted by use of epoxy into a glass sheet that allowed separate collection of the evolved gases. The TiO₂ nanotube array side of the diode was kept in 1M KOH, and the Cu-Ti-O side kept in 0.1M Na₂HPO₄ with a salt bridge linking the two sides. The AM 1.5 illumination was incident upon the TiO₂ side of the diode, which absorbs UV while passing visible light to the Cu-Ti-O side, thus minimizing any UV-assisted photocorrosion of the low bandgap material. A photocurrent density of approximately 0.25 mA/cm² is achieved. The photoconversion efficiency, calculated using $(1.23 * I)/0.1$, where I is the photocurrent density in A/cm² and 0.1 W/cm² is the power density of the incident light (1 sun), is 0.30%. Measured over a four-hour test the hydrogen generation rate of a 1 cm² sample under AM 1.5 0.1 W/cm², is ≈ 92 μL/hr, or 0.92 L/hr for a 1 m² sample.

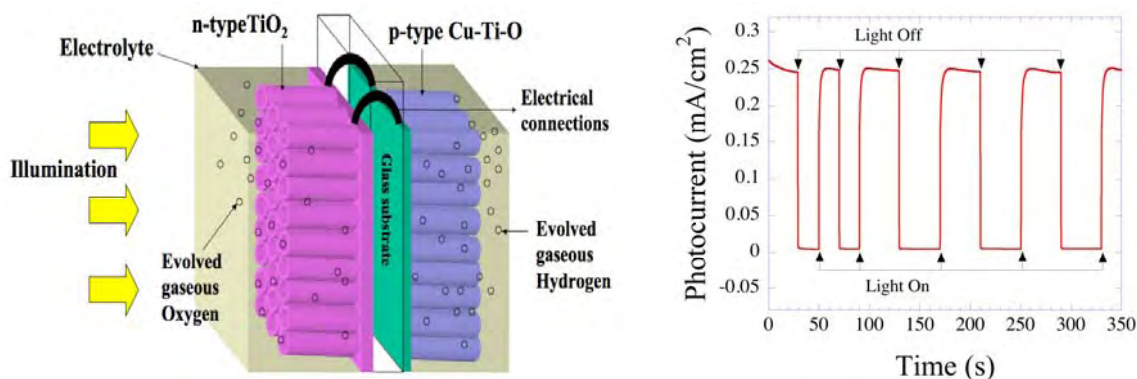


Fig. 1 Illustration of photoelectrochemical diode for water splitting comprised of n-type TiO₂ and p-type Cu-Ti-O nanotube array films, with their substrates connected through an ohmic contact. The oxygen evolving TiO₂ side of the diode absorbs UV light, passing the visible light to the hydrogen evolving Cu-Ti-O side.

Fig. 2 Photocurrent from self-biased photochemical diode of **Fig. 1**. The n-TiO₂ side is kept immersed in a 1M KOH aqueous solution, the p-Cu-Ti-O side is kept in 0.1M Na₂HPO₄ with a salt bridge linking the two solutions.

[1] G. K. Mor, H. E. Prakasham, O. K. Varghese, K. Shankar, C. A. Grimes, Vertically Oriented Ti-Fe-O Nanotube Array Films: Towards a Useful Material Architecture for Solar Spectrum Water Photolysis. *Nano Letters* 7 (2007) 2356-2364.

[2] G. K. Mor, O. K. Varghese, R. H.T. Wilke, S. Sharma, K. Shankar, T. J. Latempa, K.-S. Choi, C. A. Grimes. p-Type Cu-Ti-O Nanotube Arrays and their use in Self-Biased Heterojunction Photoelectrochemical

DOE Sponsored Publications 2006-2008

- [1] C. A. Grimes, O. K. Varghese, and S. Ranjan, *Light, Water, Hydrogen: The Solar Production of Hydrogen by Water Photoelectrolysis*. Springer, Norwell, MA. 1st. Ed. November 2007. ISBN 978-0-387-33198-0. e-ISBN 978-0-387-6828-9
- [2] M. Paulose, K. Shankar, S. Yoriya, H. E. Prakasam, O. K. Varghese, G. K. Mor, T. A. Latempa, A. Fitzgerald, C. A. Grimes. Anodic Growth of Highly-ordered TiO₂ Nanotube Arrays to 134 μm in Length. *J. Physical Chemistry B* 110 (2006) 16179-16184.
- [3] K. Shankar, G. K. Mor, H. E. Prakasam, S. Yoriya, M. Paulose, O. K. Varghese, C. A. Grimes, Highly-ordered TiO₂ Nanotube-arrays up to 220 μm in Length: Use in Water Photoelectrolysis and Dye-sensitized Solar Cells. *Nanotechnology* 18 (6): Art. No. 065707 FEB 14 2007 (11pp).
- [4] K. Shankar, G. K. Mor, A. Fitzgerald, C. A. Grimes, Cation Effect on the Electrochemical Formation of Very High Aspect Ratio TiO₂ Nanotubes In Formamide-Water Mixtures. *J. Physical Chemistry C* 111 (2007) 21-26.
- [5] K. Shankar, K. C. Tep, G. K. Mor, C. A. Grimes, An Electrochemical Strategy To Incorporate Nitrogen in Nanostructured TiO₂ Thin Films: Modification of Bandgap and Photoelectrochemical Properties. *Journal of Physics D* 39 (2006) 2361-2366.
- [6] G. K. Mor, O. K. Varghese, M. Paulose, K. Shankar, C. A. Grimes, A Review on Highly-ordered TiO₂ Nanotube-Arrays: Fabrication, Material Properties, and Solar Energy Applications, *Solar Energy Materials and Solar Cells* 90 (2006) 2011 – 2075
- [7] D. M. Grimes, C. A. Grimes, A Unique Electromagnetic Photon Field Using Feynman's Electron Characteristics and Maxwell's Equations. *Journal of Computational and Theoretical Nanoscience* 3 (2006) 649-663.
- [8] K. G. Ong, O. K. Varghese, G. K. Mor, K. Shankar, C. A. Grimes, Application of Finite Difference Time Domain to Dye-Sensitized Solar Cells: The Effect of Nanotube-array Negative Electrode Dimensions on Light Absorption. *Solar Energy Materials & Solar Cells* 91 (2007) 250-257
- [9] C. A. Grimes, Synthesis and Application of Highly-ordered Arrays of TiO₂ Nanotubes, Invited Highlight Article, *J. Materials Chemistry* 17 (2007) 1451-1457.
- [10] H. E. Prakasam, K. Shankar, M. Paulose, O. K. Varghese, C. A. Grimes, A New Benchmark for TiO₂ Nanotube Array Growth by Anodization, *J. Physical Chemistry C* 111 (2007) 7235-7241.
- [11] M. Paulose, H. E. Prakasam, O. K. Varghese, L. Peng, K. C. Popat, G. K. Mor, T. A. Desai, C. A. Grimes. TiO₂ Nanotube Arrays of 1000 μm in Length by Anodization of Titanium Foil: Phenol Red Diffusion. *J. Physical Chemistry C* 111 (2007) 14992-14997.
- [12] N. K. Allam, C. A. Grimes, Formation of Vertically Oriented TiO₂ Nanotube Arrays Using a Fluoride Free HCl Aqueous Electrolyte. *J. Physical Chemistry C* 111 (2007) 13028-13032.
- [13] S. Yoriya, M. Paulose, O. K. Varghese, G. K. Mor, C. A. Grimes, Fabrication of Vertically Oriented TiO₂ Nanotube Arrays Using Dimethyl Sulfoxide Electrolytes. *J. Physical Chemistry C* 111 (2007) 13770-13776.
- [14] L. Yang, D. He, Q. Cai, C. A. Grimes, Fabrication and Catalytic Properties of Co-Ag-Pt Nanoparticle-

Decorated Titania Nanotube Arrays. *J. Physical Chemistry C* 111 (2007) 8214-8217.

- [15] G. K. Mor, H. E Prakasam, O. K Varghese, K. Shankar, C. A. Grimes, Vertically Oriented Ti-Fe-O Nanotube Array Films: Towards a Useful Material Architecture for Solar Spectrum Water Photolysis. *Nano Letters* 7 (2007) 2356-2364.
- [16] O. K. Varghese, C. A. Grimes, Appropriate Strategies For Determining The Photoconversion Efficiency Of Water Photoelectrolysis Cells: A Review With Examples Using Titania Nanotube Array Photoanodes. *Solar Energy Materials and Solar Cells* 92 (2008) 374-384.
- [17] N. K. Allam, K. Shankar, C. A. Grimes, Photoelectrochemical and Water Photoelectrolysis Properties of Ordered TiO₂ Nanotubes Fabricated by Ti Anodization in Fluoride-free HCl Electrolytes. *Journal of Materials Chemistry* 2008. DOI: 10.1039/b718580d

In Review

- [18] S. Yoriya, G. K. Mor, S. Sharma, C. A. Grimes, Synthesis of Ordered Arrays of Discrete, Fully Separated, Partially Crystalline Titania Nanotubes by Ti Anodization Using Diethylene Glycol Electrolytes. Submitted to *J. Materials Chemistry*. 2/12/08
- [19] G. K. Mor, O. K. Varghese, R. H.T. Wilke, S. Sharma, K. Shankar, T. J. Latempa, K.-S. Choi, C. A. Grimes. p-Type Cu-Ti-O Nanotube Arrays and their use in Self-Biased Heterojunction Photoelectrochemical Diodes for Hydrogen Generation. Submitted to *Nano Letters*. 2/24/08
- [20] K. Shankar, J. Bandara, M. Paulose, Helga Wietasch, O. K. Varghese, G. K. Mor, T. J. LaTempa, M. Thelakkat and C. A. Grimes. Highly Efficient Solar Cells using TiO₂ Nanotube Arrays Sensitized with a Donor-Antenna Dye. *Nano Letters*
- [21] G. K. Mor, O. K. Varghese, R. H.T. Wilke, S. Sharma, K. Shankar, T. J. Latempa, K.-S. Choi, C. A. Grimes. p-Type Cu-Ti-O Nanotube Arrays and their use in Self-Biased Heterojunction Photoelectrochemical Diodes for Hydrogen Generation. *Nano Letters*
- [22] N. K. Allam, K. Shankar, C. A. Grimes, A General Method for the Anodic Formation of Crystalline Metal Oxide Nanotube Arrays Without the use of Thermal Annealing. Submitted to *Advanced Materials*.
- [23] N. K. Allam, X. J. Feng, C. A. Grimes, Self-assembled Fabrication of Vertically Oriented Ta₂O₅ Nanotube Arrays, and Membranes Thereof, by One-step Tantalum Anodization. Submitted to *Nano Letters* 3/31/08.

Invited Talks Citing DoE Support

- [24] C. A. Grimes, Invited Talk: Vertically-aligned Highly-ordered TiFeO_x Nanotube Arrays with Enhanced Visible Spectrum Photo-electrochemical Properties. SPIE Optics and Photonics, San Diego, August 29, 2007.
- [25] C. A. Grimes, Invited Talk: Synthesis and Five (5) Applications of Highly Ordered Arrays of TiO₂ Nanotubes. Elite Network of Bavaria (ENB) on Macromolecular Systems For Nanoscience - Chemistry, Physics, And Engineering Aspects. September, 6th - 9th 2007 in Irsee, Germany

PHOTOACTIVE INORGANIC MEMBRANES FOR CHARGE TRANSPORT

Prabir Dutta, Henk Verweij, Bern Kohler

The Ohio State University
100 West 18th Avenue, Columbus, Ohio 43210

The objective of this program is to develop integrated photochemical molecular assemblies for conversion of solar to chemical energy. The architecture involves assembly of the supramolecular system onto a zeolite membrane and to photochemically transport charge across the membrane.

I. Zeolite Membrane Development :

We have developed and reported optimized methods for growth of zeolite A and Y membranes. Current focus is on growth of oriented zeolite L membranes. Partially oriented zeolite L membranes were grown from disk-shaped zeolite L crystals to 2-7 micron thick membranes. We are examining the strategy shown in Figure 1 for complete orientation. Flat-disk zeolite L crystallites were oriented onto the surface of a thin silica layer deposited on top of an optically smooth porous alumina support. A mesoporous silica layer (200-400 nm) thick was dip-coated onto macroporous alumina supports, followed by modification of the silica surface with a silane coupling agent, 3-chloropropyltrimethoxysilane. The bi-functionality of this coupling agent was utilized to covalently link zeolite L to the support surface, thus creating an oriented zeolite L seed layer.

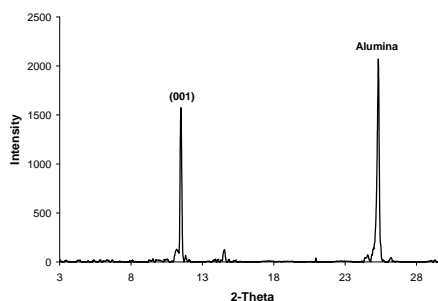
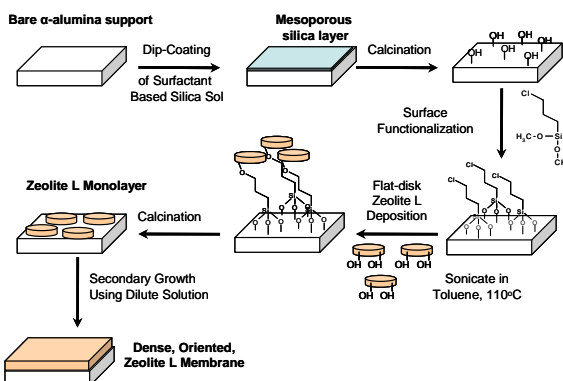
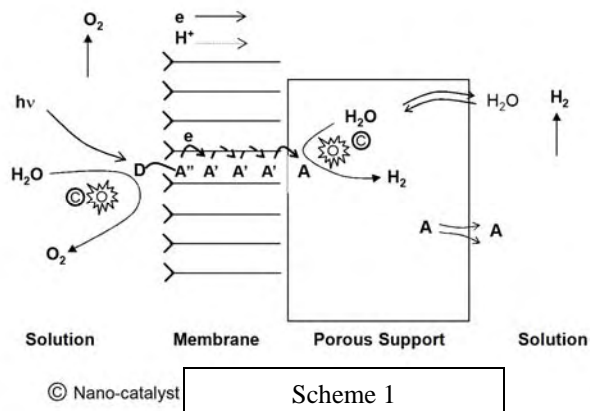
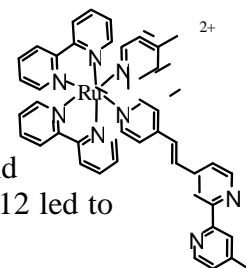


Figure 1. Left: Schematic of growing oriented zeolite L membranes. Right: XRD of seed layer deposition

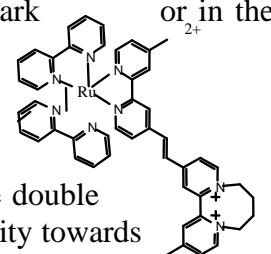
II. Photosensitizer Development

Two ruthenium polypyridyl compounds of structural formula $[(bpy)_2RuL]^{2+}$ and $[(bpy)_2RuL_{DQ}]^{4+}$ (where bpy = bipyridine, L = 1, 2-bis[4-(4'-methyl)-2,2'-bipyridyl] ethene, L_{DQ} = 1-[4-(4'-methyl)-2,2'-bipyridyl]-2-[4-(4'-N,N'-tetramethylene-2,2'-bipyridinium)] ethene) have been synthesized and characterized. Photolysis of $[(bpy)_2Ru^{(II)}L]$ complex in solutions at pH 7 and 12 led to



formation of a dimer of $[(bpy)_2Ru^{(II)}L]$. Photoreactions do not occur in the dark or in the aprotic solvent.

On the other hand, the emission intensity and lifetime of $[(bpy)_2RuL_{DQ}]^{4+}$ is strongly quenched ($> 95\%$) compared to that of the $[(bpy)_2RuL]^{2+}$ complex. This quenching is attributed to the intramolecular electron transfer from the Ru center to the diaquat (DQ) moiety across the double bond of the L_{DQ} ligand. The $[(bpy)_2RuL_{DQ}]^{4+}$ complex exhibits strong stability towards visible light due to the presence of this electron acceptor DQ. We have chosen to work with $[(bpy)_2RuL_{DQ}]^{4+}$ as the photosensitizer of choice for attaching to the zeolite membrane surface.



III. Transient Spectroscopic Studies: Transient absorption spectra for the $[(bpy)_2RuL_{DQ}]^{4+}$ photosensitizer in acetonitrile are shown in Figure 2. The rich dynamics reflect the ultrafast decay of the initial MLCT state, charge trapping on the diaquat end of the L_{DQ} ligand, and eventual charge recombination. The signals indicate that charge is efficiently transported to the L_{DQ} ligand, where it is ready to be transferred to an electron acceptor located within the zeolite framework. Electron transfer from $[(bpy)_2RuL_{DQ}]^{4+}$ anchored on the zeolite to methylviologen in the zeolite cages has been studied on nanosecond time scale by time-resolved diffuse reflectance spectroscopy. This photoreaction leads to long-lived charge separation and stabilization of the methylviologen radical in the zeolite.

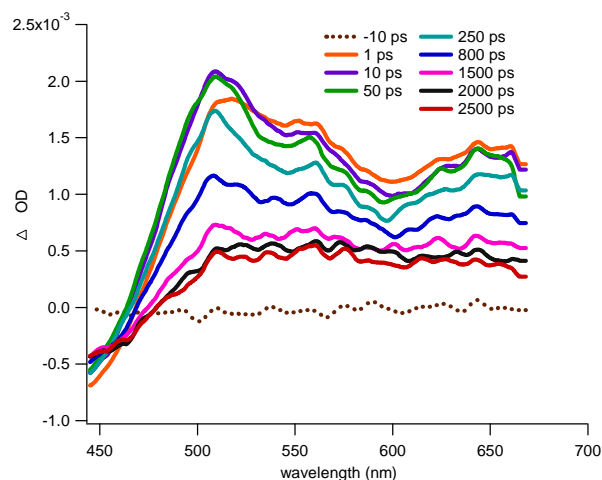


Figure 2. Broadband transient absorption of $[(bpy)_2RuLDQ]^{4+}$ excited at 400 nm with multiple transient spectra.

DOE Sponsored Publications 2006-2008

T. Kuzniatsova, Y. Kim, K. Shqau, P.K. Dutta, and H. Verweij, "Zeta-potential measurements of zeolite Y: application in homogeneous deposition of particle coatings," *Mesopor. Micropor. Mater.*, (2007), 103(1-3), 102-107.

Yanghee Kim and Prabir K. Dutta, "An Integrated Zeolite Membrane - RuO_2 Photocatalyst System for Hydrogen Production from Water" *J. Phys Chem C* (2007), 111(28), 10575-10581.

Visible-light-driven Photoreactions of $[(bpy)_2Ru(II)L]Cl_2$ in Aqueous Solutions (bpy = bipyridine, L = 1,2-bis(4-(4'-methyl)-2,2'-bipyridyl) ethene), *J. Phys Chem A*, (2008), 112(5), 808-817.

T. Kuzniatsova, Y. Kim, K. Shqau, P.K. Dutta, and H. Verweij, Synthesis of thin, oriented zeolite A membrane on macroporous support, accepted in *Advanced Functional Materials*

E. Greenbaum, Barbara Evans, Yanghee Kim and Prabir K. Dutta Mechanism of Hydrogen Production by an Artificial Photosynthetic System, submitted for publication

Jeremy White, K. Shqau, P.K. Dutta, and H. Verweij Synthesis of Randomly Oriented Zeolite L Membranes with Submicron to Micron Thicknesses, accepted in *Microporous and Mesoporous Materials*

Session V

Structures of Excited States

**TRACKING ELECTRONS AND ATOMS
IN PHOTOEXCITED MOLECULES
WITH X-RAY TRANSIENT ABSORPTION SPECTROSCOPY**

Lin X. Chen,^{a,d} Xiaoyi Zhang,^{a,b} Erik C. Wasinger,^a Jenny V. Lockard,^{a,d} Klaus Attenkofer,^b Guy Jennings,^b Ana Z. Muresan,^c Jonathan S. Lindsey^c

^aChemical Sciences and Engineering Division and ^bX-ray Science Division,
Argonne National Laboratory, Argonne, Illinois 60439, USA

^cChemistry Department, North Carolina State University, Raleigh, North Carolina 27685, USA

^dChemistry Department, Northwestern University, Evanston, Illinois, 60208, USA

Transient structural information of molecules along reaction coordinates of photochemical processes provides us insight into reaction mechanisms and the correlations of electron and nuclear movements resulting in the products in many solar energy conversion related processes. During the past decade, the laser pulse pump, X-ray pulse probe x-ray absorption spectroscopy has been developed in our lab and elsewhere. Although X-ray pulses from current synchrotron sources are much longer (i.e. ~100 ps) than fundamental chemical events (i.e. ~10-100 fs), such as bond breaking and formation, they can still be used to offer structures of thermally equilibrated transient states that were unseen before. We will present molecular structural dynamics studies of metal complexes whose ultrafast excited state dynamics and structures were investigated by femtosecond laser spectroscopy and the x-ray transient absorption spectroscopy (XTA).

Recently, we have simultaneously tracked electronic and molecular structures of a photoexcited metalloporphyrin with a 200-ps lifetime in toluene at room temperature using XTA and ultrafast optical transient absorption spectroscopy (OTA). The OTA measurements revealed an unusual stimulated emission at 630 nm with a lifetime of 0.3 - 0.4 ps in three different Ni porphyrins, only when the S_1 state was directly populated. The result suggested that the intersystem crossing from the S_2 state is much faster than the internal conversion $S_2 \rightarrow S_1$ which was considered the main decay channel for the S_2 state. Subsequent IVR and VC processes took place on in sub-ps and <20 ps respectively. The only transient excited state structure that can be captured by the 100-ps X-ray pulses from a synchrotron source (the Advanced Photon Source, or APS at Argonne) is the T_1 state with a lifetime of ~200 ps in toluene at room temperature. From the Ni K-edge XTA spectra, we were able to simultaneously track energy levels and electron occupations in molecular orbitals (MOs), as well as the molecular geometry of the excited state of NiTMP [nickel(II)tetramesitylporphyrin], in a relatively dilute toluene solution. The XTA results indicated that the excited T_1 state has *a*) an electronic configuration with singly occupied $3d_{x^2-y^2}$ and $3d_{z^2}$ MOs, *b*) an energy gap of 2.2 eV between $3d_{x^2-y^2}$ and $3d_{z^2}$ MOs, *c*) energy shifts of $3d_{x^2-y^2}$ and $4p_z$ MOs by 0.4 eV and 1.5 eV higher than those of the ground state, and *d*) an expansion of the porphyrin ring characterized by the lengthening of Ni-N and Ni-C bonds by 0.09 and 0.07 Å respectively. Moreover, XTA signals at different X-ray photon energies as functions of the delay time between the laser and the X-ray pulses were successfully collected which signifies feasibilities of acquiring the correlation and coherence between electronic configuration changes and the nuclear geometry changes, a direct visualization of Bohr-Oppenheimer approximation.

Significant transition bandwidth change in the pre-edge region at the Ni K-edge was observed, with a bandwidth of 2.3 eV for the $1s \rightarrow 3d_{x^2-y^2}$ transition in the ground state S_0 , and the 1.2 and 1.0 eV bandwidths for the $1s \rightarrow 3d_{z^2}$ and $1s \rightarrow 3d_{x^2-y^2}$ transitions respectively in the T_1 state. The broad bandwidth for the $1s \rightarrow 3d_{x^2-y^2}$ transition in the ground state is puzzling, because the potential barriers between multiple conformations are $\ll 2\text{eV}$ in solution at room temperature. Nevertheless, the bandwidth narrowing in the excited state is an indication that the potential well in the T_1 state is much narrower than that of the ground state. The XTA results for the excited state NiTMP suggest a planar geometry due to the effective expansion of the Ni(II) radius in the T_1 state. The photoinduced ligation of NiTMP was also studied showing interesting solute-solvent interactions that promoted isc.

Simultaneously tracking electronic and nuclear configurations of the excited states and reaction intermediates will have significant impacts in understanding coupling single photon event with multiple electron redox reaction mechanisms in search of efficient solar fuel generation systems.

Continuing our previous studies on the MLCT excited state of metal complexes, we have investigated the excited state structures of Pt(II) complexes as well as Pt metal nanoparticles on TiO_2 surfaces. Detailed analysis will be described briefly.

The future studies will be focused on four fronts: 1) improvement of the current XTA facility to obtain high quality data with high throughput to enable detailed structural information to be obtained for distant neighbors and multiple metal center complexes; 2) combining XTA with pump-probe S/WAS (in collaboration with David Tiede) to obtain structural information on multiple spatial scales; and 3) exploring applications with fs-ps slicing sources at the APS and ALS to resolve structures with higher time resolution; and 4) incorporating transient structural results for rationalization of photochemical mechanism and rational design of molecular systems (in collaboration with inorganic/organic/material chemists).

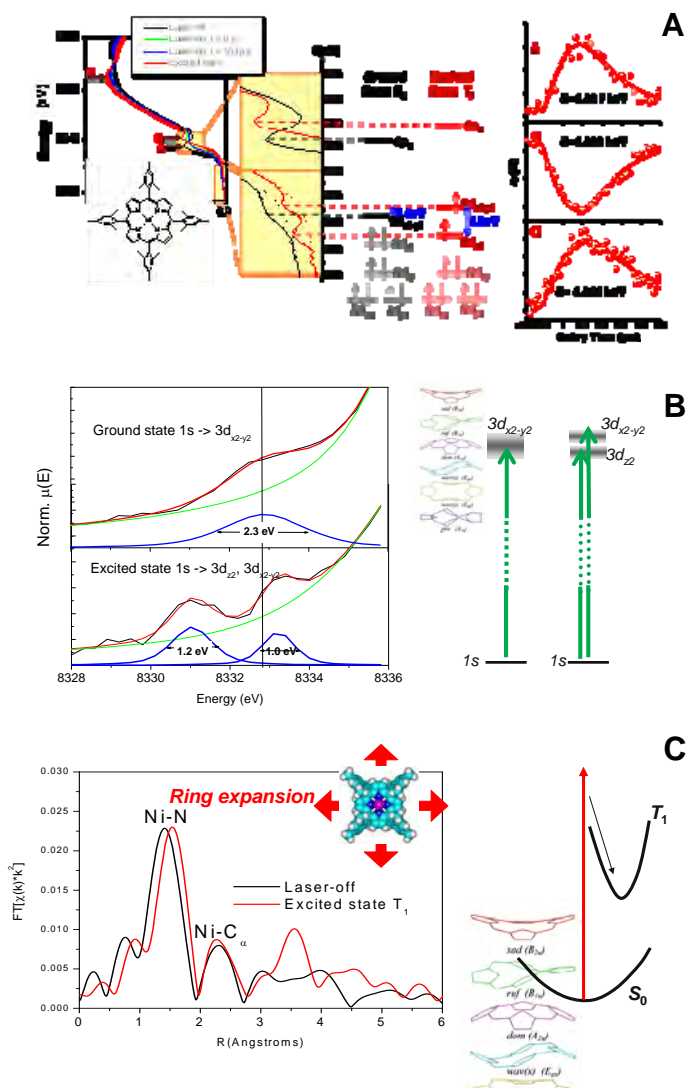


Figure 1. A. The molecular MO are mapped out for the ground and the excited state NiTMP, displayed along the kinetics curves taken at different x-ray energies as indicated; B. $1s \rightarrow 3d$ transition bandwidth change shown in the pre-edge region; and C. the porphyrin ring expansion in the excited state shown by the peak shift for the Ni-N and Ni-C distances.

Publication (2006-present):

1. XANES analysis of structural changes in a transient photoexcited state of metalloporphyrin, S. Della-Longa, L. X. Chen, P. Frank, K. Hayakawa, K. Hatada, M. Benfatto, submitted to *Inorg. Chem.* (2008)
2. Three-dimensional local structure of photoexcited Cu(I) diimine complex refined by quantitative XANES analysis, Grigory Smolentsev, Alexander V. Soldatov, Lin X. Chen, submitted to *J. Chem. Phys.*(2008).
3. Molecular Architectural Influence on Photoinduced Electron Transfer Dynamics in a Donor-Acceptor Quartet Oligomer, Lin X. Chen, Dmitrii Polshakov, Shengqiang Xiao, Yongye Liang, Jianchang Guo, Luping Yu, submitted to *J. Phys. Chem. B.* (2008).
4. Discovery of Native Metal Ion Sites Located on the Ferredoxin Docking Side of Photosystem I, Lisa M. Utschig, Lin X. Chen, Oleg G. Poluektov, *Biochemistry*, **47**, 3671-3676. (2008).
5. Selective Photocatalytic Decomposition of Nitrobenzene Using Surface Modified TiO₂ Nanoparticles, Donald Cropek, Patricia A. Kemme, Olga V. Markova, Lin X. Chen, Tijana Rajh, *J. Phys. Chem. B*, in press. (2008).
6. Aligned carbon nanotubes with built-in FeN₄ active sites for electrocatalytic reduction of oxygen, Junbing Yang, Di-Jia Liu, Nancy N. Kariuki and Lin X. Chen, *Chem. Comm.* 329-331(2008).
7. X-ray absorption spectroscopic characterization of the Compound II intermediate produced by reaction of a cytochrome P450 enzyme with peroxyxynitrite, J. Halgrimson, J. Horner, M. Newcomb, Erik C. Wasinger, Lin X, Chen, Sligar, in press *Proc. Natl. Acad. Sci. USA* (2008).
8. Pseudomonas putida CadR Selectively Recognizes Cadmium(II) Over Other Metal Ions, Hao Chen, Erik C. Wasinger, Zigang Li, Pedro Brugarolas, Lin X. Chen, and Chuan He, *submitted to J. Am. Chem. Soc.* (2008).
9. The Mechanism of the Selective Lead(II) Recognition by the PbrR691 Protein: Insights from the Spectroscopic Investigations, Peng R. Chen, Erik C. Wasinger, Jing Zhao, Daniel van der Lelie, Lin X. Chen, Chuan He, *J. Am. Chem. Soc.* **129**, 12350-12351 (2007).
10. Excited-State Relaxation Pathway and Structural Dynamics of Nickel *meso*-tetrasubstituted Porphyrins, Xiaoyi Zhang, Erik C. Wasinger, Klaus Attenkofer, Guy Jennings, Ana Z. Muresan, Jonathan S. Lindsey, Lin X. Chen, *J. Phys. Chem. A.* **111**, 11736-11742 (2007)
11. Ultrafast Structural Dynamics of Photoactive Metal Complexes in Solar Hydrogen Generation, Lin X. Chen, Dijia Liu, Erik C. Wasinger, Xiaoyi Zhang, Klaus Attenkofer, Guy Jennings, *SPIE Proceedings*, **6650**-28 (2007).

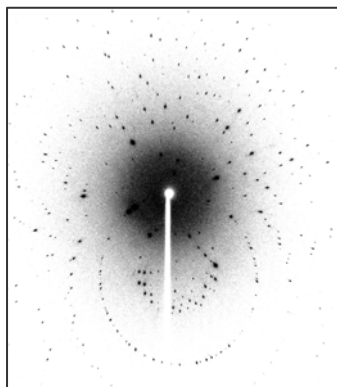
12. Photoinduced Electron Transfer in a Molecular Donor-Acceptor Quartet, Yongye Liang, Lin X. Chen, Shengqiang Xiao, Luping Yu, *Am. Chem. Soc. PMSE Preprint*, **96** 807-808 (2007).
13. Tracking Electrons and Atoms in a Photoexcited Metalloporphyrin, Lin X. Chen, Xiaoyi Zhang, Erik C. Wasinger, Klaus Attenkofer, Guy Jennings, Ana Z. Muresan, Jonathan S. Lindsey, *J. Am. Chem. Soc.* **129**, 9616-9618 (2007).
14. Novel Nanoscale Organic Materials for Optimal Photovoltaic Functions, Lin X. Chen, Dmitrii Polshakov, Shengqiang Xiao, Yongye Liang, Luping Yu, *Material Research Society Proceedings*, **974E**, CC06-11 (2007).
15. Ultrafast Structural Rearrangements in the MLCT Excited State for Copper(I) *bis*-Phenanthrolines in Solution, George B. Shaw, Christian D. Grant, Hideaki Shirota, Edward W. Castner Jr., Gerald J. Meyer, Lin X. Chen, *J. Am. Chem. Soc.* **129**, 2147-2160 (2007).
16. Molecular Structural Dynamics of Photoactive Transition Metal Complexes in Solar Energy Conversion Studied by Ultrafast Optical Spectroscopy and LITR-XAS, L. X. Chen, G. B. Shaw, E. C. Wasinger, X. Zhang, K. Attenkofer, Guy Jennings, *AIP Conference Proceedings*, **882**, 844-848 (2007).
17. Charge Separation and Surface Reconstruction: A Mn²⁺ Doping Study, Zoran V. Saponjic, Nada M. Dimitrijevic, Oleg Poluektov, Lin X. Chen, Eric Wasinger, Ulrich Welp, David Tiede, Xiaobing Zuo and Tijana Rajh, *J. Phys. Chem. B*, **110** (50), 25441-25450 (2006).
18. Dynamics of Photoinduced Electron Transfer in a Molecular Donor-Acceptor Quartet, Lin X. Chen, Shenqiang Xiao and Luping Yu, *J. Phys. Chem. B* **110**, 11730-11738 (2006).
19. The Influence of Bridging Ligand Electronic Structure on the Photophysical Properties of Noble Metal Diimine and Triimine Light Harvesting Systems, Xian-yong Wang, Andre del Guerzo, Sujoy Baitalik, Gerald Simon, George B. Shaw, Lin X. Chen, Russell Schmehl, *Photosynthetic Research* **87** 83-103(2006).

VISUALIZING GEOMETRY CHANGES ON PHOTOEXCITATION: FROM MICROSECOND TO PICOSECOND TIME RESOLUTION

Philip Coppens, Milan Gembicky, Mateusz Pitak, Shao-Liang Zheng, Marc Messerschmidt,
Chemistry Department, University at Buffalo, State University of New York, Buffalo, NY14260-3000.

The aim of the project is to extend the X-ray diffraction method beyond ground-state structure determination to the investigation of short-lived species such as occur in photo-excitation and photochemical reactions. The work will contribute to our understanding of the nature of photo-induced molecular excited states and elucidate geometry changes occurring on electron transfer within molecules, from transition metal atoms to coordinated ligands and to other molecules incorporated in the crystalline phase. In the first stage of the project a stroboscopic technique was developed in which $<100\ \mu\text{m}$ crystals are excited with a series of short laser pulses and after each pulse probed with synchronized X-ray flashes. The frequency of the pump-probe cycles ranges from 5000-25000 times per second. We have applied the technique to a series of molecules, including a photosensitizer dye, binuclear Pt and Rh metalloorganic complexes, a trinuclear Cu pyrazolate, and to molecules embedded in inert supramolecular, but fully crystalline, frameworks. The monochromatic methods are flux-limited and require a large number of pump-probe cycles to accumulate a sufficient number of counts in the detector. The large number of laser pulses needed in the stroboscopic experiment shortens the lifetime of the crystalline samples and requires frequent remounting of fresh crystals.

As many photochemical processes relevant for solar-energy capture occur on timescales faster than those of the above experiments, we are focusing our attention on development of methods for sub-microsecond diffraction. The monochromatic method limits the time-resolution that can be achieved, as an X-ray pulse-train rather than a single or very small number of synchrotron pulses is needed to ensure sufficient X-ray exposure in each of the pump-probe cycles. This

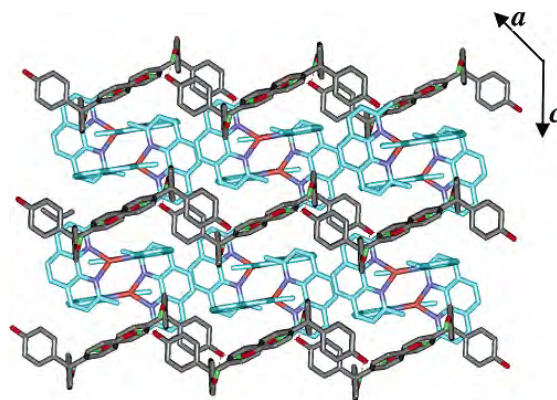


requires use of the broad-bandwidth Laue technique, in which a much larger percentage of the incident synchrotron photons is exploited, corresponding to several orders of magnitude increase in productive flux. The intensity gain achieved in the polychromatic experiment allows recording of a diffraction pattern with a single 100ps-long pulse of the synchrotron source, opening the way the mentoring of fast processes, limited only by the width of the synchrotron and laser pulses. A frame of reflections collected with a single pulse at the 14-ID beamline at APS is shown at left. A second consideration is that in ultrafast experiments a large number of reflections must be measured simultaneously which is only possible with the Laue technique.

A particular complication of the Laue method is that different reflections are recorded at different wavelengths. For a structure determination this means that the spectrum and wavelength-dependent effects such as absorption in the sample must be determined. This introduces errors, which are not serious in a standard structure determination, but considerably limit the accuracy of the measurement of rapid intensity changes intensity on light exposure. To

circumvent this problem we have developed a direct method, based on the observation that the relative intensity changes on exposure are independent of the X-ray wavelength. In the direct method the intensity change due to the laser beam for each reflection is directly derived from the raw intensities of the reflection on each pair light-on/light-off frames without wavelength scaling. A monochromatic reference structure is then used to calculate the $I(\text{on})$ reflection intensities.

In the first experiments at the newly instrumented 15-ID beamline at the Advanced Photon Source we have studied the photosensitized dye Cu(I)-dimethylphenanthroline $[\text{Cu}(\text{dmp})_2]^+$ embedded in a supramolecular solid (Fig. 2). The anionic layers between which the molecules are embedded are composed of strongly hydrogen-bonded, photochemically-inert, tri-hydroxyphenylethane molecules, which provide a strong framework, so that any molecular change does not destroy the crystal's integrity. The solid is one of a series of 8 containing supramolecular frameworks in which we have been able to embed the $[\text{Cu}(\text{dmp})_2]^+$ anion. A conventional salt of the complex was previously studied by monochromatic time-resolved methods. In the recent measurements four sets of data on the same complex were collected in order to check reproducibility of the measured changes. Results are currently being analyzed.



Acknowledgments: We are grateful to Dr. Phil Anfinrud of NIH and Profs. Shin-Ichi Adachi and Shin-Ya Koshihara (Tokyo Institute of Technology) for expert advice and help at the 14-ID beamline at the Advanced Photon Source and the NW14 station at the Advanced Ring at KEK respectively.

DOE Sponsored Publications 2006-2008

1. Supramolecular Solids and Time-Resolved Diffraction, P. Coppens, S.-L. Zheng, M. Gembicky, M. Messerschmidt and P. Dominiak, *CrystEngComm.*, **8**, 735-741 (2006),
2. The Effect of the Environment on Molecular Properties: Synthesis, Structure, and Photoluminescence of Cu(I) Bis(2,9-dimethyl-1,10-phenanthroline) Nano-Clusters in Eight Different Supramolecular Frameworks, S.-L. Zheng, M. Gembicky, M. Messerschmidt, P. Dominiak, and P. Coppens, *Inorg. Chem.*, **45**, 9281-9289 (2006).
3. On the Design of Ultrafast Shutters for Time-Resolved Synchrotron Experiments, M. Gembicky and P. Coppens, *J. Synch. Rad.*, **14**, 133-137 (2006).
4. Static and Time-resolved Photocrystallographic Studies in Supramolecular Solids, P. Coppens, S.-L. Zheng and M. Gembicky, *Zeitschr. für Kristallografie*, In Press (2008).

Session VI

Heterogeneous Systems for Solar Photoconversion II

ELECTRON TRANSFER DYNAMICS IN EFFICIENT MOLECULAR SOLAR CELLS

Aaron Staniscewski, Amanda Morris, and Gerald J. Meyer
Departments of Chemistry and Materials Science and Engineering
Johns Hopkins University Baltimore, MD 21210

A key objective of our Department of Energy supported research is to provide kinetic models for surface mediated photochemical processes relevant to solar energy conversion. Our emphasis has been on photo-induced interfacial electron transfer reactions from metal-to-ligand charge-transfer (MLCT) excited states and (more recently) porphyrinic singlet excited states anchored to mesoporous nanocrystalline (anatase) TiO₂ thin films. In recent work we have quantified mechanistic aspects of intermolecular energy and electron transfer, interfacial electron transfer, and iodine redox chemistry. Below we summarize key findings from our DOE supported research and conclude with a list of publications.

1. Lateral Energy and Charge Transfer at Sensitized TiO₂ Interfaces. Some time ago we found that long-lived MLCT excited states could be observed for Ru(II) and Os(II) compounds anchored to TiO₂ thin films that were immersed in organic solvents that did not contain ‘potential determining’ cations such as H⁺ or Li⁺. The excited states were found to undergo efficient energy transfer across the nanocrystalline TiO₂ surface. Recent Monte-Carlo simulations indicated a (30 ns)⁻¹ rate constant for intermolecular energy transfer at saturation surface coverage. This rate constant was consistent with the experimental finding that compounds with short ($\tau < 50$ ns) lifetimes decayed by a first-order kinetic pathway where longer lived excited states showed evidence for second-order annihilation reactions. Rapid energy migration could be utilized to sensitize specific sites on the semiconductor surface.

In related studies we have quantified lateral intermolecular charge transfer reactions across nanocrystalline TiO₂ surfaces. Two distinct mechanisms for such charge transfer reactions have now been identified, both of which can be driven with an applied potential and can result in complete oxidation or reduction of all the redox-active molecules on the semiconductor surface. The first mechanism, which has been known for some time, occurs by electron (hole) transfer from the conductive substrate (usually fluorine doped tin oxide) to molecules directly linked to it. Lateral electron (hole) hopping can result in complete reduction (oxidation) of all molecules within the film provided that a percolation pathway exists. We recently identified a second mechanism wherein the TiO₂ conduction band mediates the molecular redox reactions. There was no evidence for a percolation threshold and the apparent diffusion constants were about an order of magnitude larger than those previously reported. Furthermore, the observed rates for reduction were significantly different than that for oxidation. This rectifying behavior was understood based on a Gerischer-type model previously proposed for single crystal TiO₂ (rutile) electrodes. Molecular control of lateral electron transfer reactions represents an important step toward photo-driven multi-electron transfer catalysis.

A critical issue relevant to lateral energy and charge transfer reactions is the energetic position of the TiO₂ acceptor states. Ideally one would like to control and fix these energy level(s) and functionalization of the semiconductor surface with passivating molecules has been a common approach. Surface reactions with long chain hydrocarbons

that contain silane, carboxylic acid, or phosphonate groups were quantified in our laboratories by attenuated total reflection infrared spectroscopy (ATR-FTIR). The density of unfilled TiO₂ states (DOS) were probed by spectroelectrochemical, reactivity, and sensitized injection yield measurements. In almost all cases, surface functionalization was found to shift the DOS positive on an electrochemical scale (away from the vacuum level) in 0.1 M tetrabutylammonium ion containing acetonitrile electrolyte. The magnitude of the effect was found to be dependent on the surface coverage. However, in the presence of lithium cations, the onset of acceptor states was not significantly changed by any of the surface reactions investigated. The excited state injection yield after pulsed light excitation of Ru(dcb)(bpy)₂(PF₆), where dcb is 4,4'-(COOH₂)-2,2'-bpy, was 0.89 ± 0.09 for all the surface functionalized materials. Surface functionalization enhanced the open circuit photovoltage in regenerative solar cells with 0.5 M LiI/0.05 M I₂ in a manner similar to our previous reports with tripodal sensitizers.

2. Ultrafast Structural Change in Copper Diimine Compounds. In an ongoing collaboration with Professor Lin Chen, the structural changes associated with MLCT excitation of Cu^I(dmp)₂⁺ and Cu(dpp)₂⁺ (dmp = 2,9-dimethyl-1,10-phenanthroline and dpp = 2,9-dimethyl-1,10-phenanthroline) have been quantified by time resolved spectroscopies. Recent studies identified the structural origins of the observed transient spectroscopic features observed after MLCT excitation which formally generates a Cu(II) (3d⁹) state in equilibrium ground state Cu(I) (3d¹⁰) geometry. The Cu(I) ground state maintains a tetrahedral geometry while the thermally equilibrated Cu(II) MLCT state is flattened. Significantly, the singlet excited state lifetime of Cu(dmp)₂⁺* in acetonitrile was measured to be 66 fs. Rapid excited state deactivation was attributed to internal conversion and intersystem crossing at the Franck-Condon state geometry. The differentiation between this prompt fluorescence lifetime of the tetrahedral Franck-Condon geometry and the longer lived flattened geometry strongly suggest an ultrafast flattening process after light excitation of Cu^I(dmp)₂⁺.

3. Macrocyclic Pigments for Solar Energy Conversion. In collaboration with Professor Lindsey, Holten and Bocian the efficiencies of solar cells that incorporate light-harvesting arrays of organic pigments were calculated under 1 sun of air mass 1.5 solar irradiation. In one set of calculations, photocurrent efficiencies were evaluated for porphyrin, phthalocyanine, chlorin, bacteriochlorin and porphyrin-bis(perylene) pigments arrays of different length and packing densities under the assumption that each solar photon absorbed by the pigments was quantitatively converted to an electron in the external circuit. In another more realistic set of calculations, solar conversion efficiencies were evaluated units taking into account competitive excited-state relaxation pathways.

In regenerative dye sensitized solar cells, iodide was found to have a significant influence on the Zn(II)porphyrin excited state and energy conversion efficiencies. Strong evidence for iodide, as well as chloride and bromide, coordination to a several metalloporphyrins was found in absorption and photocurrent action spectra measured at different halide concentrations. The equilibrium constant for the axial ligation of halide ions to 5-(3,5-dicarboxyphenyl)-10,15,20-tri-p-tolylporphyrinatozinc(II) in propylene carbonate and attached to TiO₂ were quantified in comparative studies. These findings have implications for improving the light harvesting efficiency of dye-sensitized solar cells that employ porphyrin based chromophores. The studies also present fundamental studies of metal-ligand coordination equilibrium at semiconductor interfaces.

DOE PUBLICATIONS (2006-present)

- 1. Intermolecular Energy Transfer Across Nanocrystalline Semiconductor Surfaces.** Higgins, G.T.; Bergeron, B.V.; Hasselmann, G.M.; Farzad, F.; Meyer, G.J. *J. Phys. Chem. B* **2006**, *110*, 2598-2605.
- 2. Static and Dynamic Quenching of Ru(II) Polypyridyl Excited States by Iodide.** Marton, A.; Clark, C.C.; Srinivasan, R.; Freundlich, R.E.; Narducci Sarjeant, A.A.; Meyer, G.J. *Inorg. Chem.* **2006**, *45*, 362-369.
- 3. Tri-iodide Quenching of Ruthenium MLCT Excited State in Solution and on TiO₂ Surfaces: An Alternate Pathway for Charge Recombination.** Clark, C.C.; Marton, A.; Srinivasan, R.; Narducci Sarjeant, A.A.; Meyer, G.J. *Inorg. Chem.* **2006**, *45*, 4728-4734.
- 4. Towards Exceeding the Shockley-Queisser Limit: Photo-Induced Interfacial Charge Transfer Processes that Store Energy in Excess of the Equilibrated Excited State.** Hoertz, P.G.; Staniszewski, A.; Marton, A.; Higgins, G.T.; Incarvito, C.D.; Rheingold, A.L.; Meyer, G.J. *J. Am. Chem. Soc.* **2006**, *128*, 8234-8245.
- 5. Tuning Open Circuit Photovoltages with Tripodal Sensitizers.** Clark, C.C.; Meyer, G.J.; Wei, Q.; Galoppini, E. *J. Phys. Chem. B* **2006**, *110*, 11044-11046.
- 6. Theoretical Solar-to-Electrical Energy-Conversion Efficiencies of Perylene-Porphyrin Light-Harvesting Arrays.** Hasselman, G.M.; Watson, D.F.; Stromberg, J.; Bocian, D.F.; Holten, D.; Lindsey, J.S.; Meyer, G.J. *J. Phys. Chem. B* **2006**, *110*, 25430-25440.
- 7. Conduction Band Mediated Electron Transfer Across Nanocrystalline TiO₂ Surfaces.** Staniszewski, A.; Morris, A.J.; Meyer, G.J. *J. Phys. Chem. B* **2007**, *24*, 6822-6828.
- 8. Unexpected Ultrafast Structural Rearrangements in the MLCT Excited State of Copper(I) bis-Phenanthrolines in Solution.** Shaw, G.B.; Grant, C.D.; Castner, E.W.; Meyer, G.J.; Chen, L.C. *J. Am. Chem. Soc.* **2007**, *129*, 2147-2160.
- 9. Calculated Optoelectronic Properties of Ruthenium tris-bipyridine Dyes Containing Oligophenyleneethynylene Rigid Rod Linkers in Different Chemical Environments.** Lundqvist, M.J.; Galoppini, Meyer, G.J. Persson, P. *J. Phys. Chem. A* **2007**, *111*, 1487 – 1497.
- 10. Examination of Tethered Porphyrin, Chlorin, and Bacteriochlorin Molecules in Mesoporous Metal-Oxide Solar Cells.** Stromberg, J.R.; Marton, A.; Ling Kee, H.; Kirmaier, C.; Diers, J.R.; Muthiah, C.; Taniguchi, M.; Lindsey, J.R.; Bocian, D.F.; Meyer, G.J., Holten, D. *J. Phys. Chem. C* **2007**, *111*, 15464-15478.
- 11. Halide Coordination to Zinc Porphyrin Sensitizers Anchored to Nanocrystalline TiO₂.** Morris, A.J.; Meyer, G.J. *submitted*.
- 12. TiO₂ Surface Functionalization to Control the Density of States.** Morris, A.J.; Meyer, G.J. *submitted*.

METAL-TO-LIGAND CHARGE TRANSFER EXCITED STATES ON SURFACES AND IN RIGID MEDIA: APPLICATION TO ENERGY CONVERSION

Thomas J. Meyer, John M. Papanikolas
University of North Carolina
Department of Chemistry
Chapel Hill, N.C. 27599-3290
919-843-8313/919-962-2388
tjmeyer@unc.edu

I. Photophysical and photochemical studies of MLCT excited states in polymer films and on oxide surfaces.

Processing PEG-DMA (polyethylene glycol dimethacrylate) to make ~1 mm thick films has been developed as an alternative rigid medium to PMMA (polymethylmethacrylate). PEG-DMA films are ~10 times faster to synthesize, and have improved uniformity compared to PMMA. The rigidity of the polymerized PEG-DMA film is determined by the size of the PEG monomers. Emission measurements for Ru(phen)₃pTos₂ in various PEG films showed an expected rigidity dependence of increased emission energies and lengthened lifetimes with increasing rigidity.

Nanosecond transient absorption and emission data were collected for PEG-DMA films doped with Ru(phen)₃pTos₂ and various concentrations of TMBD (tetramethylbenzidine), an electron donor ($E^0 = 0.43$ V). Reductive quenching of the Ru(phen)₃²⁺ MLCT excited state was observed on the nanosecond time scale. The quenched emission is consistent with a random distribution of quenchers throughout the film. Analysis of the data will parameterize the effect of the medium on the distance dependence of electron transfer rate constants.

Both time-resolved and steady-state emission measurements provide evidence for excited state interactions for Ru(bpy)₂(4,4'-(PO₃H₂)₂bpy)(PF₆)₂ adsorbed to nanocrystalline 10 – 20 nm diameter nanostructured ZrO₂ and TiO₂ thin films of ~ 10 micron thicknesses. These interactions include a contribution from triplet-triplet annihilation. Photophysical measurements on Ru^{II} loaded ZrO₂ films with coadsorbed MV-COOH have shown that oxidative excited state quenching occurs followed by cross-surface back electron transfer. More complex surface structures are currently under investigation which contain: adsorbed reductive quenchers, adsorbed reductants and oxidants, and ion-paired oxidants and reductants.

II. Electrochemical and Photocatalytic Oxidation of Water by Adsorbed Ru Complexes on Metal Oxide Surfaces

Kinetic and mechanistic studies have been conducted on water oxidation by the “blue dimer” diruthenium catalyst [(bpy)₂(H₂O)RuORu(OH₂)(bpy)₂]⁴⁺ (bpy is 2,2'-bipyridine) in acidic aqueous solutions by using Ce^{IV} as a sacrificial oxidant. These results indicate that the

mechanism of water oxidation by the blue dimer strongly depends on the nature of the acid as well as its concentration. For example, in 0.1 M HNO₃ the rate determining step is oxidation of a peroxidic intermediate ((HO₂)Ru^{III}ORu^V(O)³⁺) that we have characterized by redox and acid-base titrations. In 1.0 M HNO₃ the rate determining step is oxidation of the V,IV form of the dimer, (O)Ru^VORu^{IV}(O)³⁺. Under these high anion concentration conditions, Ce(IV) depletion leads to the appearance of anated species, (O₂NO)Ru^VORu^{III}(OH₂)⁵⁺. The anated species have also been characterized by redox and acid-base titrations.

Mechanistic results have led to a new approach to water oxidation to overcome the slow step in the overall catalytic cycle. This strategy for enhancing catalytic rate is based on the addition of the kinetically facile redox mediators Ru(bpy)₂(L-L)²⁺ (L-L is 2,2'-bipyridine (bpy), 2,2'-bipyrazine (bpz) and 2,2'-bipyrimidine (bpm)) and [Ru(bpm)₃]²⁺. With this approach, rate enhancements for water oxidation by factors of up to ~25 have been achieved.

These results open the door for future catalyst design to maximize rates of catalytic water oxidation. Electrochemical rather than chemical oxidation of the blue dimer catalyst should reduce the degree of over-oxidation and allow fundamental studies over a wide pH range. We have also begun studies on the generation of oxidizing equivalents with light by photo injection from the complex Ru(pbpy)(bpy)₂²⁺ (pbpy is 4,4'-(PO₃Et₂)₂bpy) to nanocrystalline TiO₂ films. To this end, we have begun emission and ns transient absorption studies of Ru(pbpy)(bpy)₂²⁺ on TiO₂ in aqueous solutions. Our future work in this scheme for photochemical water splitting includes integrated photon-to-current efficiency (IPCE) measurements and direct monitoring of oxygen evolution by these films in the presence of catalyst.

Publications

Published

- (1) Application of Transient Infrared and Near Infrared Spectroscopy to Transition Metal Complex Excited States and Intermediates. Butler, J. M.; George, M. W.; Schoonover, J. R.; Dattelbaum, D. M.; Meyer, T. J. *Coord. Chem. Rev.* **2007**, *251*, 492–514.
- (2) Electrochemical Oxidation of Water by an Adsorbed μ -Oxo-Bridged Ru Complex. Liu, F.; Cardolaccia, T.; Hornstein, B. J.; Schoonover, J. R.; Meyer, T. J. *J. Am. Chem. Soc.* **2007**, *129*, 2446- 2447. (DOE)
- (3) Excited State Intervalence Transfer in a Rigid Polymeric Film. Fleming, C. N.; Dattelbaum, D. M.; Thompson, D. W.; Ershov, A. Y.; Meyer, T. J. *J. Am. Chem. Soc.* **2007**, *129*, 9622-9630. (DOE DE-FG02-06ER15788, LANL and NSERC)
- (4) Rigid Medium Stabilization of Metal-to-Ligand Charge Transfer Excited States. Thompson, D. W.; Fleming, C. N.; Myron, B. D.; Meyer, T. J. *J. Phys. Chem. B* **2007**, *111*, 6930-6941. (DOE-DE-FG02-06ER15788)

- (5) Vibrational and Structural Mapping of $[\text{Os}(\text{bpy})_3]^{3+/2+}$ and $[\text{Os}(\text{phen})_3]^{3+/2+}$. Demadis, K. D.; Dattelbaum, D. M.; Kober, E. M.; Concepcion, J. J.; Paul, J. J.; Meyer, T. J.; White, P. S. *Inorg. Chim. Acta* **2007**, *360*, 1143–1153. (DOE-BE-FG02-OGER15788)
- (6) Reactivity of an Adsorbed Ru(VI)-Oxo Complex: Oxidation of Benzyl Alcohol. Hornstein, B. J.; Dattelbaum, D. M.; Schoonover, J. R.; Meyer, T. J. *Inorg. Chem.* **2007**, *46* (20), 8139-8145.
- (7) Mechanisms of Water Oxidation from the Blue Dimer to Photo-system II. Liu, F.; Concepcion, J.; Cardolaccia, T.; Jurss, J.; Templeton, J.L., and Meyer, T. J. *Inorganic Chem.*, **2008**, *47*, 1727-1752.

Submitted

Mediator-Assisted Water Oxidation by the Ruthenium “Blue Dimer” *cis,cis*- $[(\text{bpy})_2(\text{H}_2\text{O})\text{RuORu}(\text{H}_2\text{O})(\text{bpy})_2]^{4+}$. Concepcion, J.; Jurss, J.; Templeton, J. L. and Meyer, T. J. *Science*, **2008**.

CONJUGATED POLYELECTROLYTES: DISRUPTED INTERACTIONS, SELF-ASSEMBLED STRUCTURES, AND HYBRID POLYMER SOLAR PHOTOCONVERSION

Kirk S. Schanze, Valeria D. Kleiman and John R. Reynolds

Department of Chemistry
University of Florida
Gainesville, FL 32611-7200

Conjugated polyelectrolytes (CPEs) are polymers that feature a π -conjugated backbone substituted with ionic solubilizing groups such as sulfonate, ammonium, carboxylate, or phosphonate ($-\text{SO}_3^-$, $-\text{NR}_3^+$, $-\text{CO}_2^-$, $-\text{PO}_3^{2-}$). CPEs are soluble in and processable from water, and they retain the favorable optoelectronic properties characteristic of the conjugated backbone (e.g., strong optical absorption, fluorescence and semiconducting properties). In addition, CPEs are amphiphilic with a strong propensity to self-assemble in solution and into nanostructured, layer-by-layer (LbL) films. This program is investigating the properties of CPEs, with emphasis placed on studies of the mechanism of “amplified quenching”, intra- and interchain excited state energy transport, self-assembly into CPE assemblies and energy transport and charge transfer in hybrid materials.

New Conjugated Polyelectrolytes: Disrupted Inter- and Intrachain Interactions. In an effort to explore how exciton transport is influenced by interactions within single conjugated chains and between chains in CPE aggregates, synthetic efforts have been directed towards the synthesis of linear and hyperbranched CPEs. In one line of work, we have developed a class of CPEs that feature branched solubilizing groups containing multiple ionic residues for each polymer repeat unit. Using a common synthetic approach, a variety of CPE structures have been prepared that

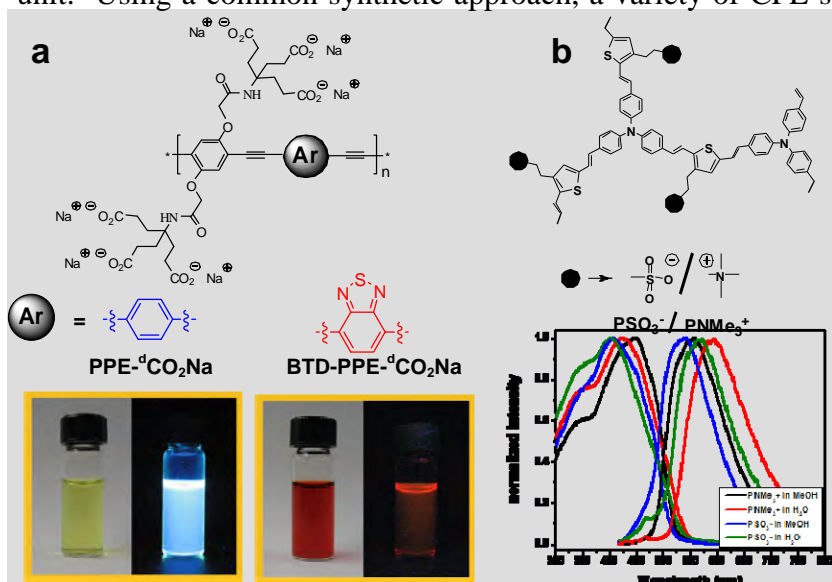


Figure 1. (a) Structure of example linear CPEs with branched ionic solubilizing groups. Photographs illustrate solutions of the polymers under visible and near-UV illumination (fluorescence). (b) Structure of example hyperbranched CPEs. Plot below illustrates the absorption and fluorescence of the materials.

differ widely in bandgap. For example, as illustrated in Figure 1a, a series of linear poly(phenylene ethynylene)-based CPEs has been prepared in which the fluorescence emission is tuned from the blue to the red. In another approach, a series of poly(fluorene)-based CPEs has been synthesized via a novel synthetic method involving thermal cleavage of organic-soluble ester precursor polymers. In a second major line of investigation, “hyperbranched” conjugated polyelectrolytes (HB-CPEs, Figure 1b) have been prepared.

The HB-CPEs feature a disrupted conjugated backbone, and they are of interest in exploring how the backbone structure influences the dynamics of singlet exciton migration.

Time-Resolved Studies of Exciton Dynamics. Time-resolved fluorescence upconversion has been applied to investigate the kinetics of exciton transport and quenching in the CPEs with branched side chains (e.g., PPE-^dCO₂Na, Fig. 1a). In one line of work we are exploring the quenching of these polymers with different concentrations of cationic cyanine dye energy acceptors and under different solvation conditions (Fig. 2). We found that, similar to our previous studies of the linear sulfonate polymer PPE-SO₃⁻, the energy migration in PPE^dCO₂⁻ leads to a strong quenching amplification, with K_{SV} on the order of 10^6 M^{-1} even for acceptors with a small overlap between emission of donor and absorption of acceptor. In addition, we followed the energy flow between donor and acceptor by measuring both the emission from the CPE and the sensitized emission from the dye as a function of dye concentration. We are currently working to model this data to extract information regarding the dynamics of diffusion of the exciton within the isolated CPE chains.

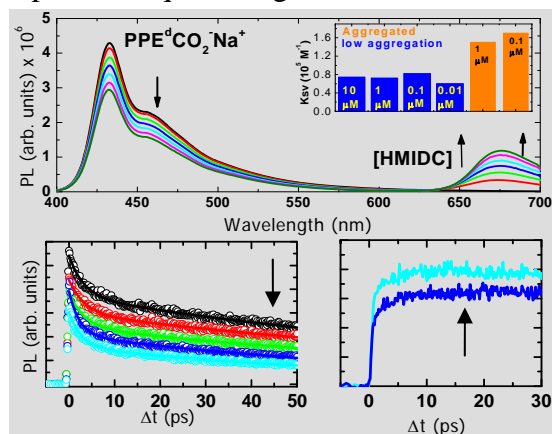


Figure 2: Emission of CPE and sensitized emission from the acceptor. Inset shows quenching dependence on aggregation and on [CPE]. A dynamic component is observed in both the ultrafast emission from CPE and the sensitized emission measured as a function of [Q].

Photophysics of CPE Films on Wide Bandgap Semiconductors. In ongoing studies we have constructed “layer-by-layer” (LbL) CPE films atop nanostructured TiO₂ and terraced SnO₂ films in order to study energy transport through the films to the semiconductor interface. The fluorescence of the CPE is quenched efficiently by the semiconductors, and transient absorption studies using films on nanostructured TiO₂ demonstrates that the quenching arises from photoinduced charge injection at the interface. The fluorescence intensity from multilayer films consisting of alternating layers of an anionic and cationic CPE atop the terraced SnO₂ increases with layer thickness, and analysis of the data suggests that singlet exciton transport is efficient through 5 bilayers (*ca.* 50 Å). Studies of photocurrent generation on CPE films on nanostructured TiO₂ indicate that charge injection is efficient, with incident photon to current efficiencies of greater than 50% observed. A study of the efficiency of charge injection vs. CPE band-gap (singlet energy) reveals that charge injection remains efficient as the polymer band-gap decreases to *ca.* 2.4 eV, and then it falls. The decrease in injection efficiency is attributed to exciton trapping by aggregates competing with transport to the CPE-semiconductor interface.

Future Plans. Work on ultrafast spectroscopy will continue studying the dynamics of exciton transport in single chain CPEs (linear chains with branched side-groups), with an emphasis placed on exploring how band-gap influences the rate of exciton transport along the chain. With the new variable band-gap CPEs with branched side chains in hand, we also will initiate studies of the efficiency and dynamics of exciton transport in LbL multilayer films in which layers that contain CPEs with different band-gap are separated by distances of nanometer dimension. Related studies will explore the efficiency of exciton transport through LbL multilayer films assembled atop wide band-gap semiconductors. Here we will utilize steady state and time resolved fluorescence spectroscopy, coupled with photocurrent efficiency measurements.

DOE Sponsored Publications 2006-2008

1. “The Role of Exciton Hopping and Förster Energy Transfer in the Amplified Quenching of Conjugated Polyelectrolytes”, J. G. Müller, E. Atas, C. Tan, K. S. Schanze and V. D. Kleiman, *J. Am. Chem. Soc.* **2006**, *128*, 4007-4016.
2. “Amplified Fluorescence Quenching of a Conjugated Polyelectrolyte Mediated by Ca²⁺”, H. Jiang, X. Zhao and K. S. Schanze, *Langmuir* **2006**, *22*, 5541-5543.
3. “A meta-Linked poly-(Phenylene Ethynylene) Conjugated Polyelectrolyte Featuring a Chiral Side Group: Helical Folding and Guest Binding”, X. Zhao and K. S. Schanze, *Langmuir* **2006**, *22*, 4856-4862.
4. “Variable Bandgap poly(Arylene Ethynylene) Conjugated Polyelectrolytes”, X. Zhao, M. R. Pinto, L. M. Hardison, J. Mwaura, J. Müller, H. Jiang, D. Witker, V. D. Kleiman, J. R. Reynolds and K. S. Schanze, *Macromolecules* **2006**, *39*, 6355-6366.
5. “Spectral Broadening in Nanocrystalline TiO₂ Solar Cells Based on poly(p-phenylene ethynylene) and polythiophene Sensitizers”, J. K. Mwaura, X. Y. Zhao, H. Jiang, K. S. Schanze and J. R. Reynolds, *Chem. Mater.* **2006**, *18*, 6109-6111.
6. “Amplified Fluorescence Quenching and Biosensor Application of a Poly(para-phenylene) Cationic Polyelectrolyte”, M. R. Pinto, C. Tan, M. B. Ramey, J. R. Reynolds, T. S. Bergstedt, D. G. Whitten, D. G. and K. S. Schanze, *Res. Chem. Intermed.* **2007**, *33*, 79-90.
7. “Base-Free Suzuki Polymerization for the Synthesis of Polyfluorenes Functionalized with Carboxylic Acids”, R. N. Brookins, K. S. Schanze and J. R. Reynolds, *Macromolecules*, **2007**, *40*, 3524-3526.
8. “Hyperbranched Conjugated Polyelectrolyte Bilayers for Solar Cell Applications”, P. Taranekar, Q. Qiao, H. Jiang, K. S. Schanze and J. R. Reynolds, *J. Am. Chem. Soc.* **2007**, *129*, 8958-8959.
9. “Effects of Polymer Aggregation and Quencher Size on Amplified Fluorescence Quenching of Conjugated Polyelectrolytes”, H. Jiang, X. Zhao and K. S. Schanze, *Langmuir* **2007**, *23*, 9481-9486.
10. “A Conjugated Polyelectrolyte Based Fluorescence Sensor for Pyrophosphate”, X. Zhao, Y. Liu and K. S. Schanze, *Chem. Commun.* **2007**, 2914-2916.
11. “Polymer Chain Length Dependence of Amplified Fluorescence Quenching in Conjugated Polyelectrolytes”, X. Zhao, H. Jiang and K. S. Schanze, *Macromolecules* 2008, web ASAP, DOI: 10.1021/ma800191q.
12. “Energy Transfer Dynamics in Conjugated Polyelectrolytes with Varying Chain Lengths”, L. Hardison, X. Zhao, H. Jiang, K. S. Schanze and V. D. Kleiman, submitted.

Session VII

Dye Sensitized Semiconductors

FUNDAMENTAL INVESTIGATIONS OF DYE/SEMICONDUCTOR INTERFACES

Yunfeng Lu, Mark T. Spitler, Dae-jin Choi, Bengt Jäckel, Robert Herrick and Bruce Parkinson
Department of Chemistry
Colorado State University
Fort Collins, CO 80523

During the last funding cycle we have been studying the fundamental properties of semiconducting oxide interfaces with covalently bound photosensitizing dyes. Understanding the energetics and structure of this interface will lead to a greater understanding of the operation and subsequent improvement of the efficiency of dye sensitized solar cells.

The first step in this project was to develop methods for preparing clean atomically flat oxide surfaces. A simple polishing and relatively low temperature annealing procedure for preparing atomically flat terraced surfaces of various single-crystal TiO_2 polymorphs was developed. Anatase (101), anatase (001), rutile (100), rutile (110) and brookite (111) surfaces could all be prepared with a terraced surface structure as revealed in AFM images. The rutile (100), (110) and anatase (101) surfaces were also shown to produce acceptable LEED patterns immediately upon insertion into a UHV system without the usual sputter and anneal cycles. A subsequent surface cleaning step using UV photooxidation in an electrolyte solution resulted in reproducible high coverages of the covalently bound sensitizing dyes. Figure 1 shows an AFM image,

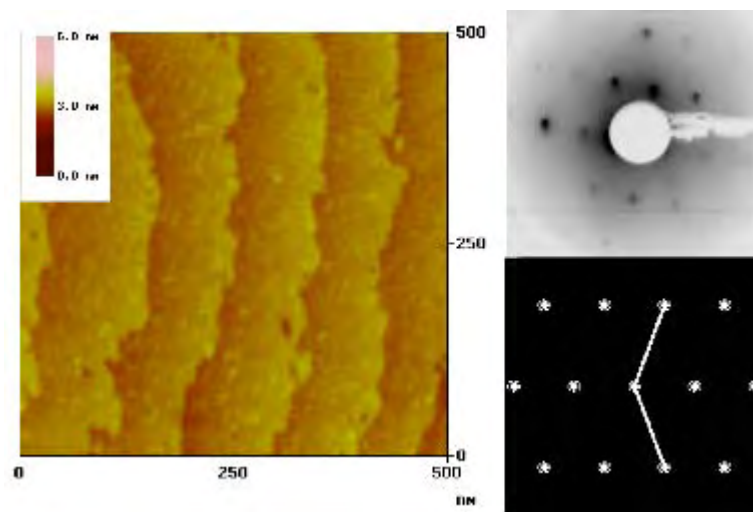


Figure 1. Left - Topographic AFM image of a natural anatase (101) crystal surface. The average step height is 0.36 nm. Upper right - Observed LEED pattern (100 eV) of the as-prepared surface. A calculated LEED pattern is given below.

Once reproducible oxide surfaces and dye coverages were achieved, a photochronocoulometric technique was developed to measure the surface coverage of the dyes, an important parameter in determining the efficiency of sensitization. The surface-bound dyes are irreversibly oxidized by

exposure to a light pulse when the n-type oxide semiconductor electrode is held in depletion. A double exponential decay of the subsequent photocurrent was then measured, where the integration of the faster decay is associated with the adsorbed dye coverage and the second much slower decay is attributed to trace regenerators, including water, in the non-aqueous electrolyte. Figure 2 shows a photocurrent transient for N3 dye adsorbed onto rutile (100). The ruthenium based N3 dye shows the expected linear dependence of the rate constant on light intensity whereas a dicarboxylated thiocyanine dye shows a square root dependence of its photooxidation rate on light intensity. The sublinear response of the thiocyanine dye is discussed in terms of the more complex surface chemistry that is known for this family of sensitizing dyes.

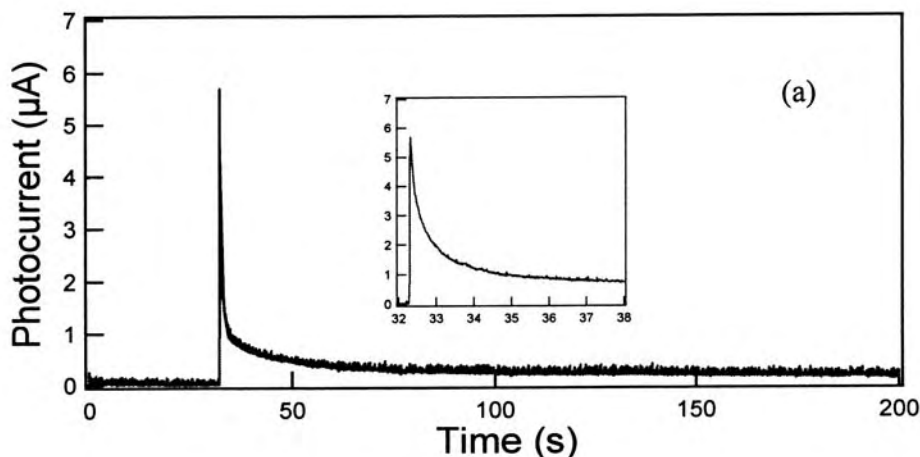


Figure 2. Transient currents for the photooxidation of N3 dye adsorbed onto a rutile (100) surface. The inset is a zoom-in at early illumination time.

A photon-initiated desorption of a dicarboxylated thiocyanine dye from a dye-sensitized semiconducting oxide crystal was observed when hydroquinone is used as a regenerator. No desorption was found under the same conditions when KI was used as the regenerator. Intermittent illumination experiments suggest that the oxidation products of the hydroquinone regenerator compete for dye adsorption sites. By comparing the photocurrent decay at both dye monomer sensitization maximum and the dimer sensitization maximum, a rearrangement of monomer into dimer was observed. A kinetic model for the photocurrent decay as a function of desorption time was derived and the desorption rate constants were obtained by fitting the experimental data to the model.

Current work is directed at the simultaneous measurement of light absorption and quantum yields for various dyes adsorbed onto TiO_2 that are crystals fabricated into ATR prisms. This experiment will determine what forms of the adsorbed dye (monomer, dimer or aggregates) are more efficient producers of photocurrent.

DOE Sponsored Publications 2006-2008

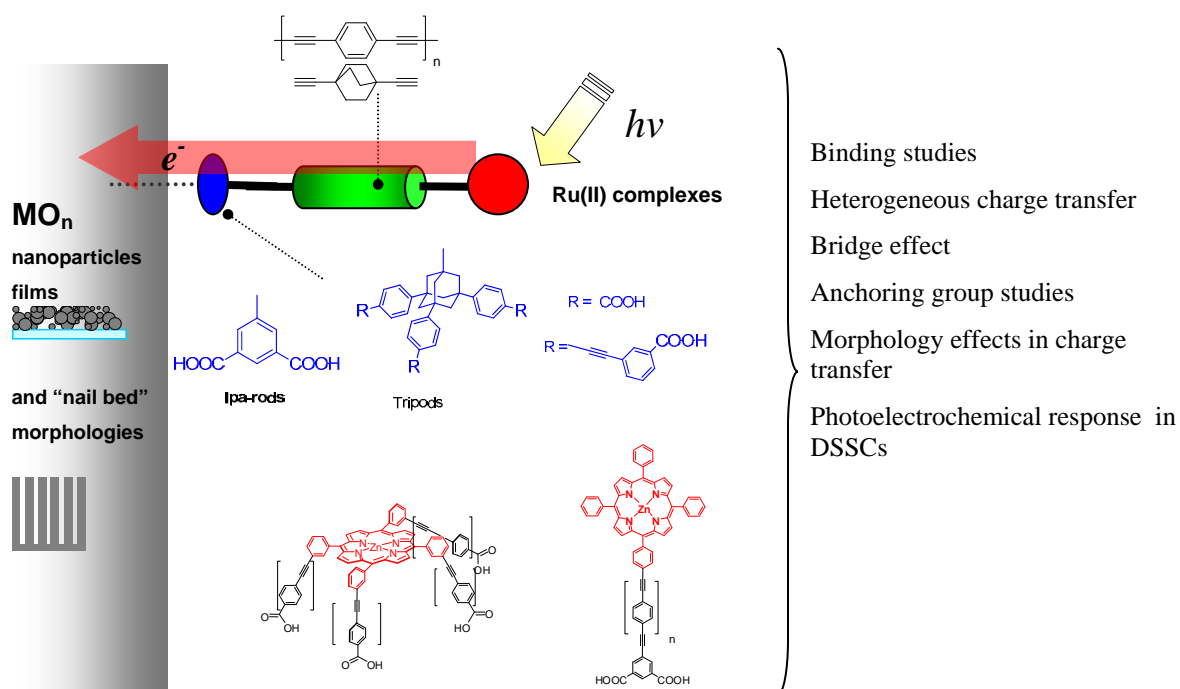
1. Aron Walsh, Su-Huai Wei, Yanfa Yan, M. M. Al-Jassim, John A. Turner, Michael Woodhouse, and B. A. Parkinson, "Structural, magnetic, and electronic properties of the Co-Fe-Al oxide spinel system", Phys. Rev. B, 76, 165119, (2007).
2. Michael Woodhouse and B. A. Parkinson, "Combinatorial Discovery and Optimization of a Complex Oxide with Water Photoelectrolysis Activity", Chemistry of Materials, 20(7), 2495-2502, (2008).
3. Michael J. Scott, Michael Woodhouse, Bruce A. Parkinson and C. Michael Elliott "Spatially Resolved Current-Voltage Measurements--Evidence for Non-Uniform Photocurrents in Dye Sensitized Solar Cells", Journal of the Electrochem. Soc., 155(3), B290-B293, (2008).
4. Yunfeng Lu, Mark T. Spitler and B. A. Parkinson, "Regenerator Dependent Photo-Induced Desorption of a Dicarboxylated Cyanine Dye from the Surface of Single Crystal Rutile", Langmuir, 23, 11673-11642, (2007).
5. Yunfeng Lu, Mark T. Spitler and B. A. Parkinson, "Photochronocoulometric Measurement of the Coverage of Surface Bound Dyes on Titanium Dioxide Crystal Surfaces", J. Phys. Chem. B, 110, 25273-25278, (2006).
6. Laura Sharp, David Soltz and B. A. Parkinson, "Growth and Characterization of Tin Disulfide Single Crystals", Crystal Growth & Design, 6(6), 1523-1527, (2006).
7. Yunfeng Lu, Bengt Jäckel and B. A. Parkinson, "Preparation and Characterization of Terraced Surfaces of Low-Index Faces of Anatase, Rutile, and Brookite", Langmuir, 22(10), 4472-4475, (2006).
8. Yunfeng Lu, Dae-jin Choi, Jimmy Nelson, O-Bong Yang and B. A. Parkinson, "Adsorption, Desorption, and Sensitization of Low-Index Anatase and Rutile Surfaces by the Ruthenium Complex Dye N3", Journal of the Electrochemical Society, 153(8), E131-E137, (2006).

MODEL DYES FOR STUDY OF MOLECULE/METAL OXIDE INTERFACES AND ELECTRON TRANSFER PROCESSES

Elena Galoppini
 Department of Chemistry
 Rutgers University
 Newark, NJ 07102

Project Summary.

The scope of this project is to understand fundamental aspects of the dye/metal oxide semiconductor interface and to develop dye-linker model compounds to study charge transfer processes at this boundary. In addition to TiO₂, ZnO and ZrO₂ nanoparticle films prepared from colloidal solutions, “nail bed” layers (ZnO nanotips and TiO₂ nanotubes) are studied to investigate the morphology effect on the interfacial processes.



Injection and recombination studies at TiO₂ and ZnO interfaces.

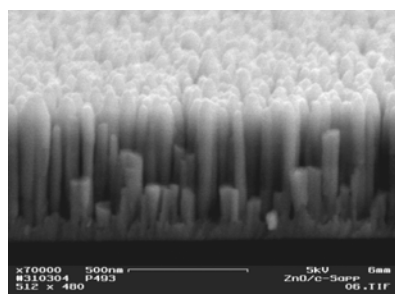
The characterization of semiconductor interfaces is of fundamental importance for solar energy conversion. The complexity of the MO_n colloidal films, made of sintered spherical nanoparticles with numerous points of contacts and cavities, and the large number of variables involved in their preparation, are a challenge for the characterization of the dye/MO_n boundary and for the study of charge transfer processes, even with well designed molecular models and with substrates that have been studied for a long time, such as TiO₂ films. A combination of (a) synthetic design, (b) spectroscopic methods, and (c) choice of

semiconductor materials is used to address this issue.

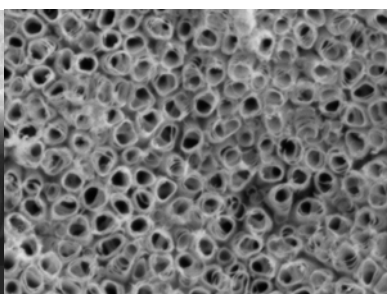
(a) We have synthesized a series of dye-linker models, with Ru(II) polypyridyl complexes and porphyrin chromophores, that bind flat to the surface of the semiconductor or bind through rigid-rod linkers with conjugated or saturated bridges ending with isophthalic or tripodal anchoring units.^{1,2,3} The models are designed to study how bridge length, dye orientation (flat vs perpendicular to the surface) and footprint anchoring groups influence the charge transfer processes and solar cells efficiencies. The synthesis of homoleptic complexes and compounds with bulky groups to minimize interactions of the chromophoric unit with nearby nanoparticles will be discussed.

(b) A new series of experiments with a selected number of dyes under vacuum conditions is in progress in the Piotrowiak group. Elimination of the solvent and oxygen will simplify the environment of the bound sensitizer and eliminate some of the inhomogeneity of the injection rates and degradation effects. Furthermore, a femtosecond mid-IR potassium niobate OPA was constructed specifically in order to permit probing of the absorption of the conduction band electron in the region of 2800-3600 nm, where it is not obscured by the spectra of the triplet MLCT state and the oxidized form of the dye. Combined with the visible range NOPA as the excitation source the system is capable of ~50 fs time resolution.

(c) A promising approach to dramatically improve dye-sensitized solar cells may lie in the development of novel semiconductor morphologies, such as TiO₂ nanotubes and ZnO



FESEM of MOCVD-grown ZnO-N on c-Al₂O₃ **Scale:** layer is ~500nm thick
Courtesy of Y. Lu



SEM image of TiO₂ nanotubes. **Scale:** Ø of each tube is ~100nm
Courtesy of K. Rajeshwar

nanotips.^{5,7} We recently reported the first study of electron transport in a functioning ZnO nanotips solar cell. Electron transport time in the cells prepared from conventional ZnO colloidal nanoparticles was comparable to that found for TiO₂ films (~10 ms) whereas in the ZnO nanotips cells it

was about two orders of magnitude faster (~30 µs). Electron transport properties of the dye/ZnO nanotips layer determined by time resolved THz spectroscopy is now under investigation with the Sundström group. In addition, the effect of the films morphology (nanoparticles vs. nanotips) on the interfacial charge transfer processes in such hybrid materials is being studied.

Photoelectrochemical properties.

Recent work in our group involves the study of porphyrin model dyes on nailbed morphologies. With Rajeshwar we are studying DSSCs prepared from vertically oriented TiO₂ nanotube arrays sensitized by porphyrin models designed to correlate changes in distance and orientation on the cells' performance. The use of dye models has proven an effective tool to probe what parameters can influence cells efficiencies. For instance, distance effects on open circuit photovoltage (Voc) values were observed by Meyer for solar cells prepared from conventional TiO₂ electrodes sensitized with Ru(II) tripods of different length.⁶ The largest Voc values were observed in the Ru(II) sensitizers attached through the longest linkers, and were

consistent with iodide oxidation taking place farther from the TiO₂ surface.

DOE Sponsored Publications 2006-2008

1. *Zn(II) Tetraarylporphyrins Anchored to TiO₂, ZnO and ZrO₂ Nanoparticle Films Through Rigid-Rod Linkers*, Rochford, J. ; Galoppini, E. *Langmuir*, (Article) **2008**, *24*, ASAP
2. *Ru(II)-Polypyridyl Complexes Bound to Nanocrystalline TiO₂ Films Through Rigid-Rod Linkers: Effect of the Linkers Length on Electron Injection Rates* Piotrowiak, P.; Galoppini, E.; Wang D.; Myahkostupov, M. *J. Phys. Chem. C* (Letter); **2007**, *111*, 2827-2829. DOI: [10.1021/jp0679257](https://doi.org/10.1021/jp0679257)
3. *Tetrachelate Porphyrin Chromophores for Metal Oxide Semiconductor Sensitization: Effect of the Spacer Length and Anchoring Group Position* Rochford, J.; Chu, D.; Hagfeldt, A.; Galoppini, E. *J. Am. Chem. Soc.* (Article); **2007** *129*, 4655-4665. DOI: [10.1021/ja068218u](https://doi.org/10.1021/ja068218u)
4. *Calculated Optoelectronic Properties of Ruthenium Tris-Bipyridine Dyes Containing Oligophenyleneethynylene Rigid Rod Linkers in Different Chemical Environments* Lundqvist, M. J.; Galoppini, E.; Meyer, G. J.; Persson P. *J. Phys. Chem. A* (Article); **2007**, *111*, 1487-1497. DOI: [10.1021/jp064219x](https://doi.org/10.1021/jp064219x)
5. *Fast Electron Transport in Metal Organic Vapor Deposition Grown Dye-sensitized ZnO Nanorod Solar Cells* Galoppini, E.; Rochford, J.; Chen, H.; Saraf, G.; Lu, Y.; Hagfeldt, A.; Boschloo, G. *J. Phys. Chem. B.* (Letter); **2006**, *110*, 16159 – 16161. DOI: [10.1021/jp062865q](https://doi.org/10.1021/jp062865q)
6. *Tuning Open Circuit Photovoltages with Tripodal Sensitizers* Clark, C. C.; Meyer, G. J.; Wei, Q.; Galoppini, E. *J. Phys. Chem. B* (Letter); **2006**, *110*, 11044-11046. DOI: [10.1021/jp064219x](https://doi.org/10.1021/jp064219x)
7. *Binding Studies of Molecular Linkers to ZnO Nanotips* Taratula, O.; Galoppini E.; Wang, D.; Chu, D.; Zhang, Z.; Chen, H.; Saraf, G.; Lu, Y. *J. Phys. Chem. B* (Article); **2006**, *110*, 6506-6515. DOI: [10.1021/jp0570317](https://doi.org/10.1021/jp0570317)

DOE-supported Ph.D. Theses

Functionalization of Semiconductor Nanomaterials for Device Fabrication **2008** Olena Taratula, Department of Chemistry, Rutgers-Newark

In Preparation

1. *Ultrafast Transport in Dye Sensitized ZnO Nanorods Investigated by Terahertz Spectroscopy* H. Němec, O. Taratula, J. Rochford, J. Zhang, Y. Lu, E. Galoppini, V. Sundström
2. *IR Surface binding studies on nanocrystalline metal oxide thin films.* Taratula, O. Shah, N.; Mendelsohn, R.; Galoppini, E. *Langmuir* (Review)
3. *Photoelectrochemical Response of Nanoporous TiO₂ Solar cells Prepared by Anodization of Titanium and Sensitized with Porphyrin Model Dyes* Rajeshwar, K; de Tacconi, R.N.; Wilaiwan, C.; Rochford, J.; Galoppini, E.

INTERFACIAL PHOTOCHEMICAL PROCESSES IN SENSITIZED NANOSTRUCTURED ELECTRODES

Arthur J. Frank, Nikos Kopidakis, Nathan R. Neale, Jao van de Lagemaat, and Kai Zhu
Chemical and Biosciences Center
National Renewable Energy Laboratory
Golden, Colorado 80401

We are conducting basic studies to understand the underlying processes that determine the electron dynamics and the light-harvesting properties of dye-sensitized photoelectrochemical solar cells. Recent major issues addressed include the kinetics and energetics of electron transport and recombination in film architecture, nanocrystal morphology, time-dependent diffusion coefficient, and surface area effects. Some specific recent achievements are summarized below.

Nanostructured architecture. Films constructed of oriented one-dimensional nanostructures, such as nanotube (NT) arrays, aligned perpendicular to the charge-collecting substrate, could potentially improve the charge-collection efficiency by promoting faster transport and/or slower recombination. The extent to which an oriented architecture could affect transport or recombination is expected to depend on mechanistic considerations, such as the density and location of structural defects, and the crystallinity. Orientative disorder in the array could also influence the transport and recombination mechanism. Understanding the principal physical and chemical factors that govern or limit cell performance is critical for underpinning the development of the next-generation sensitized nanostructured solar cells. Toward this end, we have investigated the relationship between the microstructure and the electron dynamics in dye-sensitized solar cells (DSSCs) incorporating oriented TiO₂ NT arrays or randomly packed nanoparticle (NP) films. The charge transport and recombination properties of sensitized films were studied by frequency-resolved modulated photocurrent/photovoltage spectroscopies. The morphology of the NT arrays was characterized by SEM (Figure 1), TEM, and XRD. Consistent with intuition, the charge-collection efficiencies were significantly higher in the NT-based DSSCs than their NP-based counterparts. Moreover, recombination was found to be much slower in the NT films. Counterintuitively, however, the electron transport times were comparable for both film morphologies, suggesting that some form of disorder limits transport, such as trap states associated with the polycrystallinity of the NT walls. We examine this type of disorder as well as

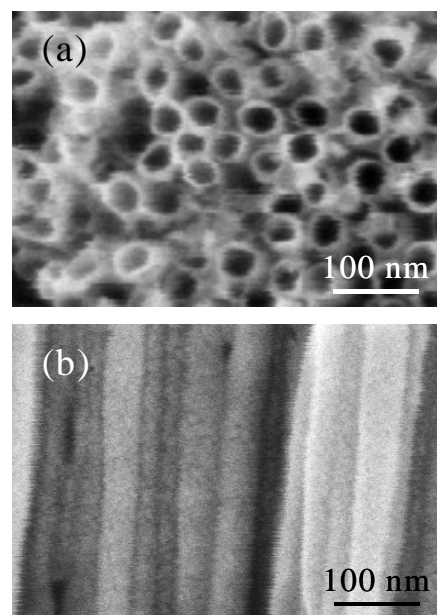


Figure 1. Surface (a) and cross-sectional (b) SEM images of TiO₂ NT arrays.

architectural disorder. The light-harvesting efficiencies and solar cell properties of NT- and NP-based DSSCs were also compared.

Surface area effects. Increasing the surface area of a film to accommodate more dye is a simple way to enhance the light-harvesting efficiency of DSSCs. Besides accommodating more dye, however, increasing the surface area also increases the recombination current density. It is generally accepted that the recombination current density scales linearly with the change in surface area. A different approach to increase the surface area is to reduce the size of the crystallites in a film, while keeping the film thickness and porosity constant. One would like to increase the surface area with a minimum increase in the recombination current density. Virtually nothing is known about the dependence of the recombination current density on the surface area for a fixed film thickness. In this study, we examined the dependence of the electron dynamics on the internal surface area of DSSCs when the average size of the crystallites in a film is systematically varied while the film thickness is held constant. Analyses of intensity-modulated photovoltage spectroscopy (IMVS) measurements reveal that the recombination current density increases superlinearly with the surface area. This superlinear dependence differs from the situation in which the average size of the crystallites in a film is fixed, and the film thickness is varied. Evidence is also presented confirming that photoinjected electrons recombine with redox species in the electrolyte via surface states rather than from the TiO₂ conduction band. The result readdresses an issue of long-standing debate.

Temporal Evolution of the Electron Diffusion Coefficient. The temporal evolution of the diffusion coefficient of electrons in DSSCs was described quantitatively using the continuous time random-walk model. An analytical expression is derived for the time-dependent diffusion coefficient, which transforms at a characteristic (Fermi) time from strongly time-dependent values (dispersive transport) at short times to relatively time-independent values (nondispersive transport) at long times. The timescale for the diffusion coefficient to reach its steady-state value is substantially longer than the Fermi time. Both the steady-state diffusion coefficient of electrons and the timescale over which transport is dispersive depend strongly on the Fermi time and the steepness of the distribution of waiting times associated with traps. At short times, electrostatic interactions with cations in the electrolyte retard the diffusion of electrons in the TiO₂ matrix in marked contrast to the situation at steady state, where ambipolar diffusion is determined solely by electron trapping. The predictions of this study should be potentially valuable in explaining the experimental results of investigations of the electron dynamics in electrolyte-filled mesoporous TiO₂ films.

Tailoring the morphology of TiO₂ Nanocrystallites. Sol-gel chemistry is the most common route for preparing TiO₂ nanocrystalline films for sensitized solar cells. Notwithstanding the research advances in nanocrystal synthesis, it is still challenging to predict a priori the crystal size and structure from a particular synthetic protocol. The synthetic knowledge to vary systematically the morphological and electronic properties of nanostructured systems in a reproducible way is important for advancing both fundamental and applied research in the DSSC area and in others. In this study, we make available reproducible routes for controlling the growth of TiO₂ nanocrystallites over a broad range of sizes and a narrow range of shapes for use in solar cells, photocatalyses, and sensors. We investigated titanium precursors, acid catalysts, and pH and show their influence on the growth direction of the nanocrystals in specific ways.

The nanocrystallites were prepared either from $\text{Ti}(\text{O}^i\text{Pr})_4$ (O^iPr = isopropoxide) in acetic acid solution or from $\text{Ti}(\text{O}^i\text{Pr})_3(\text{OAc})$ (OAc = acetate) in water followed by nitric acid acidification. Nanocrystallites formed from the first method were larger than those produced from the second method. The average size of calcined TiO_2 nanocrystallites formed from $\text{Ti}(\text{O}^i\text{Pr})_4$ varied with hydrothermal temperature from 16–36 nm, whereas the average size of those prepared from $\text{Ti}(\text{O}^i\text{Pr})_3(\text{OAc})$ varied from 13–23 nm. Significantly, the size of the crystallites displayed a linear dependence on the hydrothermal temperature. Crystal growth in acetic acid was enhanced in the [001] direction with increased autoclave temperature, whereas crystallites formed in the presence of nitric acid grew less rapidly in the [001] direction.

Future plans are directed toward understanding photochemical processes in ordered nanostructured systems.

DOE Sponsored Publications 2006-2008

“Temperature Dependence of the Electron Diffusion Coefficient in Electrolyte-Filled TiO_2 Nanoparticle Films: Evidence Against Multiple Trapping In Exponential Conduction Band Tails” Kopidakis, N; Benkstein, K.D.; van de Lagemaat, J.; Frank, A.J.; Yuan, Q.; and Schiff, E.A. *Phys. Rev. B* **2006**, 73, 045326.

“Effect of an Adsorbent on Recombination and Band-Edge Movement in Dye-Sensitized TiO_2 Solar Cells: Evidence for Surface Passivation” Kopidakis, N; Neale, N.R.; Frank, A.J. *J. Phys. Chem. B*, **2006**, 110, 12485.

“Influence of Surface Area on Charge Transport and Recombination in Dye-Sensitized TiO_2 Solar Cells” Zhu, K.; Kopidakis, N; Neale, N.R.; van de Lagemaat, J.; Frank, A.J. *J. Phys. Chem. B*. **2006**, 110, 25174. (Invited paper, Arthur J. Nozik Festschrift issue)

“Nanocrystalline TiO_2 Solar Cells Sensitized with InAs Quantum Dots” Yu, P.; Zhu, K.; Norman, A.; Ferrere, S.; Frank, A.J. Nozik, A.J. *J. Phys. Chem. B* **2006**, 110, 25451. (Invited paper, Arthur J. Nozik Festschrift issue)

“Enhanced Charge-Collection Efficiencies and Light Scattering in Dye-Sensitized Solar Cells Using Oriented TiO_2 Nanotubes Arrays” Zhu, K.; Neale, N.R.; Miedaner, A.; Frank, A.J. *Nano Lett.* **2007**, 7, 69.

“Size and Shape Control of Nanocrystallites in Mesoporous TiO_2 Films” Neale, N.R.; Frank, A.J. *J. Mater. Chem.* **2007**, 17, 3216. (Invited paper, Themed Issue on New Energy Materials)

“Removing Structural Disorder from Oriented TiO_2 Nanotube Arrays: Reducing the Dimensionality of Transport and Recombination in Dye-Sensitized Solar Cells” Zhu, K.; Vinzant, T.B.; Neale, N.R.; Frank, A.J. *Nano Lett.* **2007**, 7, 3739.

“Temporal Evolution of the Electron Diffusion Coefficient in Electrolyte-Filled Mesoporous Nanocrystalline TiO₂ Films” van de Lagemaat, J.; Zhu, K.; Benkstein, K. D.; Frank, A. J. *Inorg. Chimica Acta* **2008**, *361*, 620 (Invited paper, Michael Grätzel commemorative issue)

Session VIII

Photosynthetic Systems I

MAGNETIC RESONANCE AND PROTON LOSS STUDIES OF CAROTENOID RADICAL CATIONS

Lowell D. Kispert,¹ A. Ligia Focsan,¹ Tatyana A. Konovalova,¹ Jesse Lawrence,¹
Michael K. Bowman,¹ David A. Dixon,¹ Peter Molnar² and Jozsef Deli²

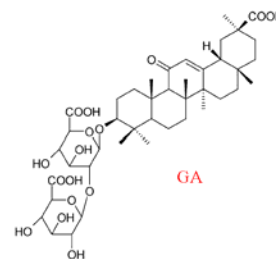
¹The University of Alabama, Department of Chemistry, Tuscaloosa, AL 35487-0336,

²Department of Biochemistry and Medical Chemistry, University of Pécs, Hungary

Carotenoids, intrinsic components of reaction centers and pigment-protein complexes in photosynthetic membranes, play a photoprotective role and serve as a secondary electron donor. Before optimum use of them can be made in artificial photosynthetic systems, their multiple roles in living materials must be understood which requires extensive characterization of their electron transfer, radical trapping ability, stability, structure in and on various hosts, and photochemical behavior. We focus here on the role of carotenoid radicals in photoprotection.

It was determined that length of the polyene molecules is important in formation of the radical cations. No radical cations were obtained from retinoids (C₂₀) treated with BF₃-diethyl etherate or SbCl₃, while the carotenoids (C₄₀), in the same conditions, are capable to produce radical cations by one-electron transfer.

An artificial matrix can modify the properties of carotenoids (Car). We found that Car form 1:2 complexes with β -glycyrrhizic acid (GA) in aqueous solution as well as in polar organic solvents which increased the scavenging rate of Car toward OOH radicals by more than 10 times. Furthermore, GA forms inclusion complexes with carotenoid radical cations, resulting in their stabilization, increases the lifetime and yields of the Car-quinone charge transfer complex and decreases the rate of electron transfer.



Our DFT, pulsed ENDOR and HYSCORE studies of carotenoids adsorbed on silica-alumina or imbedded in metal-substituted MCM-41 artificial matrices and then irradiated, have revealed the formation of the radical cations and neutral radicals. The neutral radicals are formed from the radical cation in the presence of light and/or by hydrolysis as a result of proton loss from particular positions at the cyclohexene rings or from the methyl groups attached to the polyene chain. DFT calculations have predicted that, in general, the most stable neutral radicals are those formed by proton loss at the C4(4') methylene position. In violaxanthin, the epoxide group at positions C5(5')-C6(6') blocks the loss at C4(4') position. In the case of lutein, the most stable radical is formed as a result of proton loss at C6', followed by the neutral radical formed by loss at C4, at the opposite cyclohexene ring.

Crystal structures of the light harvesting center LHCII (Figure 1) containing the carotenoids involved in photoprotection against excessive sunlight were examined. We found that the type and location of the carotenoids are ideal to be effective quenchers of the excess energy from nearby chlorophyll (Chl) molecules once long-lived neutral radicals were formed.

Femtosecond transient absorption measurements performed by Fleming's group have revealed the formation of the radical cation of zeaxanthin in LHCII in the quenched state. Further irradiation would cause the radical cation to deprotonate preferentially at positions situated in the cyclohexene rings forming the neutral radical. The cyclohexene rings of zeaxanthin are in close proximity of the stromal and luminal aqueous surfaces that surround LHCII. It is known from

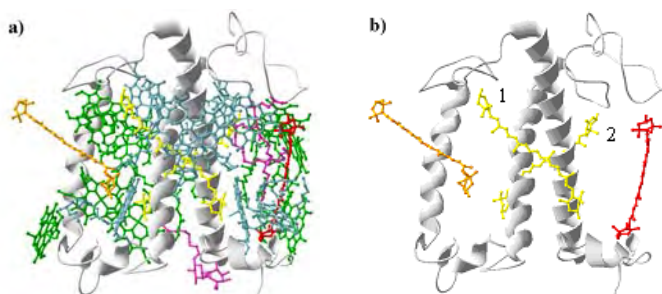


Figure 1. a) LHCII monomer of pea (PDB code: 2BHW): Grey, polypeptide; red, xanthophyll cycle carotenoid; orange, 9'-*cis* neoxanthin; yellow, lutein; blue, Chla; green, Chlb; pink, lipids. b) the location of Car in LHCII.

electrochemical measurements that the radical cation ($pK_a \sim 4-7$) can spontaneously deprotonate in the presence of water to form the neutral radicals. In the case of violaxanthin deprotonation is not possible at the cyclohexene rings, preventing the formation of the neutral radical. The next available positions for proton loss in the case of violaxanthin are C9(9') and C13(13') which are located in the hydrophobic area of the thylakoid membrane. The formation of the neutral radical of zeaxanthin in the presence of water and/or excess light in LHCII can explain why, in xanthophyll cycle, zeaxanthin only (and not violaxanthin) becomes a quencher under high light irradiation.

There are also two lutein (isomer of zeaxanthin) molecules in LHCII positioned in an X shape. Lutein 1 is known to be the main xanthophyll involved in Chl triplet quenching. Its position in LHCII, with one ring containing the C6' position toward the stroma and one ring (containing the next energetically available position, C4, for proton loss) toward the lumen, is favorable for the formation of the neutral radical. Similarly, lutein 2 could also form neutral radicals by proton loss at the cyclohexene rings. Loss from the methyl groups at the polyene chain is less likely due to the hydrophobic media that surround the lutein molecules, their polyene chains being firmly fixed in two elongated hydrophobic cavities on both sides of the supercoil. Moreover, the precursor radical cation of lutein has not been observed.

A third carotenoid situated in LHCII, 9'-*cis* neoxanthin, is an energy transfer agent and is not known to be involved in quenching. The structure of neoxanthin given below (Figure 2) indicates an epoxide at the C5'-C6' position, and an allene group at the opposite end. Our previous studies of allenic carotenoids have shown that R/S isomerization via radical cations or dications is energetically unfavorable and the radical cations and dications are unstable. Also, based on the results for violaxanthin, the epoxide group would prevent the loss of the proton. Future plans are to determine by DFT calculations and EPR and Raman measurements, the radicals formed for 9'-*cis* neoxanthin in different matrices.

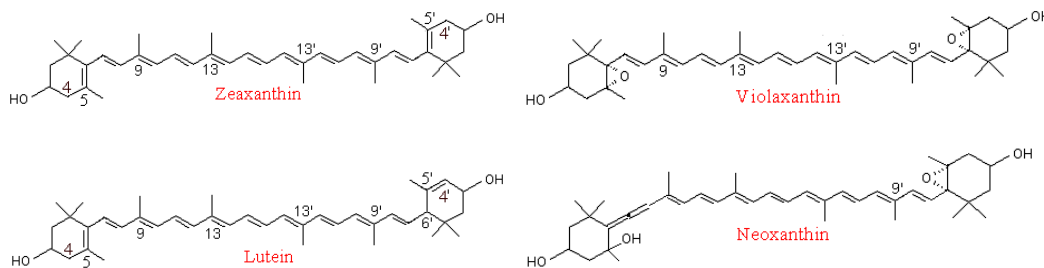


Figure 2. Carotenoids in LHCII; studied: zeaxanthin, violaxanthin and lutein; to be studied: 9'-*cis* neoxanthin.

DOE Sponsored Publications 2006-2008

1. Host-Guest Complexes of Carotenoids with β -Glycyrrhizic Acid
N. E. Polyakov, T. V. Leshina, N. F. Salakhutdinov, and L. D. Kispert, *J. Phys. Chem. B*, **110**, 6991-6998 (2006).
2. Antioxidant and Redox Properties of Supramolecular Complexes of Carotenoids with β -Glycyrrhizic Acid
N. E. Polyakov, T. V. Leshina, N. F. Salakhutdinov, T. A. Konovalova, L. D. Kispert, *Free Rad. Biol. Med.*, **40**, 1804-1809 (2006).
3. DFT and Experimental Examination of the Oxidation/Reduction of a Thiol-Substituted Carotenoid with Gold versus Glassy Carbon Electrodes
Y. Gao, A. L. Focsan, Y. Y. Li, and L. D. Kispert, *J. Phys. Chem. A*, **110**, 10091-10097 (2006).
4. Density Functional Theory Study of the β -Carotene Radical Cation and Deprotonated Radicals
Y. Gao, A. L. Focsan, L. D. Kispert, and D. A. Dixon, *J. Phys. Chem. B*, **106**, 24750-24756 (2006).
5. Electron Paramagnetic Resonance Analyses of Biotransformation Reactions With Cytochrome P-450 Immobilized on Mesoporous Molecular Sieves
M. Rosales-Hernández, L. Kispert, E. Torres-Ramírez, D. Ramírez-Rosales, R. Zamorano-Ulloa, J. Trujillo-Ferrara, *Biotechnol. Lett.*, **29**: 919-924 (2007).
6. Pulsed EPR and DFT Characterization of Radicals Produced by Photo-Oxidation of Zeaxanthin and Violaxanthin on Silica-Alumina
A. L. Focsan, M. K. Bowman, T. A. Konovalova, P. Molnár, J. Deli, D. A. Dixon, and L. D. Kispert, *J. Phys. Chem. B*, **112**, 1806-1819 (2008).
7. Pulsed ENDOR Studies of Carotenoid Oxidation in Cu(II)-Substituted MCM-41 Molecular Sieves
J. Lawrence, A. L. Focsan, T. A. Konovalova, P. Molnár, J. Deli, M. Bowman, and L. D. Kispert, *J. Phys. Chem. B*, in press 2008.
8. Comparative Studies on Cation Radical Formation of Carotenoids and Retinoids
G. Kildahl-Andersen, T. A. Konovalova, A. L. Focsan, L. D. Kispert, T. Anthonsen, and S. Liaaen-Jensen, *Tetrahedron Letters*, **48**, 8196-8199 (2007).
9. ENDOR Spectroscopy, Chapter 4 in *Handbook of Applied Solid State Spectroscopy*
L. D. Kispert and L. Piekara-Sady, D. R. VIJ, Editor, Springer Science Publishers, NY, 2006.

10. Applications of EPR Spectroscopy to Understanding Carotenoid Radicals, in *Carotenoids: Physical, Chemical and Biological Functions and Properties*
L. D. Kispert, L. Focsan and T. Konovalova, J. T. Landrum, Editor, CRC Press, in press 2008.
11. Formation of Carotenoid Neutral Radicals in Photosystem II
Yunlong Gao, K. E. Shinopoulos, C. A. Tracewell, A. L. Focsan, G. W. Brudvig and L. D. Kispert, *Biochemistry*, submitted 2008.

DOE Supported Ph.D. Dissertation

12. EPR and DFT Studies of Proton Loss From Carotenoid Radical Cations
Alexandrina Ligia Focsan, Ph.D. Dissertation, The University of Alabama, 2008.

PHOTOSYNTHETIC LIGHT HARVESTING AND ITS REGULATION

Graham R. Fleming,^{1,2} Krishna K. Niyogi,^{3,2} Elizabeth Read,^{1,2} Tessa Calhoun,^{1,2} Gabriela Schlau-Cohen,^{1,2} Naomi Ginsberg,^{1,2} Tae Ahn,^{1,2} Roberto Bassi⁴

1. Department of Chemistry
University of California, Berkeley
Berkeley, CA 94720
2. Physical Biosciences Division
Lawrence Berkeley National Laboratory
Berkeley, CA 94720
3. Department of Plant and Microbial Biology
University of California, Berkeley
Berkeley, CA 94720
4. Department of Science and Technology
University of Verona
Italy, 37134

A consequence of the nanoscale dimensions of photosynthetic pigment-protein complexes is that the chromophores are close enough to interact strongly and produce delocalized states. However, techniques to reveal whether true quantum mechanical aspects were important in these systems—quantum coherence effects—were lacking. Two-dimensional (2D) Fourier-transform femtosecond spectroscopy, developed in our group, records the signal at the amplitude level, and is thus sensitive to the quantum phase. In the first study of this type on the FMO protein from a green sulfur bacterium, we observed complex oscillations which persisted for at least 650 fs (Fig 1).

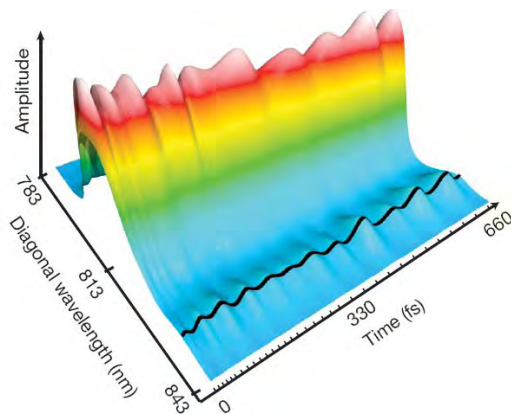


Figure 1 Diagonal slice as a function of time through a two-dimensional electronic spectrum of the FMO light harvesting complex. The oscillations in amplitude represent the quantum phase information as the system evolves in time.

The oscillations can be described as originating from electronic beats between the exciton states of the FMO complex. This leads to the suggestion that FMO may function as a quantum device in which, analogous to quantum search algorithms such as Grover's algorithm, the excitation explores multiple sites simultaneously and, provided the final state underwent rapid dephasing, finds the target with much higher efficiency than in a classical random walk. Using a related

technique—two color coherence electronic spectroscopy—we showed that the fluctuations of the excited B and H levels (B is accessory bacteriochlorophyll and H is bacteriopheophytin) are strongly correlated which again leads to long lived coherence. Recently we carried out 2D spectroscopy of LHCII, the most abundant light harvesting protein. Again a strong beat pattern persisting for quite long times was evident.

Analysis of LHCII data is underway. We have taken 2D spectra of the LH4 protein from purple bacteria whose structure is not known at atomic resolution. The 2D spectra enable us to rule out the proposed structure and suggest a quite different structure showing the potential of 2D spectroscopy for structural studies. We plan to develop the use of polarization techniques to enhance the structural content of 2D spectra.

Energy dependent quenching (qE) is a vital mechanism for regulating photosynthetic light harvesting in higher plants. We previously demonstrated a positive correlation of charge transfer (CT) between coupled zeaxanthin (Zea) and chlorophyll (Chl) molecules and all the physiological characteristics of qE. We have now shown that this charge-transfer quenching takes place in all three of the minor complexes (CP24, CP26, CP29) and have identified the specific chlorophyll molecules involved in CP29. We propose that reversible conformational changes in CP29 can tune the electronic coupling between the chlorophylls, thereby modulating the energy of the Chl-Zea state and switching on and off the charge-transfer quenching during qE. Recent structural models of the PSII super complex place the minor complexes between the bulk LHCII antenna and the reaction center core, making the minor complexes ideally placed to act as valves to control the flow of excitation to the primary electron donor.

DOE Sponsored Publications 2006-2008

1. Triplet-Triplet Energy Transfer Coupling: Theory and Calculation, Z-Q Qiang, C-P Hsu and G.R. Fleming, *J. Chem. Phys.* **124**, 044506 (2006).
2. Two-Dimensional Electronic Spectroscopy of Molecular Complexes, M. Cho, Tobias Brixner, Igor Stiopkin, Harsha Vaswani and G.R. Fleming, *J. Chinese Chem. Soc.* **53**, 15-24 (2006).
3. Electronic 2D Spectroscopy of Light Harvesting, T. Brixner, J. Stenger, H.M. Vaswani, M. Cho, R.E. Blankenship and G.R. Fleming. *Femtochemistry VII* eds. A.W. Castleman Jr. and M.L. Kimble, Elsevier (Amsterdam) 331-336 (2006).
4. Nonlinear Femtosecond Optical Spectroscopy Techniques in Photosynthesis, D. Zigmantas, Y-Z Ma, E.L. Read and G.R. Fleming. *In Biophysical Techniques in Photosynthesis II*, Eds. T.J. Aartsma and J. Matysik, Springer (Dordrecht) 201-222 (2008).
5. One- and Two-Color Photon Echo Peak Shift Studies of Photosystem I, H.M. Vaswani, J. Stenger, P. Fromme and G.R. Fleming. *J. Phys. Chem. B.* **110**, 26303-26312 (2006).
6. Two-Dimensional Electronic Spectroscopy of the B800-B820 Light-Harvesting Complex, D. Zigmantas, E.L. Read, T. Mancal, T. Brixner, A.T. Gardiner, R.J. Cogdell and G.R. Fleming. *PNAS*, **103**, 12672-12677 (2006).
7. Two Dimensional Fourier Transform Electronic Spectroscopy: Evolution of Cross Peaks in

- the Fenna-Matthews-Olson Complex, G.S. Engel, E. L. Read, T. R. Calhoun, T. K. Ahn, T. Mancal, R. E. Blankenship, and G. R. Fleming. *In Ultrafast Phenomena XV* (Springer, Berlin), 392-394 (2007).
8. Two Dimensional Optical Spectroscopy of Multi-chromophore Protein Complexes. G.R. Fleming, D. Zigmantas, E. L. Read, T. Mancal and G. S. Engel. *In Ultrafast Phenomena XV* (Springer, Berlin) 326-328 (2007).
 9. Evidence for wavelike energy transfer: Quantum coherence in photosynthetic systems. G. S. Engel, T. Calhoun, E.L. Read, T. K. Ahn, T. Mancal, R. E. Blankenship and G. R Fleming. *Nature* **446**, 782 (2007).
 10. Determination of Electronic Mixing in Purple Synthetic Bacteria by Two-Color Three Pulse Photon Echo Peak Shift. D. Y. Parkinson, H. Lee and G. R. Fleming. *In Ultrafast Phenomena XV* (Springer, Berlin) 537-539 (2007).
 11. Excited State Structural Dynamics of the Charge Transfer State of Peridinin, M. A. Prantil, A. J. Van Tassel, R. G. Hiller, and G. R. Fleming. *Israel Journal of Chemistry*, **47**, 17-24 (2007).
 12. Measuring Electronic Coupling in the Reaction Center of Purple Photosynthetic Bacteria by Two Color Three Pulse Photon Echo Peak Shift Spectroscopy, D. Y. Parkinson, H. Lee, and G. R. Fleming. *J. Phys. Chem. B*, **111**, 7449-7456 (2007).
 13. Coherence dynamics in photosynthesis: protein protection of excitonic coherence, H. Lee, Y.C. Cheng and G. R. Fleming, *Science* **316**, 1462 (2007).
 14. Multidimensional Ultrafast Spectroscopy Special Feature: Cross-peak-specific two dimensional electronic spectroscopy. E. L. Read, G. S. Engel, T. Calhoun, T. Mancal, T.K. Ahn, R. E. Blankenship and G. R. Fleming, *PNAS*, **104**, 14203-14208 (2007).
 15. Zeaxanthin Radical Cation Formation in Light Harvesting Complexes of Higher Plant Antennae, T. J. Avenson, T. K.Ahn, D. Zigmantas, R. Bassi, M. Ballottari, K. K. Niyogi, and G. R. Fleming *J. Biol Chem*, **283**, 6, 3550-3558 (2008).
 16. Efficient Simulation of Three-Pulse Photon-Each Signals and the Application to Detect Electronic Coupling in a Bacterial Reaction Center, Y-C. Cheng, H. Lee, and G. R. Fleming *Journal of Physical Chemistry A*, **111**, 9499-9508 (2007).
 17. Elucidation of population and coherence dynamics using cross-peaks in two-dimensional electronic spectroscopy, Y-C Cheng, G. S. Engel and G. R. Fleming, *Chemical Physics*, **341**, 285-295 (2007).
 18. Coherence Quantum Beats in Two-dimensional Electronic Spectroscopy, Y-C. Cheng and G. R. Fleming, *J. Phys. Chem. A*, (In Press).
 19. Visualization of Excitonic Structure in the Fenna-Matthews-Olson Photosynthetic Complex by Polarization-Dependent Two-Dimensional Electronic Spectroscopy, E. L. Read, G. S. Schlau-Cohen, G. S. Engel, J. Wen, R. E. Blankenship and G. R. Fleming, *Biophys. J.*, (In Press).
 20. Architecture of a charge-transfer state regulating light harvesting in a plant antenna protein, T. K. Ahn, T. J. Avenson, M. Ballottari, Y-C Cheng, K. K. Niyogi, R. Bassi and G. R. Fleming, *Science*, (In Press).

21. Kinetic modeling of charge-transfer quenching in the CP29 minor complex. Y.C. Cheng, T.K. Ahn, T.J. Avenson, D. Zigmantas, K.K. Niyogi, M. Ballottari, R. Bassi, and G.R. Fleming, *J Phys Chem B*, (Submitted).

Session IX

Molecular Complexes for Energy and Charge Transfer

ENERGY AND CHARGE TRANSPORT IN SELF-ASSEMBLED SYSTEMS FOR ARTIFICIAL PHOTOSYNTHESIS

Michael R. Wasielewski

Department of Chemistry and Argonne-Northwestern Solar Energy Research (ANSER) Center
Northwestern University, Evanston, IL 60208-3113

Scope of the project. We are investigating several related, fundamental problems critical to developing an integrated system for artificial photosynthesis. Studies are in progress to understand how structural dynamics control long distance charge separation and storage in donor-bridge-acceptor (D-B-A) systems by attacking this problem on time scales ranging from femtoseconds to milliseconds using both transient optical and EPR spectroscopy. We are developing the fundamental requirements for energy and charge transport in self-assembling systems having emergent properties as a result of the assembly (e.g. Figure 1). We are also exploring how multiple photoinduced charge separation pathways can be used to accumulate redox equivalents at a single redox site to drive catalysts for fuel formation.

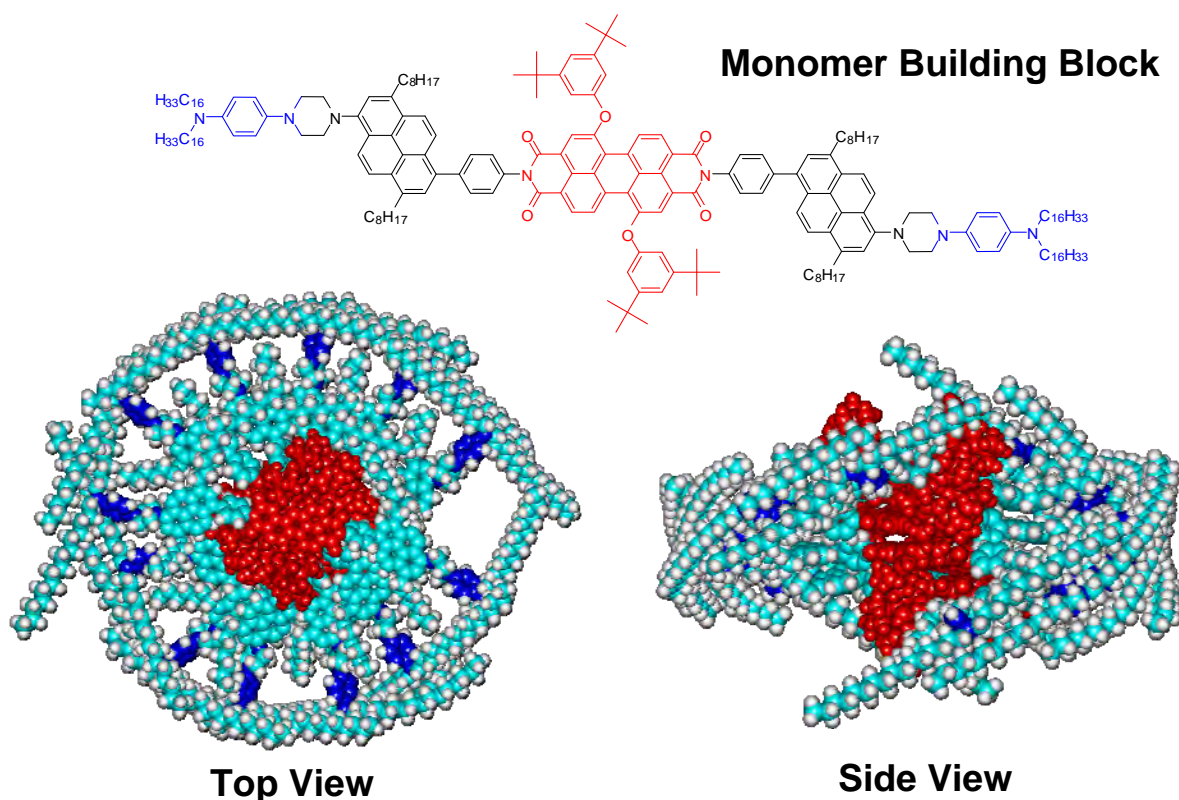


Figure 1. Structures of the donor-acceptor building block and two views of its self-assembled helical hexamer as determined using SAXS in methylcyclohexane solution.

Recent Results. In this presentation we will describe new molecules designed to provide building blocks for the self-assembly of integrated artificial photosynthetic systems for solar energy conversion. We are currently exploring covalent building blocks within which the initial

photoinduced multi-step electron transfer is followed by competitive charge transfer throughout the extended self-assembled structure leading to long distance charge transport. The structures shown in Figure 1 depict a donor-acceptor system in which two-step charge separation occurs following photoexcitation. This building block self-assembles into a stacked, helical supramolecular structure in which the electron donors and acceptors are segregated. The long lifetime of the photogenerated radical ion pair within the covalent building block allows competitive charge hopping to occur between non-covalent acceptors in the segregated charge pathway within the supramolecular structure. The structure of the supramolecular assembly shown in the Figure 1 was determined *in solution* using X-ray scattering techniques at the Advanced Photon Source (APS) at Argonne National Laboratory. The structures are determined at concentrations comparable to those at which spectroscopic measurements of their energy and electron transfer dynamics are made; thus providing a direct measure of how structure controls artificial photosynthetic function within the assembly. Implementation of segregated pathways for electron and hole transport using self-assembly is important for developing materials for integrated systems for artificial photosynthesis as well as for organic photovoltaics.

Ever since the crystal structure of the LH-II antenna protein from purple photosynthetic bacteria revealed that bacteriochlorophylls arrayed in a ring structure are used for light harvesting, considerable effort has been invested in making biomimetic chromophore rings, which offer insights into the photophysics of energy collection and transfer in photosynthetic proteins. We have now prepared a zinc chlorophyll (ZnChl) derivative, Figure 1, that self-assembles into a cyclic tetramer and exhibits intramolecular energy transfer rates comparable to those observed for covalent ring structures. Once again, the structure of this self-assembled light-harvesting cyclic Chl array was determined using SAXS in solution at the APS. The larger transition dipole moment for the lowest energy electronic transition of ZnChls compared to that of porphyrins increases the rate of Förster (through-space) energy transfer between the chlorophylls.

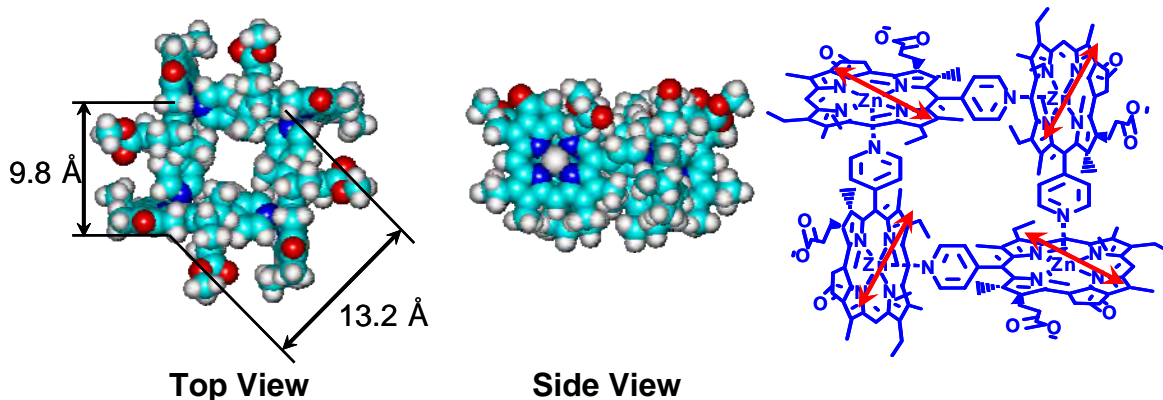


Figure 2. Left and center: Structure of the self-assembled cyclic ZnChl tetramer for light harvesting determined using SAXS in toluene solution. Right: the chemical structure showing the orientation of the Q_y optical transition moments.

Future Plans. Our overarching plan is to understand the properties of photodriven redox systems well enough to produce an integrated artificial photosynthesis system that harvests light, separates charge and delivers that charge to catalysts for solar fuels formation.

DOE Sponsored Publications 2006-2008

1. Electron Hopping in π -stacked Covalent and Self-assembled Perylenediimides Observed by ENDOR Spectroscopy, M. J. Tauber, J. M. Giaimo, R. F. Kelley, B. Rybtchinski, and M. R. Wasielewski, *J. Am. Chem. Soc.* **128**, 1782-1783 (2006).
2. Energy, Charge, and Spin Transport in Molecules and Self-Assembled Nanostructures Inspired by Photosynthesis, M. R. Wasielewski, *J. Org. Chem.* **71**, 5051-5066 (2006).
3. Time-resolved EPR Studies of Photogenerated Radical Ion Pairs Separated by *p*-Phenylene Oligomers and Triplet States Resulting from Charge Recombination, Z. E. X. Dance, Q. Mi, D. W. McCamant, M. J. Ahrens, M. A. Ratner, and M. R. Wasielewski, *J. Phys. Chem. B* **110**, 25163-25173 (2006).
4. Linker-Controlled Energy and Charge Transfer within Chlorophyll Trefoils, R. F. Kelley, M. J. Tauber, and M. R. Wasielewski, *Angew. Chem. Int. Ed.* **45**, 7979-7982 (2006).
5. Hole Mobility in DNA A-Tracts, F. D. Lewis, H. Zhu, P. Daublain, B. Cohen, and M. R. Wasielewski, *Angew. Chem. Int. Ed.* **45**, 7982-7985 (2006).
6. Photoinduced Charge Separation in Self-Assembled Cofacial Pentamers of Zinc-5,10,15,20-Tetrakis(perylenediimide)porphyrin, M. J. Ahrens, R. F. Kelley, Z. E. X. Dance, and M. R. Wasielewski, *Phys. Chem. Chem. Phys.* **9**, 1469-1478 (2007).
7. A Perylenedicarboxamide Linker for DNA Hairpins, F. D. Lewis, L. Zhang, R. F. Kelley, D. McCamant, and M. R. Wasielewski, *Tetrahedron* **63**, 3457-3464 (2007).
8. Solution-Phase Structure of an Artificial Foldamer: X-Ray Scattering Study, R. F. Kelley, B. Rybtchinski, M. T. Stone, J. S. Moore, and M. R. Wasielewski, *J. Am. Chem. Soc.* **129**, 4114-4115 (2007).
9. Ultrafast Energy Transfer within Cyclic Self-Assembled Chlorophyll Tetramers, R. F. Kelley, R. H. Goldsmith, and M. R. Wasielewski, *J. Am. Chem. Soc.* **129**, 6384-6385 (2007).
10. Intramolecular Electron Transfer within a Covalent, Fixed Distance Donor-Acceptor Molecule in an Ionic Liquid, J. V. Lockard and M. R. Wasielewski, *J. Phys. Chem. B*, **111**, 11638-11641 (2007).
11. Scaling Laws for Charge Transfer in Multiply Bridged Donor-Acceptor Molecules in a Dissipative Environment, R. H. Goldsmith, M. R. Wasielewski, and M. A. Ratner, *J. Am. Chem. Soc.* **129**, 13066-13071 (2007).
12. Controlling Energy and Charge Transfer in Linear Chlorophyll Dimers, R. F. Kelley, M. J. Tauber, T. M. Wilson, and M. R. Wasielewski, *Chem. Commun.*, 4407-4409 (2007).

13. Dynamics and Efficiency of DNA Hole Transport via Alternating AT vs. poly(A) Sequences, F. D. Lewis, P. Daublain, B. Cohen, J. A. Vura-Weis, and M. R. Wasielewski *J. Am. Chem. Soc.* **129**, 15130-15131 (2007).
14. Direct Observation of the Preference of Hole Transfer Over Electron Transfer for Radical Ion Pair Recombination in Donor-Bridge-Acceptor Molecules, Z. E. X. Dance, M. J. Ahrens, A. M. Vega, A. Butler-Ricks, D. W. McCamant, M. A. Ratner, and M. R. Wasielewski, *J. Am. Chem. Soc.* **130**, 830-832 (2008).
15. Excited Singlet States of Covalently Bound, Cofacial Dimers and Trimers of Perylene-3,4:9,10-bis(dicarboximide)s, J. M. Giaimo, J. V. Lockard, L. E. Sinks, A. M. Vega, T. M. Wilson, and M. R. Wasielewski, *J. Phys. Chem. A* **112**, 2322-2330 (2008).
16. Reversible Bridge-Mediated Excited State Symmetry Breaking in Stilbene-Linked DNA Dumbbells, F. D. Lewis, P. Daublain, L. Zhang, B. Cohen, J. A. Vura-Weis, M. R. Wasielewski, V. Shafirovich, Q. Wang, and T. Fiebig, *J. Phys. Chem. B* **112**, 3838-3843 (2008).
17. Intramolecular Energy Transfer within Butadiyne-Linked Chlorophyll and Porphyrin Dimer-Faced, Self-assembled Prisms, R. F. Kelley, S. J. Lee, T. M. Wilson, Y. Nakamura, D. M. Tiede, A. Osuka, J. T. Hupp, and M. R. Wasielewski, *J. Am. Chem. Soc.* **130**, 4277-4284 (2008).
18. Intersystem Crossing Mediated by Photoinduced Intramolecular Charge Transfer: Julolidine-Anthracene Donor-Acceptor Molecules, Z. E. X. Dance, S. M. Mickley, M. J. Ahrens, A. Butler-Ricks, M. A. Ratner, and M. R. Wasielewski, *J. Phys. Chem. A* (ASAP).
19. Fast Energy Transfer within a Self-Assembled Cyclic Porphyrin Tetramer, R. A. Jensen, R. F. Kelley, S.-J. Lee, M. R. Wasielewski, J. T. Hupp, and D. M. Tiede, *Chem Commun.* (in press).
20. The Influence of Guanine on DNA Hole Transport Efficiency, F. D. Lewis, P. Daublain, B. Cohen, J. Vura-Weis, and M. R. Wasielewski, *Angew. Chem. Int. Ed.* (in press).
21. Unexpectedly Similar Charge Transfer Rates through Benzo-annulated Bicyclo[2.2.2]octanes, R. H. Goldsmith, J. Vura-Weis, A. M. Vega, S. Borkar, A. Sen, M. A. Ratner, and M. R. Wasielewski, *J. Am. Chem. Soc.* (in press).
22. Challenges in Distinguishing Superexchange and Hopping Mechanisms of Intramolecular Charge Transfer through Fluorene Oligomers, R. H. Goldsmith, O. DeLeon, T. M. Wilson, D. Finkelstein-Shapiro, M. A. Ratner, and M. R. Wasielewski, *J. Phys. Chem. A.* (in press).

Fundamental Studies of Charge Migration and Delocalization Relevant to Solar Energy Conversion

Michael J. Therien
Department of Chemistry
Duke University
Durham, NC 27708-0354

This program seeks to understand the molecular-level principles by which complex chemical systems carry out photochemical charge separation, transport, and storage, and how these insights will impact the design of practical solar energy conversion and storage devices. Towards these goals, this program focuses on: (1) carrying out fundamental mechanistic and transient dynamical studies of proton-coupled electron-transfer (PCET) reactions; (2) characterizing and interrogating via electron paramagnetic resonance (EPR) spectroscopic methods novel conjugated materials that feature large charge delocalization lengths; and (3) exploring excitation delocalization and migration, as well as polaron transport properties of meso-scale (nano-to-micron-sized) assemblies that are capable of segregating light-harvesting antennae, nanoscale wire-like conduction elements, and distinct oxidizing and reducing environments. Examples of projects carried out over the past two years include:

Excited State Dynamics of Nanoscale, Chromophore-Containing Polymersomes. Polymersomes, self-assembled vesicles are comprised of amphiphilic diblock copolymers, demonstrate numerous properties in common with liposomes, their lipid counterparts, yet exhibit mechanical strengths 5-50 times greater. These features, coupled with the fact that the polymersome hydrophobic bilayer is 2-3 times thicker than that of classical liposomes suggest that polymersomes can incorporate, segregate, and disperse functional elements that are both larger and more morphologically diverse than that demonstrated to date in liposomes. Developing multi-component solar energy-transducing polymersomes requires fundamental studies of the electronic, optical, and photophysical properties of polymersomes that contain functional electrooptic elements. Within polymersome membrane environments, long polymer chains constrain ethyne-bridged oligo(porphinato)zinc(II) based supermolecular fluorophore (**PZn_n**) conformeric populations and disperse these **PZn_n** species within the hydrophobic bilayer. Ultrafast excited-state transient absorption and anisotropy dynamical studies of NIR-emissive polymersomes in which the **PZn_n** fluorophore loading per nanoscale vesicle is varied between 0.1-10 mole %, enable the exploration of concentration-dependent mechanisms for nonradiative excited-state decay. These experiments correlate fluorophore structure with its gross spatial arrangement within specific nanodomains of these nanoparticles, and reveal how compartmentalization of fluorophores within reduced effective dispersion volumes impacts bulk photophysical properties. As these factors play key roles in determining the energy transfer dynamics between dispersed fluorophores, this work underscores that strategies that modulate fluorophore and polymer structure to optimize dispersion volume in bilayered nanoscale vesicular environments will further enhance the emissive properties of these nanoscale constructs.

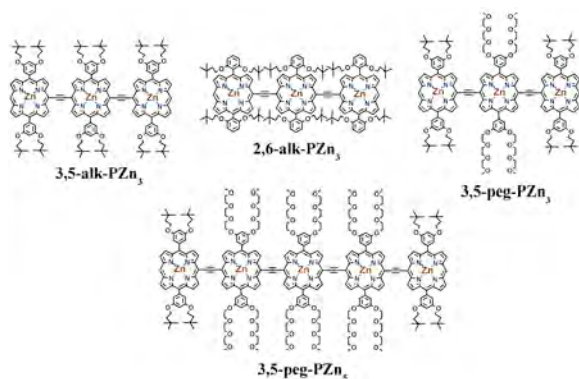
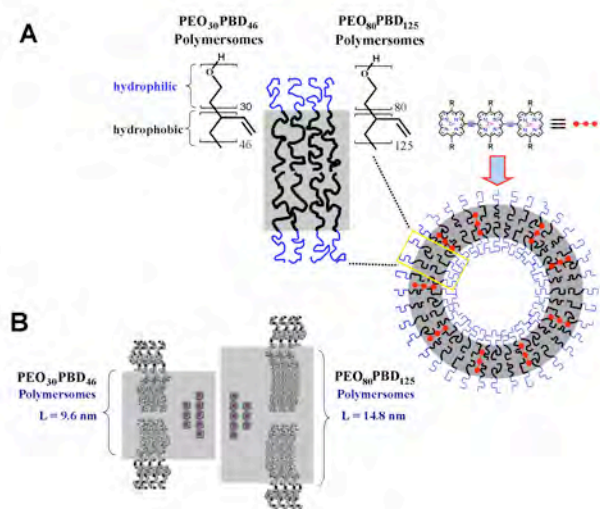
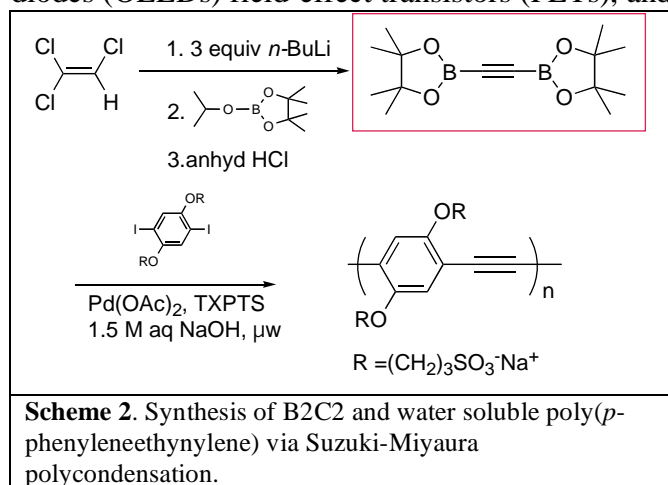


Chart 1. Structures of ethyne-bridged porphyrin arrays **3,5-peg-PZn₃**, **3,5-alk-PZn₃**, **2,6-alk-PZn₃** and **3,5-peg-PZn₅**



Scheme 1. (A) Depiction of **PZn₃** fluorophore dispersion within PEO-PBD NIR-emissive polymersome environments. (B) Hydrophobic bilayer thicknesses (*L*) of **PEO₃₀-PBD₄₆** and **PEO₈₀-PBD₁₂₅** polymersomes; generic **PZn₃** and **PZn₅** fluorophores are also shown, to scale, for comparison.

Synthesis of Water-Soluble Poly-(p-phenyleneethynylene) in Neat Water Under Aerobic Conditions via Suzuki-Miyaura Polycondensatin using a Novel Diborylethyne Synthon. Ethyne-bridged conjugated polymers impact a wide-range of technologies; the efficacy of these species derives not only from their established semiconducting and optical properties, but also from the facts that these rigid, rod-like structures are readily processible, and manifest high photo and thermal stabilities. Poly(*p*-phenyleneethynylene)s (PPEs) define the archetypal examples of ethyne-bridged conjugated polymers; these species have been utilized in organic light-emitting diodes (OLEDs) field-effect transistors (FETs), and solar energy conversion devices. As such,



Scheme 2. Synthesis of **B2C2** and water soluble poly(*p*-phenyleneethynylene) via Suzuki-Miyaura polycondensation.

considerable effort has been placed in the development of synthetic protocols for repeating arene-ethyne structural motifs. High efficiency lightweight, flexible solar energy conversion devices will undoubtedly require the elucidation of hole and electron transport media that differ substantially with respect to those delineated to date. The performance of organic conducting and semi-conducting structures is related directly to the nature of the charge/spin carriers, the extent to which these carriers can be spatially delocalized, the factors that control charge (spin) migration dynamics, and the extent and efficiency which these materials

absorb the solar spectrum. In an effort to fabricate a wide range of poly(*p*-arylene-ethynylene)s that feature enhanced electrooptic properties relevant to solar energy conversion, we have developed a novel ethyne synthon, 1,2-bis(4',4',5',5'-tetramethyl[1',3',2']dioxaborolan-2'-yl)ethyne (**B2C2**). We have shown the utility of **B2C2** in the Suzuki-Miyaura polycondensation

reaction, synthesizing a water-soluble poly(*p*-phenyleneethynylene) (**PPES**) from {[2,5-diiodo-1,4-bis(3-propoxy-sulfonicacid) benzene] sodium salt} in neat water under an aerobic atmosphere. This environmentally benign protocol for the preparation of ethyne-bridged conjugated polymers overcomes key drawbacks of commonly employed Sonogashira coupling and acyclic diyne metathesis methods, which include: the introduction of butadiyne defects along the polymer backbone, a requisite inert-atmosphere, and incompatibility of water-solubilizing functional groups with oligomerization reaction conditions. Importantly, this conjugated rigid-rod polymer synthesis represents a unique example in which polymerization, purification, and isolation steps can be accomplished using only H₂O as a solvent; further this approach opens routes to water-soluble, processable optoelectronic materials that have heretofore been inaccessible.

DOE Sponsored Publications 2006-2008:

- (1) Conjugated Chromophore Arrays with Unusually Large Polaron Delocalization Lengths, K. Susumu, P. R. Frail, P. J. Angiolillo, and M. J. Therien, *J. Am. Chem. Soc.* **2006**, *128*, 8380-8381.
- (2) One-Dimensional Diffusion Limited Relaxation of Photoexcitations in Suspensions of Single-Walled Carbon Nanotubes, R. M. Russo, E. J. Mele, C. L. Kane, I.V. Rubtsov, M. J. Therien, and D. E. Luzzi, *Phys. Rev. B.* **2006**, *74*, 0414051-0414054.
- (3) A Temperature-Dependent Mechanistic Transition for Photoinduced Electron Transfer Modulated by Excited-State Vibrational Relaxation Dynamics, Y. K. Kang, T. V. Duncan, and M. J. Therien, *J. Phys. Chem. B.* **2007**, *111*, 6829-6838.
- (4) Synthesis of Water-Soluble Poly-(*p*-phenyleneethynylene) in Neat Water Under Aerobic Conditions via Suzuki-Miyaura Polycondensation using a Diborylethyne Synthon, Y. K. Kang, P. Deria, P. J. Carroll, and M. J. Therien, *Org. Lett.* **2008**, *10*, 1341-1344.
- (5) Ultrafast Excited State Dynamics of Nanoscale Near Infrared Emissive Polymersomes, T. V. Duncan, P. P. Ghoroghchian, I. V. Rubstov, D. A. Hammer, and M. J. Therien, *J. Am. Chem. Soc.* Accepted for publication.
- (6) Orientational Dependence of Cofacial Porphyrin-Quinone Electronic Interactions within the Strong Coupling Regime, Y. K. Kang, J. Zheng, I. V. Rubtsov, D. N. Beratan, and M. J. Therien, *J. Am. Chem. Soc.* Submitted.

POTENTIAL OF “MOLECULAR WIRES” FOR SOLAR PHOTOVOLTAICS

John R. Miller, Andrew Cook, Paiboon Sreearunothai, Sadayuki Asaoka, Norihiko Takeda, Sean McIlroy, Julia M. Keller* and Kirk Schanze*

Chemistry Department, Brookhaven National Laboratory, Upton, NY 11973,

*University of Florida, Gainesville, FL.

Long, conjugated molecules can act as semiconducting “molecular wires.” Alone, attached to surfaces or in concert with nanoparticles, they appear to have enormous potential for development of inexpensive solar photovoltaics. A field called “plastic solar,” has created solar cells having efficiencies reaching 5%. To explain our motivation this talk will briefly review that field, which is encountering barriers to the advances that are needed for eventual goal of cheaper-than-oil solar electricity. Fundamental science offers chances to mitigate those barriers. We will argue that popular methods make little use of the potential of conjugated molecules to act as “wires,” due in part to a limited understanding of what that potential is. We argue that past difficulties with transport confines peoples’ thinking. Limitations on transport, particularly for excitons, are almost seen as absolute, although no fundamental basis is known for such a belief; indeed some reports support the hypothesis of long distance transport. Experiments described here seek to understand started how fast charges move in conjugated molecules and whether there are limits to the distances they move without trapping. It will be important to obtain similar information for excitons. We argue that this kind of knowledge about transport of charges and excited states is a wise starting point. We begin in solution where the experiments are more tractable, with the intent to expand our understanding of what is possible. Later steps would confront the questions of how to express these properties in the solid-state, and how to utilize them to create completely new kinds of solar cells. The experiments described here will focus on charge transport through long molecules in fluids and the corresponding molecular properties that determine such transport.

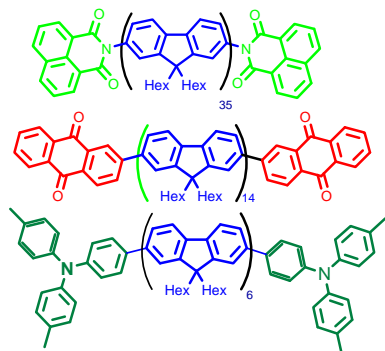
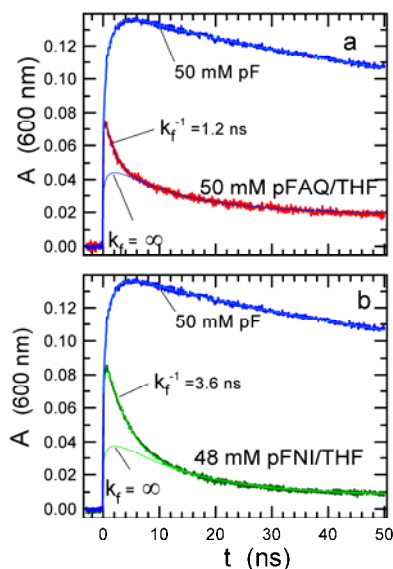
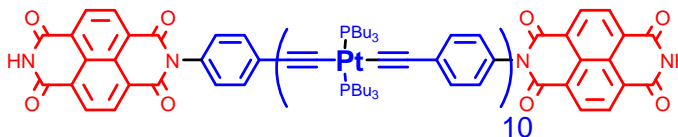


Figure 1 shows structures of conjugated polyfluorenes having charge trapping end caps. The intent is to rapidly inject charges into these molecules and learn whether and how fast the charges can transport of tens of nm or longer to the caps. Measurements with high time resolution have observed the transport within these molecules (Figure 2). Recent application of preparative GPC has given molecules having lengths to 100 nm with moderate polydispersities. Pulse radiolysis at BNL’s Laser Electron Accelerator Facility (LEAF) enables rapid injection of charges into molecules such as these. LEAF’s ~ 5 ps electron pulses are now augmented by the development of a fast, single-shot detection method (UFSS) that allows observation of the behavior of charges with 15 ps time resolution. An additional discovery is that measurable numbers of electrons are attached very rapidly these molecules, bypassing the requirements for diffusion that usually limit the time resolution of charge injection experiments.



These experiments find that electrons transport over distances exceeding 150\AA and perhaps 300\AA in a few ns. While charges are injected randomly along the length of the molecule, the results are consistent with the idea that the dispersion in transport times is due to spread of initial injection sites, without significant contributions from traps, such as “kinks” or chemical defects. In this sense the transport appears to be homogeneous. It appears that a charge created in the “wire” reaches the electron-accepting end cap group with high probability. The results also indicate that end-capping is not complete. At present the precision of the conclusions about homogeneity of transport is limited by the incomplete end-capping and insufficient knowledge of exactly how many end caps are missing.

Similar charge electron transport is also observed in molecules having metal atoms as part of the conjugated chain. Given that the delocalization length is shorter in the platinum-conjugated chains, transport might be expected to be slower. For this molecule, $\text{Pt}_{10}(\text{NDI})_2$, the charge transport to the naphthalenediimide end caps was faster than observations, $k > 7 \times 10^9 \text{ s}^{-1}$, based on experiments with 125 ps time resolution. The UFSS method will be applied to this molecule pending instrumental modifications. This and similar molecules with $n < 10$, are oligomers, having a definite number of repeat units and complete end-capping.



Another oligomer investigated in collaboration with H. Imahori and Y. Shibano has up to sixteen fluorene repeat units and fullerene end caps. Electron transport is fast, but measurable using the UFSS method. The Pt containing and fullerene capped oligomers appear to have faster charge transport than the polymers having similar lengths described above. These oligomers are different in having a) 100% end capping b) definite lengths and c) electron-trapping end caps that are not conjugated to the chains, but are connected through saturated linkages.

Near-term future plans include a characterization of charge transport in end-capped polyfluorenes as a function of length to 100 nm in polar fluids. We will seek methods to obtain more complete end capping or to develop separations techniques to remove those molecules not having end caps. Also sought will be new molecules or methods to determine charge transport in non-polar media and in solids. We will apply the UFSS to measurement of electron transfer rates in small molecules. We will also investigate electron transfer in small molecules. Unusual features of charge attachment to benzoquinone will be explored with a method that may be capable of continuously tuning energetics to electron attachment reactions over $\sim 200 \text{ meV}$ free energy change. Application of this method will provide insight into the possibility that electron transfer to create the lowest excited state is forbidden because it requires a two-electron transition.

DOE Sponsored Publications 2006-2008

- (1) Rate and driving force for protonation of aryl radical anions in ethanol, Funston, A. M.; Lyman, S. V.; Saunders-Price, B.; Czapski, G.; Miller, J. R. *Journal of Physical Chemistry B* **2007**, *111*, 6895-6902.
- (2) Radical ion states of platinum acetylide oligomers, Cardolaccia, T.; Funston, A. M.; Kose, M. E.; Keller, J. M.; Miller, J. R.; Schanze, K. S. *Journal of Physical Chemistry B* **2007**, *111*, 10871-10880.
- (3) Nature and energies of electrons and holes in a conjugated polymer, polyfluorene, Takeda, N.; Asaoka, S.; Miller, J. R. *Journal of the American Chemical Society* **2006**, *128*, 16073-16082.
- (4) Spectroscopy and transport of the triplet exciton in a terthiophene end-capped poly(phenylene ethynylene), Funston, A. M.; Silverman, E. E.; Schanze, K. S.; Miller, J. R. *Journal of Physical Chemistry B* **2006**, *110*, 17736.
- (5) Electron and Hole Transport to Trap Groups at the Ends of Conjugated Polyfluorenes, Sadayuki Asaoka, Norihiko Takeda, Tomokazu Iyoda, Andrew R. Cook and John R. Miller (submitted).

Session X

Photosynthetic Systems II

REGULATION OF THE ELECTRON TRANSFER PATHWAYS IN NATURAL PHOTOSYNTHESIS

Oleg G. Poluektov, Lisa M. Utschig, and David M. Tiede
Chemical Sciences and Engineering Division
Argonne National Laboratory
Argonne, IL 60439

Our research is focused on investigation of fundamental mechanisms for solar energy conversion in natural photosynthesis. By understanding structure-function relationships in biological photosynthesis we can establish principles for the design of biomimetic systems for solar energy conversion.

Early photosynthetic events involve light-induced electron transfer (ET) between donor-acceptor molecules (cofactors) embedded within highly structured matrices in reaction center (RC) proteins. RCs are unique examples of molecular systems in which both the cofactors and the surrounding media are tuned for optimized solar energy conversion. Here we describe our research which addresses the protein's role in controlling and defining optimal pathways for proton-coupled ET reactions. Our experimental approach includes the application of a suite of advanced, multi-frequency, time-resolved magnetic resonance techniques together with capabilities to prepare specialized RC samples. Our close interactions and collaborations with Argonne and external colleagues bring the essential complementary research techniques and additional tailored samples. These include transient optical and X-ray techniques, natural and artificial photosynthetic model systems.

Background. The key reaction of photosynthetic energy conversion involves rapid, sequential electron transfer steps resulting in charge separation. In the RC of *Rhodobacter sphaeroides* an electron is transferred within 200 ps from the excited singlet state of the primary donor P through an intervening bacteriopheophytin acceptor, H_A , to the primary quinone acceptor Q_A , forming the metastable charge separated state, $P^+Q_A^-$. This state can decay either by back recombination to the ground state PQ_A or by forward ET from Q_A^- to the membrane-diffusible electron carrier quinone, Q_B . Following two subsequent ET events and the uptake of two protons, Q_B is reduced to its hydroquinone. The resulting proton gradient across the membrane drives ATP synthesis.

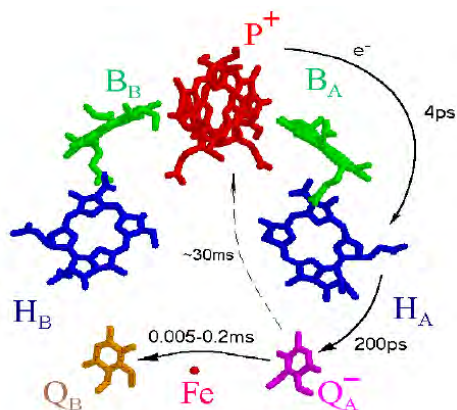


Figure 1. Arrangement of cofactors of the RC as revealed by X-ray crystallography.

Conformational gating of interquinone ET. It is well established that the $Q_A^-Q_B \rightarrow Q_AQ_B^-$ ET is a conformationally gated reaction. The nature of the gate remains unclear. Previously we demonstrated that the earlier proposed movement of Q_B from the “proximal” to the “distal” site is not a gate for interquinone ET. Can it be that Q_A is involved in this conformational gating? Using advanced time-resolved (TR) high-frequency (HF) EPR techniques (in collaboration with G. Kothe, Freiburg University) we found that the geometry of Q_A^- , observed on a nanosecond time scale after light-induced ET to Q_A , deviates from the Q_A geometry determined by X-ray diffraction analysis. This observation suggests that the

conformational state of Q_A possibly plays an important role in forward ET. We proposed that at longer times after photo-excitation of the RC, the geometry of Q_A^- relaxes to that determined by X-ray diffraction. Thus this light-induced reorientation of Q_A^- in its binding pocket might be a rate limiting step of the interquinone ET reaction. This model logically accounts for the striking “Kleinfeld effect”: ET from Q_A^- to Q_B proceeds in RCs cooled to cryogenic temperature under illumination but does not proceed in RCs cooled in the dark.

In order to assess our model and examine possible reasons for the different Q_A geometries obtained from TR EPR vs. X-ray crystallography, we have performed a systematic study of the effects of radiation on Fe-removed/Zn-replaced RC crystals using HF (130 GHz) EPR spectroscopy. Our experiments demonstrate that radiation induces free radical formation and subsequent bond breakage as well as cofactor oxidation state changes that alter the native activity of the protein. We suggest that radiation induced reduction of the quinones can provide an explanation for the multiplicity of quinone binding sites observed in RC crystal structures, and for discrepancies between spectroscopic and crystallographic measurements of quinone site structures.

Imaging ET pathways in the photosynthetic RC. Protein reorganization around Q_A and H_A is believed to be an important factor in controlling ET from P to Q_A and stabilization of $P^+Q_A^-$. Recently we reported a new method to potentially reconstruct the delocalization of the donor and acceptor wave functions through the protein. This affords the possibility to locate probable ET pathways, i.e., through the nuclei having maximum overlap of the donor and acceptor wave functions. The method is based on a new phenomenon we detected in the TR electron-nuclear double resonance (ENDOR) spectra of the spin-correlated radical pairs (SCRPs) in photosynthetic RCs. The observed effects result from both the increased spectral resolution and orientational selectivity provided by HF EPR and are manifest as narrowing of the ENDOR lines resulting in substantially increased spectral resolution.

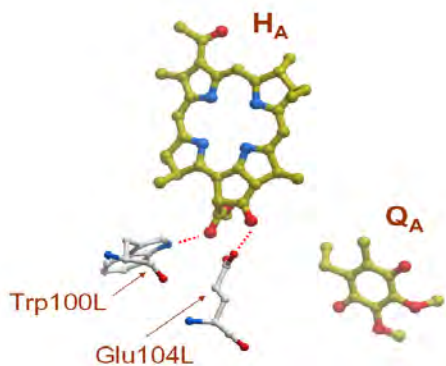


Figure 2. H-bonds (dotted lines) between pheophytin (H_A) and Trp100L, Glu104L are identified as probable bridges in ET between P and Q_A .

hypothesis that matrix relaxation responsible for regulation of ET step leading to stabilized charge separation in the bacterial RCs occurs around the pheophytin cofactor.

In the future we will extend our research of the protein’s role in controlling and defining optimal pathways for ET reactions on genetically modified RCs, RC samples freeze trapped in different conformational states, photosystem I, and model biomimetic ET systems where proton-coupled ET plays an important role for stabilization of charge separated states.

DOE Sponsored Publications 2006-2008

1. Thurnauer, M. C., Poluektov, O. G., and Kothe G. (2008) High-Field EPR Studies of Electron Transfer Intermediates in Photosystem I. In: Advances in Photosynthesis and Respiration Series, Vol. 24, (Golbeck, J., H., ed) Photosystem I: The Light-Driven Plastocyanin: Ferredoxin Oxidoreductase, pp. 339-360. Springer, Dordrecht, The Netherlands.
2. Raitsimring, A. M., Astashkin, A. V., Baute, D., Goldfarb, D., Poluektov, O. G., Lowe, M. P., Zech, S. G., and Caravan, P. Determination of the Hydration Number of Gadolinium(III) Complexes by High-Field Pulsed ^{17}O ENDOR Spectroscopy, *ChemPhysChem*, 2006, 7, 1590-1597.
3. Smirnova, T. I., Chadwick, T. G., MacArthur, R., Poluektov, O., Song, L., Ryan, M., and Bankaitis, V. A. The Chemistry of Phospholipid Binding by the *Saccharomyces cerevisiae* Phosphatidylinositol Transfer Protein Sec14p as Determined by Electron Paramagnetic Resonance Spectroscopy, *J. Biol. Chem.*, 2006, 281, 34897-34908.
4. Dimitrijevic, N. M., Poluektov, O. G., Saponjic, Z., and Rajh, T. Complex and Charge Transfer between TiO_2 and Pyrroloquinoline Quinone, *J. Phys. Chem. B*, 2006, 110, 25392-25398.
5. Saponjic, Z. V., Dimitrijevic, N. M., Poluektov, O., Chen, L. X., Wasinger, E., Welp, U., Tiede, D., Zuo, X., and Rajh, T. Charge Separation and Surface Reconstruction: A Mn^{2+} Doping Study, *J. Phys. Chem. B*, 2006, 110, 25441-25450.
6. Dubinskij, A. A., Utschig, L. M., and Poluektov, O. G. Spin-Correlated Radical Pairs: Differential Effect in High-Field ENDOR Spectra, *Appl. Magn. Reson.*, 2006, 30, 269-286.
7. Smirnova, T. I., Smirnov, A. I., Pachtchenko, S., and Poluektov, O. G. Geometry of Hydrogen Bonds Formed by Lipid Bilayer Nitroxide Probes: A High Frequency Pulsed ENDOR/EPR Study, *J. Am. Chem. Soc. (Communication)*, 2007, 129, 3476-3477.
8. Smirnova, T. I., Chadwick, T. G., Voinov, M. A., Poluektov, O., van Tol, J., Ozarowski, A., Schaaf, G., Ryan, M. M., and Bankaitis, V. A. Local Polarity and Hydrogen Bonding Inside Sec14p Lipid-binding Cavity: High-Field Multifrequency EPR Studies, *Biophys. J.*, 2007, 92, 3686-3695.
9. Poluektov, O. G., Utschig, L. M., Thurnauer, M. C., and Kothe, G. Exploring Hyperfine Interactions in Spin-Correlated Radical Pairs from Photosynthetic Proteins: High-Frequency ENDOR and Quantum Beat Oscillations, *Appl. Magn. Reson.*, 2007, 31, 123-143.
10. Ponomarenko, N., Poluektov, O., Li, L., Bylina, E., Ismagilov, R., and Norris, J. Structural Aspects of Interactions Between the Primary Donor and Cytochrome in Heterodimer Mutant Reaction Centers of *Blastochloris viridis*, *Photosyn. Res.*, 2007, 91, 142.
11. Poluektov, O., Utschig, L., Paschenko, S., Lakshmi, K., and Tiede, D. Time-Resolved High-Field EPR Spectroscopy of Natural Photosynthesis: Photoinduced Electron Transfer Pathways in Photosystem I, *Photosyn. Res.*, 2007, 91, 150-151.
12. Lakshmi, K., Poluektov, O., Lee, S., Chand, S., and Wagner, A. Snapshot of Biological Proton-Coupled Electron-Transfer: Tyrosine Intermediates in Photosystem II, *Photosyn. Res.*, 2007, 91, 176.

13. Dimitrijevic, N. M., Saponjic, Z. V., Rabatic, B. M., Poluektov, O. G., and Rajh, T. Effect of Size and Shape of Nanocrystalline TiO₂ on Photogenerated Charges. An EPR Study, *J. Phys. Chem. C Lett.*, 2007, *111*, 14597-14601.
14. Heinen, U., Utschig, L. M., Poluektov, O. G., Link, G., Ohmes, E., and Kothe, G. Structure of the Charge Separated State P⁺₈₆₅Q⁻_A in the Photosynthetic Reaction Centers of *Rhodobacter sphaeroides* by Quantum Beat Oscillations and High-Field Electron Paramagnetic Resonance: Evidence for Light-Induced Q⁻_A Reorientation, *J. Am. Chem. Soc.*, 2008, *129*, 15935-15946.
15. Kothe, G., Norris, J. R., Poluektov, O. G., and Thurnauer, M. C. (2008) High-Time Resolution Electron Paramagnetic Resonance - Study of Quantum Beat Oscillations Observed in Photosynthetic Reaction Center Proteins. In: *Advances in Photosynthesis and Respiration Series*, Vol. 26, (Matysik, J., and Aartsma, T., J., eds) *Biophysical Techniques in Photosynthesis*, Springer, Dordrecht, The Netherlands.
16. Poluektov, O. G. and Utschig, L. M. (2008) Protein Environments and Electron Transfer Processes Probed with High-Frequency ENDOR. In: *Advances in Photosynthesis and Respiration Series*, Vol. 27, (Hunter, C. N., Thurnauer, M. C., Daldal, F., and Beatty, J. T., eds) *The Purple Phototrophic Bacteria : Genetics, Molecular Biology, Biochemistry and Biophysics*. Springer, Dordrecht, The Netherlands, in press.
17. Utschig, L. M., Chen, L. X., and Poluektov, O. G. Discovery of Native Metal Ion Sites Located on the Ferredoxin Docking Side of Photosystem I, *Biochemistry*, 2008, *47*, 3671-3676.
18. Utschig, L. M., Chemerisov, S. D., Tiede, D. M., and Poluektov, O. G. EPR Study of Radiation Damage in Photosynthetic Reaction Center Crystals, *Biochemistry*, submitted for publication.
19. Moore, G. F., Hamburger, M., Gervaldo, M., Poluektov, O. G., Rajh, T., Gust, D., Moore, T. A., and Moore, A. L. A Bioinspired Construct that Mimics the Proton Coupled Electron Transfer between P680⁺ and the TyrZ-His190 Pair of Photosystem II, *J. Am. Chem. Soc.*, in preparation.

PHOTOACTIVITY AND ELECTRON TRANSFER EXTREMES IN MACROMOLECULAR BIOSYSTEMS

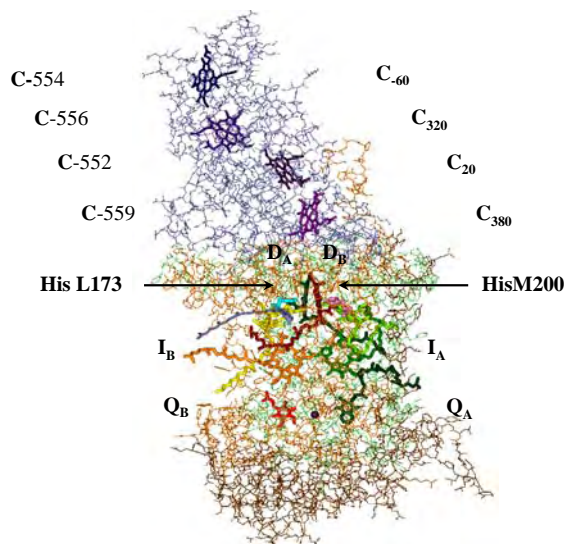
Nina Ponomarenko, Oleg Poluektov*, Petersen Hasjim, Anthony Marino, Alice Wang, Alec Block, Elzbieta Gasyna, Zbigniew Gasyna, and James Norris

Department of Chemistry
University of Chicago
Chicago IL 60637

*Chemistry Division
Argonne National Laboratory
Argonne, IL 60439

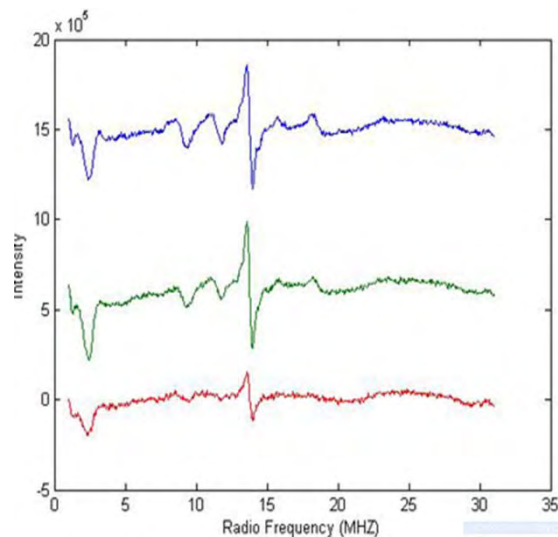
To explore the role of solvent in photoactivity and electron transfer in the solid state, our investigations have explored electron transfer in three extreme systems: 1) the highly photoactive reaction center of *B. viridis* modified by genetic manipulation, 2) the light harvesting complex LH1 of photosynthetic bacteria that exhibits low temperature electron transfer but no photoactivity, and 3) the natural biopolymer melanin which exhibits some photoactivity but more importantly protects against oxidative damage. Each system offers insight into different aspects of photoactivity and electron transfer.

1) The reaction center of *B. viridis* is a sophisticated molecular wire. The tightly bound cytochrome c of the RC complex from *B. viridis* contains four hemes that differ in their reduction potentials and optical and EPR spectra. They are arranged in a linear sequence of potentials P–C₃₈₀–C₂₀–C₃₂₀–C₆₀ running through the long axis of the protein (adjacent figure). As revealed by the X-ray structure along with the amino acid sequence, three hemes are His–Met

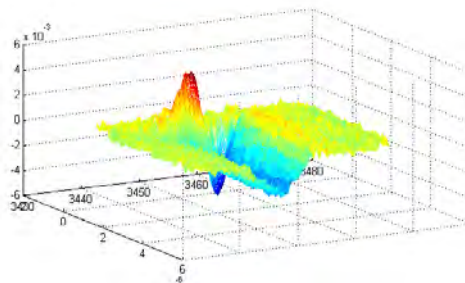


coordinated and the fourth is bis–His coordinated. Oligonucleotide–mediated mutagenesis has been employed to produce two symmetry–related mutants of photosynthetic bacterium *B. viridis*. Histidine residues associated with the central Mg²⁺ ions of the two bacteriochlorophylls (Bchls) of the special pair primary donor (His–L173 or His–M200) have been replaced with leucine, affording bacteriochlorophyll/bacteriopheophytin heterodimers. The reaction centers isolated from mutants were characterized by EPR as well as optical absorption spectroscopy. The changes in photoinduced electron transfer resulting from the presence of the heterodimer are revealed by detailed, high–field EPR studies. The various redox stages available in the *B. viridis* reaction center will be described. Studies of these heterodimer mutants contribute to our understanding of electron transfer involving the native special pair primary donor and the functioning of the cytochrome molecular wire.

2) The LH1 photosynthetic antenna is remarkable for lack of photochemical activity and its ability to undergo ‘isoenergetic’ electron transfer in both the liquid and solid states. ENDOR spectra of chemically oxidized LH1 provide additional insights into the dynamics of electron transfer within the LH1 at low temperature (adjacent figure). As the EPR line width decreases with increased fraction of oxidized Bchl, the corresponding ENDOR spectrum characteristic of monomeric Bchl cation diminishes, consistent with more and more electron transfer. Along with diminishing monomeric ENDOR signals, no additional ENDOR peaks appear for electrons delocalized in two or three Bchls. The absence of additional ENDOR signals such as those that arise from the special-pair cation of the reaction center suggests that electron transfer in LH1 is thermally activated. When the fraction of oxidized Bchls in LH1 is small, the energy level gap between the adjacent Bchls of LH1 is relatively large. Consequently, a high probability exists for cations to be trapped in sites that do not have sufficient thermal energy to move to a neighboring Bchl. As the fraction of Bchls oxidized in LH1 increases, the average number of spins in LH1 increases, the average energy gap decreases and so fewer and fewer spins are trapped in particular Bchls. The random movement of un-trapped holes prevents detection by ENDOR. Uniformity in the protein environment of the Bchl cations is the key to efficient ‘isoenergetic’ electron transfer in the solid state.



3) An important issue in solar energy trapping and storage is long-term photochemical stability. In solar energy devices light can also damage both the active components as well as the packaging matrix. Protection from light generated redox stress is a challenging issue, especially if the lifetime of a solar conversion device is expected to exceed 10 years. Nature not only has an example of efficient solar energy harvesting in photosynthesis but also provides a paradigm of highly effective photo-protection in the melanins. The melanins exhibit complex, low-yield photochemistry and excellent antioxidant properties. Melanin protects against photochemistry by converting radiation into heat and by scavenging reactive oxygen species. However, melanin can also produce dangerous superoxide. Semiquinone-like free radicals of melanin are formed in low yield by light and are detectable by time resolved EPR (TREPR) (adjacent figure). TREPR spectra of melanin irradiated with light exhibit complex electron spin polarization that can be used to unravel the Jekyll-Hyde photochemistry of the melanins. The ultimate goal of these studies is to understand how melanin provides photoprotection versus photodamage using TREPR and static magnetic fields. The antioxidant principles uncovered in melanin are expected to be useful in providing long term stability for solar energy devices.



DOE Sponsored Publications 2006–2008

1. Das, R., M. K. Bowman and J.R. Norris, Simplification of complex EPR spectra by cepstral analysis, *Journal of Physical Chemistry, A* 111, 4650–4657 (2007).
2. Hasjim, P. L. and J. R. Norris, Electron spin polarization of radical pairs in simple molecular wires, *Journal of Physical Chemistry C*, 111, 5203–5210 (2007).
3. Ostafin, A. E.; Popova, J. A.; Payne, C. K.; Mizukami, H., and J.R. Norris, Temperature dependent UV–Vis spectral changes in hydrogen– and deuterium–bonded photosynthetic reaction centers of *Rhodohacter sphaeroides*, *Photosynthetica* 44, 433–438 (2006).
4. Kobori, Y. and J. Norris, 1D Radical Motion in Protein Pocket: Proton–Coupled Electron Transfer in Human Serum Albumin, Communication, *J. Am. Chem Soc.* 128, 4–5 (2006).
5. Baxter, R. H. G., E. Krausz and J. R. Norris, Photoactivation of the photosynthetic reaction center of *B. viridis* in the crystalline state, *J. Phys. Chem. B.* 110, 1026–1032(2006).

Session XI

Quantum Particles for Solar Photoconversion

FEMTOSECOND KERR-GATED FLUORESCENCE MICROSCOPY

L. Gundlach, L. Schneemeyer, M. Myahkostupov and P. Piotrowiak
Department of Chemistry
Rutgers University
Newark, New Jersey 07102

We present a Kerr-gated microscope capable of collecting 2D fluorescence images of films, nanowires and molecules with sub-100 fs resolution. The chief objective of developing the described instrument was to bridge the temporal resolution gap between the bulk femtosecond pump-probe experiments and time-resolved microscopy. The approach is simple and involves the insertion of a nonlinear optical Kerr gate into the output pathway of a wide-field microscope. In addition to the dramatically improved temporal resolution, the wide-field design allows simultaneous tracking of several molecules or nanoparticles and ultrafast lifetime imaging of heterogeneous surfaces. Kerr gating relies on transient birefringence induced by a laser pulse in a nonlinear medium placed between crossed polarizers. The collected emission light passes through the Kerr shutter only when the gating pulse is incident upon the medium. The transmitted light is detected by a CCD camera. By delaying the gating pulse with respect to the excitation pulse in the same fashion as in ultrafast pump-probe experiments, the time evolution of the imaged object, $I(x,y;t)$, can be followed and the emission decays can be assembled. In addition to the time resolved imaging mode of operation, the Kerr-gated microscope can be arranged in a spectrally dispersed configuration and function as a femtosecond fluorescence spectrometer.

Several preliminary examples of the application of the ultrafast microscope will be reported. The ultimate temporal resolution of the setup was tested by collecting Kerr-gated plasmon emission images of a cluster of 40 nm Au nanoparticles on SiO₂ (Fig.1). The measurements yielded plasmon lifetime of less than 60 fs. This value is consistent with the ultrafast dephasing in metals due to the very rapid e-e scattering.

One of the key applications of microscope will be the study of exciton localization and carrier transport in semiconductor nanowires, ‘nanobelts’ and carbon nanotubes. We monitored

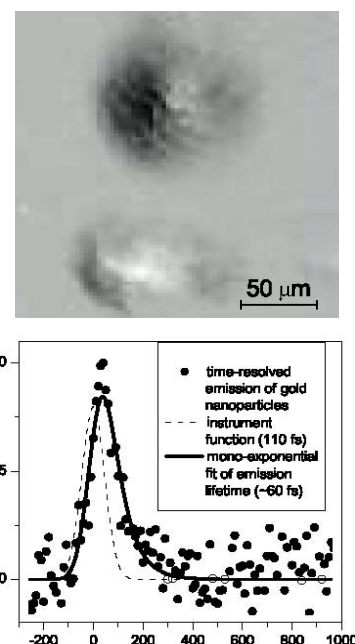


Fig.1. Gated image of a cluster of Au-nanoparticles (top) and the plasmon emission lifetime of ~60 fs (bottom).

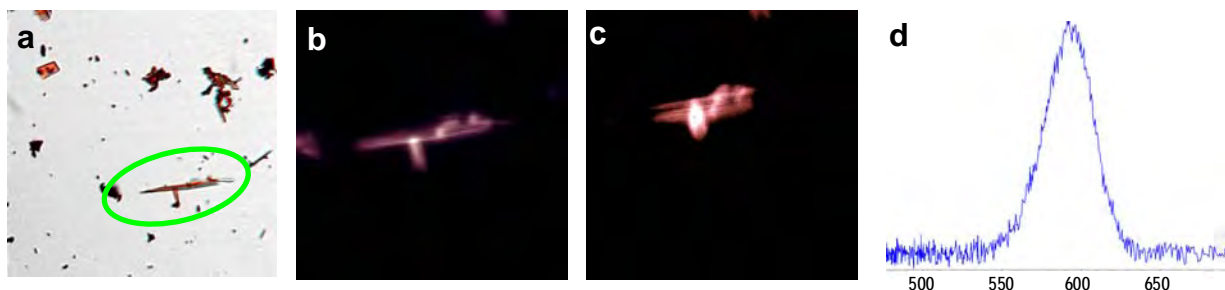


Fig.2. (a) A 50 μm long CdS_xSe_{1-x} nanobelt; (b and c) emission images collected without and with the Kerr gate assembly in the light path; (d) CW emission spectrum of a single nanobelt collected using the microscope.

the exciton dynamics in a single ‘nanobelt’ of the mixed chalcogenide, $\text{CdS}_x\text{Se}_{1-x}$ (Fig.2). Complex, multicomponent dynamics, with a strong, nonlinear dependence on the excitation power has been observed. On the basis of the correlation between the temporal evolution of the image and that of the fluorescence spectrum (Fig.3a and 3b) this behavior is tentatively ascribed to exciton relaxation and subsequent carrier transport to the trapping sites. Different models consistent with the presence of the prompt emission and the delayed red-shifted component are being considered.

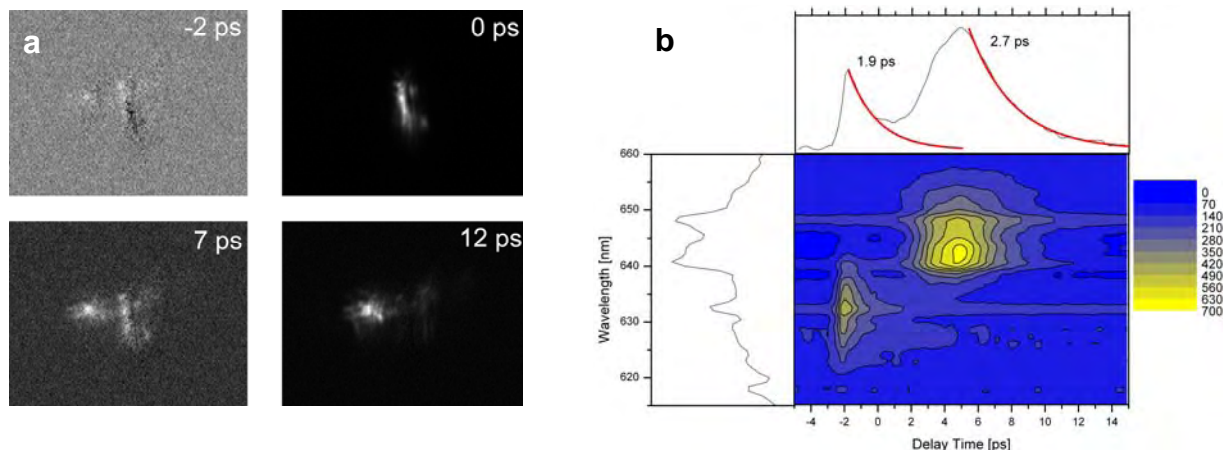


Fig.3. (a) Kerr-gated temporal evolution of the fluorescence image of the $\text{CdS}_x\text{Se}_{1-x}$ nanobelt shown in Fig. 2a 2b and 2c; (b) spectrally and temporally resolved fluorescence of the same object.

The time evolution of the fluorescence image of the ‘nanobelt’ in Fig. 2 and 3 will be shown in a film with ~ 200 fs frame resolution. The complex behavior of a single light emitting ‘nanobelt’ underscores the importance of imaging methods which combine high temporal, spatial and spectral resolution. Further experiments on the $\text{CdS}_x\text{Se}_{1-x}$ system, including variable temperature and polarization dependence measurements, are in progress.

Lastly, we report the results of a separate project, in which strong vibrational state dependence of interfacial electron transfer between the short-lived S_1 state of a surface bound azulene chromophore and colloidal TiO_2 was observed. Two distinct regimes were found: a low energy one corresponding to the injection into trap states and a high energy one, which corresponds to the injection into the bulk conduction band of the semiconductor. The state dependent injection is achieved in a straightforward manner by tuning the wavelength of the femtosecond excitation pulse across the S_0 - S_1 band. Thanks to the well defined vibronic structure of the absorption band and the wide separation between S_1 and S_2 electronic states, the effect can be unambiguously attributed to the amount of vibrational excitation deposited in the system.

The energy of the S_1 state and azulene’s redox potential indicate that the S_1 state lies very close to the conduction band edge of TiO_2 . As a consequence, with appropriate adjustment of the excited state oxidation potential, it ought to be possible to achieve exoergic electron injection from the higher vibrational levels of the S_1 state, while injection from the lower vibrational states would remain endoergic. Indeed, we were able to attain the desired matching of energy levels in 6-methylazulene-2-carboxylic acid (Fig.4). This molecule exhibits a sharp, ~ 5 -fold increase of the electron injection yield when excited at ~ 0.45 eV above the origin of the S_1 band. The amount of necessary excess energy is approximately equivalent to 3 quanta of the skeletal breathing mode

of azulene. The dependence of the yield and rate of an interfacial redox process on the excess vibrational energy deposited into the molecular chromophore has interesting implications for photovoltaic materials and hybrid molecular/solid state electronic devices.

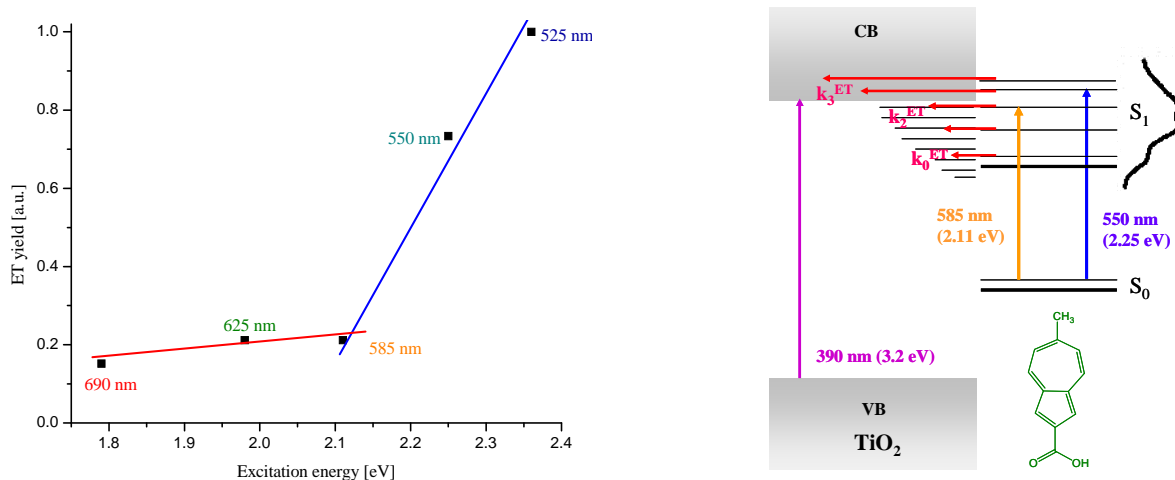


Fig. 4. Dependence of electron injection from the short-lived S_1 state of azulene into the conduction band of colloidal TiO_2 on the excess vibrational excitation energy.

DOE Sponsored Publications 2006-2008

1. *Femtosecond Kerr-Gated Wide-Field Fluorescence Microscopy*, L. Gundlach, P. Piotrowiak, *Opt. Lett.*, in print.
2. *Novel Setup for Time-Resolved Fluorescence Microscopy*, L. Gundlach, P. Piotrowiak, *Proc. SPIE 6643*, 66430E1-E7, 2007.
3. *Ru(II)-bpy Complexes Bound to Nanocrystalline TiO_2 Films Through Phenyleneethynylene Linkers: Effect of the Linkers Length on Electron Injection Rates*, M. Myahkostupov, P. Piotrowiak, D. Wang, E. Galoppini, *J. Phys. Chem. C*, 2007, *111*, 2827.
4. *Inhomogeneity of Electron Injection Rates in Dye-Sensitized TiO_2 : Comparison of the Mesoporous Film and Single Nanoparticle Behavior*, T.D.M. Bell, C. Pagba, M. Myahkostupov, J. Hofkens, P. Piotrowiak, *J. Phys. Chem. B.*; 2006; *110*, 25314-25321.
5. *Inhomogeneity of Electron Injection Rates in Dye-Sensitized TiO_2 : Continuous Mesoporous Films and Single Particle Behavior*, T.D.M. Bell, C. Pagba, M. Myahkostupov, J. Hofkens, P. Piotrowiak, *Proc. SPIE 6325*, 63250X-X7, 2006.

MULTIPLE EXCITON GENERATION: SILICON QDS, QD ARRAYS, QD SOLAR CELLS, AND CONTROVERSY

A.J. Nozik, M.C. Beard, R.J. Ellingson, M. Law, J.M. Luther, J.C. Johnson, Q. Song, M.C. Hanna, and J.E. Murphy
National Renewable Energy Laboratory
Golden, CO 80401

We have observed very efficient multiple exciton generation (MEG) in PbSe, PbS, PbTe, and Si colloidal nanocrystals (quantum dots (QDs)) at threshold photon energies of 2-3 times the HOMO-LUMO transition. For Si, the first indirect semiconductor exhibiting MEG and the most important semiconductor for solar cell applications, QDs with a radius about equal to the exciton Bohr radius (5 nm) show only a small blue shift (weak quantum confinement) but still exhibit efficient MEG.. This has very important implications for QD solar cell applications.

Very recently, some controversy has arisen regarding the reproducibility of reported MEG efficiencies in InAs and CdSe QDs. This controversy will be addressed and possible reasons for non-reproducibility of certain measurement techniques will be discussed...

We have studied MEG in close-packed PbSe QD arrays where the QDs are electronically coupled in the films and thus exhibit good carrier mobility. We have demonstrated that the MEG efficiency in such conductive PbSe QD films is comparable to isolated QDs in colloids. This is important since a promising device geometry for MEG solar cells is a 3D QD array forming a film that is the intrinsic region of a *p-i-n* or *metal-i-metal* structure; the extended states formed from the electronically coupled QDs allow the delocalized photogenerated carriers to separate, traverse the film, and be collected at the electrical contacts.. Exchanging the bulky capping ligands used in the QD synthesis with shorter molecules after film formation dramatically increases the carrier mobility of QD films by reducing the interdot spacing while retaining well-passivated surfaces. Distinct excitonic features, similar to that in isolated QDs in solution, are preserved in these electronically- coupled arrays. This is important because one might expect that creating extended states in QD arrays should greatly reduce the MEG QY. The ability to effectively couple QDs without reduction of MEG is very encouraging for the development of novel high-efficiency solar cells employing close-packed arrays of QDs.

A more simple analysis was developed and applied to extract both the MEG efficiency and the absorption cross section of colloidal Si QDs and QD films at the pump wavelength. The ratio of the normalized change in transmission soon after the excitation pulse (3 ps) to that after all Auger recombination is complete (750 ps) is plotted versus photon fluence and the following equation is fit to the data to extract the value of QY and σ :

$$R_{pop} = \frac{\left(\frac{\Delta T}{T_0}\right)_{t=3ps}}{\left(\frac{\Delta T}{T_0}\right)_{t=750ps}} = \frac{J_0 \cdot \sigma \cdot QY \cdot \delta}{1 - \exp(-J_0 \cdot \sigma)}$$

:

where R_{pop} is defined as the ratio of exciton populations at 3 and 750 ps after excitation, J_0 is the photon fluence, σ is the absorbance cross section at the pump wavelength, QY is the number of excitons created per excited QD, and δ is the decrease in single exciton population over the time frame of the experiment. This analysis technique provides a reliable way to accurately determine the QY of exciton generation and also enables the direct measurement of the absorption cross section (σ) of the QDs at the pump wavelength.

We have developed a simple, all-inorganic metal/QD/metal sandwich cell that produces a large short-circuit photocurrent ($\sim 20\text{-}25\text{ mA/cm}^2$) via a Schottky junction at the negative electrode. The PbSe NC film, deposited *via* layer-by-layer (LbL) dip coating, yields an EQE of 65% across the visible and up to 25% in the infrared region of the solar spectrum, with a power conversion efficiency of 2 to 2.5%. Our QD devices produce short-circuit currents equivalent to or perhaps even larger than existing nanostructured solar cells, including the best organic and dye-sensitized devices, without the need for sintering, superlattice order or separate phases for electron and hole transport.

Device fabrication consisted of depositing a 60–300 nm-thick film of monodisperse, spheroidal PbSe QDs onto indium tin oxide (ITO) coated glass using a layer-by-layer dip coating method, followed by evaporation of a top metal contact. Large-area, crack-free and mildly conductive QD films result. The QDs, randomly packed within the films, are covered in adsorbed ethanedithiolate and show *p*-type DC conductivity under illumination. When tested in nitrogen ambient under 100 mW/cm^2 simulated sunlight, EDT-treated devices exhibit large short-circuit photocurrent densities (JSC) and modest open-circuit voltages (VOC) and fill factors (FF), with the most efficient devices yielding $JSC = 20\text{-}25\text{ mA/cm}^2$, $VOC = 240\text{ mV}$, $FF = 0.41$ and an overall efficiency of 2.1 to 2.4%. There are a few drawbacks to the device that deserve mention and future work. First, the Schottky junction is at the back rather than the front contact. This forces us to build relatively thin cells, which makes it difficult to achieve enough light absorption to yield higher EQEs and complicates our search for MEG photocurrent. Applying a small reverse bias during EQE measurements further enhances the photocurrent in the blue, but proper analysis of photoconductive gain is required in order to separate photoconductive gain from MEG to explain the origin of the additional current. It is also necessary to develop the means to prevent oxidation of the QD film in air. Finally, as a Schottky cell our device can produce only a relatively small VOC, in theory little more than $E_g/2q$. A QD *p-n* or *p-i-n* structure would be superior in this respect.

In summary, we report MEG in the most important, abundant, and non-toxic semiconductor (Si) near its optimum QD bandgap for solar conversion efficiency, and we introduced an all-inorganic Schottky junction QD solar cell that produces a large short-circuit photocurrent via dissociation of excitons and separation of free carriers in a single photoactive material. The latter demonstrates that large EQEs are obtainable from QD solar cells without the need for sintering, superlattice order or separate phases for electron and hole transport. Future work will focus on developing a deeper understanding of (1) the MEG process in QDs, the role of surface chemistry, and how to optimize MEG by lowering the threshold photon energy toward $2E_g$ and producing a step-function characteristic versus photon energy, and (2) inter-QD electronic coupling, surface passivation, doping, and junction formation in QD films. .

DOE Sponsored Publications 2006-2008

1. M. C. Hanna and A. J. Nozik, "Solar Conversion Efficiency of Photovoltaic and Photoelectrolysis Cells with Carrier Multiplication Absorbers", *J. Appl. Phys.* **100**, 074510/1-074510/8 (2006).
2. J. E. Murphy, M. Beard, and A. J. Nozik, "Time-Resolved Photoconductivity of PbSe Nanocrystal Arrays", *J. Phys. Chem. B* **110**, 25455-25461 (2006).
3. P. Yu, K. Zhu, A. G. Norman, S. Ferrere, A. J. Frank, and A. J. Nozik, "Nanocrystalline TiO₂ Solar Cells Sensitized with InAs Quantum Dots", *J. Phys. Chem. B* **110**, 25451-25454 (2006).
4. A. Shabaev, Al. L. Efros, and A. J. Nozik, "Multiexciton Generation by a Single Photon in Nanocrystals", *Nano Lett.* **6**, 2856-2863 (2006).
5. J. E. Murphy, M. C. Beard, A. G. Norman, S. P. Ahrenkiel, J. C. Johnson, P. Yu, O. I. Micic, R. J. Ellingson, and A. J. Nozik, "PbTe Colloidal Nanocrystals: Synthesis, Characterization, and Multiple Exciton Generation," *J. Am. Chem. Soc.* **128**, 3241 (2006).
6. Paci, I., J.C. Johnson, X. Chen, G. Rana, D. Popovic, D.E. David, A.J. Nozik, M.A. Ratner and J. Michl, "Singlet Fission for Dye Sensitized Solar Cells: Can a Suitable Sensitizer be Found," *J. Amer. Chem. Soc.* **128**, 16546-16553 (2006).
7. X. Ai, M. C. Beard, K. P. Knutsen, S. E. Shaheen, G. Rumbles, and R. J. Ellingson, Photoinduced Charge Carrier Generation in a Poly(3-hexylthiophene) and Methanofullerene Bulk Heterojunction Investigated by Time-Resolved Terahertz Spectroscopy", **110**, 25462-25471 (2006).
8. C. Engtrakul, Y.-H. Kim, J. M. Nedeljkovic, S. P. Ahrenkiel, K. E. H. Gilbert, J. L. Alleman, S. B. Zhang, O. I. Micic, A. J. Nozik, and M. J. Heben, "Self-Assembly of Linear Arrays of Semiconductor Nanoparticles on Carbon Single-Walled Nanotubes", *J. Phys. Chem. B* **110**, 25153 (2006).
9. Ai, X.; Xu, Q.; Jones, M.; Song, Q.; Ding, S.-Y.; Ellingson, R. J.; Himmel, M.; Rumbles, G., "Photophysics of (CdSe)ZnS Colloidal Quantum Dots in an Aqueous Environment Stabilized with Amino Acids and Genetically-Modified Proteins", *Photochemical & Photobiological Sciences* **6**, 1027 (2007).
10. Luther, J. M.; Beard, M. C.; Song, Q.; Law, M.; Ellingson, R. J.; Nozik, A. J., "Multiple Exciton Generation in Films of Electronically Coupled PbSe Quantum Dots", *Nano Letters* **7**, 1779 (2007).
11. Jones, M.; Metzger, W. K.; McDonald, T. J.; Engtrakul, C.; Ellingson, R. J.; Rumbles, G.; Heben, M. J., "Extrinsic and Intrinsic Effects on the Excited-State Kinetics of Single-Walled Carbon Nanotubes", *Nano Letters* **7**, 300 (2007).
12. Beard, M. C.; Knutsen, K. P.; Yu, P.; Luther, J. M.; Song, Q.; Metzger, W. K.; Ellingson, R. J.; Nozik, A. J., "Multiple Exciton Generation in Colloidal Silicon Nanocrystals", *Nano Letters* **7**, 2506 (2007).
13. Luque, A., A. Martí and A.J. Nozik, "Solar Cells Based on Quantum Dots: Multiple Exciton Generation and Intermediate Bands," *MRS Bull.* **32**, Special Issue on Photovoltaics, 236-241 (2007).
14. Ellingson, R. J., "Solar cells: slicing and dicing photons", *Nature Photonics* **2**, 72 (2008).
15. Law, M., . Luther, J.M. Song, Q., Perkins, C.L., Nozik, A.J. "The Structural, Optical and Electrical Properties of PbSe Nanocrystal Solids Treated Thermally and with Simple Amines" *JACS*, 2008 (in press).

16. Luther, J.M., M. Law, Q. Song, C.L. Perkins, M.C. Beard and A.J. Nozik, “Structural, Optical, and Electrical Properties of Self-Assembled Films of PbSe Nanocrystals Treated with 1,2-ethanedithiol, ACS Nano **2**, 271–280 (2008).
17. Johnson, J.C., Nozik A.J., Chen, X., Rana, G., Paci, I., Ratner, M.A. Michl, J., “Photophysical Properties of Covalently Linked Molecular Dimers Based on Biradicaloids: Evidence for Singlet Fission,” J. Am. Chem. Soc., (2008) to be submitted.
18. Nozik, A.J., “Multiple Exciton Generation in Semiconductor Quantum Dots”, Chem. Phys. Letters, Frontiers in Chemistry, in press (2008).
19. Johnson, J.C. , Gerth, K., Song, Q., James E. Murphy, Arthur J. Nozik , “Ultrafast exciton fine structure relaxation dynamics in lead chalcogenide nanocrystals: Nano Lett, (2008) in press.
20. Luther, J.M., Law, M., Beard, M.C., Song, Q., Reese, M.O., Ellingson, R.J., and Nozik, A.J. “Schottky Solar Cells Based on Colloidal Nanocrystal Films, Nature Materials, (2008) submitted.

PHOTOPHYSICS OF INDIVIDUAL SINGLE-WALLED CARBON NANOTUBES

Lisa J. Carlson, Libai Huang, Hermen Pedrosa, and Todd D. Krauss
Department of Chemistry
University of Rochester
Rochester, New York 14627-0216

Single-walled carbon nanotubes (SWNTs) are tubular graphitic molecules with exceptional and unusual mechanical, electrical, and optical characteristics. Regarding their potential as novel materials for solar energy conversion, SWNTs could play a role as photosensitizers, photogenerators of charge carriers, or charge transport materials. The goal of this project is to develop a more complete understanding of the optical properties of SWNTs, in particular those that are especially relevant to solar photochemistry.

SWNT Fluorescence Efficiency: Despite recent interest in the optical properties of SWNTs, large gaps in the fundamental understanding of their photophysical characteristics remain. In particular, an accurate value for the SWNT fluorescence efficiency has not yet been determined. From a fundamental point of view, a molecule's fluorescence efficiency is one of its most important photophysical parameters, and often influences whether a system incorporating this molecule is selected for development into photonics-based applications. For an ensemble of nanotubes, the fluorescence quantum yield (QY) is extremely low, typically less than 0.1%, which is somewhat surprising given that fluorescence from individual SWNTs can be detected with reasonable signal to noise.

We have determined the fluorescence QY of individual SWNTs, obtained by simultaneously dispersing dilute suspensions of SWNTs and CdTe/ZnS quantum dots (QDs) onto a substrate and monitoring their single-molecule emission by epifluorescence microscopy.

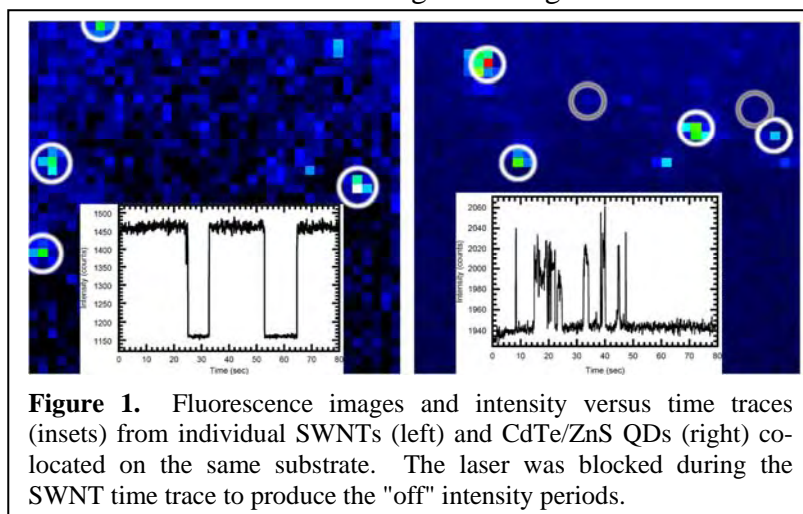


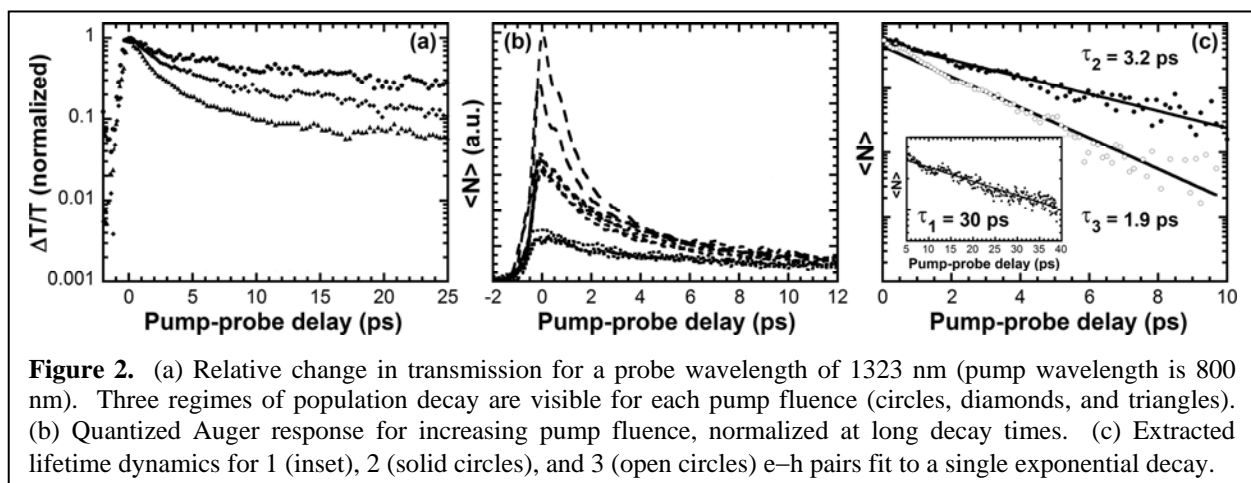
Figure 1. Fluorescence images and intensity versus time traces (insets) from individual SWNTs (left) and CdTe/ZnS QDs (right) co-located on the same substrate. The laser was blocked during the SWNT time trace to produce the "off" intensity periods.

Comparisons between the relative fluorescence intensities of the SWNTs and QDs allowed for a direct determination of the SWNT QY given that the QY of single QDs is well defined. We have found that the SWNT QY is $\sim 3 \pm 1\%$, almost two orders of magnitude larger than that determined for an ensemble. We will discuss whether the measured QY represents an intrinsic property of various nanotube structures, (n,m) , or is influenced by other factors such

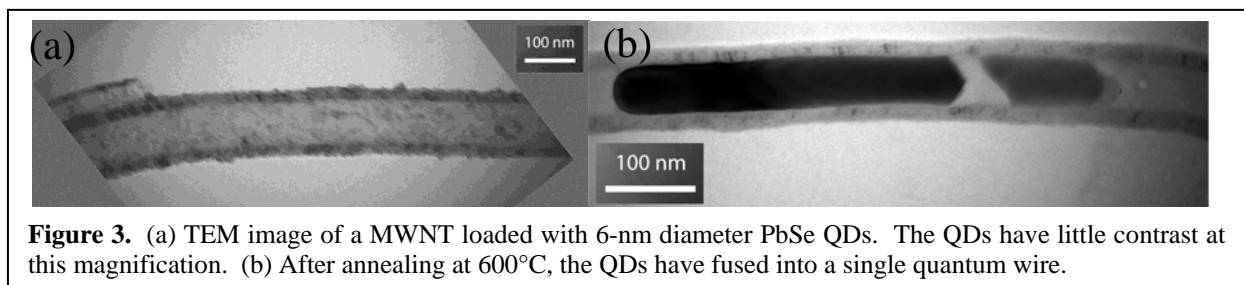
as the local environment, intertube interactions, defects, and "dark" exciton states.

SWNT Excited State Dynamics: Further, it is also not well understood how, and on what timescales, photoexcited excitons in SWNTs relax back to the ground state. To that end,

transient absorption spectroscopy was used to examine the relaxation dynamics of photoexcited nanotubes and to elucidate the nature of the SWNT excited state. Not unexpectedly, SWNT excited state relaxation is complex, spanning timescales covering several orders of magnitude. For SWNT bundles only, very fast initial recovery times (300–500 fs) were observed that corresponded to excited state relaxation through the metallic nanotubes in the bundle. For semiconducting SWNTs, a slower decay component was observed (40–60 ps) that corresponded to electron–hole recombination (Figure 2a). As the excitation intensity was increased, multiple electron–hole pairs were generated in the SWNT; however, these e–h pairs annihilated each other completely in a few picoseconds (Figure 2b,c). Studying the dynamics of this annihilation process revealed the lifetimes for 1, 2, and 3 e–h pair states, which further confirmed that the photoexcitation of SWNTs produces not free electrons, but rather one-dimensional bound electron–hole pairs (i.e., excitons).



Future Directions: SWNTs have absorption transitions in the near infrared and a strong Coulomb interaction between electrons and holes. Thus, these materials are potential good candidates for the generation of multiple excitons from absorption of a single photon (MEG), which is a way of potentially increasing solar cell efficiency as with other nanometer scale materials [1]. We will use ultrafast spectroscopy to generate, detect, and characterize multiple electron–hole pairs in SWNTs through MEG processes. Also, we recently discovered that PbSe QDs loaded inside a multi-walled nanotube (MWNT) will fuse and form extended wire-like crystals upon heating, using the MWNT as a template (Figure 3). We also plan to investigate the photoinduced charge transfer and transport between encapsulated PbSe QDs and quantum wires, and supporting metallic nanotubes (of much narrow diameter) in these hybrid nanostructures.



References

1. A. J. Nozik, "Quantum Dot Solar Cells," *Physica E* **14**, 115–120 (2002).

DOE-Sponsored Publications 2006–2008

1. L. Huang and T. D. Krauss, "Single carbon nanotube photonics and the role of excitons," in Physical Chemistry of Interfaces and Nanomaterials V, Eds: M. Spitler and F. Willig, *Proc. of the SPIE*, 6325, 1–7 (2006).

2. L. J. Carlson, S. E. Maccagnano, J. Silcox, M. Zheng, and T. D. Krauss, "Fluorescence Efficiency of Individual Carbon Nanotubes," *Nano Lett.* **7**, 3698–3703 (2007).

3. L. J. Carlson and T. D. Krauss, "Photophysics of Individual Single-Walled Carbon Nanotubes," *Acc. Chem. Res.* **41**, 235–243 (2008).

4. R. Haggemueller, S. S. Rahatekar, J. A. Fagan, J. Chun, M. L. Becker, R. R. Naik, T. Krauss, L. Carlson, J. Kadla, P. Trulove, D. Fox, Z. Fang, S. Kelley, J. W. Gilman, "A Comparison of Quality of Dispersion of Single Wall Carbon Nanotubes using Different Surfactants and Biomolecules," *Langmuir* (in press, 2008).

5. H. N. Pedrosa and T. D. Krauss, "Fluorescence from Isolated Carbon Nanotubes in Cross-linked Micelles," (submitted, 2008).

6. R. Priefer, K. E. Leach, T. D. Krauss, J. R. Drapo, M. L. Ingalsbe, M. A. van Dongen, J. C. Cadwalader, M. A. Baumler, and M. S. Pinto, "Multilayer Film Preparation of PVPh from Aqueous Media," (submitted, 2008).

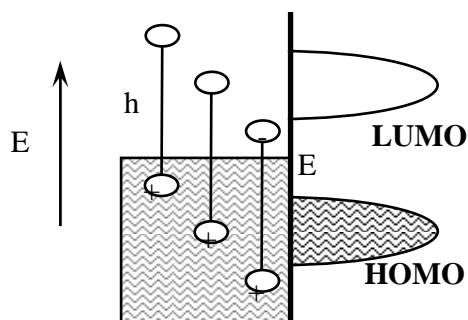
PHOTOVOLTAGE AND HOT ELECTRONS IN SILVER NANOCRYSTALS

Peter Redmond, Xiaomu Wu, Haitao Liu, and Louis Brus
Chemistry Department
Columbia University
New York, NY, 10027

The goal of our DOE research is to create fundamental understanding of how visible light interacts with matter, and how neutral excitations evolve into separated electrons and holes. We specifically focus on metallic nanocrystals, and on metallic carbon nanotubes and graphene. In metallic carbon nanotubes, using a combination of Rayleigh and Raman spectroscopy, we have explored the coupling between vibrations and isoenergetic electron-hole excitations. The graphene program began recently. Graphene has the potential to form an optically transparent, electrically efficient electrode for charge separation and collection in solar cells. Our immediate goal is to understand how Raman spectroscopy can be an informative diagnostic for single sheet graphene -- size, crystallinity, chemical doping, and chemical derivitization. We are also exploring chemical reactions involving graphene, and specifically the fundamental mechanism and reaction intermediates present in reaction with dioxygen. We are also exploring the nature of edge pi electron states on finite graphene pieces.

In my most recent DOE talk I spoke about excitons in carbon nanotubes, and in this talk I focus on photochemical charge separation that can occur following plasmon excitation of Ag nanocrystals.

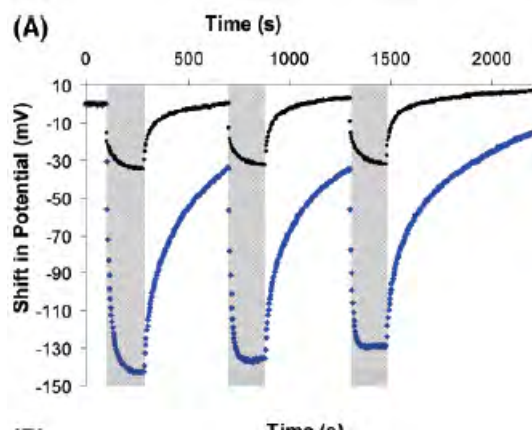
Our DOE work on Ag nanocrystals began in an effort to understand reports of intense, single molecule SERS (Surface Enhance Raman Scattering). Our experimental approach involved confocal microscopic techniques, coupled with topological AFM characterization and white light (dark field) Rayleigh Plasmon optical scattering. We studied SERS signals from single molecules on optically separated Ag nanocrystal groupings. We found that the huge SERS signal comes from molecules at the junctions of ca. 30 nm Ag nanocrystals; Raman enhancements in junctions can be 12 orders of magnitude, while enhancements near single nanocrystals are 5-6 orders of magnitude. This increase in junctions has a clear theoretical origin in the mutual polarization of two almost touching metallic particles. While the plasmon is a volume excitation in a single isolated metallic particle, in two nearly touching nanocrystals the plasmon is a metallic skin excitation in the junction.



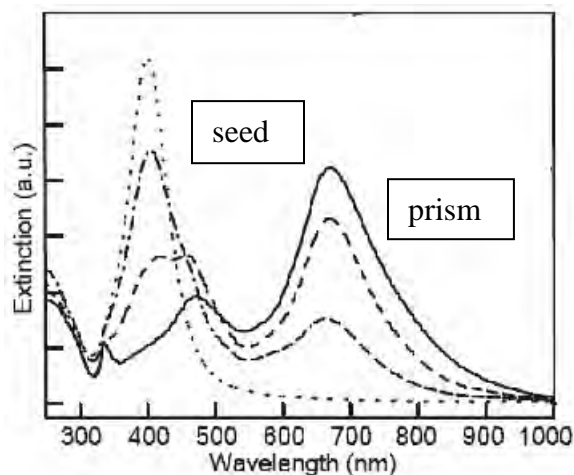
this relaxation is mainly due to surface scattering: volume induced relaxation is slow. If an

Molecules are chemisorbed on Ag and Au nanoparticles. The single molecule SERS blinking appears to represent adsorption-desorption events. Thus electron exchange between irradiated Ag nanocrystals and adsorbed molecules creates a much stronger SERS effect than simple field enhancement at the surface. Optically excited "hot" electrons and holes in the Ag nanocrystal relax to the Fermi level within femtoseconds. It is clear in the literature that

adsorbed molecule has its HOMO or LUMO resonant with a hot hole or electron, the quantum yield can be high for transient carrier capture on the molecule. For example, the low lying pyridine LUMO is resonant with hot electrons at visible wavelengths – this exchange coupling is the reason that pyridine SERS is especially strong. The pyridine anion is stable, and the electron quickly transfers back into the metal at a lower energy. There is no permanent charge transfer.



measured in the open circuit potential. Under steady state illumination photovoltage increases until some reduction process occurs. Ag^+ in solution is easily reduced by the photovoltage, leading to growth in the Ag nanocrystal size. The rate of Ag^+ reduction as a function of photovoltage can be understood using the Butler-Volmer equation.



dimension is determined by the irradiation wavelength via the plasmon spectrum. The process becomes sublinear at relatively low light intensities, apparently due to the low Ag^+ equilibrium concentration. This photovoltage mechanism explains recent experimental results involving single and dual wavelength irradiation, and the core/shell synthesis of Ag layers on Au seeds.

We discovered that adsorbed sodium citrate, a common aqueous stabilizing agent, undergoes irreversible hot hole oxidation when the Ag plasmon is irradiated. In a photo-Kolbe reaction, CO_2 is released when an adsorbed carboxylic acid anion is oxidized. An electron is irreversibly transferred to the colloidal Ag nanocrystal, creating a cathodic photovoltage. This photovoltage is an increase in the double layer potential. If citrate stabilized Ag nanocrystals are adsorbed on an ITO electrode in an electrochemical cell, photovoltage can be directly

Photovoltage allows us to understand the room light induced photo conversion of aqueous 8 nm Ag nanocrystal seeds into 70 nm single crystal plate prisms, due to surface plasmon excitation. The process requires dioxygen, and the transformation rate is first-order in seed concentration. Although citrate is necessary for the conversion, and is consumed, the transformation rate is independent of citrate concentration. The mechanism involves oxidative etching of the Ag seed, creating an Ag^+ concentration ca. 10^{-8} M. Silver ion photoreduces onto an Ag prism that has a large cathodic photovoltage. The lateral prism

DOE Sponsored Publications 2006-2008

- 1) Gordana Dukovic, Milan Balaz, Peter Doak, Nina D. Berova, Ming Zheng, Robert S. Mclean, and Louis Brus "Racemic Single-walled carbon nanotubes exhibit circular dichroism when wrapped with DNA" , *J. Am. Chem. Soc.* *128*, 9004 (2006).
- 2) Peter L. Redmond, Erich C. Walter, Louis E. Brus, "Photo-induced Thermal Copper Reduction onto Gold Nanocrystals Under Potentiostatic Control", *J. Phys. Chem. B* *110*, 25158 (2006)
- 3) Feng Wang, Weitao Liu, Y.Ron Shen, Yang Wu, Matthew Y. Sfeir, Limin Huang, James Hone, Stephen O'Brien, Louis E. Brus, and Tony F. Heinz "Multiphonon Raman Scattering from Individual Single-Walled Carbon Nanotubes" *Phys. Rev. Lett.* *98*, 047402 (2007)
- 4) Peter L. Redmond, Xiaomu Wu and Louis Brus, "Photo-Voltage and Photo-Catalyzed Growth in Citrate Stabilized Colloidal Silver Nanocrystals", *J. Phys. Chem. C*, *111*, 8942 (2007).
- 5) Y. Wu, J. Maultzsch, E. Knoesel, B. Chandra, M. Huang. M. Sfeir, L. Brus, J. Hone, T. Heinz, "Variable Electron-Phonon Coupling in Isolated Metallic Carbon Nanotubes Observed by Raman Scattering", *Phys. Rev. Lett.* *99*, 027402 (2007).
- 6) Peter L. Redmond, Louis E. Brus " "Hot Electron" Photo-Charging and Electrochemical Discharge Kinetics of Silver Nanocrystals", *J. Phys. Chem C* 2007. *111*. 14849-14854.
- 7) Xiaomu Wu, Peter L. Redmond, Haitao Liu, Yihui Chen, Michael Steigerwald, and Louis Brus "Photovoltage Mechanism for Room Light Conversion of Citrate Stabilized Silver Nanocrystal Seeds to Large Nanoprisms" 2008 submitted to JACS
- 8) Li Liu, Sunmin Ryu, Michelle R. Tomasik, Elena Stolyarova, Naeyoung Jung, Mark S. Hybertsen, Michael L. Steigerwald, Louis E. Brus, George W. Flynn "Graphene Oxidation: Thickness Dependent Etching and Strong Chemical Doping" 2008 submitted to Nano Letters

Posters

"ELECTROCHEMICALLY WIRED" SEMICONDUCTOR NANOPARTICLES: TOWARD VECTORAL ELECTRON TRANSPORT IN HYBRID MATERIALS"

Neal R. Armstrong, Jeffery Pyun, S. Scott Saavedra
 Department of Chemistry
 University of Arizona
 Tucson, Arizona 85721
nra@email.arizona.edu

Semiconductor nanoparticles (SC-NPs, e.g. CdSe and related II-VI materials) possess photocatalytic capabilities for hydrogen generation, and can be used as the primary light-absorbing material in emerging photovoltaic technologies – provided that the photo-corrosion of these nanoparticles can be suppressed by sufficiently electron-rich solutions or polymer hosts. Our strategy has been to develop electron-rich thiophene-terminated capping ligands for SC-NPs, which allow us to capture these materials in, or at the surface of, electrodeposited, polymers such as PEDOT or P3HT.

Recent experiments focus on nano-texturing of the electrodeposited polymer host to provide the highest possible surface area for exposure of the “wired” SC-NPs. Pulsed-potential-step (PPS) protocols are effective in controlling the morphology of both PEDOT and P3HT polymer films (Fig. 2). Studies in progress seek to compare the capture efficiency, and photoactivity of SC-NPs using two complementary approaches: (1) the textured polymer host contains electroactive termini which covalently bond with the capping ligands of the SC-NP; (2) the surface of the textured polymer host contains ligand groups which displace ligands (e.g. pyridine) surrounding the SC-NP, providing for NP capture.

UV-photoelectron spectroscopy (UPS) is now routinely used to characterize these frontier orbital energies, using monolayer tethered SC-NPs on Au. Results will be presented which compare frontier orbital energies of the bare SC-NP with those following ligand capping, and comparing those results from studies of capping of the bulk semiconductor (e.g. single crystal CdSe).



Fig. 1 – Schematic view of the photoelectrochemical reaction of an electrochemically “wired” semiconductor nanoparticle, involving hole-capture by an electron-rich polymer host and electron capture by a solution electron acceptor (e.g. H^+).^{1,2,7}

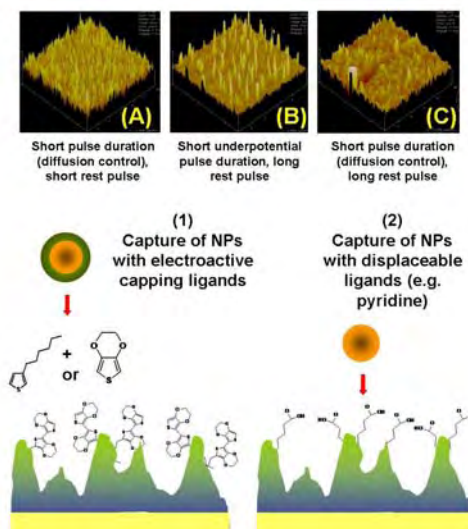


Fig. 2 – (upper) AFM images of textured, electrodeposited poly(thiophene) films as a function of pulse-potential step protocols (lower) Schematic views of SC-NP capture at the surfaces of textured, electrodeposited polymer films. Scenario (1): NP is capped with electroactive ligands and electropolymerized into polymer film in parallel with solution monomers. Scenario (2): The SC-NP is capped with easily displaceable ligands –electrodeposited polymer film is decorated with electroactive monomers terminated in ligands which can capture single monolayers of SC-NPs.

ARE THE ELECTRONIC PROPERTIES OF CONJUGATED POLYMERS DEFORMABLE?

Josh Bolinger, Leonid Fradkin, Kwang-Jik Lee, Rodrigo E. Palacios, and Paul F. Barbara

Center for Nano and Molecular Science and Technology

University of Texas

Austin, TX and 78746

The injection of positive charge carriers (holes) into conjugated polymer chains is a critical process in solar cells based on organic materials and organic/inorganic hybrid materials. We have observed that hole injection into single conjugated polymer chains is light-assisted and highly cooperative. This unprecedented effect may underlie critical, poorly understood organic electronic device phenomena such as the build-up of functional deeply-trapped-charge layers in polymer light emitting displays and the poor fill factors in organic photovoltaic devices.

The charging/discharging dynamics were investigated indirectly by a variety of single molecule fluorescence spectroscopy electro-optical techniques see Fig. 1.

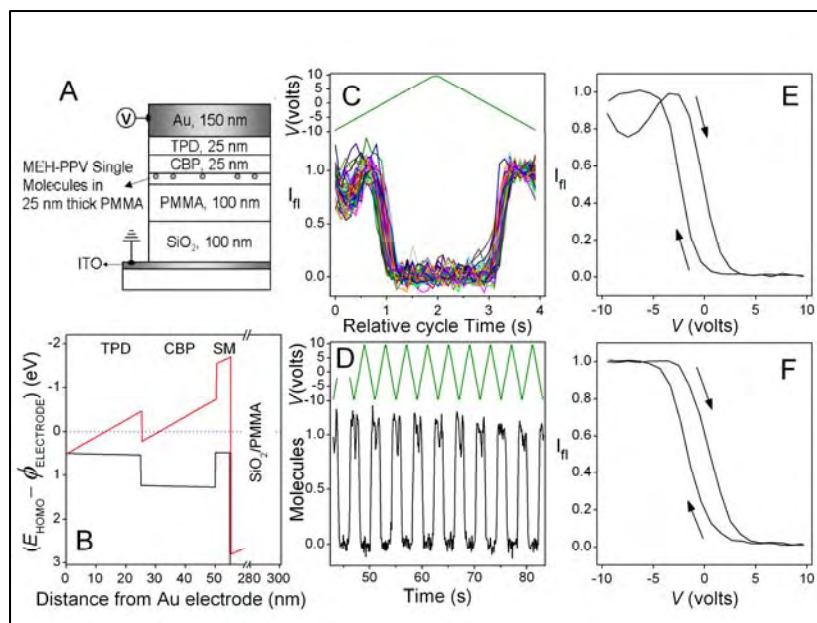


(Fig. 1. (A) Hole-injection device structure. (B) HOMO energy levels relative to the work function of the hole-injection electrode for the device shown in A. The black and red lines are Poisson-Boltzmann simulations at 0V (at equilibrium) and 10V (before charging) respectively. (C) single-molecule fluorescence-intensity trajectories (D) Ensemble average of ~100 single-molecule normalized fluorescence-intensity trajectories obtained while applying a triangular bias (top green line) (E,F) Ensemble average of ~100 single-molecule

F-V trajectories obtained at: high vacuum (10^{-7} Torr) (E) and 5 Torr of O_2 (F).)

The hole-injection from a layer of carbazole (a strong organic hole-donor), into isolated, single polymer chains of the conjugated polymer (MEH-PPV) imbedded in a multilayer device (Fig 1A) was studied. The experimental amount and rate of hole-injection from the carbazole HTL into individual polymer chains was monitored indirectly by single molecule fluorescence spectroscopy. We assign the injection of holes reported herein to a previously unreported light-induced hole transfer mechanism (denoted by LIHT) involving light assisted injection of holes from the carbazole layer into single MEH-PPV polymer chains. The single polymer chain charging process is sufficiently hysteretic that charge can be reproducibly “stored” on a single polymer chain at intermediate bias (4 V) for long periods (>40 s, in the dark), in analogy to an electronic memory.

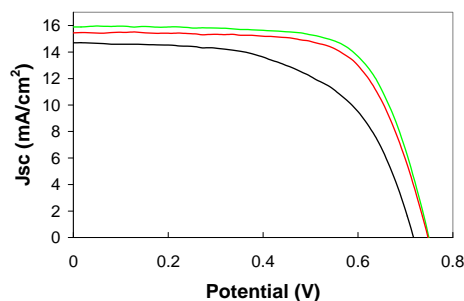
IMPROVING THE EFFICIENCY OF DYE SENSITIZED SOLAR CELLS FOR HYBRID DYE CELL/SILICON CONCENTRATOR SYSTEMS

Greg. D. Barber, Anna Lee, Thomas E. Mallouk
Materials Research Institute and Department of Chemistry
The Pennsylvania State University
University Park, PA 16802

This DOE sponsored research is focusing on the development of a high performance concentrator system that combines low cost dye sensitized solar cells (DSSCs) and a smaller area silicon concentrator cell. The performance is limited by the efficiency of the DSSC component and modeling shows 8% efficient DSSCs are needed to attain ~20% efficient modules. We are studying novel designs for DSSCs involving photonic crystal scattering layers and self-assembling dye/columnar TiO₂ nanostructures. The effect of processing environment on photo-generated charge transport of nano-TiO₂ is also being studied to improve dye cell performance.

Photonic Crystal Coupled DSSCs. We showed previously that inverse opal TiO₂ coupled to dye-sensitized nanocrystalline TiO₂ gave a ~25% enhancement in the red response of a DSSC cell. This enhancement was modeled by Miguez et al. and shown to arise from evanescent wave coupling of the two layers. We have now made structures to test these theoretical predictions. In the optimal FTO/nc-TiO₂/inverse opal configuration, it is experimentally difficult to join the photonic crystal to the nc-TiO₂. Nevertheless, a substantial improvement in average DSSC efficiency from ~6.5% to 8.3% was observed for DSSCs that contained inverse opal photonic crystal scattering layers.

Figure 1. I-V curves of 240 and 270 nm pore size inverse opal (red and green respectively) photonic crystal enhanced DSSCs versus equivalent thickness nanoparticulate DSSC (black).



Self Assembled Columnar Dye Sensitized Solar Cells.

Experiments by Frank, Yang, and Hupp show that columnar or nanotube architectures offer advantages for electron transport in DSSCs. A significant challenge is to make crystalline, high aspect ratio structures on transparent conductor electrodes, with adequate surface area for binding dye molecules. We are exploring a self assembly approach to grow oriented anatase on anode materials through the use of a controlled hydrolysis processes using various titanium precursors and capping reagents that can contain (or be substituted by) dye molecules. Initial results will be discussed.

Effect on Processing Environment on Dye Sensitized Solar Cells. We are also studying the effect of processing environment on photogenerated charge transport properties of conventional nanoparticulate TiO₂ films. The ordinary procedure in DSSC processing is to process in air but previous research shows sintering of submicrometer titania depends significantly on oxygen and water vapor pressure. Initial results show sintering in oxygen and a high humidity environment improves the efficiency of commercially available 32 nm average particle size anatase. We are now studying this process with hydrothermally synthesized nano-TiO₂.

DESIGN OF MOLECULAR RECTIFIERS FOR SOLAR PHOTOCATALYTIC CELLS

Snoeberger R, Schmuttenmaer CA, Crabtree RH, Brudvig GW, Batista VS

Yale Chemistry Department
New Haven, CT, 06520-8107

Solar photocatalysis with robust, nontoxic and inexpensive semiconductor materials could drive a wide range of ‘contrathermodynamic’ –light driven, uphill– reactions not possible thermally, including ‘green’ production of chemical fuels by artificial photosynthesis. However, the design principles for efficient heterogeneous photocatalysis remain unclear and are the subject of our research. Biomimetic Mn catalysts have been studied to understand O₂ evolution by water splitting.¹ Sensitized TiO₂ nanoparticles (NPs), used in Grätzel cells, are robust materials for efficient light-harvesting by photoexcitation of surface complexes and interfacial electron transfer (IET). We integrate these two strategies to investigate heterogeneous photocatalysis based on TiO₂ NPs functionalized with Mn complexes, combining computational modeling, synthesis (Crabtree’s poster) and spectroscopy/electrochemistry (Schmuttenmaer’s poster).

Our computational studies predict ultrafast IET and visible-light sensitization of TiO₂ nanoparticles, when surfaced modified by covalently attaching mixed-valent Mn dimers known to be effective catalysts for water splitting. However, photoactivation of the Mn catalysts by accumulation of multiple oxidizing equivalents is challenging since the photooxidized Mn complexes compete with the TiO₂ sacrificial electron acceptor and induce recombination, as recently probed by time-resolved EPR measurements.² Here we report the design of linkers that are oxidation resistant and hinder recombination functioning as molecular rectifiers. In particular, the terpyridine-functionalized acetylacetonate linker described in Fig. 1 (see also Crabtree’s poster) is resistant to oxidation due to its low lying electronic states, sensitizes TiO₂ NPs to visible light with Mn(II)-terpyridine surface complexes, and induces favorable directionality of electron transfer as shown in Fig. 1 (see also Schmuttenmaer’s poster).³ The relative positioning of the energy levels in the donor and acceptor parts of the linker, favors injection, hinders recombination, and determines rectification properties with subpicosecond IET and recombination times that are several (14) orders of magnitude longer.

References cited

- (1) Limburg, J.; Vrettos, J. S.; Liable-Sands, L. M.; Rheingold, A. L.; Crabtree, R. H.; Brudvig, G. W. *Science* **1999**, 283, 1524.
- (2) Abuabara, S. G.; Cady, C. W.; Baxter, J. B.; Schmuttenmaer, C. A.; Crabtree, R. H.; Brudvig, G. W.; Batista, V. S. *J. Phys. Chem. C* **2007**, 111, 11982.
- (3) McNamara, W.; Snoeberger, R.; Schmuttenmaer, C. A.; Crabtree, R. H.; Brudvig, G. W.; Batista, V. S. *in prep*, **2008**.

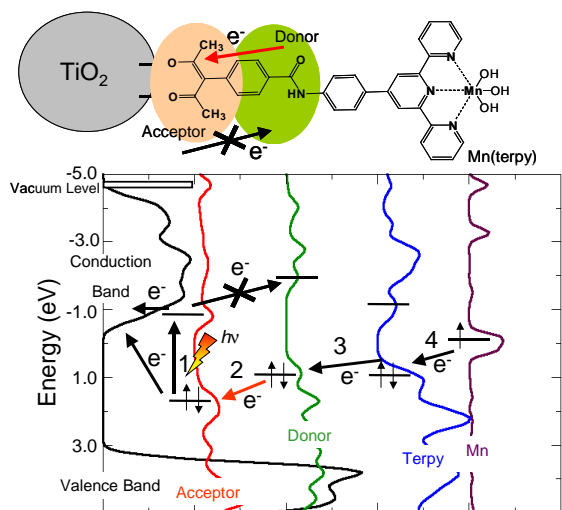


Figure 1: Mn complex/TiO₂-NP and DOS energy diagram illustrating the rectification principle for solar photoactivation of surface catalysts.

MULTIPLE EXCITON GENERATION AND CHARGE CARRIER DYNAMICS IN ELECTRONICALLY COUPLED FILMS OF PbSe NANOCRYSTALS

Matthew C. Beard, M. Law, J.M. Luther, Q. Song, R.J. Ellingson, Sukgeun Choi, M. Hanna, and
A. J. Nozik
National Renewable Energy Laboratory
Golden, CO 80401

We report on the ultrafast carrier dynamics in isolated semiconductor NCs and in films of PbSe semiconductor nanocrystals. We recently reported that in hydrazine treated PbSe nanocrystal films the MEG efficiency remains about the same as in untreated NCs, however, the inter-NC coupling increases. The biexciton lifetime (Auger recombination rate) increased by a factor of ~ 3 for the coupled NCs and the mobility, measured using time-resolved THz spectroscopy (TRTS), greatly increases. Recently we have developed a simple, metal/PbSe-NC/metal cell via a Schottky junction at the negative electrode that produces a large short-circuit photocurrent. In this cell the PbSe NCs films are chemically treated using 1,2-ethanedithiol (EDT) to produce highly photoconductive films that yield EQEs of 65% across the visible and up to 25% in the infrared region of the solar spectrum. We have studied carrier-dynamics in films of PbSe NCs chemically treated using EDT and find that the biexciton lifetime increases by a factor of 10 relative to isolated NCs. We also have found evidence for a reduced MEG QY in these treated films.

We show that TRTS measurements can distinguish between free- and bound carriers and is a powerful technique to study transport phenomenon in nanoscale architectures. We report on the free-carrier QYs upon photoexcitation in coupled NC films. By employing both TRTS and TA we hope to gain a better understanding of carrier cooling, MEG, and delocalized charge transport in these films and report preliminary results towards that end.

We have measured the n and k of our layer-by-layer PbSe nanocrystal films and constructed an optical model in order to understand the optical generation rate in our devices. Our results indicate a reduced dielectric constant of PbSe nanocrystals relative to bulk values. We report preliminary results on understanding the EQE in order to determine whether MEG-produced carriers contribute to the high photocurrents observed in our devices. We discuss limitations of our device structure in observing MEG photocurrents and report progress towards overcoming those limitations.

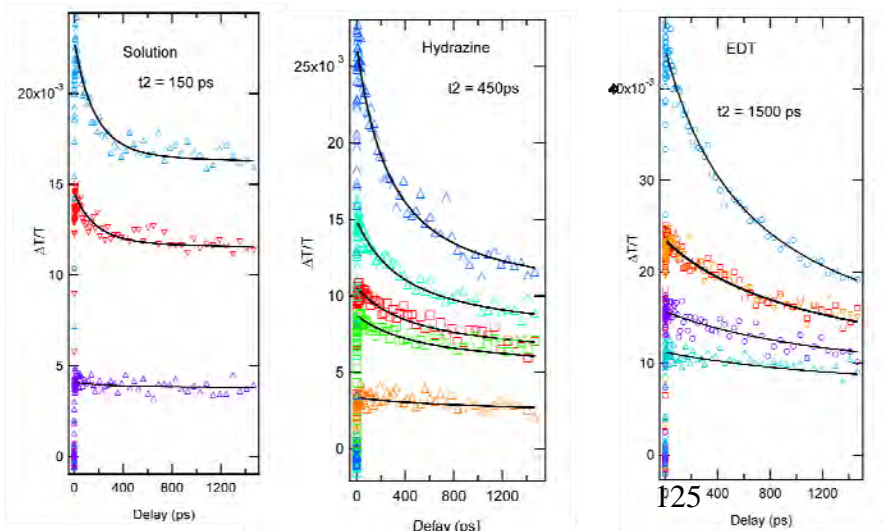


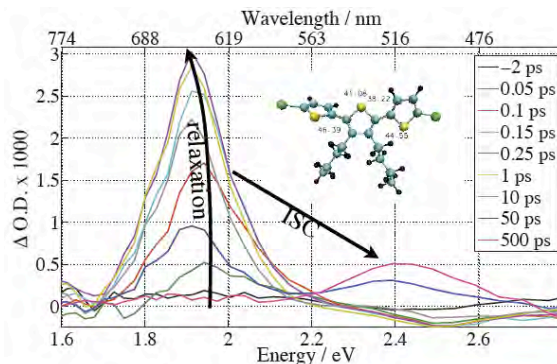
Figure. Transient bleaching dynamics in 2050 nm PbSe nanocrystals in (a) solution, (b) hydrazine treated films and (c) EDT treated films. The photoexcitation energy was less than the MEG threshold. As the photo fluence is increased a fast component due to Auger recombination grows in. The biexciton lifetime increases substantially as a function of the electronic coupling.

PHOTOPHYSICS OF THIOPHENE BASED LIGHT HARVESTERS

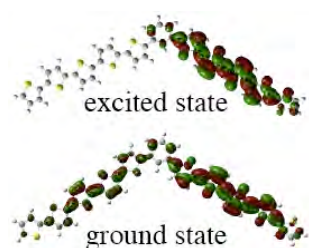
Adam Huss, Nathan Wells, Kent Mann, Wayne Gladfelter, and David Blank
Department of Chemistry
University of Minnesota
Minneapolis, MN 55455

Using a host of time resolved spectroscopies, complemented with time dependent density functional theory (TD-DFT) calculations, we have investigated the excitation and subsequent excited state relaxation dynamics in a series of thiophene based molecular systems. The molecules include the basic building blocks of substituted terthiophenes, phenyl core thiophene dendrimers, and low molecular weight regio-regular poly(3-hexylthiophene). These materials have been shown to serve as both light harvesters and electron donors (hole conductors) in dye-sensitized and organic photovoltaics. Here we have concentrated on the initial events of light absorption and subsequent intramolecular nuclear and electronic relaxation. When the molecular size exceeds the size of the exciton, relaxation dynamics can be coupled to spatial migration of the excitation.

Figure 1 shows transient absorption spectroscopy of 3',4'-dibutyl-5,5''-dibromo-2,2':5',2''-terthiophene following excitation at 400 nm. Transient absorption from the excited singlet state appears in the first ~100 fs near 650 nm. Close inspection of this feature reveals that it shifts to lower energy as it grows. This time resolved spectral diffusion provides a measure of the relaxation in the initially created excited state. On longer time scales the singlet absorption at 650 nm retreats and is replaced by absorption from the triplet state at 520 nm. This gives us a measurement of the intersystem crossing rate (~50 ps). By varying the substituents we are able to systematically tune the singlet-triplet energy gap and compare the ISC rates with predictions of the relative energies of these states from TD-DFT calculations. Asymmetric substitutions can lead to charge transfer character in the excited state with associated influence on the relaxation.



On longer time scales the singlet absorption at 650 nm retreats and is replaced by absorption from the triplet state at 520 nm. This gives us a measurement of the intersystem crossing rate (~50 ps). By varying the substituents we are able to systematically tune the singlet-triplet energy gap and compare the ISC rates with predictions of the relative energies of these states from TD-DFT calculations. Asymmetric substitutions can lead to charge transfer character in the excited state with associated influence on the relaxation.



The phenyl core thiophene dendrimers are well-defined larger molecular systems that allow investigations of the localization of the excited state that is driven by nuclear relaxation. The figure to the left shows a calculation of the relaxed ground and excited states of a piece of a dendrimer where two thiophene arms are placed meta to each other on the central core. Using fluorescence upconversion we are able to follow the spatial realignment and energetic relaxation of the excited state. A surprisingly large fraction of the excited state relaxation takes place in < 100 fs and is the result of planarization between rings driven by displaced torsional coordinates. Using 2-color 3-pulse echo peak shift spectroscopy we have found that the initial spectral migration in polythiophenes (spanning > 0.5 eV) is coherent rather than the often proposed mechanism in conjugated polymers of stochastic self trapping.

HOLE TRANSFER IN TETRAPYRROLIC DYADS: $^2A_{1U}$ VERSUS $^2A_{2U}$ GROUND STATES

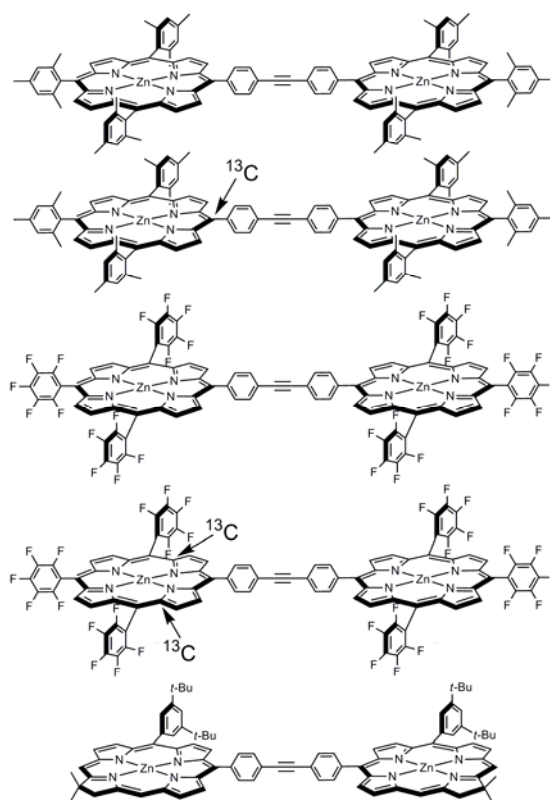
James R. Diers,^a Patchanita Thamyongkit,^b Ana Muresan,^b Masahiko Taniguchi,^b
Dewey Holten,^c Jonathan S. Lindsey,^b and David F. Bocian^a

^aDepartment of Chemistry University of California, Riverside CA 92521-0403

^bDepartment of Chemistry, North Carolina State University, Raleigh, NC 27695-8204

^cDepartment of Chemistry, Washington University, St. Louis, MO 63130-4889

Efficient solar-energy conversion requires that holes generated after excited-state electron-injection can move efficiently away from the anode, thereby preventing charge-recombination. Thus, understanding hole mobility in prototypical light-harvesting and charge-separation systems is of fundamental interest. Towards this goal, the ground-state hole-transfer characteristics of the monocations of several different types of tetrapyrrolic dyads have been investigated using EPR spectroscopy. The structures of the arrays are shown in the accompanying chart. All of the dyads are zinc chelates linked by a diphenylethyne group via the meso-positions of the macrocycle. Two of the dyads are based on porphyrins, one contains three mesityl substituents at the non-linking meso positions of the macrocycle, and the other contains three pentafluorophenyl substituents at these positions. The third dyad is based on a chlorin (one reduced pyrrole ring). The ground states of the cations of the fluorinated porphyrin and chlorin dyads are $^2A_{1u}$, whereas the ground state of the cation of the mesityl-substituted porphyrin dyad is $^2A_{2u}$. The spin density in the $^2A_{1u}$ ground state resides primarily at the α and β positions of the pyrrole rings, whereas the spin density in the $^2A_{2u}$ ground state reside primarily at the meso carbons and the pyrrole nitrogens. Previous EPR studies have shown that meso-linked dyads with $^2A_{2u}$ ground states exhibit hole-transfer rates that are fast on the EPR time scale ($<10^6$ s⁻¹). The fast rates are attributed to the fact that the linker is at a site of large spin density. The fundamental question to be addressed is whether the hole-transfer rate remains fast when the linker is at a site of low (or nil) spin density, such as in the meso-linked dyads with $^2A_{1u}$ ground states. The EPR studies are facilitated by the examination of α -pyrrole ^{13}C labeled fluorinated porphyrins. The ^{13}C labels afford hyperfine interactions at the site of significant spin density.



**PHOTOINITIATED ELECTRON COLLECTION
IN MIXED-METAL SUPRAMOLECULAR COMPLEXES:
DEVELOPMENT OF PHOTOCATALYSTS FOR HYDROGEN PRODUCTION**

Karen J. Brewer, Shamindri Arachchige, Ran Miao, Jared Brown, David Zigler
Department of Chemistry
Virginia Tech, Blacksburg, VA 24061-0212 (kbrewer@vt.edu)

The goal of this project was to prepare and study mixed-metal supramolecular complexes as light activated electron collectors with a focus on their application as solar photocatalysts for hydrogen production. The coupling of multiple charge transfer light absorbing (LA) units in combination with an electron collector (EC) provides light activated collection of reducing equivalents, photoinitiated electron collection (PEC), Figure 1. Recently we have shown that all three Ru,Rh,Ru complexes shown in Figure 1 undergo photoinitiated electron collection at the Rh center and photochemically reduce water to hydrogen in the presence of DMA, TEOA or TEA as electron donors and details of this study will be presented.

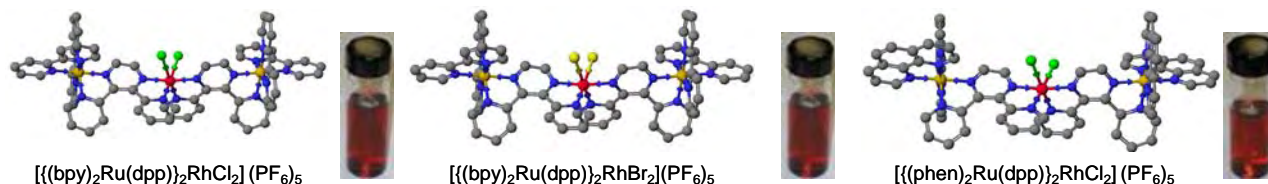


Figure 1. Mixed-Metal Supramolecular Photocatalysts for H_2 Production from H_2O .

Recently we have prepared Ru,Rh dyads that still maintain the reactive $Rh^{III}Cl_2$ site, Figure 2. These complexes displayed somewhat unexpected properties as compared to the previously prepared Ru,Rh,Ru triads. Orbital inversion is seen in the dyad with the dpp^{0-} couple preceding Rh reduction suggesting nearly isoenergetic Rh and dpp orbitals in this structural motif. This is further exemplified by the quenching of the Ru→dpp CT emission in both systems to a similar degree indicating a low lying 3MMCT state in both complexes. The photophysical and photochemical properties of these Ru,Rh dyads and triads will be described.

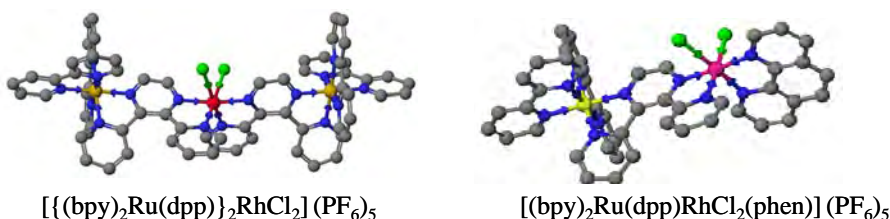


Figure 2. Mixed-Metal Supramolecular Ru,Rh dyad and Ru,Rh,Ru triad bridged by dpp.

A new type of molecular architecture that couples multiple LA units through bridging ligands and a central metal has been established to undergo photoinitiated electron collection. These systems collect electrons on bridging ligand acceptor orbitals and include coupled reactive Pt sites. One example of this type of Pt based system is $[(bpy)_2Ru(dpp)]_2Ru(dpq)PtCl_2]^{6+}$. We have recently shown that following MLCT excitation, $[(bpy)_2Ru(dpp)]_2Ru(dpq)PtCl_2]^{6+}$ undergoes reduction in the presence of an electron donor leading the multielectron reduced form, $[(bpy)_2Ru(dpp^-)]_2Ru(dpq^-)PtCl_2]^{3+}$.

FORMATION OF CAROTENOID NEUTRAL RADICALS IN PHOTOSYSTEM II

Yunlong Gao,^a Katherine E. Shinopoulos,^a Cara A. Tracewell,^a
A. Ligia Focsan,^b Lowell D. Kispert^b and Gary W. Brudvig^a

^aDepartment of Chemistry, Yale University, P.O. Box 208107, New Haven, CT 06520-8107

^bDepartment of Chemistry, University of Alabama, P.O. Box 870336, Tuscaloosa, AL 35487

Carotenoids are known to function in photosynthetic systems as light-harvesting pigments, as photoprotective molecules in triplet energy-transfer processes, as scavengers of singlet molecular oxygen and as components that stabilize pigment-protein structures. More recently, photosystem II (PSII) has been found to utilize β -carotene as a redox center whereby the carotenoid acts as a molecular wire to facilitate long-range electron transfer. The β -carotene radical cation is easily deprotonated in model systems, and the deprotonation is facilitated in the presence of a good proton acceptor such as water. β -carotene radicals produced in the model system Cu(II)-MCM-41 were studied by ENDOR and UV/visible spectroscopies. ENDOR studies showed that the neutral radicals of β -carotene were produced in humid air under fluorescent light. The maximum absorption wavelengths of the radicals were measured and were additionally predicted using TD-DFT calculations. An absorption peak at 750 nm, which was assigned to the neutral radical with a proton loss from the 4(4') position of the β -carotene radical cation in the model system, has also been observed in photosystem II (PS II) samples using near-IR spectroscopy after illumination at 20 K. This peak was previously unassigned in PS II samples. The intensity of the absorption peak at 750 nm relative to the absorption of chlorophyll and β -carotene radical cations increased with increasing pH of the PS II sample, providing further evidence that the absorption peak is due to the deprotonation of the β -carotene radical cation. Based on a consideration of possible proton acceptors that are adjacent to the 4(4') positions of β -carotenes in photosystem II, as modeled in the X-ray crystal structure of Loll et al. (2005) *Nature* **438**, 1040-1044, electron transfer pathways from β -carotene molecules with adjacent proton acceptors to P680^{•+} are proposed.

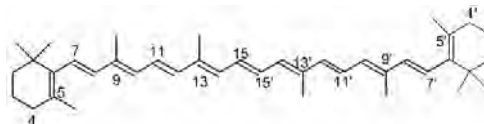


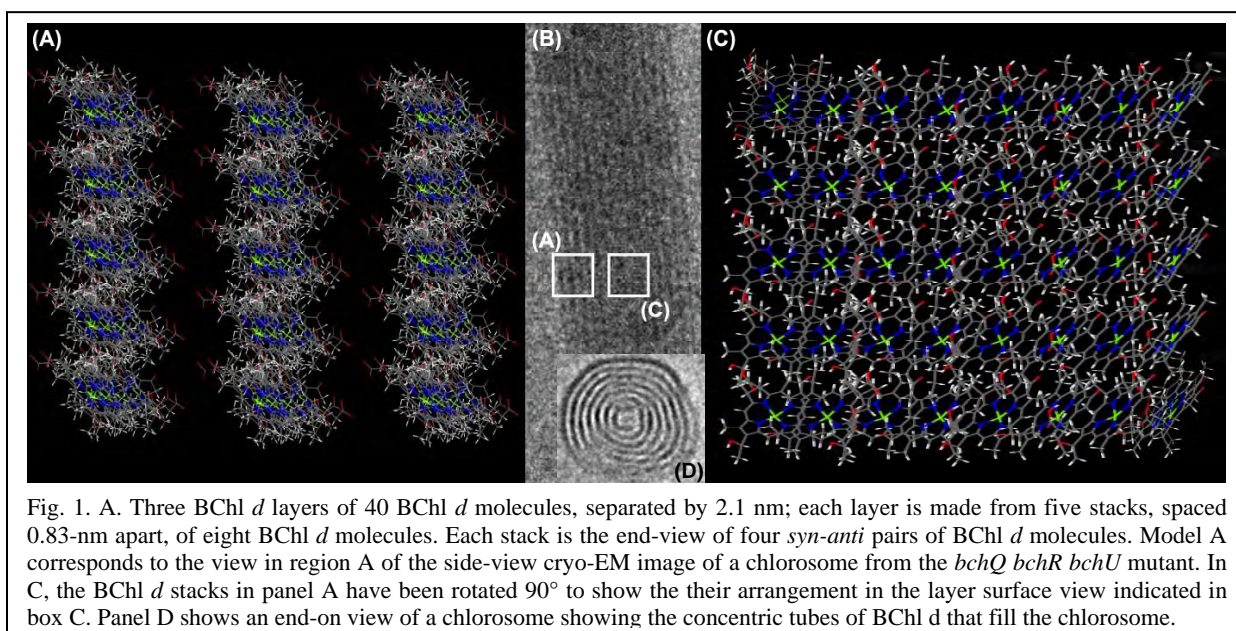
Figure 1. The structure of all-*trans* β -carotene.



LIGHT ENERGY TRANSDUCTION IN GREEN SULFUR BACTERIA

Donald A. Bryant, Julia A. Maresca, Aline Gomez Maqueo Chew, Zhenfeng Liu, Amaya M. Garcia Costas, and Fang Shen
Department of Biochemistry and Molecular Biology,
The Pennsylvania State University
University Park, PA 16802 USA

Chlorosomes are the largest known light-harvesting antennae and are found in members of three bacterial phyla: *Chlorobi*, *Chloroflexi*, and *Acidobacteria*. Chlorosomes from the green sulfur bacterium *Chlorobium tepidum* have lipid monolayer envelopes that are stabilized by ten different proteins. CsmA is the most abundant protein (~2500 molecules/chlorosome); it binds bacteriochlorophyll (BChl) *a* and forms a paracrystalline baseplate complex. *C. tepidum* chlorosomes contain about 200,000-250,000 BChl *c* molecules, which self-assemble and are not specifically associated with any protein. By combining genome sequence information, molecular genetics, and biochemical approaches, we have defined the pathways for the synthesis of carotenoids, BChl *a* and BChl *c*, and we have constructed a large number of mutant strains that have allowed us to characterize the structural and functional properties of chlorosomes. Recently, we have collaborated with Swapna Ganapathy, Dr. Huub DeGroot, Dr. Alfred Holzwarth, Dr. Egbert Boekema, and Dr. Gert Oostergetel to solve the structure of the BChl *d* molecules in chlorosomes of a *bchQ bchR bchU* mutant of *C. tepidum* by using a combination of cryo-electron microscopy, solid-state NMR, and molecular modeling methodologies. These studies reveal for the first time that the basic assembly units of the supramolecular structure are *syn-anti* pairs of stacked BChl *d* molecules in which the farnesyl tails point in opposite directions. The *syn-anti* paired BChl *d* molecules form stacks that are spaced 0.83 nm apart, and the tetrapyrrole rings lie in layers separated by 2.1 nm. These BChl *d* molecules form supramolecular nanostructures built from concentric tubes of different diameters but with constant layer spacing (2.1 nm; see Fig. 1).



ENHANCEMENT OF PHOTOELECTROCHEMICAL PROPERTIES VIA ELECTROCHEMICAL MORPHOLOGY CONTROL OF PHOTOELECTRODES

Kyoung-Shin Choi
Department of Chemistry
Purdue University
West Lafayette, IN 47907

In the preparation of polycrystalline electrodes for use in solar energy conversion (e.g. solar hydrogen production, photovoltaic devices), increasing interfacial areas without sacrificing charge transport properties is critical. However, when nanocrystalline electrodes are prepared to achieve high surface areas, the equally enhanced grain boundary areas often significantly interfere with their charge transport properties. This causes photon-generated electrons and holes to recombine before they are used in desired processes. In this context, dendritic architectures may be highly beneficial; in dendritic growth, crystals form a physically continuous network by nature, while creating high surface areas. In addition, fibrous or rod-type morphologies are also of strategic importance as fibers and rods can be extended farther from the substrates increasing interfacial areas while the one dimensional architecture efficiently minimizes the randomness of charge carrier pathways. In this presentation, we will present various polycrystalline architectures that can be exploited to enhance photoelectrochemical properties (e.g. dendritic, fibrous, and rod-type morphologies). We will discuss key electrochemical synthetic conditions to stabilize each morphology and their effect on photoelectrochemical properties. An example shown in Figure 1 demonstrates the photocurrent enhancement of dendritic Cu_2O electrodes achieved by optimizing details of dendritic growth (e.g. nucleation density, degree of branching, crystal size).

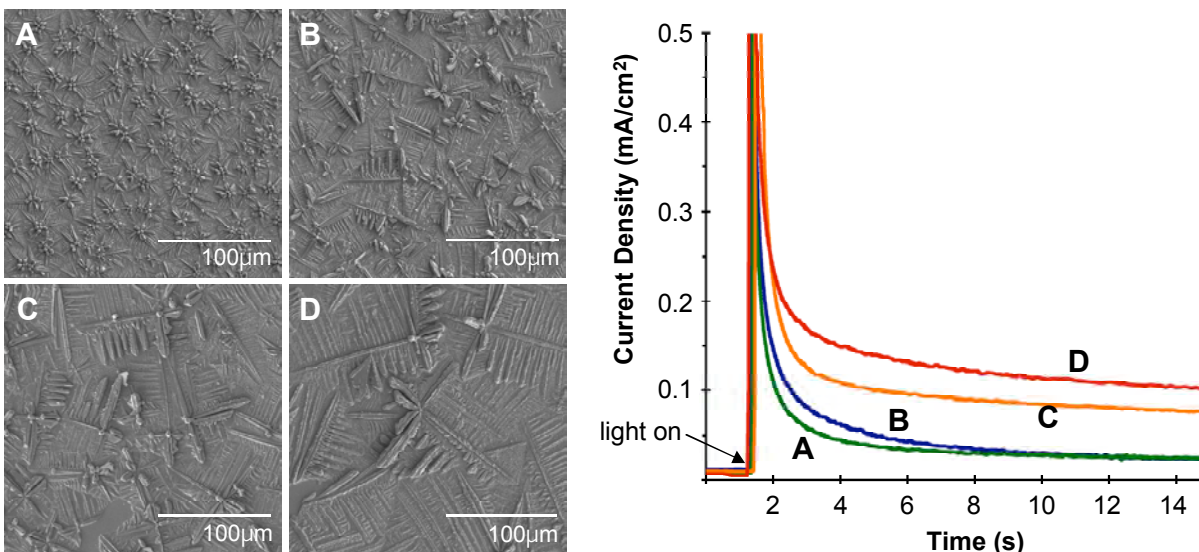


Figure 1. Photocurrent measurement of dendritic Cu_2O films with varying nucleation densities and degrees of branching.

ACETYLACETONATE AS A ROBUST ANCHOR AND ELECTRON CONDUIT FOR SOLAR CELL DYES

McNamara W, Cady C, Snoeberger R, Schmuttenmaer CA, Brudvig GW, Batista VS, Crabtree RH

Yale Chemistry Department
New Haven, CT, 06520-8107

Current Grätzel cells are not robust because humidity detaches the classic carboxylate anchors. Our terpyridine catechol linker¹ proved stable to humidity but was still detached by oxidation. Since oxidation is our goal, this was fatal. We now show that an acetylacetonate-terpyridine (**3**) is a robust linker, not only to humidity but also to oxidation.² The terpyridine-functionalized acetylacetonate described here is capable of binding Mn(II) and sensitizing visible light induced interfacial electron transfer (IET) into TiO₂ nanoparticles (NPs). DFT studies (Batista poster) are key in designing anchors with the right relationship of the HOMO and LUMO energies of the components involved. Spectroscopy allows characterization of the surface-attached species. Detection of interfacial electron transfer by terahertz spectroscopy (Schmuttenmaer poster) completes the first stage of the study.

The synthesis of the terpyridine-catechol material has been described in our published paper.¹ The terpyridine-functionalized acetylacetonate was synthesized via catalytic L-proline mediated CuI coupling (Fig 1). Terpyridine **2** was synthesized from *p*-nitrobenzaldehyde by a conventional annulation procedure. DFT calculations validated the design for our IET application.

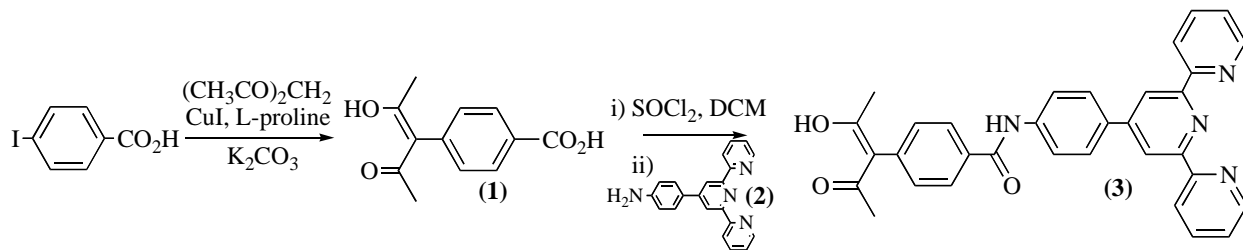


Fig 1 Synthetic route

The resulting material, **3**, proved to attach readily to TiO₂ NPs, as shown by IR and UV-vis spectroscopy. The material attached to TiO₂ (**4**) was stable to a water wash as well as to oxone solution (a powerful oxidant). **4** also took up Mn(II) from solution to give the N-bound adduct as shown by EPR and UV-vis spectroscopy. Cooling to 6K followed by illumination at 400 nm resulted in IET as shown by the decay of the Mn(II) EPR signal and rise of a THz absorption by the photoinjected electron. In the dark, the electron returned to the Mn site, restoring the EPR spectrum of Mn(II). The physical and chemical properties of **3** look promising for further study such as synthesis of the 'black dye' Ru analogue for robust attachment.

References cited

1. Abuabara SG, Cady CW, Baxter JB, Schmuttenmaer CA, Crabtree RH, Brudvig GW, Batista VS, *J Phys Chem C*, **2007**, *111*, 11982-11990.
2. McNamara W, Snoeberger R, Schmuttenmaer CA, Crabtree RH, Brudvig GW, Batista VS, *in preparation*.

TOOLS FOR ELUCIDATING MECHANISM FOLLOWING ADAPTIVE CONTROL AND PROGRESS TOWARDS CONTROL OF MULTIPLE EXCITON GENERATION

Niels H. Damrauer, Matthew A. Montgomery, Erik M. Grumstrup
Department of Chemistry and Biochemistry
University of Colorado at Boulder
Boulder, CO 80304

The control of electronically, structurally, and reactively complex systems is now possible using iterative learning in many-parameter spaces of shaped laser fields. However, maturation of this technique known as adaptive femtosecond pulse shaping requires that control be complemented with new information about these complex systems that leads to their controllability. This presentation explores recent progress in our laboratory developing experimental and statistical tools for exploration of control mechanism following unbiased many parameter adaptive searches. We also present initial results of experiments that aim to control multiple exciton generation in PbSe quantum dots.

Our starting place has involved the implementation of statistical analysis-based dimension reduction strategies following many-parameter adaptive control of excited-state population in coordination complexes in solution. While developed for a specific system under laser control, these strategies are general and allow us to identify the fewest number of independent control variables. These variables have proven useful for visualizing control surfaces. Further, we are able to systematically interrogate these surfaces as a means of exploring how the system changes spectroscopically as laser-pulse fitness improves.

In addition to these statistical strategies we are developing spectroscopic techniques to interrogate control mechanism following adaptive control. We are creating methodology that utilizes the same experimental setup in place during control; namely, pulse shaping in concert with pump/probe spectroscopy. Our initial efforts show that pulse amplitude-shaping allows for facile generation of phase-locked pulse pairs and subsequent measurement of two-dimensional electronic spectra. We are now developing strategies based on phase and amplitude switching that address whether laser-pulse frequency-dependent phase is a necessary component of control in any successful adaptive experiment. We anticipate that this general technique will be useful for proving whether a control mechanism relies on the manipulation of coherences in complex systems.

Finally, we present initial progress towards the control of multiple exciton generation. As shown in *Fig. 1*, we have observed the iterative maximization of a transient bleach signature (relative to pulse intensity) of $\sim 7-8$ nm PbSe quantum dots excited at ~ 3 times the band gap. These data are preliminary and serve at this point only to show that our experimental infrastructure is in place.

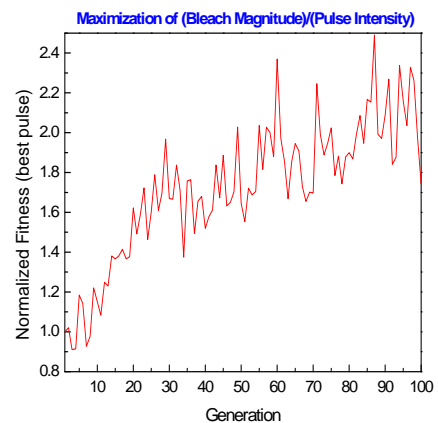


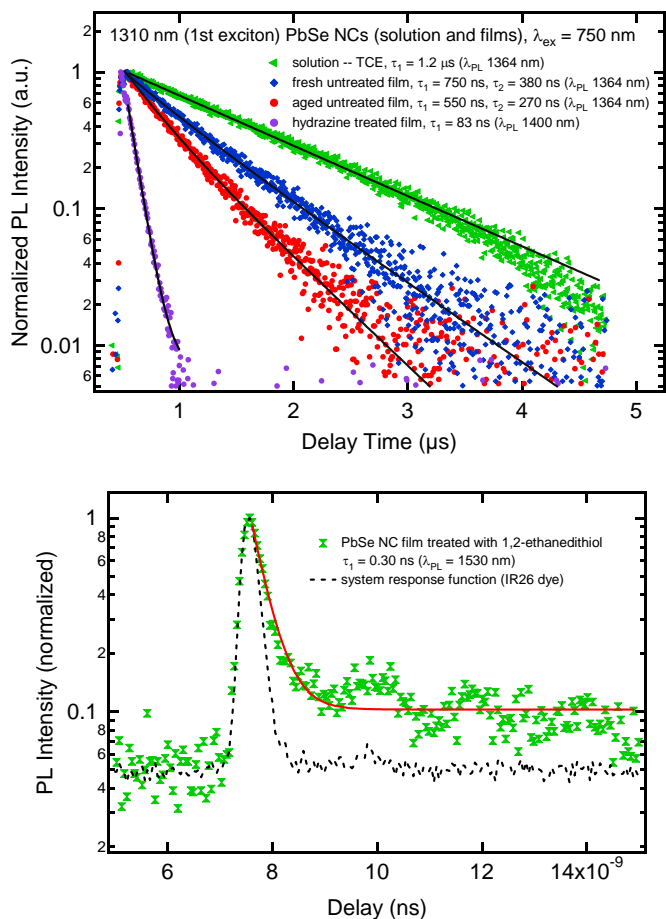
Fig. 1: Preliminary adaptive maximization of the band-gap bleach in PbSe quantum dots normalized to pulse intensity.

CW- AND TIME-RESOLVED PHOTOLUMINESCENCE STUDIES OF SEMICONDUCTOR NANOCRYSTALS AND NANOCRYSTAL ARRAYS FOR EFFICIENT SOLAR ENERGY CONVERSION

R. J. Ellingson, M. Law, J. Luther, Q. Song, J. C. Johnson, B. Hughes, K. A. Gerth, A. Midgett, O. Semonin, M. C. Beard, and A. J. Nozik
Center for Chemical Sciences and Biosciences, Energy Sciences Directorate
National Renewable Energy Laboratory
Golden, CO 80401

Observations of efficient multiple exciton generation (MEG) in colloidal semiconductor nanocrystals (NCs) of lead-salts, CdSe, InAs/CdSe and Si motivate concentrated effort to understand how NC films (arrays) can be designed to facilitate efficient exciton dissociation, low recombination loss, and high mobility. Indeed, in the wake of considerable progress in observing MEG spectroscopically, and contradictory reports on the observation and efficiency of MEG in CdSe and InAs NCs, a conclusive demonstration of MEG-enhanced photocurrent would represent critical data for both basic science as well as technology development efforts. We have pursued the fabrication of films of strongly coupled NCs to study the parameters and processes essential to photoconversion, and in particular to study the photon energy dependence of exciton production (and conversion) efficiency.

Using time-resolved photoluminescence, we study the effect on carrier lifetimes of various chemical treatments to NC-based films. Although our earlier investigations showed that the MEG QYs for solution, untreated film, and hydrazine treated film do not differ significantly, carrier lifetimes show dramatic variation with the chemical preparation. Initial optical and electrical characterization of the NC films and film-based devices shows that enhanced coupling improves charge transport while decreasing the carrier lifetime by as much as three orders of magnitude. Film morphology plays a critical role in these properties. Our recent progress includes the development of a layer-by-layer process for solution-based fabrication of nanocrystal solids, performing a ligand exchange step following each layer's deposition. Simple Schottky barrier devices have been fabricated and characterized. Resulting devices show high photocurrents and efficiencies $\geq 2\%$.



MASS TRANSFER OF POLYPYRIDYL COBALT COMPLEXES WITHIN MESOPOROUS TiO₂ DYE-SENSITIZED SOLAR CELL PHOTOANODES

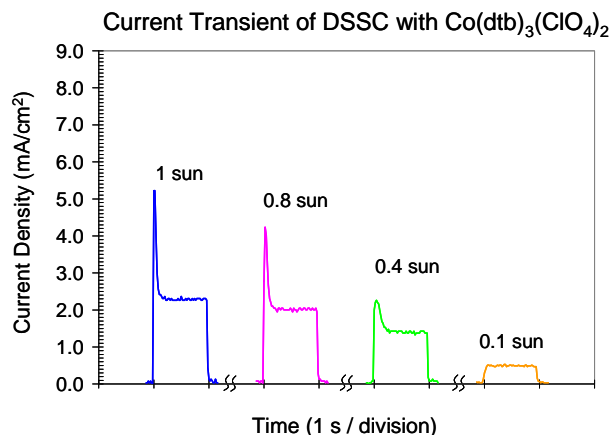
Jeremy J. Nelson, Tyson J. Amick, C. Michael Elliott
Chemistry Department
Colorado State University
Fort Collins, CO 80523

Dye-sensitized solar cells (DSSCs) offer the potential for reasonably efficient solar energy conversion at low cost. In a properly functioning DSSC, electrons must be shuttled from the cathode to the oxidized dye. Despite its other drawbacks, I⁻/I₃⁻ has proven most efficient in this electron transfer mediation. However, certain polypyridyl Co(II) complexes (e.g., Co(dtb)₃(ClO₄)₂, where dtb = 4,4'-di-*tert*-butyl-2,2'-bipyridine) have been shown to be reasonably efficient mediators in DSSCs, although thus far less so than I⁻/I₃⁻. Slower dye reduction by Co(dtb)₃²⁺ was previously demonstrated, but recent investigations reveal an important difference in their rates of diffusion as well, particularly within the nanocrystalline TiO₂ layer.

Transient experiments conducted at short circuit indicate that DSSCs with cobalt mediators display a qualitatively different response to the onset of illumination than do DSSCs with I⁻/I₃⁻. Specifically, a sharp decline in the initial current over ~1 s or less is observed with cobalt-mediated cells, suggestive of solution polarization resulting from the insufficient diffusion of mediator between the two electrodes. Consistent with this hypothesis are the observations that viscosity and Co(dtb)₃²⁺ concentration significantly affect the transient behavior.

To confirm this hypothesis, rotated disk electrode (RDE) experiments were performed to determine the rate of diffusion of Co(dtb)₃²⁺ complexes through typical nanocrystalline TiO₂ films. Using a thermal platinization treatment, fluorine-doped tin(IV) oxide (FTO) glass was modified to effect the oxidation of both Co(dtb)₃²⁺ and I₃⁻. An electroinactive, nanocrystalline TiO₂ film was deposited and the entire assembly was used to fabricate a RDE. Diffusion coefficients of both Co(dtb)₃²⁺ and I₃⁻ through the film and through bulk solution were determined using Koutecký-Levich analyses. Attempts to investigate the effect of a monolayer of a bis(bipyridyl)ruthenium dye adsorbed to the TiO₂ on diffusion were complicated by a concurrent decrease in electron transfer rates at the FTO surface.

As the solvent and mediator concentration are quite different in DSSC experiments than for RDE experiments, it was necessary to account for the difference in solution viscosities. Using experimentally determined values for the viscosities, it has been calculated that the effective diffusion coefficients through TiO₂ films in DSSCs are ~2 x 10⁻⁷ cm² s⁻¹ for Co(dtb)₃²⁺ and ~2 x 10⁻⁶ cm² s⁻¹ for I₃⁻.



OPTICAL AND ELECTROCHEMICAL PROPERTIES OF SHELL-CORE DENDRIMERS: RUTHENIUM COORDINATION COMPLEXES CAPPED WITH SIZED PHENOTHIAZINE-SUBSTITUTED BIPYRIDINES

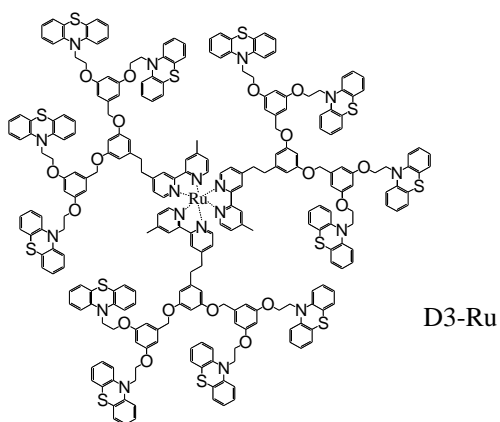
Marye Anne Fox, James K. Whitesell, and Linyong Zhu

Department of Chemistry and Biochemistry

University of California, San Diego

La Jolla, CA 92093

Achieving long-lived charge separation in integrated arrays containing photosensitizers, electron donors and semiconductor nanoparticle arrays has been an important objective for over a decade. Recently, we have prepared a range of dendrimers as photoactive integrated systems have a regular, highly-branched, three-dimensional architecture.



	$E_{1/2}$ / Volt +/\$\pm\$0.1 V	$E_{1/2}$ / Volt +/\$\pm\$0.1 V	Quantum yield +/\$\pm\$0.03	Decay	Decay	Decay
			$\lambda_{ex} = 455$ nm	$\lambda_{ex} = 355$ nm	$\lambda_{ex} = 455$ nm	$\lambda_{ex} = 532$ nm
	PTZ ⁺⁰	Ru ^{3+/2+}		Fraction(τ /ns)	Fraction(τ /ns)	Fraction(τ /ns)
D0	--	1.10	0.120	1.00(805)	1.00(790)	1.00(795)
D1	0.61	1.27	0.025	0.80(75) + 0.20(900)	0.86(69) + 0.14(900)	0.80(74) + 0.20(890)
D2	0.62	1.25	0.022	0.33(104) + 0.51(350) + 0.16(870)	0.38(89) + 0.51(295) + 0.13(780)	0.33(86) + 0.50(287) + 0.17(760)
D3	0.67 (irr)	1.29 (irr)	0.070	0.39(154) + 0.61(445)	0.36(130) + 0.64(445)	0.45(185) + 0.55(480)

* $E_{1/2}$ value +0.31 V vs SSCE; with Fe³⁺. Irr = irreversible

Their electrochemistry is the same, except that **D3** shows irreversible features; absorption spectra are familiar; emission spectra are broader but are clearly ascribed to a familiar MLCT state, which is populated in high yield and probably decays by similar pathways. There are no extraneous ultra-fast processes causing premature self-quenching of incident excitation. Therefore, we conclude that these, or closely related species, may serve as highly absorptive efficient antenna systems. Such arrays have found practical use in photosensitization of thin film semiconductor devices, which require high densities of surface-bound dyes.

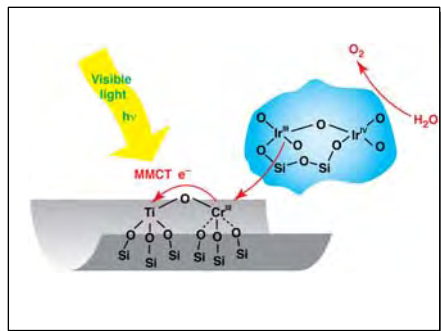
DOE Sponsored Publications 2004-2007

1. Tao Gu, James K. Whitesell, and Marye Anne Fox, "Electrochemical Charging of a Fullerene-Functionalized Self-Assembled Monolayer on Au (111)," *J. Org. Chem.* **2004**, 69, 4075-4080.
2. Mariana Rusa, James K. Whitesell, and Marye Anne Fox, "Controlled Fabrication of Gold/Polymer Nanocomposites with a Highly Structured Poly(*N*-acylethyleneimine) Shell," *Macromolecules* **2004**, 37, 2766-2774.
3. T. Hirakawa, J.K. Whitesell, and Marye Anne Fox, "Effect of Temperature and CO₂ Pressure on the Photocatalytic Oxidation of *n*-Octanol on Hydrophobic TiO₂ Suspended in Aerated Supercritical CO₂," *J. Phys. Chem. B* **2004**, 108, 10213-10218.

BINUCLEAR TiOCr CHARGE-TRANSFER CHROMOPHORE DRIVEN VISIBLE LIGHT WATER OXIDATION AT Ir OXIDE NANOCLUSTER

H. Han and H. Frei
Physical Biosciences Division
Lawrence Berkeley National Laboratory
Berkeley, CA 94720

We are developing all-inorganic photocatalytic units on nanoporous silica supports consisting of a heterobinuclear metal-to-metal charge-transfer (MMCT) site for visible light absorption coupled to a multi-electron transfer catalyst. In this work, an Ir oxide nanocluster was used as water oxidation catalyst. IrO_x is an established material for efficient water oxidation with a turnover frequency similar to that of the natural water oxidation complex. We have recently demonstrated water oxidation under visible light at IrO_x nanoclusters inside the channels of mesoporous silica MCM-41 by coupling the catalyst to single Cr^{VI} centers anchored on the pore surface. In this photocatalytic system, the oxidized donor that drives the catalyst is a transient hole on O generated by excitation of the Cr^{VI}-O^{II} → Cr^V-O^I LMCT chromophore with 460 nm light. The hole on the O has a potential around +3 V while the minimal potential for O₂ evolution from H₂O is 1.23 V, which shows that the Cr^{VI}/IrO_x photocatalytic unit cannot be thermodynamically efficient. Therefore, a crucial step towards energetically efficient photocatalytic water oxidation is the replacement of the CrO LMCT chromophore by a binuclear MMCT chromophore. In such a unit, the redox potential of the donor center can be adjusted to better match the thermodynamic requirements of the catalyst by selecting an appropriate donor metal and oxidation state.



We have assembled TiOCr^{III} units with high selectivity in MCM-41 pores and coupled them to Ir oxide nanoclusters. The TiOCr^{III} MMCT chromophore was structurally characterized by EXAFS, XANES, EPR and vibrational spectroscopy. In-situ FT-Raman spectroscopy revealed water oxidation upon irradiation of the TiOCr^{III} chromophore with visible light by growth of O₂⁻ (superoxide) at 994 cm⁻¹ in H₂O, and at 961 cm⁻¹ (¹⁸O¹⁶O⁻) and 930 cm⁻¹ (¹⁸O₂⁻) in H₂¹⁸O. The isotopically labeled product confirms that the superoxide species originate from oxidation of water. EPR spectroscopy of the suspension showed that the superoxide species are interacting with a Ti center. These observations are explained by photocatalytic oxidation of water at Ir oxide nanoclusters followed by trapping of the evolving O₂ by transient Ti^{III} centers to yield Ti^{IV}--O₂⁻. The proposed mechanism is supported by the detection of Ti^{III} in the EPR spectrum if the persulfate acceptor is absent in the photolysis experiment. The steady state buildup of Ti^{III} implies that Ir oxide nanoclusters are efficiently coupled to the Cr centers, and that electron donation from IrO_x to Cr^{IV} competes successfully with back electron transfer from Ti^{III}. This MMCT unit constitutes the first example of an all-inorganic visible charge-transfer chromophore with selectable donor redox potential for driving water oxidation. The flexibility of assembling such inorganic molecular charge-transfer sites and coupling them to catalysts opens up the development of robust photocatalysts in nanoporous scaffolds with tailored light absorption properties and matched redox potentials.

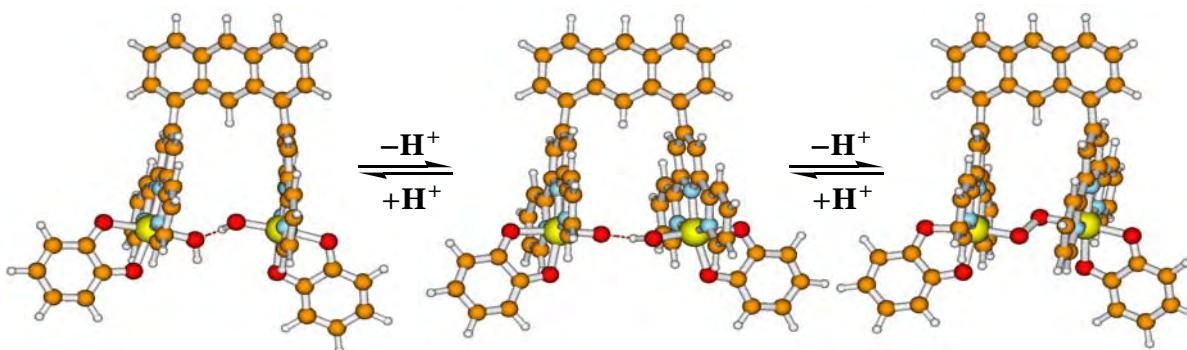
WATER OXIDATION BY A RUTHENIUM COMPLEX WITH NON-INNOCENT QUINONE LIGANDS

Etsuko Fujita,¹ James T. Muckerman,¹ Ming-Kang Tsai,¹ Dmitry E. Polyansky,¹
Tohru Wada,² Koji Tanaka²

¹ Chemistry Department, Brookhaven National Laboratory, Upton, NY 11973-5000

² Coordination Chemistry Laboratories, Institute for Molecular Science, 5-1 Higashiyama,
Myodaiji, Okazaki, Aichi 444-8787, Japan

A novel dinuclear Ru complex, $[\text{Ru}_2(\text{OH})_2(3,6\text{-Bu}_2\text{Q})_2(\text{btpyan})](\text{SbF}_6)_2$ (3,6-Bu₂Q = 3,6-di-*tert*-butyl-1,2-benzoquinone, btpyan = 1,8-bis(2,2':6',2''-terpyrid-4'-yl)anthracene), that contains redox active quinone ligands exhibits excellent electrocatalytic activity for water oxidation when immobilized on an indium-tin-oxide electrode.¹ The novel features of the dinuclear and related mononuclear Ru species with quinone ligands, and comparison of their properties to those of the Ru analogues with the bpy ligand (bpy = 2,2'-bipyridine) replacing quinone, are discussed together with new theoretical and experimental results that show striking features for both the dinuclear and mononuclear species.² The identity and oxidation state of key mononuclear species, including the previously reported oxyl radical, have been reassigned. Our gas-phase theoretical calculations indicate that the Tanaka Ru-dinuclear catalyst seems to maintain predominantly Ru(II) centers while the quinone ligands and water moiety are involved in redox reactions throughout the entire catalytic cycle for water oxidation. $[\text{Ru}_2(\text{O}_2^-)(\text{Q}^{-1.5})_2(\text{btpyan})]^0$ is a key intermediate and the most reduced catalyst species that is formed by removal of all four protons before four-electron oxidation takes place. The current status and new directions for kinetic and mechanistic investigations, and key issues and challenges in water oxidation with the Tanaka catalyst (and its analogues with Cl- or NO₂-substituted quinones and a species with a xanthen bridge instead anthracene) will be discussed.



References

1. Wada, T.; Tsuge, K.; Tanaka, K. *Inorg. Chem.* **2001**, *40*, 329-337.
2. Muckerman, J. T.; Polyansky, D. E.; Wada, T.; Tanaka, K.; Fujita, E. *Inorg. Chem.* **2008**, *47*, 1787-1802.



PROTEIN-PROTEIN INTERACTIONS IN THE HELIOBACTERIAL REACTION CENTER

John H. Golbeck

Department of Biochemistry and Molecular Biology; Department of Chemistry
The Pennsylvania State University
University Park, PA 16802 USA

All Type I photosynthetic reaction centers harbor three [4Fe-4S] clusters F_X , F_B and F_A that function as a molecular wire to vector electrons from the site of light-induced charge separation to the soluble protein, ferredoxin. These three Fe/S clusters are well-characterized in Photosystem I, but have only recently been characterized in the homodimeric Type I reaction center from *Heliobacterium modesticaldum*. We reported earlier that the terminal [4Fe-4S] clusters F_A and F_B reside on a loosely bound ferredoxin-like protein named PshB (Heinnickel et al., 2005). Time-resolved optical spectroscopy showed that on a single-turnover flash, only 50% of electrons were transferred to the F_A and F_B ; the other 50% underwent charge recombination from F_X . One likely possibility is that only 50% of the PshB binding sites are occupied on the heliobacterial reaction center (Heinnickel et al. 2006). Interestingly, the gene that codes for PshB is part of a dicistronic operon that contains a gene for a second ferredoxin-like protein (Figure 1).

```
PshB  MAYKITDACTACGACMDGCCVGAIVEGKKYSITSDCVDCGVCADKCPVDAIIPG
PshB1 MUYKISDACCVACGACEDACPVNAIIKGDVYSITDACCIDCGTCADTCPAGAISEG
```

Figure 1. Amino acid sequence of PshB and PshB1

We have cloned this gene and overexpressed the protein in *Escherichia coli*. Reconstitution studies with inorganic reagents have shown that this protein similarly harbors two [4Fe-4S] clusters (Figure 2). Incubation of the reconstituted protein with heliobacterial reaction center cores results in a long charge-separated state characteristic of electron transfer past F_X to one of the terminal Fe/S clusters, F_A or F_B . These results indicate that this second ferredoxin-like protein, which we have named PshB1, is capable of functioning as a terminal electron acceptor in a manner similar to that of PshB. Thus, the heliobacterial reaction center core is capable of interacting with two, loosely bound ferredoxins that fill the role of the tightly bound PsaC protein in Photosystem I. Studies are underway to determine whether the relative binding affinities of PshB and PshB1 and to determine which is the physiological acceptor protein *in vivo*.

Heinnickel, M., Shen, G., Agalarov, R., and Golbeck, J. H. (2005) Resolution and reconstitution of a bound Fe-S protein from the photosynthetic reaction center of *Heliobacterium modesticaldum*, *Biochemistry* 44, 9950-9960.

Heinnickel, M., Shen, G., and Golbeck, J. H. (2007) Identification and characterization of PshB, the dicluster ferredoxin that harbors the terminal electron acceptors F_A and F_B in *Heliobacterium modesticaldum*, *Biochemistry* 46, 2530-2536

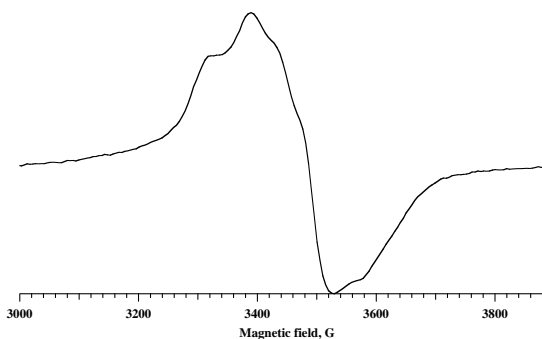
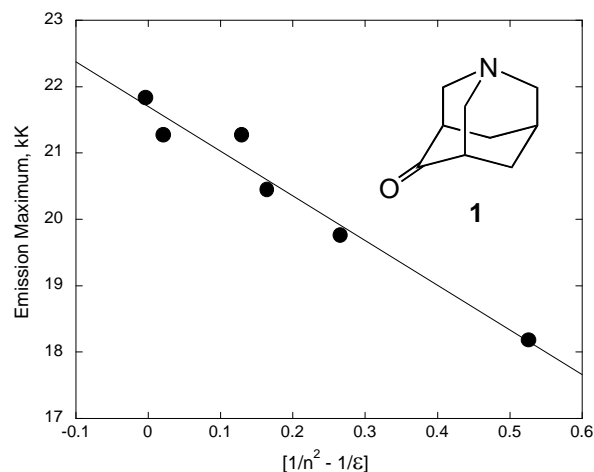


Figure 2. EPR Spectrum of chemically reduced PshB2

SOLVATOCHROMISM MEASURES ENERGETIC DISORDER IN POLYMER CHARGE-TRANSPORT SYSTEMS

Brandon Deason, Ian R. Gould and Dmitry Matyushov
Department of Chemistry and Biochemistry
Arizona State University
Tempe, AZ 85287

The role of energetic disorder in determining the efficiencies of photoinduced charge separation and migration in organic polymer systems has not been properly established. Here we describe a solvatochromic method for quantitative determination of energetic disorder for charge-transfer systems. Initial work has concentrated on characterization of the probe molecule, dicyanovinylazaadamantane, **1**, and development of the proper band-shape analysis theory. **1** is unique in having both charge-transfer absorption and emission bands that are well separated from locally excited absorptions. The internal, non-solvent, reorganization parameters have also been independently measured. CT absorption and emission spectra have been recorded in solvents of varying polarity, from cyclohexane to acetonitrile. Band-shape analysis provides accurate solvent reorganization parameters. Preliminary observations in polymer systems are also reported.



Emission maximum of **1** versus Pekar factor, in various solvents.

CHARGED DEFECTS IN π -CONJUGATED POLYMERS

Brian A. Gregg, Dong Wang, Nikos Kopidakis, Xin Ai and Matthew O. Reese
Chemical and Biosciences Center
National Renewable Energy Laboratory
Golden, Colorado 80401

All semiconductors contain defects and the defect density usually increases as the degree of crystallinity decreases. Defects, whether purposely added as dopants or not, often control the electrical behavior of inorganic semiconductors. In the newer field of organic semiconductors, however, little is known about the number, influence or chemical identity of defect states. In fact, in most theoretical models of transport in π -conjugated polymers, the presence of charged defects is simply ignored. We study the ostensibly pure π -conjugated polymers regioregular poly(3-hexylthiophene), P3HT, and poly(4-methoxy-1-decyloxy-2,5-phenylenevinylene), MDMO-PPV. We show, consistent with the measurements of others, that they contain 11 - 15 orders of magnitude more charged species at equilibrium than they would if they were defect-free. A Poole-Frenkel-like model is proposed as an alternative to existing models of transport and conductivity in these semiconductors.

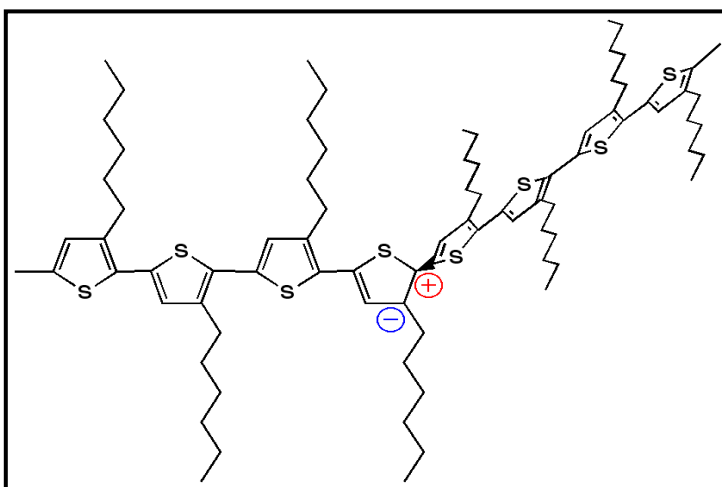


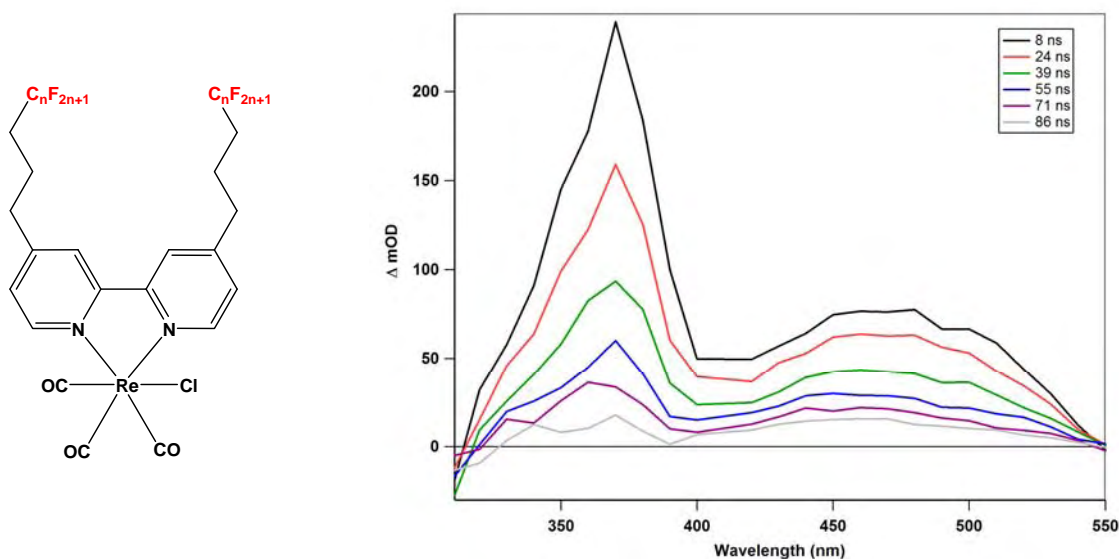
Illustration of a possible charged defect in solid films of poly(3-hexylthiophene).

Inspired by the passivation of defects in amorphous silicon by treatment with hydrogen, we introduce chemical treatments that modify the photophysical and electrical properties of these polymers. Treatment with nucleophiles such as methoxide ion leads to a decrease in positive charge density and film conductivity, and an increase in carrier mobility, fluorescence intensity and lifetime. Treatment with electrophiles such as dimethyl sulfate causes no change in positive charge density but increases the conductivity and hole mobility, and almost doubles the exciton diffusion length. Both treatments improve the stability of the polymers against photo-oxidative damage.

MECHANISTIC INVESTIGATIONS OF THE PHOTOCATALYTIC REDUCTION OF CO₂ IN SUPERCRITICAL CO₂

David C. Grills, Etsuko Fujita, Mark D. Doherty
Chemistry Department
Brookhaven National Laboratory
Upton, NY 11973

Our research focuses on gaining a fundamental understanding of the processes involved in the chemical conversion of solar energy, with a goal of developing systems that are capable of efficiently storing solar energy in the form of useful fuels and chemicals. One avenue of research is the photocatalytic reduction of CO₂ to CO in supercritical CO₂ (scCO₂). The use of scCO₂ as a solvent has several advantages over the use of conventional organic solvents. In particular, it eliminates any possibility of coordinating solvent molecules binding to the active site of the catalyst and hindering reaction with CO₂. Furthermore, the concentration of CO₂ in scCO₂ can be extremely high (typically 20 M). In order to study the photocatalytic reduction of CO₂ in scCO₂, we have synthesized photocatalysts that exhibit extremely high solubility in scCO₂ (see below). The catalysts, of general formula [(4,4'-(C_nF_{2n+1}CH₂CH₂CH₂)₂-2,2'-bpy)Re(CO)₃Cl], possess long perfluorinated tails that enhance their solubility in scCO₂ dramatically compared to their non-fluorinated analogs. We have used a number of steady-state and time-resolved spectroscopic techniques to examine the photophysics and photochemistry of these catalysts in both conventional solvents and scCO₂, and have compared the results with the unsubstituted parent catalyst, (2,2'-bpy)Re(CO)₃Cl. Preliminary investigations into the photocatalytic reduction of CO₂ to CO with the fluorinated catalysts in scCO₂ will also be presented.



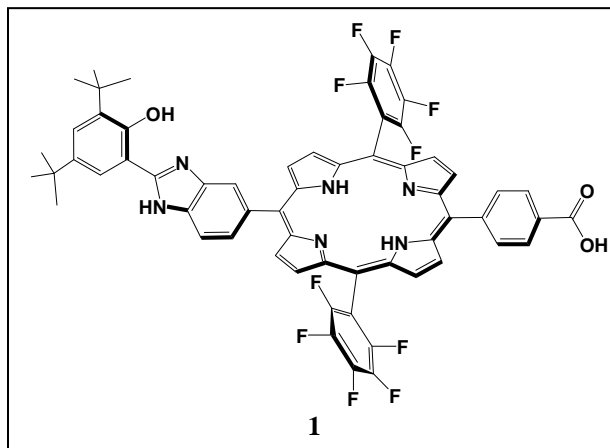
Transient absorption spectra recorded after 409 nm laser flash photolysis of [(4,4'-(C₆F₁₃CH₂CH₂CH₂)₂-2,2'-bpy)Re(CO)₃Cl in scCO₂ (2500 psi, 35.0 °C).

A BIOINSPIRED CONSTRUCT THAT MIMICS THE PROTON COUPLED ELECTRON TRANSFER BETWEEN P680⁺ AND THE TyrZ-His190 PAIR OF PHOTOSYSTEM II

Gary F. Moore,¹ Michael Hamburger,¹ Miguel Gervaldo,¹ Amy Keirstead,¹ Gerdenis Kodis,¹ Oleg G. Poluektov,² Tijana Rajh,² Devens Gust,¹ Thomas A. Moore,¹ and Ana L. Moore¹
¹Center for Bioenergy and Photosynthesis, Department of Chemistry and Biochemistry, Arizona State University, Tempe, AZ 85287-1604; ²Center for Nanoscale Materials and Chemical Sciences and Engineering Division, Argonne National Laboratory, Argonne, IL 60439

The most sustainable source of electrons for solar production of hydrogen or other fuels is water. In photosystem II, tyrosine Z (TyrZ) functions as a redox mediator between the photo-oxidized primary donor (P680⁺) and the Mn-containing oxygen evolving complex (OEC). The oxidation of TyrZ by P680⁺ likely occurs with a shift of the phenolic proton to its hydrogen-bonded partner, a histidine residue (His190). This change in the protonation state of TyrZ is thought to play an important role in the electron transfer by poising the potential of the mediator between that of P680⁺ and the Mn cluster of the OEC, so that transfer of an electron from TyrZ to P680⁺ and from the Mn cluster to the oxidized TyrZ are both thermodynamically favorable.

We report the synthesis and spectroscopic investigation of a photochemically active mimic of the chlorophyll-Tyr-His complex, molecule **1**. The molecule was adsorbed onto



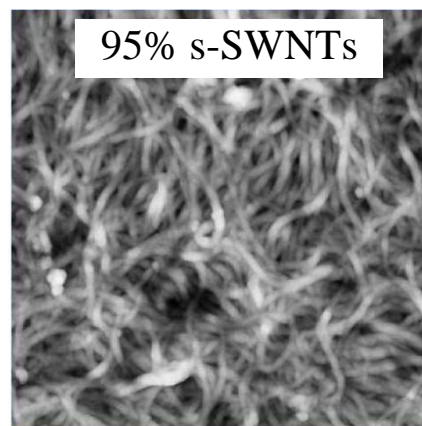
nanoparticulate TiO₂, which serves as an electron acceptor. Excitation of the porphyrin yields the first excited singlet state, which decays by photoinduced electron transfer to the semiconductor, yielding the porphyrin radical cation. Using low-temperature photoinduced D- and X-band EPR spectroscopy, we have found that when this construct is illuminated as a suspension in acetonitrile at 80 K, 95% of the resulting holes migrate from the porphyrin to the phenol moiety. When a similar experiment is performed at 4 K, 52% of the holes are trapped on the porphyrin, reminiscent of the observation of a trapped high-potential state in the natural system. Warming the sample to 80 K allows migration to the phenol, so that 95% of the holes reside on that entity. Only ~350 mV of redox potential is lost when the hole moves from the porphyrin to the phenol.

This construct exhibits key features of the mediated, high potential electrochemistry of photosynthesis. The molecule incorporates a built-in high potential mediator thermodynamically capable of coupling the anode of a photoelectrochemical cell to an appropriate water-oxidizing catalyst. The construct uses a bioinspired concept, a step-wise electron transfer process with tight control of proton activity, to move the oxidation potential from the sensitizer to a mediator. Key features of the system are that a considerable fraction of the high oxidation potential of the porphyrin is maintained in the phenol radical and the notoriously irreversible phenol redox chemistry is instead reversible (an imperative for a mediator).

PHOTOCHEMICAL PROPERTIES OF SINGLE-WALLED CARBON NANOTUBES: PRECISELY TUNED CHIRALITY MIXTURES AND SWNT-HYDROGENASE COMPLEXES

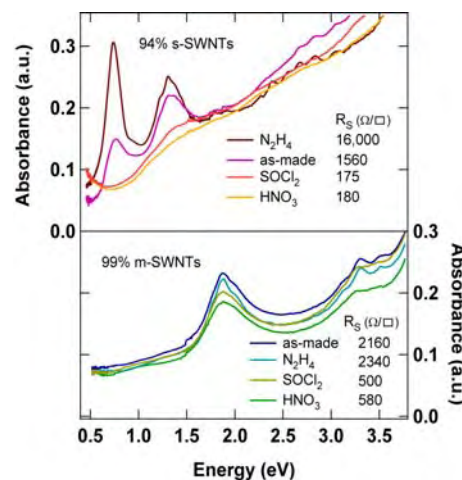
J.L. Blackburn, M.C. Beard, T.M. Barnes, D. Svedruzic, P.W. King, and M.J. Heben
Energy Sciences
National Renewable Energy Laboratory
Golden, Colorado 80401

Carbon single-wall nanotubes (SWNTs) exist in a variety of lattice conformations. As-produced samples are mixtures of metallic (m) and semiconducting (s). This poses a problem for building advanced architectures for solar energy conversion. For example, the presence of m-SWNTs can quench photoexcited states in s-SWNTs, and s-SWNTs interposed between m-SWNTs can inhibit charge transport. Moreover, the basic properties of the individual tube-types are obscured when mixtures are studied, especially in the condensed phase.



Using SWNTs produced in-house by laser vaporization, colloidal solutions enriched in m- or s-SWNTs were prepared by density gradient centrifugation.¹ Aliquots containing different proportions of m- and s-SWNTs were extracted and evaluated as to m- and s-SWNT content by comparing the integrated areas of the first metallic (M_{11}) and second semiconducting (S_{22}) optical transitions. Specifically chosen fractions were combined to prepare films with a wide range of precisely controllable m/s ratios.²

These films, best described as three-dimensional networks of highly conductive quantum wires with tunnel barriers between individual wires, were examined by a variety of spectroscopic and electrical techniques. The critical factors determining carrier transport are: (1) the density of carriers available for conduction, (2) the degree of carrier delocalization and role of tube-tube barriers, and (3) the effect of redox doping. Such studies are critical for understanding charge carrier dynamics following photoexcitation in transient absorption, microwave conductivity, and time-resolved terahertz conductivity experiments, and for constructing complex structures involving SWNTs for photoconversion.



During the past year we also continued our investigations of SWNTs complexed to the hydrogenase enzyme CaHydI. In contrast to our previous photoluminescence studies³ which probed only s-SWNTs, Raman spectroscopy was used to follow charge transfer interactions mediated by the adsorbed enzyme with both m- and s-SWNTs.⁴

¹Arnold, et al., *Nature Nanotech.* 2006, **1**, 60; ²Blackburn, et al., accepted to *Nano* 2008;

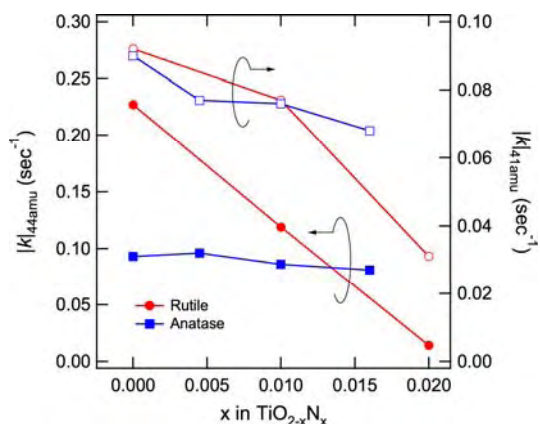
³McDonald, et al., *Nano Lett.* 2007, **7**, 3528; ⁴Blackburn, et al., accepted to *Dalt. Trans.* 2008.

PHOTOACTIVITIES OF N-DOPED RUTILE AND ANATASE SURFACES

Takeo Ohsawa, Sau. H. Cheung, Michael A. Henderson, Scott A. Chambers
Chemical and Materials Sciences Division
Pacific Northwest National Laboratory, Richland, WA 99352, USA

TiO₂ has been widely studied as heterogeneous photocatalyst since the discovery of its utility for the photoelectrolysis of water.¹ One of the major limitations of TiO₂ is that it absorbs relatively little of the solar spectrum. Asahi *et al.*² suggest that one way around this problem is by anion doping. Following this suggestion, many studies have been performed under visible-light irradiation using what is claimed to be N-doped TiO₂. It is critical to determine how N interacts with the TiO₂ lattice in order to understand the resulting electronic structure and photocatalytic activity. Our previous work has shown that the N solubility limit within the anion sublattice in rutile and anatase is ~2 atomic %.³ The N dopant substitutes for lattice O in both polymorphs as N³⁻ and adds 2*p* states above the valence band maximum, thereby reducing the interband optical absorption threshold to ~2.5 eV. Above the 2% solubility limit, N doping results in formation of an amorphous N-bearing phase with unknown photocatalytic properties.

In this presentation, we show that the hole-mediated photoactivities of structurally well-defined N-doped TiO₂ (TiO_{2-x}N_x, *x* ≤ 0.02) rutile (110) and anatase (001) films are significantly different. Trimethyl acetic acid (TMAA) was selected as a photochemical probe molecule because it undergoes acid dissociation on the TiO₂ surfaces to form densely-packed, stable trimethyl acetate (TMA) adlayers at RT. Exposing these surfaces to UV light results in e⁻/h⁺ pair formation in the substrate followed by a hole-mediated reaction in which TMA decomposes to CO₂ and a mixture of C₄s (isobutane and isobutene).⁴ The undoped rutile TiO₂(110) surface is shown to be over twice as active for TMA photodecomposition as compared to the undoped anatase TiO₂(001) surface, dispelling the notion that anatase is necessarily the more photoactive of the two polymorphs. However, as substitutional N is doped into the films, the hole mediated photoactivity of rutile TiO₂(110) significantly declines, as shown in the figure above, while the activity of the anatase TiO₂(001) surface is only mildly affected. These results show that holes are readily trapped (and neutralized) at N-dopant sites in rutile, but these sites in anatase do not inhibit hole migration and hole-mediated photochemistry.



CO₂ (mass 44, filled symbols) and C₄ (mass 41, empty symbols) rate constants, *k*, for photodecomposition of TMA as a function of substitutional N dopant concentration for epitaxial anatase TiO_{2-x}N_x(001) (blue squares) and rutile TiO_{2-x}N_x(110) (red circles).

1. Fujishima, A.; Honda, K. *Nature* **1972**, 238, 37.
2. Asahi, R.; Morikawa, T.; Ohwaki, T.; Aoki, K.; Taga, Y. *Science* **2001**, 293, 269.
3. (a) Cheung, S. H.; Nachimuthu, P.; Joly, A. G.; Engelhard, M. H.; Bowman, M. K.; Chambers, S. A. *Surf. Sci.* **2007**, 601, 1754; (b) Chambers, S. A.; Cheung, S. H.; Shutthanandan, V.; Thevuthasan, S.; Bowman, M. K.; Joly, A. G. *Chem. Phys.* **2007**, 339, 27.
4. Henderson, M. A.; White, J. M.; Uetsuka, H.; Onishi, H. *J. Am. Chem. Soc.* **2003**, 125, 14974.

A STABLE MOLECULAR CATALYST FOR OXYGEN EVOLUTION FROM WATER

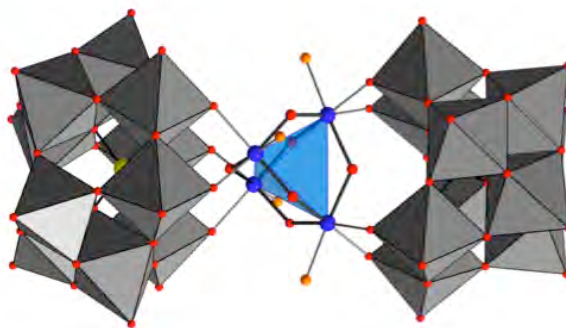
Yurii V. Geletii, Zhuangqun Huang, Yu Hou, Aleksey Kuznetsov, Tianquan Lian, Jamal Musaev, Craig L. Hill

Department of Chemistry and Cherry L. Emerson Center for Scientific Computation,
Emory University
Atlanta, Georgia 30322

Progress has been made on three fronts:

I. Design and realization of a stable molecular catalyst for oxidation of water to dioxygen.¹ Such a soluble complex could well be compatible (interface-able) with photosensitizer and/or catalytic H₂ evolution systems of many types. The complex Rb₈K₂[{Ru₄O₄(OH)₂(H₂O)₄}(γ-SiW₁₀O₃₆)₂]-25H₂O (**1**), comprises a [Ru₄(μ-O)₄(μ-OH)₂(H₂O)₄]⁶⁺ core stabilized by two oxidatively resistant (organic-structure-free) polytungstate ligands, [γ-SiW₁₀O₃₆]¹⁰⁻ (Ru-Ru distances of 3.47-3.66 Å; see Figure). Like the manganese oxo cluster catalyst for H₂O oxidation/O₂ evolution in green plants (OEC in Photosystem II), **1** undergoes 4 sequential reversible oxidations and then evolves O₂. While this work is only just starting, **1** addresses some core challenges in splitting H₂O with sunlight – it catalyzes the rapid oxidation of H₂O to O₂, does so in aqueous solution at pH 7, and is quite stable under turnover conditions.

Figure. Structure (right) of the polyanion in **1**, highlighting the central [Ru₄(μ-O)₄(μ-OH)₂(H₂O)₄]⁶⁺ core (ball-and-stick representation, Ru: blue, μ-O: red, O(H₂): orange, H omitted for clarity) and the slightly distorted Ru₄ tetrahedron (transparent blue). The polytungstate fragments are shown as gray polyhedra; Si as yellow spheres.



II. Characterization of the first triads comprising [Ru(bpy)₃]ⁿ⁺-TiO₂ (Grätzel cell components) with redox and catalytically active POMs including **1.** We have prepared successfully the triad and studied the charge transfer dynamics by time-resolved fluorescence and transient absorption spectroscopy in the visible and infrared.

III. Computational investigation of the geometrical and electronic structures of **1 and related complexes.** We have elucidated electronic structure of the complex **1**, and have analyzed the nature of its frontier orbitals at the DFT/B3LYP level of theory. The same theoretical approach was applied to elucidate the mechanism of O₂-based oxidation from [γ-1,2-H₂SiRu₂W₁₀O₄₀(H₂O)₂]⁴⁻ (**2**), which is the predicted precursor of complex **1**.

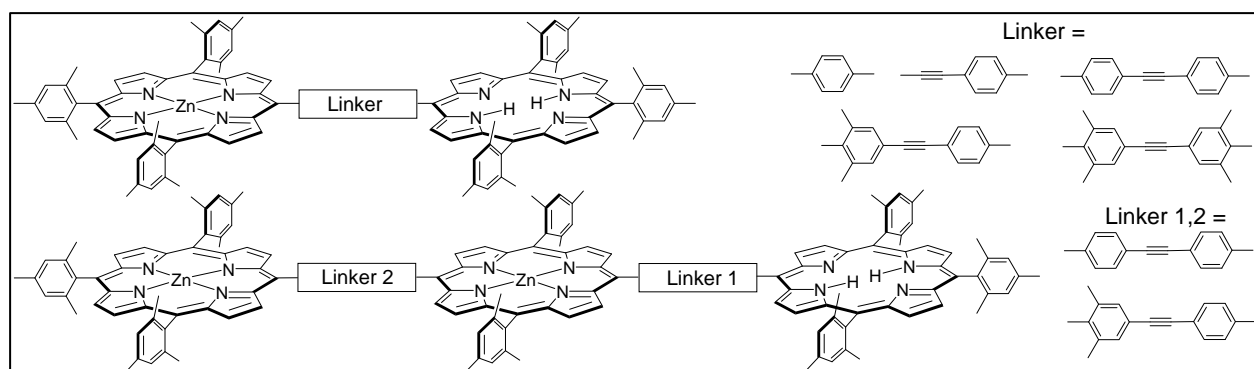
1. Geletii, Yurii V.; Botar, Bogdan; Kögerler, Paul; Hillesheim, Daniel A.; Musaev, Djameladdin G.; Hill, Craig L., An All-Inorganic, Stable, and Highly Active Tetraruthenium Homogeneous Catalyst for Water Oxidation. *Angew. Chem. Int. Ed.* **2008**, 47, “Early View” (published online 3/20/08). Selected as the VIP (Very Important Paper) by the reviewers and editor).

DETERMINATION OF THE RATES OF GROUND-STATE HOLE TRANSFER IN ONE-ELECTRON OXIDIZED TETRAPYRROLE ARRAYS VIA TIME-RESOLVED OPTICAL SPECTROSCOPY

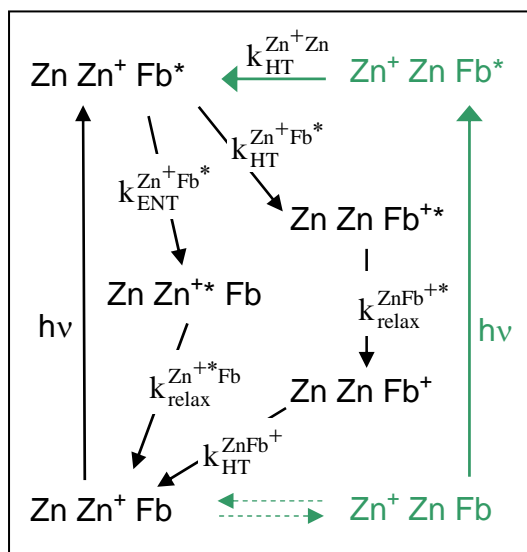
Hee-eun Song¹, Christine Kirmaier¹, Masahiko Taniguchi², James R. Diers³,
David F. Bocian³, Jonathan S. Lindsey², and Dewey Holten¹

Departments of Chemistry ¹Washington University, St. Louis, MO 63130; ²North Carolina State University, Raleigh NC 27695; ³University of California Riverside, Riverside CA 92521

A detailed understanding of ground-state hole migration in molecular architectures is essential for the design and construction of solid-state molecular-based solar-energy conversion systems. In particular, direct knowledge of the rates of ground-state hole-transfer between identical sites is central to the design of solar cells and any type of system that requires meta-stabilization of charge-separated states and/or the effective elimination of charge recombination. To this end, time-resolved absorption studies are being performed to directly obtain the rates of hole transfer between zinc porphyrins in triads that contain a free base porphyrin that serves as an optical probe; companion studies on benchmark dyads and monomers are being performed.



The structures of representative dyads and triads are shown above. One electron is removed from the zinc porphyrin(s) electrochemically, followed by ultrafast absorption measurements in which the free base porphyrin is selectively excited. The processes denoted in black in the kinetic scheme at the right (involving only the adjacent zinc and free base porphyrins) are those that also occur in the corresponding dyads. The processes denoted in green are those that occur exclusively in the triads. Comparison of the kinetic profiles for triads and dyads allows determination of the rate constant for hole transfer between adjacent zinc porphyrins joined by a specific linker. Studies are underway on analogous arrays that give the rate constants for hole transfer between free base porphyrins.



EXCITED-STATE AND PROTON-COUPLED ELECTRON-TRANSFER PROPERTIES OF TUNGSTEN-ALKYLIDYNE CHROMOPHORES AND ASSEMBLIES

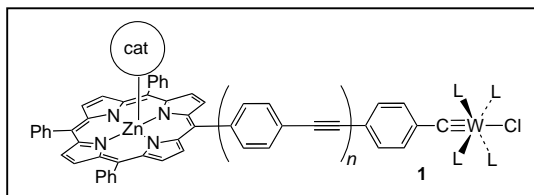
Brian W. Cohen, Michael I. Newsom, Benjamin Lovaasen, and Michael D. Hopkins

Department of Chemistry, 929 E. 57th Street

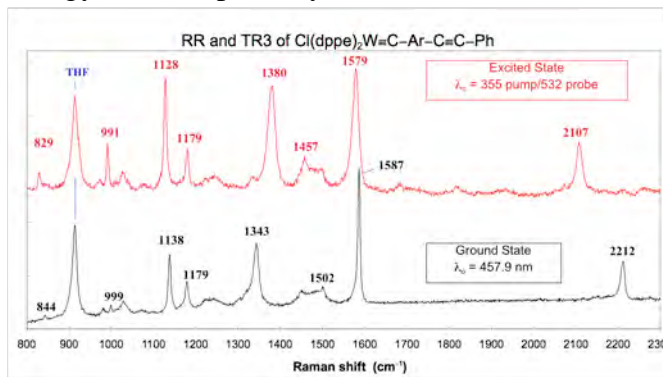
University of Chicago

Chicago, IL 60637

We are investigating inorganic complexes and assemblies with highly reducing excited-states suitable for the photochemical reduction of inert substrates such as CO₂. Among potential building blocks for these assemblies, our attention has been drawn to metal-alkylidyne complexes (*Coord. Chem. Rev.* **2005**, 249, 1396) because they possess broadly tunable redox, optical and photophysical properties and participate in proton-coupled electron-transfer reactions, which are anticipated to be important for catalyst regeneration and for the storage of proton/electron equivalents. One family of assemblies being studied is represented by **1**.



Recent research along two complementary tracks will be described. One set of studies has focused on characterizing the photophysical and excited-state properties of **1** and its constituents. Selective isotopic labeling (¹³C, ²H) within the W(CPh) unit of W(CPh)L₄Cl compounds, systematic variation of its ancillary ligands, and temperature-dependent luminescence studies of W(CAr)L₄Cl compounds containing extended phenylene-ethynylene Ar groups have provided insight into the key nonradiative-decay and energy-transfer pathways. In addition, the excited-state structures of the W(CAr)L₄X arms of **1** have been characterized by time-resolved XAFS ($n = 0$; in collaboration with Dr. Lin Chen, Argonne National Lab) and time-resolved resonance Raman spectroscopy ($n = 2, 3$; right); these results, together with ground-state structural studies of oxidized chromophores, point to small reorganization energies for the photoredox processes.



A second study has centered on elucidating the properties of the PCET reactions of W(CPh)L₄Cl complexes. For this purpose the family of compounds W(CPh)(dmpe)₂Cl, [W(CPh)(dmpe)₂Cl]⁺, and [HW(CPh)(dmpe)₂Cl]⁺ has been prepared and characterized by X-ray crystallography and variable-temperature multinuclear NMR spectrometry, and the thermodynamics of electron, proton, and hydrogen-atom transfer determined. The unusual seven-coordinate hydride ion has been found to be nonrigid in solution at room temperature and pentagonal-bipyramidal at low temperature and in the solid state, and is an unusually weak cationic acid (pK_a > 20). Importantly, it may be formed either via protonation of d² W(CPh)(dmpe)₂Cl or H-atom transfer to d¹[W(CPh)(dmpe)₂Cl]⁺.

FUNDAMENTAL STUDIES OF LIGHT-INDUCED CHARGE TRANSFER, ENERGY TRANSFER, AND ENERGY CONVERSION WITH SUPRAMOLECULAR SYSTEMS

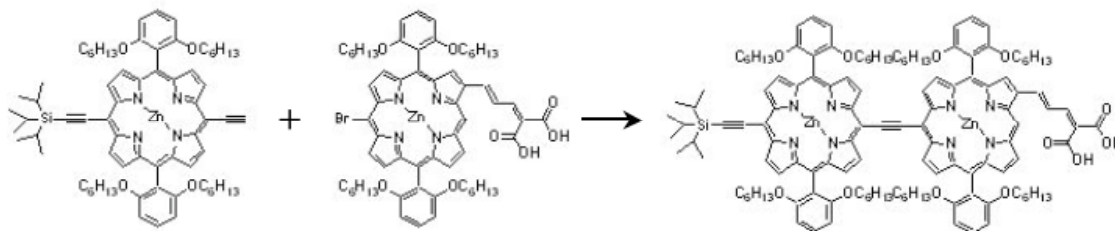
Joseph T. Hupp

Department of Chemistry
Northwestern University
Evanston, IL, 60093

This project seeks to exploit supramolecular chemistry: a) to interrogate and understand fundamental aspects of light-induced charge transfer and energy transfer, and b) to construct solar energy conversion systems that make use of unique assembly motifs to address key conversion efficiency issues.

We have been exploring dye systems that allow us to harvest a large fraction of the visible and near-IR spectrum. Our attention has been on highly conjugated porphyrin systems. These offer much higher extinction coefficients than the standard ruthenium dyes employed in Gratzel cells and much better spectral coverage than conventional porphyrin molecules. Higher extinction allows lower-area cells to be constructed. These, in turn, provide a path to lower dark currents and, in principle, higher photovoltages. Our recent focus has been on three issues: 1) dye attachment and loading, 2) “exciton” localization and delocalization within large assemblies, and 3) intra-assembly electron transfer within such assemblies. Results from these studies will be presented, along with preliminary results from sensitization of photoelectrochemical cells.

Shown below is a representative example of the dyes being developed. (Notably, the example features a terminal alkyne – a functional group that, after deprotection, should allow for multilayer formation via Sharpless-type “click” chemistry.) We find that dye loading is superior with malonate anchors (shown) in comparison to carboxylates. In the example shown, the anchor is positioned at a beta rather than meso site. Electronic structure calculations show that a node exists at the beta site in the HOMO, but not in the LUMO. The implication is that beta anchored assemblies will be wired well for electron injection (from the LUMO), but wired poorly for recombination (back ET to the LUMO). The opposite situation exists for meso-tethered dyes, i.e. the electronic structure should favor comparatively slow injection and comparatively rapid recombination (perhaps even geminate recombination). We suspect that efficient geminate recombination accounts for many of the unexplained efficiency shortfalls with previous cells sensitized with porphyrins.



Representative references: R. F. Kelley, et al., *J. Am. Chem. Soc.*, **2008**, *130*, 4277-4284.

A. B. F. Martinson, T. W. Hamann, M. J. Pellin, J. T. Hupp, *Chem. Eur. J.*, **2008**, “early view.”

R. A. Jensen, R. F. Kelley, S. J. Lee, M. R. Wasielewski, J. T. Hupp, D. M. Tiede, *Chem. Comm.*, **2008**, 1886.

COVALENT AND NON-COVALENT COUPLING OF NOVEL CHROMOPHORES FOR HIGH SINGLET FISSION YIELDS

Justin C. Johnson, Akin Akdag, Xudong Chen, Josef Michl, Arthur J. Nozik

Although singlet fission (the splitting of one singlet exciton into two triplets) was intensively researched decades ago, it has only recently been considered as a means for improving the efficiency of solar photoconversion devices. In order to optimize the singlet fission yield in practical chromophores, several molecular parameters must be considered. The dependence of the molecular photophysics, especially triplet yield, on coupling strength, geometry, and energy level alignment in designed molecular dimers and crystals has been investigated both theoretically and experimentally under a variety of conditions. The focus of recent efforts has been on derivatives of 1,3-diphenylisobenzofuran (DPIBF). DPIBF has an energy level structure such that the double-triplet state is expected to lie slightly lower in energy than the lowest energy singlet state. Thus, with appropriate coupling between chromophores, DPIBF should undergo singlet fission without competition from vibrational relaxation or reversal due to fast triplet-triplet annihilation.

Interchromophore coupling is a critical issue in singlet fission studies. DPIBF dimers with various coupling strengths and geometries were synthesized and studied optically. Thin solid films of varying crystallinity were also fabricated. The time-resolved spectroscopic results suggest a possible new mechanism for the singlet fission process in weakly coupled covalently-bound dimers, involving an intermediate state stabilized by polar media. This process may be distinct from singlet fission in solid films, where excitations are strongly delocalized and singlet fission can potentially proceed with a higher rate and efficiency than in isolated dimers. Design of new molecules and aggregates to produce high singlet fission yields for utilization in practical devices is ongoing and guided by these initial efforts toward a fundamental understanding of the dynamics of the process.

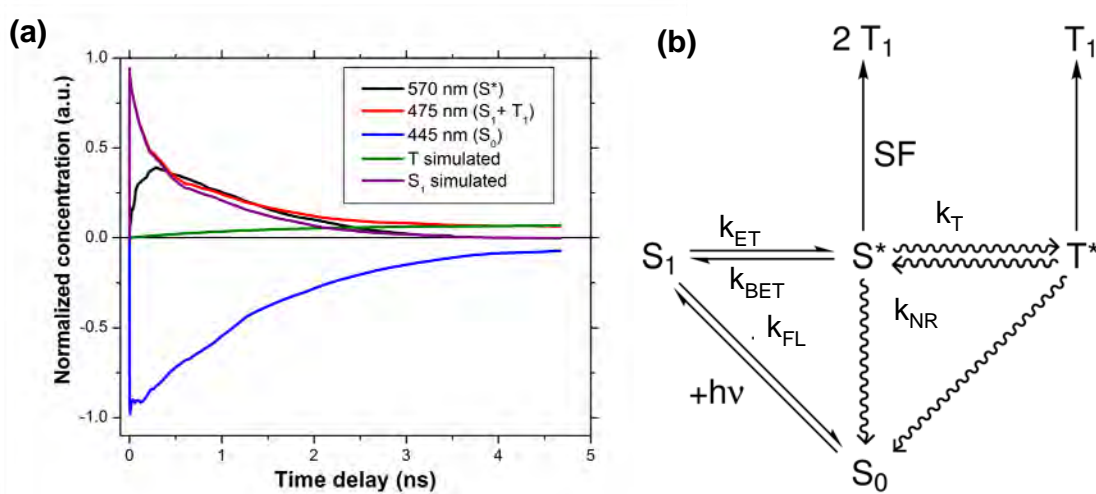


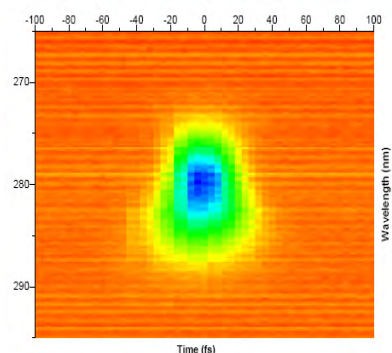
Figure 1. (a) Kinetics of electronic state population after photoexcitation derived from global target analysis of pump-probe probe data from DPIBF dimers in polar solution. (b) Proposed kinetic scheme of intermediate and triplet formation.

TOWARDS MULTIDIMENSIONAL SPECTROSCOPY OF QUANTUM DOTS

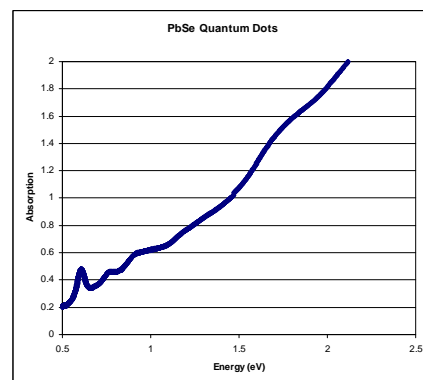
Byungmoon Cho, William K. Peters, Robert J. Hill, and David M. Jonas
Department of Chemistry and Biochemistry
University of Colorado
Boulder, Colorado 80309-0215

Multiple Exciton Generation (MEG) is a potential route to more efficient photovoltaic devices. Theories proposed to explain reports of MEG differ in the dephasing dynamics which convert the coupled hot single exciton and multiple exciton states into metastable multiple excitons, with corresponding differences in the MEG yield. We will discuss progress towards multidimensional spectroscopy of semiconductor quantum dots, where we have goals of measuring the coupling and dephasing between the hot single exciton and multiple exciton states.

To carry out these experiments, we have built a visible femtosecond Non-collinear Optical Parametric Amplifier (NOPA) pumped by a cw pumped Ti:sapphire regenerative amplifier (Coherent REGA). The design closely follows that of Riedle and co-workers, using the frequency doubled (400 nm) output of the REGA as the pump and a white light continuum as the signal in the optical parametric amplifier. Pulse durations of 15 fs have recently been reported for this type of NOPA. The measured NOPA pulse spectra at a center wavelength of 560 nm indicated a transform limited pulse duration of 17 fs. Although initial pulse characterization by non-collinear Second Harmonic Generation (SHG) autocorrelation suggested a near transform limited 19 fs pulse duration, measurements by SHG Frequency Resolved Optical Gating indicated a bandwidth limitation due to excess thickness of the SHG crystal (100 micron BBO). SHG FROG measurements (Figure 1) using a specially fabricated KDP wedge, where the thickness can be adjusted down to zero, indicate a 24 fs pulse duration with improved cubic dispersion compensation needed to reach the transform limit. Pulse to pulse energy stability is better than 1% and should be improved by replacement of lossy REGA compressor gratings. A kHz near-IR NOPA is under construction.



Our size-selective synthesis of PbSe quantum dots closely follows the work of Luther et al. Crude initial estimates from the absorption spectrum suggest a 7 nm diameter with a size distribution of 15% for the spectrum shown in Figure 2. We are setting up measurements of photoluminescence spectra and learning to do TEM. For time resolved experiments, we have put together a sample cell which is sealed from the atmosphere and rotates at 3000 rpm. For a 30 micron spot size, this allows experiments at up to 100 kHz repetition rate to probe a fresh sample. We are currently measuring hot single exciton lifetimes above the MEG threshold in PbSe dots with pump-probe and transient grating techniques.



EXCITON DYNAMICS IN GASE QUANTUM DOT AGGREGATES

David F. Kelley

University of California, Merced
Merced, CA, 95344

GaSe is a layered semiconductor that forms disk-like nanoparticles having diameters of 2.5 to 12 nm. Recent AFM images confirm electron diffraction and spectroscopic results indicating that the particles are single tetra-layers, see figure 1, below.

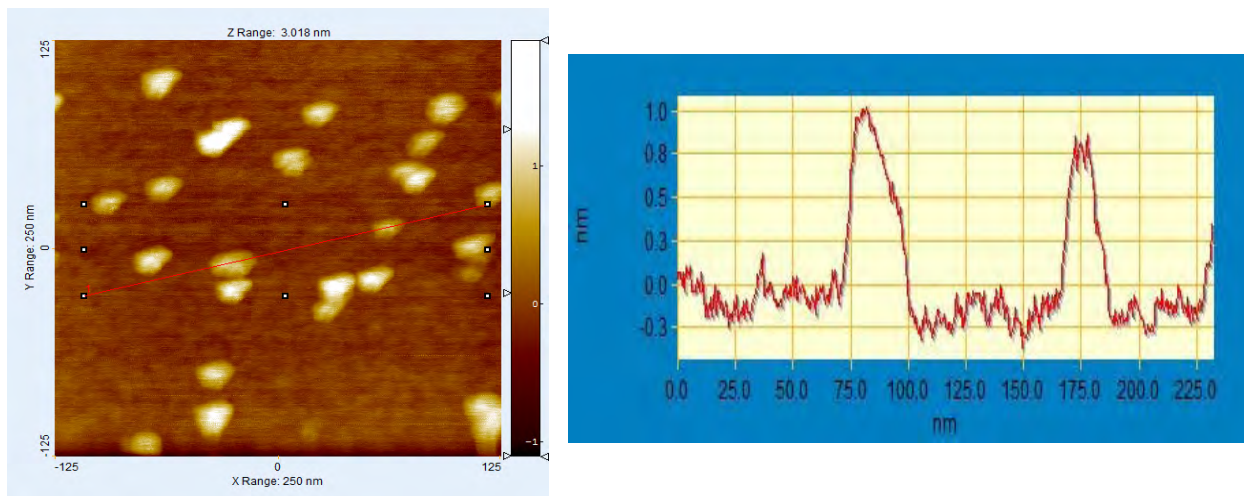


Figure 1. Preliminary AFM images GaSe nanoparticles on a gold surface. All particles show heights of about 1.0 nm, consistent with the assignment to single tetra-layers and the known crystal structure. At higher concentrations, (not shown) images of aggregates are also observed. The large apparent diameters are due to the finite AFM tip size. (Images courtesy of Prof. Tao Ye, U. C. Merced.)

We have recently established that the extent to which the particles aggregate in solution and in liquid crystals is a very sensitive function of their surface chemistry. The particles are normally ligated with TOP and TOPO ligands. These ligands can be displaced by less bulky octanal ligands, resulting in much more strongly interacting aggregates, as seen in the absorption spectrum, figure 2. Dynamical studies measuring exciton motion and superradiance in these aggregates are currently in progress.

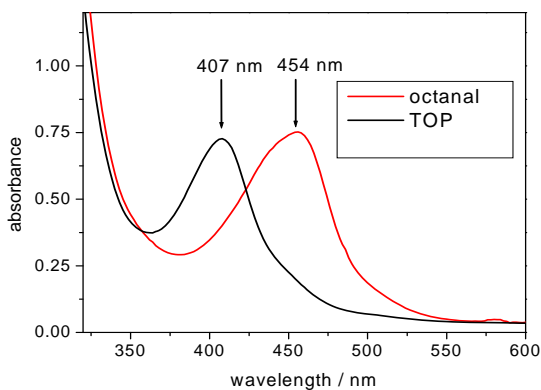


Figure 2. Absorption spectra of GaSe nanoparticles in TOP (black curve) and in TOP with 5% octanal (red curve). The presence of the octanal induces particle aggregation, causing the spectrum to shift about 50 nm to the red.



SNAPSHOTS OF BIOLOGICAL PROTON-COUPLED ELECTRON TRANSFER: PULSED ELECTRON PARAMAGNETIC RESONANCE SPECTROSCOPY OF TYROSINE INTERMEDIATES IN PHOTOSYSTEM II

Oleg Poluektov,² Sophia Lee,¹ Shreya Chand,¹ Arlene Wagner² and K. V. Lakshmi¹

¹*Department of Chemistry and Chemical Biology, Rensselaer Polytechnic Institute, Troy, NY 12180*

²*Chemistry Division, Argonne National Laboratory, Argonne, IL 60439*

The solar water-splitting protein complex, photosystem II (PSII), catalyzes one of the most energetically demanding reactions in Nature by using light energy to drive the catalytic oxidation of water. Proton-coupled electron transfer (PCET) reactions, which are exquisitely tuned by smart protein matrix effects, are central to this water-splitting chemistry. PSII contains two symmetrically placed tyrosine residues, Y_D and Y_Z, one on each subunit of the heterodimeric core

(Figure 1). The functions of these symmetry-related tyrosines are quite distinct, a versatility provided by their distinct local environments in PSII. Y_Z is kinetically competent and has been proposed to be directly involved in the PCET reactions of water oxidation. In contrast, the Y_D PCET redox poises the catalytic Mn₄

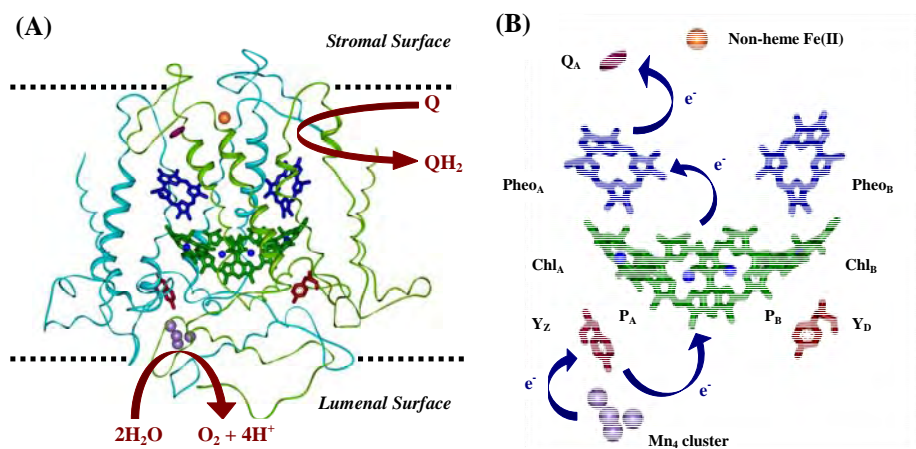


Figure 1. (A) Schematic of the D1 and D2 polypeptide chains of PSII displaying the charge-transfer cofactors and the net reactions of light-driven water oxidation and quinone reduction. (B) The primary electron-transfer pathway of PSII. Also shown are the redox-active tyrosine residues that participate in proton-coupled electron transfer reactions.

cluster and may electrostatically tune the adjacent monomeric redox-active chlorophyll and β -carotene in the secondary ET pathway of PSII. This study focuses on disentangling individual steps of the photo-induced PCET events that lead to the formation of the redox-active tyrosyl radical, Y_D[•], in PSII. Owing to the cryogenic turnover properties of PSII, it is possible to photo-oxidize Y_D at 1.8 K where both the proton and protein motions are limited. Annealing this state at a slightly higher temperature allows proton movement and relaxation of the protein environment. It is our hypothesis that the electron transfer, proton movement and associated conformational changes of the Y_D-binding pocket are the individual steps of the PCET reaction. Together, these reactions result in highly-efficient unidirectional proton and electron transfer at Y_D. Using pulsed high-frequency EPR and ¹H and ²H ENDOR spectroscopy, we elucidate the sequence of events that lead to PCET at the Y_D site of PSII. These studies provide ‘snapshots’ of functional PCET intermediates and, for the first time, make it possible to directly observe the mechanism of PCET in biological energy transduction.

CHEMICAL CONTROL OVER THE ELECTRICAL PROPERTIES OF GaAs AND Zn_3P_2 SEMICONDUCTOR SURFACES AND PHOTOELECTRODES

Gregory M. Kimball, Matthew C. Traub, and Nathan S. Lewis

Division of Chemistry and Chemical Engineering

California Institute of Technology

210 Noyes Laboratory, 127-72, Pasadena, CA 91125

Semiconductor surface chemistry underlies the performance of solar energy conversion systems based on the photoelectrochemical production of electricity or fuels. Particularly in nanocrystalline structures, the high surface area creates an even greater need for surfaces that are chemically inert and electrically passive. We report recent results demonstrating chemical control of the electrical properties of both GaAs nanocrystals powders and Zn_3P_2 large-grain polycrystals.

We have demonstrated an effective protocol to synthesize crystalline GaAs nanocrystals and to chemically passivate native surface states. Treatment of HCl-etched GaAs nanocrystals with hydrazine or sodium hydrosulfide resulted in a functionalized semiconductor surface. After annealing, the N 1s peak of N_2H_2 -exposed GaAs nanocrystals shifted by 3.2 eV to a lower binding energy as determined by XPS. The band-gap photoluminescence was weak from the Cl⁻ and N_2H_2 or sulfide-terminated nanocrystals, but the annealed nanocrystals displayed strongly enhanced band-edge PL, indicating that the surface states of GaAs nanocrystals were effectively passivated by this two-step, wet chemical treatment (Fig. 1).

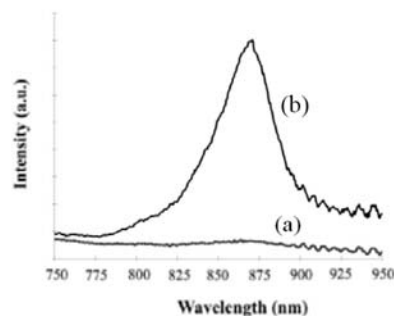


Fig. 1. Steady-state photoluminescence intensity of N_2H_2 -functionalized samples (a) before and (b) after annealing.

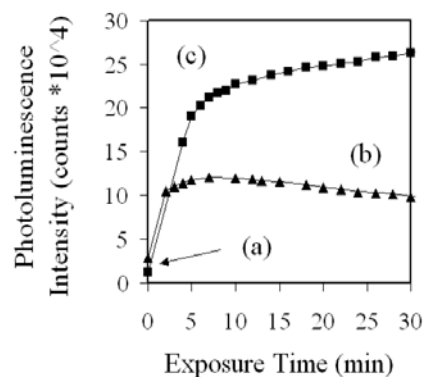


Fig. 2. Steady-state photoluminescence intensity data for Zn_3P_2 surfaces (a) as polished, (b) etched with bromine in methanol, and (c) etched and treated with ammonium sulfide in t-butanol.

Zinc phosphide (Zn_3P_2) is a promising material for solar energy conversion. Zn_3P_2 has many attractive properties including a direct gap near the terrestrial optimum (1.5 eV), electrically passive grain boundaries, and constituent elements that are earth abundant as well as inexpensive. Etching with bromine in methanol is shown both to readily remove native oxide and to dramatically enhance photoluminescence. Sulfur passivation with ammonium sulfide in t-butanol provides a Zn_3P_2 surface that is both strongly photoluminescent and resistant to degradation by air oxidation (Fig. 2). After treatment, the P2p photoelectron spectrum showed a new species attributable to P-S bonding at 132.1 eV. We hypothesize that a P-S surface layer forms above the Zn_3P_2 bulk and protects the underlying semiconductor.

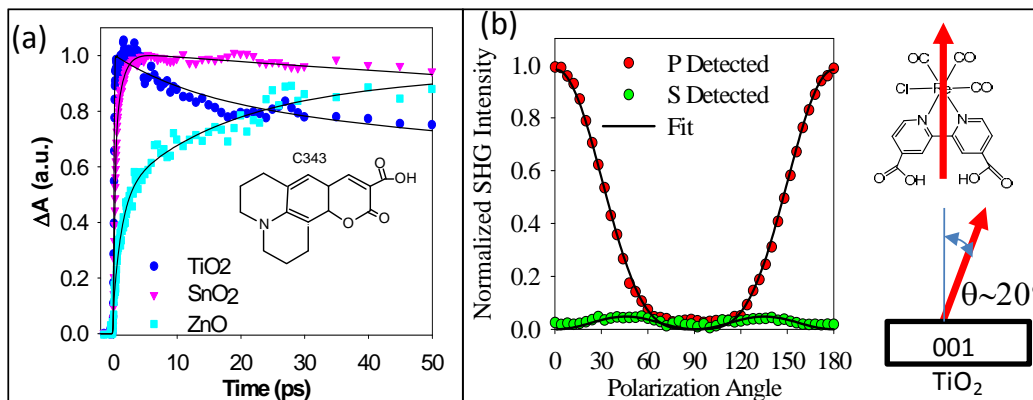
SEMICONDUCTOR DEPENDENCE OF INTERFACIAL ELECTRON TRANSFER

Jier Huang, Dave Stockwell, Chantelle Anfuso, Baohua Wu and Tianquan Lian
Department of Chemistry
Emory University
Atlanta, GA 30322

Photoinduced interfacial electron transfer (ET) from molecular adsorbates to metal oxide nanoparticles is a fundamental process that is relevant to the design and improvement of many nanoparticle based devices, such as dye sensitized solar cells. There have been many reports of ultrafast electron transfer from $\text{Ru}(\text{dcbpyH}_2)_2(\text{NCS})_2$ (**N3**) [dcbpy = 2,2'-bipyridine-4,4'-biscarboxylic acid] and related sensitizer molecules to TiO_2 nanocrystalline thin films. Slower injection processes were often reported on other metal oxides, such as SnO_2 and ZnO . It is unclear whether there is a general trend of semiconductor dependence and what may be responsible for such trend. To address these questions, we have compared the injection kinetics from a series of small organic sensitizers (coumarins and oligoenes) to TiO_2 , SnO_2 and ZnO . These molecules have excited oxidation potentials high above the conduction band edge, reducing the influence of poorly characterized defects states on the injection process. They are also chosen to facilitate comparisons with computation modeling (conducted by V. Batista's group at Yale University), which is crucial to the understanding of the semiconductor dependence. To provide further test of computational models, the geometry of adsorbate on single crystal surfaces was also measured by Second Harmonic Generation (SHG) Spectroscopy.

As shown in Figure 1a, average injection times from Coumarin 343 to TiO_2 , SnO_2 , and ZnO , are $< 100\text{fs}$, $\sim 1\text{ps}$ and $\sim 10\text{ps}$ respectively. Similar trends were observed for a series of phenyl substituted oligoenes. We will discuss these trends, comparison with computational modeling and possible reasons for the semiconductor dependence. Shown in Figure 1b is the dependence of SHG signal on the polarization angle of incident fundamental beam (at 800 nm) for $\text{Re}(\text{dcbpy})(\text{CO})_3\text{Cl}$ (**ReC0A**) on Rutile TiO_2 (001) surface. We will discuss a preliminary analysis of adsorbate orientation (relative to surface normal) obtained from the measured ratios of the SHG signals at different polarization combinations.

Fig. 1 a) comparison of electron injection rate from coumarin 343 to TiO_2 , SnO_2 and ZnO . b) the polarization dependence of SHG signal of **ReC0A** on rutile TiO_2 (001).



ACCESSING THE NEAR-INFRARED SPECTRAL REGION WITH STABLE, SYNTHETIC WAVELENGTH-TUNABLE BACTERIOCHLORINS

Masahiko Taniguchi,^a David L. Cramer,^a Anil D. Bhise,^a Hooi Ling Kee,^b David F. Bocian,^c
Dewey Holten,^b and Jonathan S. Lindsey^a

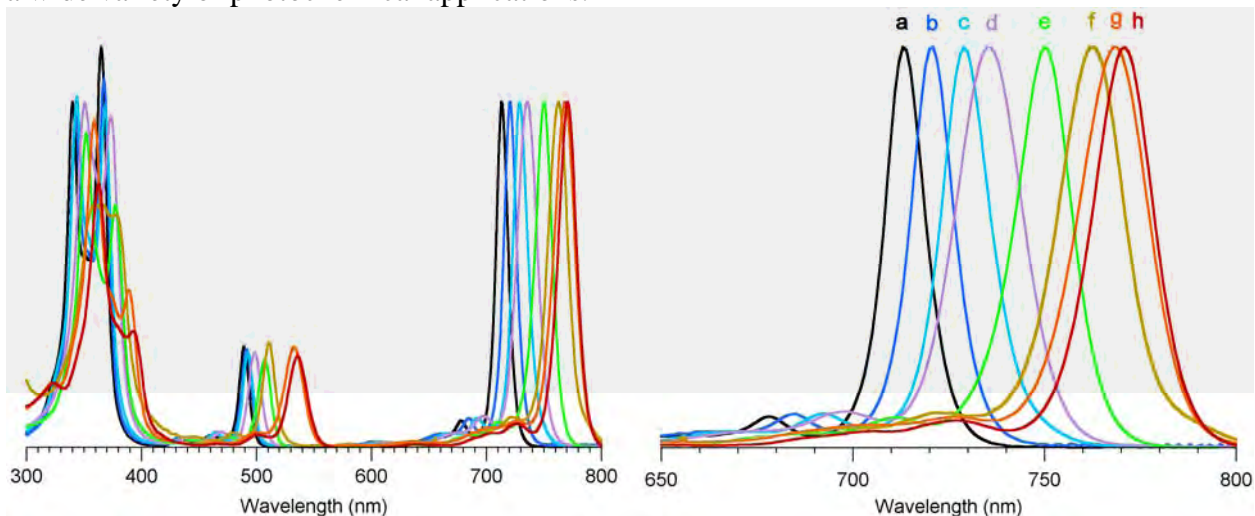
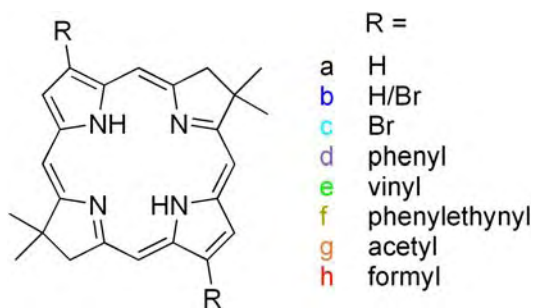
^aDepartment of Chemistry, North Carolina State University, Raleigh, NC 27695

^bDepartment of Chemistry, Washington University, St. Louis, MO 63130

^cDepartment of Chemistry, University of California Riverside, Riverside, CA 92521

The near-infrared (NIR) spectral region has been comparatively underutilized for diverse materials and medical applications owing to the lack of chromophores that afford stability, solubility, synthetic malleability, and tunable photophysical features. Bacteriochlorins are attractive candidates in this regard; however, preparation via modification of naturally occurring bacteriochlorophylls or reduction of porphyrins or chlorins has proved cumbersome. To overcome such limitations, a dibromobacteriochlorin (**BC-Br³Br¹³**) was prepared *de novo* by the acid-catalyzed condensation of an 8-bromo-dihydrodipyrriin-acetal. **BC-Br³Br¹³** bears (1) a geminal dimethyl group in each reduced ring to block adventitious dehydrogenation, and (2) bromo groups at the 3- and 13-positions (R = Br) for further chemical modifications. **BC-Br³Br¹³** was derivatized via Pd-mediated reactions to give bacteriochlorins bearing diverse substituents at the 3- and 13-positions (R = phenyl, vinyl, phenylethynyl, acetyl, formyl), and a benchmark bacteriochlorin lacking such substituents (R = H).

Depending on the substituents at the 3- and 13-positions, the position of the long-wavelength absorption maximum [$Q_y(0,0)$ band] lies between 713 and 771 nm, the fluorescence emission maximum lies between 717 and 777 nm, and the fluorescence quantum yield ranges from 0.15 to 0.070. The ability to introduce diverse auxochromes and the tunable absorption and emission spectral properties suggest that synthetic bacteriochlorins are viable candidates for a wide variety of photochemical applications.

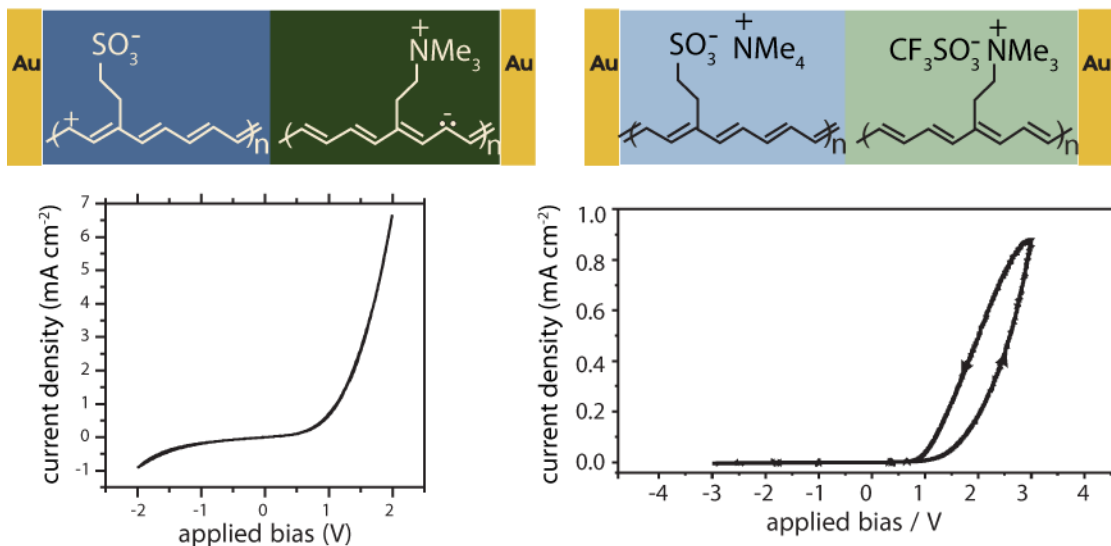


CONJUGATED IONOMERS FOR PHOTOVOLTAIC APPLICATIONS: ELECTRIC FIELD DRIVEN CHARGE SEPARATION AT ORGANIC JUNCTIONS

Fuding Lin, Ethan Walker, David Stay, Yongjun Wang, and Mark Lonergan
Department of Chemistry, The Materials Science Institute
University of Oregon
Eugene, OR 97403

The photovoltaic properties and electrical asymmetries of junctions based on conjugated ionomers (ionically functionalized conjugated polymers), such as those shown below, are reported. Unlike conventional organic photovoltaic junctions, these interfaces are designed to generate a built-in electric field through charge depletion, much like in the classic inorganic pn junction. In the doped example on the left, charge separation is driven by the exchange of electronic charge carriers as in the silicon pn junction. In the undoped example on the right, charge separation is driven by ion exchange across the interface. In both case, the generation of a built-in electric field is made possible by the covalently bound counter-ions. These immobile counter-ions stabilize the junction with respect to either a bulk redox reaction on the left or the exchange of salt on the right. Both systems show the asymmetric current-voltage behavior typical of a photodiode.

Spectrally resolved photoresponse, impedance analysis, and current-voltage measurements (transient and steady-state) are reported in an effort to understand the asymmetries observed in these systems and characterize their photovoltaic properties. The mechanisms of electrode polarization and mixed ionic/electronic transport appear intermediate between more traditional electrochemical and solid-state junctions. The implications of the unique mechanistic aspects of carrier transport and polarization on photovoltaic applications are discussed. New materials synthesis to control ionic functional group density, which is essential for controlling junction properties, is also presented.



MOLECULAR LEVEL ORGANIZATION OF HETEROMETALLIC OXIDES/ORGANICS FOR PHOTOCATALYSIS

Paul A. Maggard
Department of Chemistry
North Carolina State University
Raleigh, NC 27695

Standard solid-state synthesis has been the predominant method for preparing large band gap metal-oxides that can absorb ultraviolet light and photocatalytically react with water to produce hydrogen. However, this synthetic route also represents a relatively limited way to explore higher-level structural designs that could lead to the more optimal atomic and electronic structures necessary for discovering new types of photocatalysts. Our research efforts have focused on the synthesis of new heterometallic-oxide/organic solids based on: 1) structural incorporation of organic ligands which enables a finer molecular-level structural control, and 2) molten-salt flux reactions for controlled growth of particle sizes from nanometers up to micrometers as well as in flux-assisted ion exchange reactions. Our new metal oxides also contain specific combinations of d^0 (e.g., Ta^{5+}) with d^{10} (e.g., Ag^+) electron configurations to create an optimal band-energy profile for visible-light absorption and catalysis.

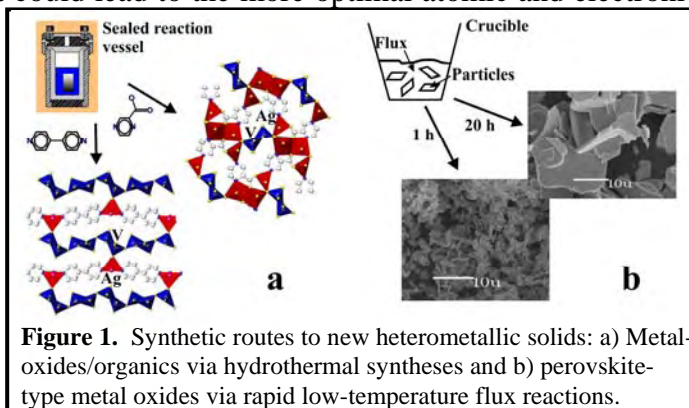


Figure 1. Synthetic routes to new heterometallic solids: a) Metal-oxides/organics via hydrothermal syntheses and b) perovskite-type metal oxides via rapid low-temperature flux reactions.

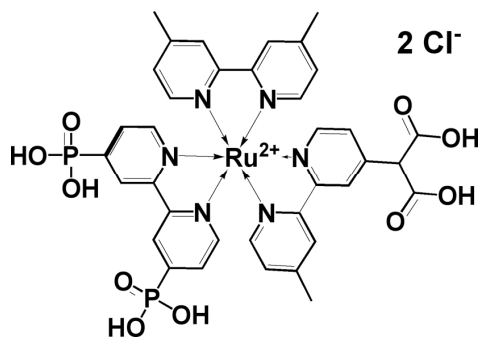
Several new heterometallic-oxide/organic solids (e.g., $MM'OL$; $M/M' =$ transition metals with d^0 and d^{10} electron configurations; $L =$ coordinating ligand) in the Cu/Re , Ag/Re , Cu/V and Ag/V systems have been synthesized by hydrothermal techniques. These compounds exhibit optical bandgap sizes in the visible-light energy range, at ~ 400 – 500 nm for the Ag -based systems and at ~ 500 – 650 nm for the Cu -based systems. Further, coordination of selected organic ligands to the oxide framework has yielded a wide range of structural diversity in which to probe and elucidate the structural principles of their formation. As will be presented in the poster, the new synthetic explorations have demonstrated the accessibility of a diverse array of structural motifs, including clusters, chains, and layers, and that are a function of both the solvent pH and the ligand geometry and size. This work has enabled new investigations into the effects of coordination environments and framework dimensionalities on the measured bandgap sizes and types, absorption coefficients, and relative band potentials of heterometallic oxides. At a larger size-scale regime, the molten-salt flux growth of heterometallic-oxide particles (e.g., $MM'O$) in the Ag/Nb and Cu/Nb systems has been investigated towards achieving a finer control over particle sizes and morphologies, as well as for improved product homogeneity. Current results will be presented that illustrate the formation of 'nano-terraced' surface features on $AgNbO_3$ particles grown from molten salts (e.g., Na_2SO_4), and which have been investigated for their role in activating its surfaces for the photocatalytic reaction with water. In addition, new research will be presented on the use of molten-salt fluxes for facilitating rapid ion-exchange reactions that accomplish the insertion of Cu^+/Ag^+ ions into layered tantalate and niobate perovskites.

SEMICONDUCTOR-SENSITIZER-CATALYST SYSTEMS FOR OVERALL WATER SPLITTING USING VISIBLE LIGHT

W. Justin Youngblood, Seung-Hyun Anna Lee, Deanna Lentz, Hideo Hata, Renzhi Ma, Paul G. Hoertz, Thomas A. Moore,[†] Ana L. Moore,[†] Devens Gust,[†] and Thomas E. Mallouk
Department of Chemistry, Department of Chemistry and Biochemistry[†]
The Pennsylvania State University and Arizona State University[†]
University Park, PA 16802 and Tempe, AZ 85287[†]

The design of visible light water splitting catalysts is a long-standing problem that continues to be of both fundamental and practical interest. By linking molecular sensitizers to both oxide semiconductor particles and oxygen-evolving iridium oxide colloids, we are making donor-sensitizer-acceptor triads and studying them as components of photoelectrochemical and photocatalytic water splitting systems.

While oxynitride semiconductor-based water splitting photocatalysts have been reported by Domen and coworkers, there has so far been little success in developing molecular catalysts for the overall water splitting reaction. We recently showed (*J. Phys. Chem. B.* **2007**, *111*, 6945) that ruthenium poly(pyridyl) sensitizers with pendant malonate or succinate ligands could stabilize 2 nm diameter IrO₂ colloids, and that the resulting sensitizer-linked colloids are very good photocatalysts for water oxidation. We now report that a ruthenium tris(bipyridyl) sensitizer containing both malonate and phosphonate ligands (below) can link the stabilized IrO₂ clusters to a high surface area TiO₂ electrode. Transient absorbance experiments show that the photoexcited sensitizer rapidly injects an electron into the TiO₂ film, and that electron transfer from IrO₂ to Ru³⁺ then occurs on a timescale of ~3 ms. At open circuit, back electron transfer from TiO₂ to Ru³⁺ is much faster (~0.3 ms). In a three-electrode cell, the sensitized electrode acts as a photoanode for overall water splitting with 0.8% quantum yield at 450 nm. An open circuit photovoltage of 880 mV is obtained, and hydrogen is evolved at the Pt cathode. We are now exploring other ligands and assembly strategies in order to decrease the rate of back electron transfer from the TiO₂ electrode and increase the fraction of sensitizer molecules that are linked in the TiO₂-sensitizer-IrO₂ triad arrangement.



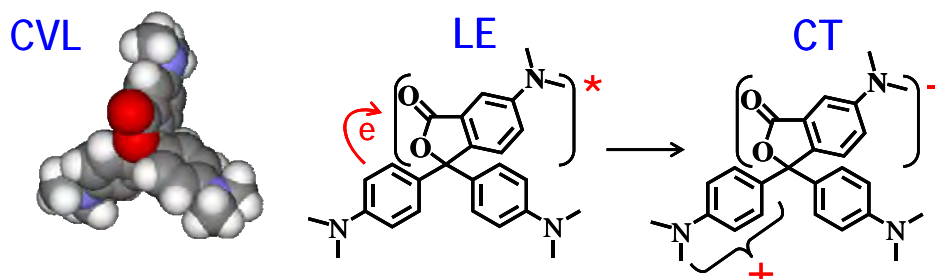
In order to extend this idea to photocatalytic systems, we need to use semiconductors with more negative conduction band edge potentials than TiO₂ and catalyze the reduction of water by photoinjected electrons. Another important requirement is to prevent the hydrogen-evolving catalyst from catalyzing the recombination reaction of hydrogen and oxygen. With oxynitride photocatalysts, Maeda and Domen have found that Rh/Cr₂O₃ core-shell nanoparticles have the desired catalytic selectivity. We have therefore studied the photocatalytic activity of Rh nanoparticles dispersed on HCa₂Nb₃O₁₀ sheets and Nb₂O₅ nanotubes. We have found unusually good dispersion of Rh and high photocatalytic activity for hydrogen generation from aqueous methanol solutions with these catalysts. Electron microscopy and zeta potential measurements suggest that covalent Nb-O-Rh bonding stabilizes sub-1 nm Rh catalyst particles on the niobium oxide supports. We are currently studying the reduction of Cr(VI) onto these clusters.

CHARGE TRANSFER IN CRYSTAL VIOLET LACTONE: CONVENTIONAL SOLVENTS AND IONIC LIQUIDS

Mark Maroncelli and Xiang Li

Department of Chemistry, Penn State University,
104 Chemistry Building, University Park, PA 16802

Crystal violet lactone (CVL) is one of those rare molecules that exhibits dual fluorescence in liquid solution. Recent work by Karpiuk¹ has established the origin of this dual fluorescence to be an excited-state electron transfer between a locally excited state of the aminophthalimide ring and one of the dimethylanilino groups, as indicated below. We have been exploring the use of this reaction as a probe of electron transfer in ionic liquids.



In conventional solvents the equilibration between the LE and CT states occurs on the 10-100 ps time scale and the equilibrium constant is a simple function of solvent dielectric parameters. In typical aprotic solvents bi-exponential kinetics are observed, as expected for a simple 2-state reaction. The reaction rates observed are strongly correlated to the integral solvation times and are roughly in keeping with expectations for a small-barrier reaction dominated by outer sphere reorganization.

In ionic liquids the reaction is much slower than in conventional solvents, consistent with the much slower solvation times found in ionic liquids. But, because solvation and reaction occur on comparable time scales, the reaction kinetics are more complex than in conventional solvents. The kinetics also depend markedly on excitation wavelength (which is not the case in conventional solvents). This dependence is indicative of the dynamic heterogeneity that we believe is characteristic of many fast processes taking place in ionic liquids.

In this poster, we summarize our current understanding of the nature of the solvent control over this excited-state electron transfer reaction in conventional solvents, ionic liquids, and their mixtures.

References:

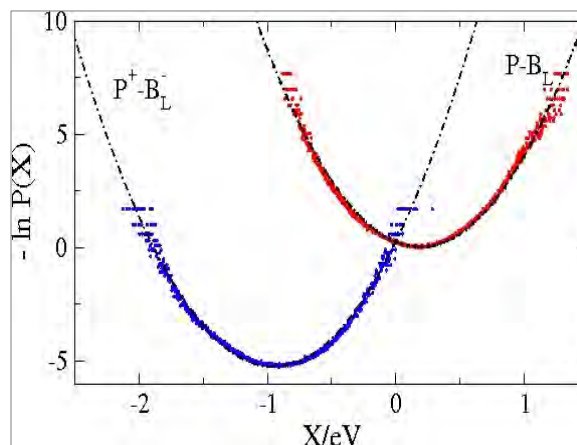
J. Karpiuk, "Dual Fluorescence from Two Polar Excited States in One Molecule. Structurally Additive Photophysics of Crystal Violet Lactone," *J. Phys. Chem. A* **108**, 11183-11195 (2004).

ENERGETICS OF NATURAL PHOTOSYNTHESIS AND MECHANISMS OF REDUCTION OF CHARGE RECOMBINATION

D. N. LeBard and D. V. Matyushov
Center for Biological Physics
Arizona State University
Tempe, AZ, 85287-1504

Recombination of the photoinduced charge-separation transition presents a significant bottleneck for the efficiency of solar energy conversion. In addition to technological solutions, general ideas of how to efficiently fight recombination rates are required. The current understanding of photoinduced charge transitions in molecules rests on ideas incorporated into the Marcus theory of electron transfer which does not allow much flexibility in eliminating recombination rates. In general terms, the current fundamental prescription to reduce recombination is to move the reaction into a deeply inverted region where efficiency of Franck-Condon overlap is greatly reduced.

We propose that a significant reduction of recombination rates can be achieved in systems allowing the splitting of the Stokes shift (distance between the minima) from the curvatures of the free energy surfaces of electron transfer. Our ultimate goal is to formulate a set of physical requirements for the solar systems to achieve such splitting and potentially lead to lower recombination rates. While studying particular synthetic systems will be our next step, we first have looked at natural bacterial photosynthesis for signatures of this mechanism.



In this presentation we report our finding¹ that a significant separation of the Stokes shift from the reorganization energy is indeed realized in natural systems. We presents the results of Molecular Dynamics (MD) simulations showing how this mechanism is realized in bacterial reaction centers, along with initial mechanistic insights into the role of proteins in achieving the splitting. Figure 1 shows our preliminary results of the free energy surfaces of primary charge separation from MD simulations for which half of the Stokes shift is equal to 0.6 eV and the reorganization energy is 1.6 eV (these two quantities are equal in the standard models). The discrepancy of this magnitude can potentially shift the reaction either to the normal region of electron transfer or much deeper in the inverted region than is currently anticipated for a given driving force of the reaction.

Fig. 1: Free energy surfaces of primary charge

[1]. D. N. LeBard and D. V. Matyushov, J. Phys. Chem., to be submitted.

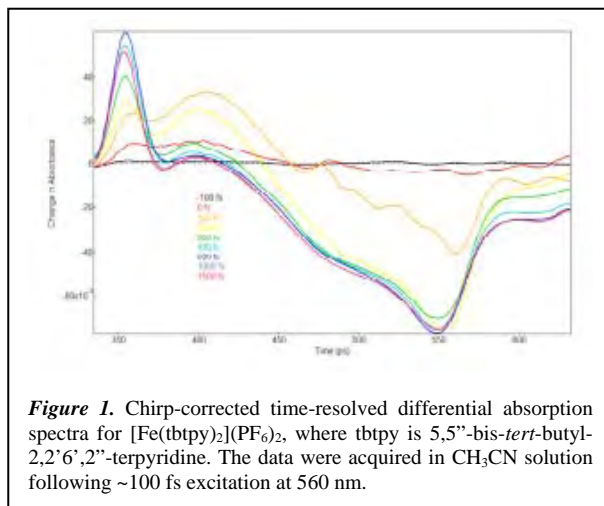
CONTROL OF ULTRAFAST CHARGE TRANSFER-STATE DEACTIVATION IN FIRST-ROW TRANSITION METAL CHROMOPHORES

Allison Brown, Lindsey Jamula, and James K. McCusker*

Department of Chemistry
Michigan State University
East Lansing, MI 48824

Since the 1991 report by O'Regan and Grätzel of a photovoltaic device based on nanocrystalline TiO₂, the possibility of creating efficient solar cells based on the concept of semiconductor sensitization has fueled substantial efforts involving a large number of research groups around the world. Solar energy conversion efficiencies as high as 11% have been reported using Ru^{II}-based charge-transfer complexes as the chromophore. Though impressive, it is likely that the efficiency of these cells will have to improve by at least another factor of two if they are to become economically competitive with fossil fuels for the production of electricity on a large scale. The prospects for achieving this by tweaking the current system are not particularly encouraging at present given that improvements in cell efficiency appear to have reached a plateau over the past several years.

With these issues in mind, we are exploring the possibility of using chromophores based on first-row transition metal complexes in dye-sensitized solar cells. In addition to the substantial reduction in cost associated with these materials, the fundamental changes in redox kinetics upon moving to the first transition series may open up new avenues for optimizing cell regeneration. We have demonstrated that one critical problem with Fe^{II}-based chromophores is ultrafast intramolecular deactivation of the initially formed charge-transfer state to low-lying ligand-field state(s) of the compound (Figure 1); once formed, these ligand-field states are low enough in energy and/or have weak enough coupling to the conduction band of TiO₂ as to preclude interfacial electron transfer. Similar observations in Cr^{III} complexes suggests this may be an intrinsic problem with first-row complexes that must be overcome if further progress on the application of these chromophores in dye-sensitized solar cells is to be achieved.

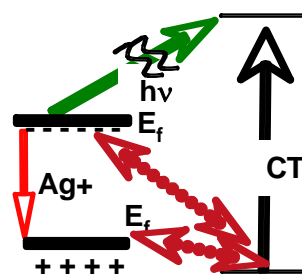


We are pursuing this issue on several fronts. In terms of synthesis, we are developing new ligands designed around vibrational coordinates that we believe may be coupled to charge transfer-to-ligand field relaxation. These new chromophores are then subject to an array of steady-state and time-resolved spectroscopic probes in order to assess changes in the MLCT excited-state lifetime. Analogous studies on fully assembled solar cells employing these chromophores will then allow us to quantify injection dynamics to provide the metrics we need to achieve in order to make this class of chromophores a viable option in this technology.

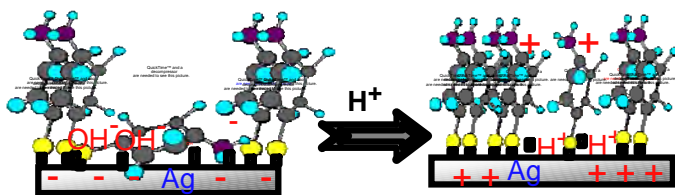
STAGES IN PHOTOCHEMICAL SOLAR CONVERSION: CATALYTIC H₂ EVOLUTION AS THE PARTICLES SEE IT

Getahun Merga,¹ Laura C. Cass, Daniel M. Chipman, and Dan Meisel
Radiation Laboratory and Department of Chemistry & Biochemistry
University of Notre Dame, Notre Dame, Indiana 46556

Metallic particles are often suggested as catalysts to provide conversion from single- to multi-electron redox for the reduction half-cycle of water splitting. A model to describe the mechanism for this reaction, adopted from electrochemical hydrogen evolution, was developed some time ago, but molecular level understanding of this reaction is still missing. Utilizing a recently developed synthesis for the production of silver particles that contain only silver, water, and their ions in suspension, we follow H₂ evolution using surface enhanced Raman spectroscopy (SERS). We show that the particles are stabilized by hydroxide ions or silver ions at high and low pH's, respectively. Suspensions of these particles are extremely stable even at very high particle concentrations (up to ~2 M). We determine the concentration of each species in suspensions of particles of predetermined sizes in the range of ~15-230 nm with relatively narrow size distributions. These particles are used to catalyze the reduction of water by radiolytically generated strongly reducing radicals. A well-studied, adsorbed, probe molecule, *p*-aminothiophenol (*p*-ATP), reports detailed information on processes at the particle surface using SERS. The intensity of the SERS spectra during the production of H₂ was determined under various



Scheme 1: Fermi level changes and its coupling to the *p*-ATP probe.



Scheme 2: Flat to perpendicular conformation change in response to PZC and pK_a transitions.

experimental conditions. The spectra diminish upon injection of electrons into the particles but are recovered on adding Ag⁺ ions. These effects result from changing the Fermi level of the particle. Coupling of the particles' Fermi level to the ground state vibrational levels of the probe molecule is altered in response to the position of the Fermi level, affecting the charge-transfer component of the SERS enhancement (Scheme I). This provides an estimate of the overpotential for the particles during the hydrogen evolution reaction. Effects of pH on the SERS intensity are similar. Preliminary experiments suggest conversion from one orientation of the probe to another (Scheme 2). Alternatively, preliminary computations of model prototypes of the probe on silver raise the possibility that changes in the Fermi levels alter the ground state charge distribution between the probe and the particle, leading to different enhancements of different modes.

¹ Permanent Address: Dept. of Chemistry, Andrews University, Berrien Springs, Michigan, 49104

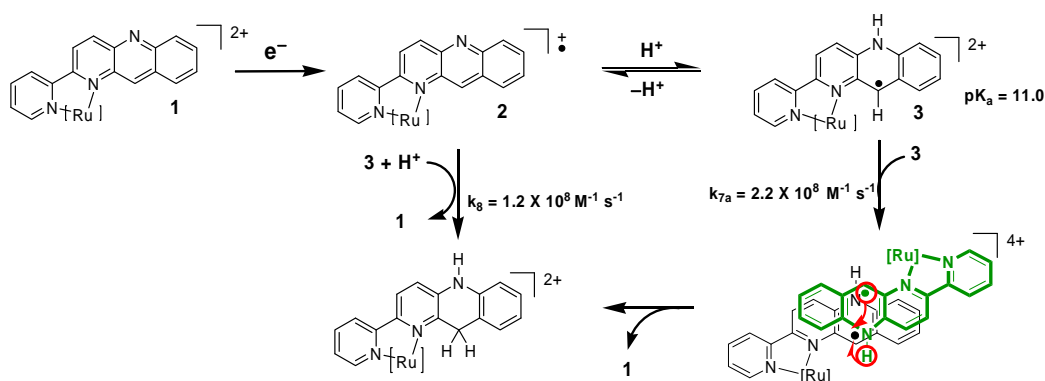
PHOTOCHEMICAL GENERATION OF A HYDRIDE DONOR AND ITS REACTIONS

James T. Muckerman,¹ Dmitry E. Polyansky,¹ Patrick Achord,¹
Koji Tanaka,² and Etsuko Fujita¹

¹ Chemistry Department, Brookhaven National Laboratory, Upton, NY 11973-5000

² Coordination Chemistry Laboratories, Institute for Molecular Science, 5-1 Higashiyama,
Myodaiji, Okazaki, Aichi 444-8787, Japan

An NADPH-like hydride donor $[\text{Ru}(\text{bpy})_2(\text{pbnHH})]^{2+}$ can be cleanly formed by the reductive quenching of the metal-to-ligand charge-transfer (MLCT) excited state of $[\text{Ru}(\text{bpy})_2(\text{pbn})]^{2+}$ by triethylamine upon irradiation with visible light ($< 600 \text{ nm}$) with a quantum yield for the formation of $[\text{Ru}(\text{bpy})_2(\text{pbnHH})]^{2+}$ of 0.21 at $\lambda = 355 \pm 6 \text{ nm}$.¹ The mechanistic pathways of formation of the $[\text{Ru}(\text{bpy})_2(\text{pbnHH})]^{2+}$ species from $[\text{Ru}(\text{bpy})_2(\text{pbn})]^{2+}$ were studied in an aqueous medium. Formation of the one-electron-reduced species as a result of reduction by a solvated electron ($k = 3.0 \times 10^{10} \text{ M}^{-1} \text{ s}^{-1}$) or $\text{CO}_2^{\bullet-}$ ($k = 4.6 \times 10^9 \text{ M}^{-1} \text{ s}^{-1}$), or reductive quenching of an MLCT excited state by 1,4-diazabicyclo[2.2.2]octane ($k = 1.1 \times 10^9 \text{ M}^{-1} \text{ s}^{-1}$) was followed by protonation of the reduced species ($\text{p}K_a = 11$). Dimerization ($k = 2.2 \times 10^8 \text{ M}^{-1} \text{ s}^{-1}$) of the singly-reduced, protonated species, $[\text{Ru}(\text{bpy})_2(\text{pbnH}^\bullet)]^+$, followed by disproportionation of the dimer as well as the cross reaction between the singly-reduced, protonated and non-protonated species ($k = 1.2 \times 10^8 \text{ M}^{-1} \text{ s}^{-1}$) results in the formation of the final $[\text{Ru}(\text{bpy})_2(\text{pbnHH})]^{2+}$ product together with an equal amount of the starting complex, $[\text{Ru}(\text{bpy})_2(\text{pbn})]^{2+}$.² At 0.2 °C, a dimeric intermediate, most likely a π -stacking dimer, was observed that decomposes thermally to form an equimolar mixture of $[\text{Ru}(\text{bpy})_2(\text{pbnHH})]^{2+}$ and $[\text{Ru}(\text{bpy})_2(\text{pbn})]^{2+}$ ($< \text{pH } 9$). The absence of a significant kinetic isotope effect in the disproportionation reaction of $[\text{Ru}(\text{bpy})_2(\text{pbnH}^\bullet)]^+$ and its conjugate base ($> \text{pH } 9$) indicates that disproportionation occurs by a stepwise pathway of electron transfer followed by proton transfer.



¹ D. Polyansky, D. Cabelli, J. T. Muckerman, E. Fujita, T. Koizumi, T. Fukushima, T. Wada, and K. Tanaka, *Angew. Chem. Int. Ed.* **46**, 4169 (2007).

² D. E. Polyansky, D. Cabelli, J. T. Muckerman, T. Fukushima, K. Tanaka, and E. Fujita, *Inorg. Chem.* ASAP DOI: 10.1021/ic702139n (2008).

THEORETICAL/COMPUTATIONAL PROBES OF INTER- AND INTRAMOLECULAR ELECTRON TRANSFER: ELECTRONIC STRUCTURE AND ENERGETICS

Marshall D. Newton
Chemistry Department, Brookhaven National Laboratory
Upton, New York 11973-5000

The ability to control the kinetics of electron transfer (ET) and to design systems with desired kinetic behavior requires a quantitative understanding of basic structural and energetic quantities. We have employed *ab initio* electronic structure models to calculate several of these, including solvent-dependent bimolecular association constants, reorganization energies (both molecular (λ_{in}) and solvent (λ_s)), and electronic coupling elements (H_{DA}). The solvent is represented in terms of a dielectric continuum model with a realistic molecular cavity (PCM), and in the case of bimolecular encounter complexes, the formulation of the quantum mechanical correction for so called basis set superposition error (BSSE) is extended so as to accommodate the presence of the solvent continuum as well as the geometrical relaxation of intramolecular monomer reactants in response to the variation of their intermolecular configurations.

As an example of bimolecular association preceding ET, we have studied the self exchange between TCNE and its radical anion (TCNE $^{\cdot-}$) in three solvents of varying polarity: THF ($\epsilon=7$), CH₂Cl₂ ($\epsilon=9$) and CH₃CN ($\epsilon=37$). In proceeding from vacuum to solution, the calculated stabilization energy is reduced from -18 kcal/mol to ~ -3 kcal/mol, the calculated energy surface becomes flatter, with a somewhat larger minimum energy separation of the monomer units (r_{DA}), and the corresponding minimum energy (TCNE₂) $^{\cdot-}$ structures are, respectively, delocalized and charge-localized. In a comparison of radical anion (TCNE/TCNE $^{\cdot-}$) and radical cation (TTF/TTF $^{\cdot+}$) systems, we calculated H_{DA} and λ_{in} using DFT (B3LYP), and together with the electrostatic effective charges obtained from these calculations, and a Poisson equation solver (Delphi), we evaluated λ_s for 7 different solvents ranging from chloroform ($\epsilon=5$) to propylene carbonate ($\epsilon=65$). The resulting vertical ET energies agreed with observed values to within $\sim \pm 10\%$. The continuum calculations used no empirical information other than standard ϵ values and van der Waals radii.

The above ET reactants involve 'direct' ET between D and A moieties. In the case of bridge-mediated ET, the validity of the commonly used 2-state ($n=2$) electronic model (initial and final ET states) must be carefully evaluated, since electronic states of intermediate bridge sites may lie close enough to D and A states to require explicit inclusion in a multistate model ($n>2$). We have examined this issue for some pyrazine bridged Ru complexes (with RJ Cave), using the generalized Mulliken Hush model (GMH), in which the electronic state space is selected (a set of $n \geq 2$ adiabatic states), and then the charge-localized diabatic states are defined as the eigenstates of the dipole moment operator. Addressing questions as to whether the estimate of H_{DA} improves as one increases n , and in what sense the GMH approach 'converges' with n , we conclude that the 2-state model gives the best estimate of effective coupling, finding that similar magnitudes are obtained by superexchange correction of H_{DA} values obtained for larger spaces ($n=3-5$).



TWO-COLOR TWO-DIMENSIONAL FOURIER TRANSFORM ELECTRONIC SPECTROSCOPY WITH A PULSE-SHAPER

J. A. Myers, K. L. M. Lewis, P. F. Tekavec, J. P. Ogilvie

Department of Physics and Biophysics
University of Michigan, Ann Arbor, MI, 48109

Two-dimensional electronic spectroscopy (2DES) has recently emerged as a powerful technique for studying energy transfer and electronic coupling in photosynthetic systems. Despite the rich chemical information available from 2DES, the relative difficulty of implementing the experiment has limited the degree to which this method has been utilized. This is particularly true at visible wavelengths where the demand for high phase-stability generally requires diffractive-optics-based^{1,2} or actively phase stabilized approaches. It has been suggested that absorptive 2D spectra could be obtained using a combination of a collinear pump pulse pair and noncollinear probe.³ Recently, 2D spectra have been collected in this “pump-probe” geometry at infrared⁴ and near-infrared wavelengths,⁵ greatly simplifying the experimental approach of 2DES. Here we implement a method that employs an acousto-optic pulse-shaper used in a pump-probe geometry to obtain absorptive spectra in a simple dye system at visible frequencies.

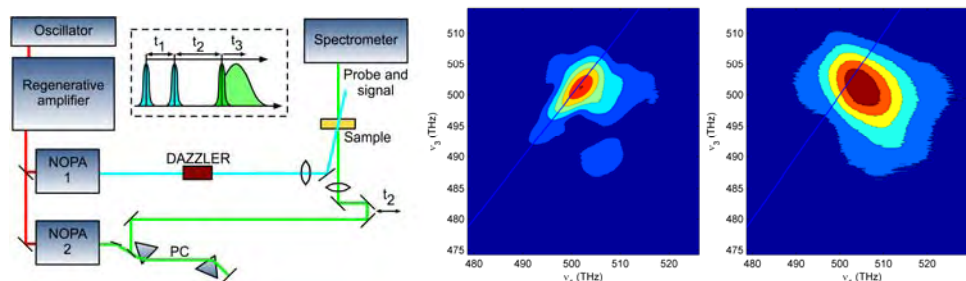


Fig. 1. Straightforward experimental setup for pump-probe 2DES employing a pulse-shaper. Inset shows the pulse sequence at the sample. Right: 2DES spectra for cresyl-violet in ethanol for $t_2=0$ (left) and $t_2=5$ ps (right).

To increase the spectral resolution and information content of 2D spectra, the separation into absorptive and dispersive components is desirable.³ The pulse-shaper-based pump-probe geometry takes advantage of the high degree of precision with which a pulse-shaper can create phase-locked pulse pairs and automatically retrieves absorptive 2D spectra. Our experimental setup is shown in Fig. 1, where the first two pulses in the sequence are created by a Dazzler pulse-shaper. Two non-collinear optical parametric amplifiers (NOPAs), allow two-color measurements to explore energy transfer and electronic coupling over a broad frequency range. To demonstrate the method we have performed 2DES on cresyl violet in ethanol. At early t_2 , the data is elongated along the diagonal, reflecting inhomogeneous broadening in the system. At later times the diagonal elongation vanishes as the system loses memory of its initial excitation frequency. Future work will employ the two-color pulse-shaping-based approach to study energy transfer and electronic coupling in photosynthetic complexes.

(1) Cowan, M. L.; Ogilvie, J. P.; Miller, R. J. D. *Chemical Physics Letters* **2004**, *386*, 184-189.

(2) Brixner, T.; Stiopkin, I. V.; Fleming, G. R. *Optics Letters* **2004**, *29*, 884-886.

(3) Faeder, S. M. G.; Jonas, D. M. *Journal Of Physical Chemistry A* **1999**, *103*, 10489-10505.

(4) DeFlores, L. P.; Nicodemus, R. A.; Tokmakoff, A. *Optics Letters* **2007**, *32*, 2966-2968.

(5) Grumstrup, E. M.; Shim, S.-H.; Montgomery, M. A.; Damrauer, N. H.; Zanni, M. T. *Opt. Exp.* **2007**, *15*, 16681.

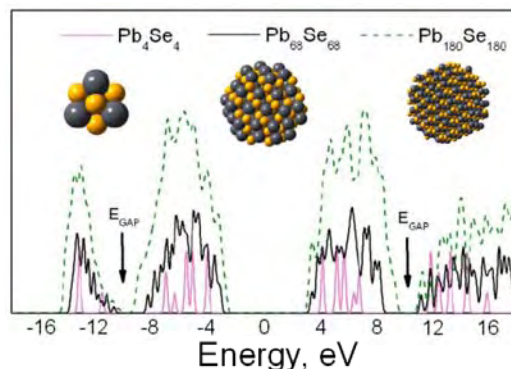
**PHOTOCHEMICAL DYNAMICS ON THE NANOSCALE:
TIME-DOMAIN *ab initio* STUDIES OF QUANTUM DOTS
AND MOLECULE-SEMICONDUCTOR INTERFACES**

Oleg V. Prezhdo

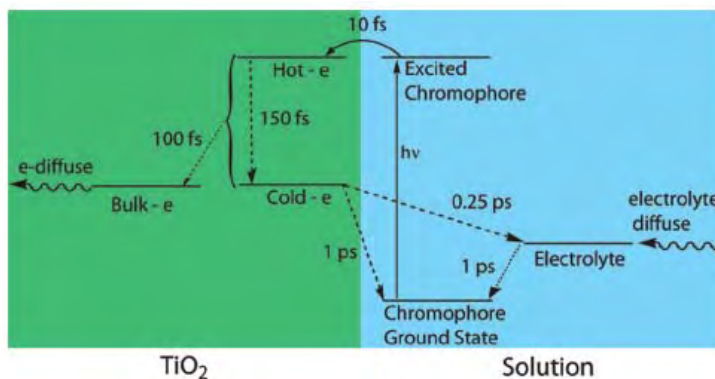
Department of Chemistry
University of Washington
Seattle, WA 98195-1700

Novel photovoltaic and photochemical materials require an understanding of their dynamical response on the nanometer scale. A great deal of experimental and theoretical work has been devoted to characterizing the excitation, charge, and vibrational dynamics in quantum dots, carbon nanotubes, conducting polymers, inorganic semiconductors and molecular chromophores. We have developed state-of-the-art non-adiabatic molecular dynamics techniques and implemented them within time-dependent density functional theory in order to model the ultrafast photoinduced processes in these materials at the atomistic level, and in real time.

Quantum dots (QD) are quasi-zero dimensional structures with a unique combination of molecular and bulk properties. As a result, QDs exhibit new physical properties such as carrier multiplication, which has the potential to greatly increase the efficiency of solar cells. The electron-phonon and Auger relaxation in QDs compete with carrier multiplication. Our detailed studies of the competing processes in PbSe QDs rationalize why carrier multiplication was first observed in this material.



Electron transfer across molecular/bulk interfaces is the subject of active research, creating many challenges due to the stark differences between the quantum states of molecules and periodic systems, as well as the often disparate sets of theories and experimental tools used by chemists and physicists. Charge transport across the interface remains a key to such fields as molecular electronics, photocatalysis, electrolysis, and photo-voltaics. The theoretical studies provide an exclusive perspective on the photoinduced interfacial transfer dynamics.



Our real-time atomistic simulations create a detailed picture of these materials, allow us to compare and contrast their properties, and provide a unifying description of quantum dynamics on the nanometer scale.

COMBUSTION SYNTHESIS AND CHARACTERIZATION OF NANOCRYSTALLINE TUNGSTEN OXIDE

Walter Morales, Norma de Tacconi and Krishnan Rajeshwar
Center for Renewable Energy Science & Technology (CREST)
University of Texas at Arlington
Arlington, TX 76019

The energy payback time associated with the semiconductor active material is an important parameter in a photovoltaic solar cell device. Lowering the energy requirements for the semiconductor synthesis step or making it more energy-efficient is thus critical toward making the overall device economics more competitive relative to other non-polluting energy options. In this poster presentation, combustion synthesis is demonstrated to be a versatile and energy-efficient method for preparing inorganic oxide semiconductors such as tungsten trioxide (WO_3).¹ The energy efficiency of combustion synthesis accrues from the fact that high process temperatures are *self-sustained* by the exothermicity of the combustion process and the only *external* thermal energy input needed is for dehydration of the fuel/oxidizer precursor mixture and bringing it to ignition. Importantly, we show that in this approach, it is also possible to tune the optical characteristics of the oxide semiconductor (i.e., shift its response toward the visible range of the electromagnetic spectrum) in situ by doping the host semiconductor during the formative stage itself (see Figure 1). As a bonus, the resultant material shows enhanced surface adsorption properties such as markedly improved organic dye uptake relative to benchmark samples obtained from commercial sources. Finally, this synthesis approach requires only very simple equipment, a feature that it shares with other “mild” inorganic semiconductor synthesis routes such as sol-gel chemistry, chemical bath deposition, and electrodeposition.

Oxide semiconductors are eminently attractive candidates as photocatalysts for H_2 generation from water. Unlike other candidates such as GaP, InP, or CdTe, oxides such as WO_3 do not contain precious metals or toxic elements. The lower optical band gap of combustion-synthesized WO_3 (~2.5 eV) relative to TiO_2 (~3.0-3.2 eV)—a veritable workhorse in the water-splitting community—results in a more substantial utilization of the solar spectrum. The origin of this optical response shift was further probed by XRD and XPS. While all the diffraction peaks for monoclinic WO_3 were faithfully reproduced in the combustion-synthesized WO_3 samples relative to the commercial benchmark sample, the peaks in the former were significantly broadened because of the diminution of particle size and the strain induced in the oxide lattice by doping. The present study constitutes the first use of combustion synthesis for preparing nanosized particles of WO_3 .¹

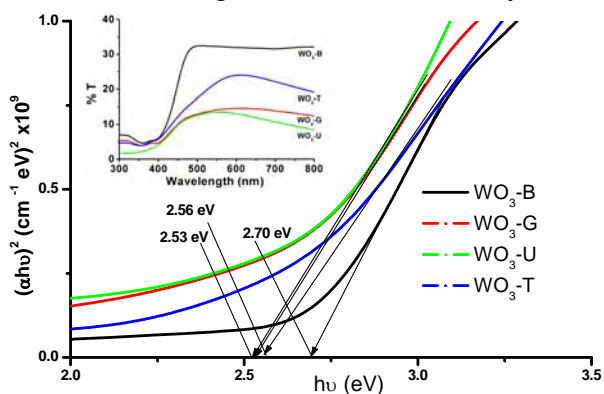


Figure 1. Tauc plots for combustion-synthesized WO_3 samples (G, U and T) obtained for the diffuse reflectance data shown in the inset. ‘B’ is a commercial sample.

(1) Morales, W.; Cason, M.; Aina, O.; de Tacconi, N. R.; Rajeshwar, K. *J. Am. Chem. Soc.* (in press).

MICROWAVE CONDUCTIVITY STUDIES OF PHOTO-INDUCED CARRIERS IN SINGLE-WALLED CARBON NANOTUBES

Garry Rumbles, Nikos Kopidakis, Andrew Ferguson, Jeff Blackburn, Michael Heben
Chemical and Biosciences Center
National Renewable Energy Laboratory
Golden, Colorado, 80305-3393

Using transient microwave conductivity we have recently studied a number of photo-induced electron transfer processes of CdS grown on TiO₂, a soluble derivative of C₆₀ (PCBM) dispersed in poly(3-hexylthiophene) (P3HT), P3HT on planar magnesium-doped zinc oxide (ZMO) and, more recently, single-walled carbon nanotubes (SWNTs) dispersed in polymer matrices.

To understand the nature of excitations in carbon nanotubes, samples of SWNTs isolated in an inert polymer, carboxymethyl cellulose (CMC), were studied. Figure 1 shows two transients exciting high into the SWNT absorption profile at 800 nm, and also closer to the optical band edge at 1700 nm. The transients are dominated by fast, instrument limited, decay, but with a long-lived decay component that is more prominent when exciting at the higher energy. These data indicate that the bulk of the carriers are lost within the exciting laser pulse, with the long-lived tail attributed to a small amount of carrier, probably electron, trapping, leaving a few mobile holes. The origin of the fast loss mechanism will be examined in the presentation, with the relevant importance of carrier recombination and exciton formation discussed. The efficiency of this process appears to be dependent on the excitation wavelength, as shown by the two action spectra, shown in Figure 1, where the photoconductivity is monitored coincident with excitation (EOP), and after 100 ns.

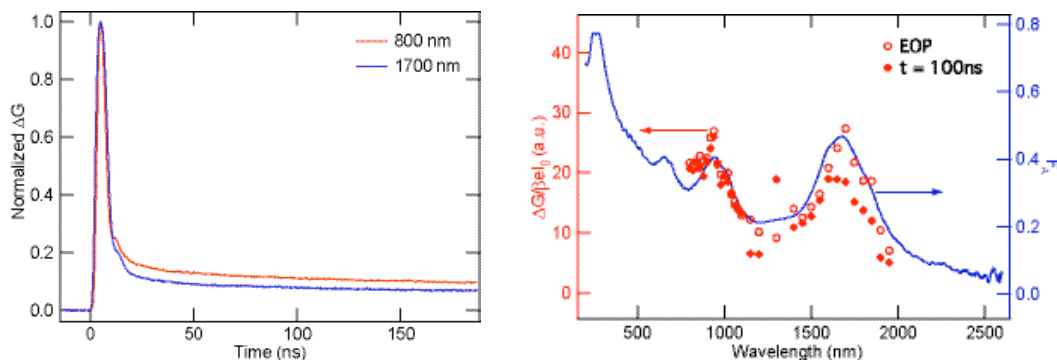


Figure 1 – Microwave conductivity data for a sample of isolated SWNTs embedded in a CMC matrix. Left: Normalized transient microwave conductivity transients exciting at 800 nm and 1700 nm. Right: Fraction of light absorbed, F_A , compared to microwave conductivity action spectra recorded at $t = 0$ ns (EOP) and $t = 100$ ns.

The mobility of carriers in SWNTs is reported to be extremely high (ca. 50000 cm²/Vs). Although the peak photoconductivity signal for the SWNTs is large, it is substantially lower than what would be predicted for such a high mobility. This discrepancy may arise from the influence of the finite-length nanotubes. To test this hypothesis, we have carried out a study of a series of samples containing SWNTs of differing length. A discussion of the results of these studies will also be part of the presentation.

QUENCHING OF TRIPLET EXCITONS IN CONJUGATED POLYELECTROLYTES

Hui Jiang[†], John R. Miller[‡] and Kirk S. Schanze[†]

[†]Chemistry Department, University of Florida, Gainesville, FL 32611

[‡]Chemistry Department, Brookhaven National Laboratory, Upton, NY

The properties of the singlet exciton in conjugated polyelectrolytes (CPEs) have been studied extensively due to the fact that the fluorescence is quenched with extraordinary efficiency by small molecules with opposite charge compared to the polymer. This “superquenching” or “amplified quenching” effect is ascribed to the delocalization and rapid diffusion of the singlet exciton along the conjugated polymer backbone. However, compared to the singlet exciton, much less is known regarding the properties of the triplet exciton in conjugated polymers or conjugated polyelectrolytes. In order to gain insight concerning the properties of the triplet exciton in CPEs, we have investigated the quenching of triplet excitons in the anionic polymer (TH-PPE) and a corresponding model compound (TH-PE) by 9-aminomethylanthracene (AMA) which is a cationic triplet energy acceptor.

The triplet excited state of TH-PPE and TH-PE is monitored by laser flash photolysis. The triplet is long-lived ($\tau > 10 \mu\text{s}$) and it absorbs strongly in the red part of the visible spectrum. The quenching of the triplet states of TH-PPE and TH-PE by AMA was studied in methanol (MeOH) and ethylene glycol (EG) by monitoring the transient absorption decay at the maximum wavelength of the triplet state absorption. The resulting kinetic data is analyzed in terms of the initial amplitude, which is associated with “static” (i.e., instantaneous) quenching, and the lifetime, which is associated with a dynamic quenching process. As shown in Figure 1 for TH-PPE, dynamic (lifetime) quenching for both TH-PPE and TH-PE dominates, and the recovered bimolecular quenching constants agree well with the calculated values of the diffusion rate in both solvents. A careful analysis reveals that in contrast to singlet excitons, due to the long lifetime of the triplet exciton in conjugated polymers and conjugated polyelectrolytes, the dynamic quenching process governed by bimolecular diffusion prevails, so that the amplified quenching effect is not observed for the triplet excitons (Scheme 1).

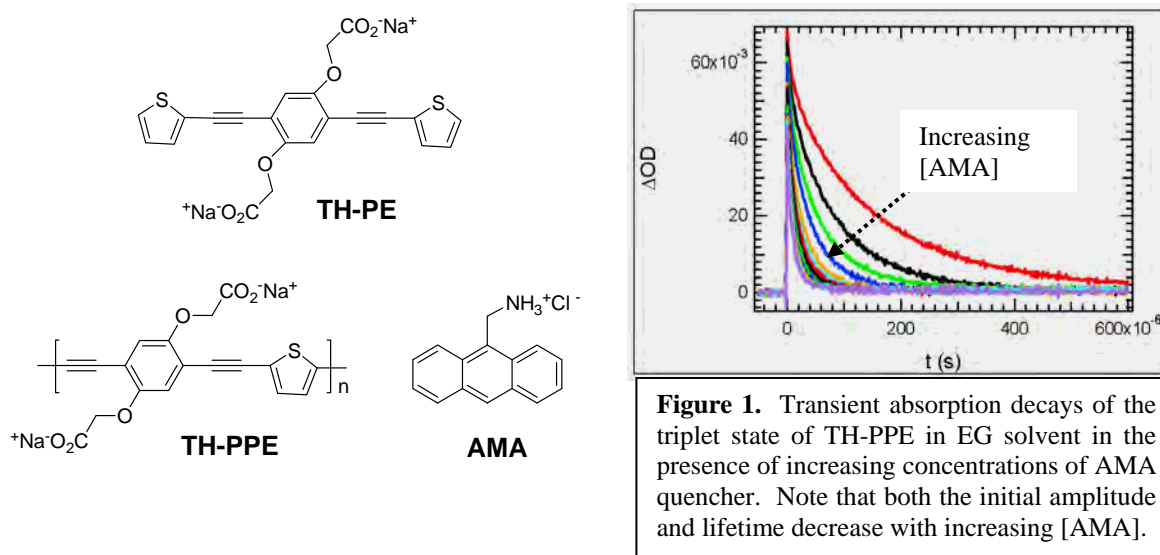


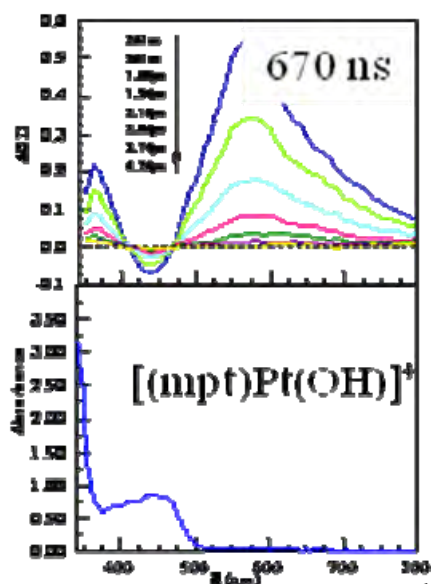
Figure 1. Transient absorption decays of the triplet state of TH-PPE in EG solvent in the presence of increasing concentrations of AMA quencher. Note that both the initial amplitude and lifetime decrease with increasing [AMA].

EXCITED STATE ENERGETICS AND PHOTOREDOX REACTIONS OF Pt(II) TERPYRIDYL COMPLEXES

Kalpana Shankar, Heidi Hester, Duraisamy Kumaresan, Kristi Lebkowski and Russell Schmehl
Department of Chemistry
Tulane University
New Orleans, LA 70118

With the recent discoveries of square planar Pt(II) imine complexes having long lived excited states in solution at room temperature, the need for systematic and thorough characterization of the excited state has increased. In addition, the palette of complexes available now provides an avenue for investigating intra- and intermolecular photoinduced electron transfer reactions in these complexes. Of particular interest is the possibility of coupling one electron oxidation or reduction reactions in an effort to drive net chemical conversion (i.e. reduction of protons to hydrogen, etc.).

Among Pt(II) terpyridyl complexes, a few have been found to have relatively long (>100 ns) excited state lifetimes in solution at room temperature. One emphasis of our recent work has been to understand the structural and electronic factors that result in complexes with long lived



excited states. Our efforts have focused on the examination of transient absorption spectra and temperature dependent luminescence lifetimes for a series of [(mpt)PtX]ⁿ⁺ (X = Cl, CN, py, CCR, OH; mpt = 4'-(p-methylphenyl)-2,2',6',2''-terpyridine) complexes, yielding activation parameters for nonradiative relaxation. The results have been coupled with time dependent density functional calculations to provide clues for the design of additional chromophores.

Pt(II) complexes having modified terpyridyl ligands and/or aryl acetylide ligands as the fourth ligand fall into this class and they have been shown to yield hydrogen upon photolysis in the presence of a sacrificial electron and proton donor. We will present results on the fate of the Pt(II) acetylide complexes following hydrogen production indicating that acetylide loss and ligand reduction definitely accompany hydrogen generation. No direct evidence for colloidal Pt formation was obtained.

The complexes also exhibit irreversible one electron oxidation since disproportionation leads to formation of six coordinate Pt(IV) complexes. Photochemical approaches provide a means to make the Pt(III) species by quenching the excited states with electron accepting quenchers. Initial luminescence quenching and transient absorption results of photooxidation experiments will be presented. Efforts to obtain Pt(III/II) potentials through Rehm-Weller analysis have been frustrated. We have also investigated the reductive quenching of several (L)Pt(II) terpyridyl complexes (L= Cl, CN, aryl acetylide) and have determined excited state potentials for one electron reduction.

CHARACTERIZATION OF CHARGE INJECTION AND CHARGE SEPARATION IN FUNCTIONALIZED TiO₂ FOR USE IN SOLAR HYDROGEN PRODUCTION

Clyde W. Cady, James M. Schleicher, Gonghu Li, William R. McNamara, Robert C. Snoeberger, Victor S. Batista, Robert H. Crabtree, Gary W. Brudvig, and Charles A. Schmuttenmaer

Department of Chemistry
Yale University

225 Prospect St. P.O. Box 208107, New Haven, CT 06520-8107

Nanocrystalline wide-band gap semiconductors such as TiO₂ have shown great promise in the areas of dye-sensitized solar cells and photocatalytic materials. One of the most important aspects of their performance is the ability to accept and transport photoexcited electrons. This work builds on our recent report¹ in which a variety of experimental and computational techniques verified charge injection and separation from a terpyridine-Mn(II) complexes linked via catechol to TiO₂ nanoparticles (NPs). We have since characterized a variety of anchors, linkers, and types of TiO₂ NPs, and show how a combination of THz spectroscopy, UV/vis studies, and low-temperature EPR spectroscopy can provide a full picture of these processes.

As seen in Figure 1, the processes of interest are the injection time scale, the duration of charge separation at room temperature (not shown in Figure 1), the time scale for Mn(II) oxidation and subsequent reduction at 6 K, and the mobility of the electron once injected into the TiO₂ NP (also not shown in Figure 1). We find injection time scales that are typically dominated by a fast component that is shorter than our 300 fs experimental time resolution (in excellent agreement with computational results, see Batista's poster), which may or may not be accompanied by a slower component depending on the anchor/linker/metal complex and the nature of the TiO₂ NPs.

We are developing new oxidation-resistant linkers that are also stable in aqueous environments, and are as efficient for charge injection as conventional linkers. The anchor molecules we have investigated are R-Si(O-)₃ (i.e., siloxane), and acetylacetonate (acac). We have compared the linkers *n*-1,3-propdiyl, no linker, and carboxamidophenyl (see Crabtree's poster). We have compared metal complexes Mn^{II}(OAc)₂, with cis-bis(isothiocyanato) bis(2,2'-bipyridyl-4,4'-dicarboxylato)-ruthenium(II) bis-tetrabutylammonium (also known as "red dye, or N719).

We find that injection dynamics and efficiency for the acac/phenylene/amide/phenylene/trpy anchor/linker complex are as good as that for red dye covalently bonded to TiO₂. We find that the siloxane/*n*-1,3-propdiyl anchor/linker yields essentially no charge injection. In addition, amorphous regions in the colloidal TiO₂ NP samples have a tremendous influence on carrier mobility upon photoinjection.

1. Sabas G. Abuabara, Clyde W. Cady, Jason B. Baxter, Charles A. Schmuttenmaer, Robert H. Crabtree, Gary W. Brudvig and Victor S. Batista, *J. Phys. Chem. C*, **111**, 11982 – 11990 (2007).

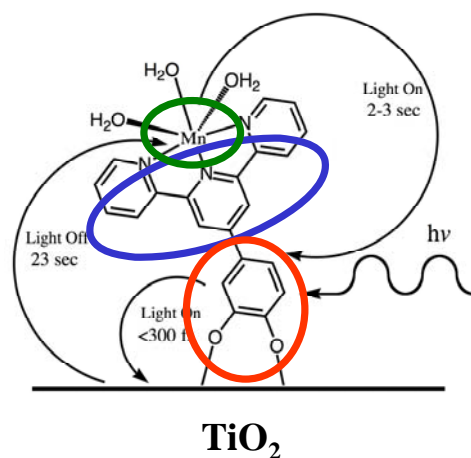
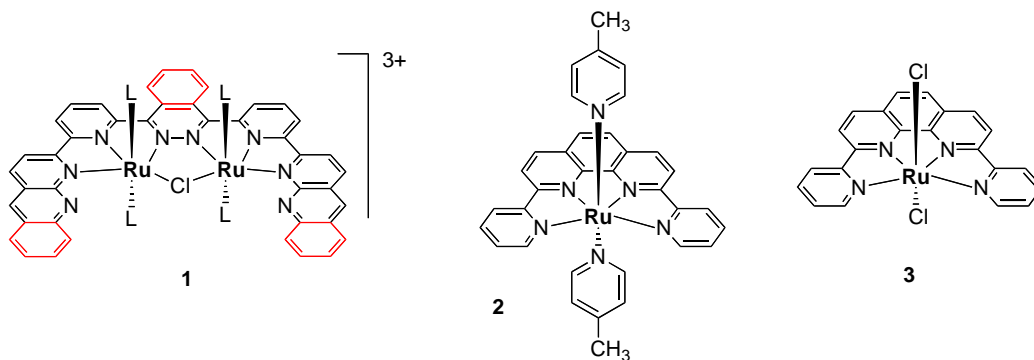


Figure 1. Photoinitiated processes in catechol-trpy-Mn(II) complex on TiO₂. Time scales determined from THz spectroscopy, computational studies, and low-temperature EPR spectroscopy.

INVESTIGATION OF RUTHENIUM-BASED WATER OXIDATION CATALYSTS

Ruifa Zong, Huan-Wei Tseng, Zeping Deng, Dong Wang, Bin Wang, Randolph Thummel
Department of Chemistry
University of Houston
Houston, TX 77204-5003

We have reported that a series of dinuclear Ru(II) complexes with structures similar to **1** in the presence of Ce(IV) as a sacrificial oxidant catalyze the oxidation of water to produce O₂.¹ Kinetic measurements are made using an oxygen sensitive fluorescence probe while calibration and end point readings (turnovers) are carried out by GC analysis. Mononuclear complexes have also been found to catalyze water oxidation and a wide variety of Ru(II) pyridine and polypyridine complexes have been examined, using mono-, bi-, tri-, and tetradentate ligands. We are following a synthesis driven approach in hopes of establishing a structure-activity correlation that would aid in optimization of catalyst performance as well provide some understanding of mechanism.



A crystal structure of a catalyst of type **1** verifies the bridging chloride and indicates considerable in-plane distortion of the equatorial ligand. The structure of the equatorial ligand has been varied both in the central linker and the peripheral binding unit (see red). The axial ligands (L) are mostly 4-substituted pyridines as well as imidazoles. When oxadiazole is the linker the Ru centers are pulled apart and no longer Cl-bridged. Due to the ligand-induced constraints of tetradentate binding in systems such as **2**, the metal center is more accessible and considerable catalytic activity is observed (TN = 416).² To further exploit this situation we have prepared a new Ru polypyridine reagent, [Ru(DPP)Cl₂] (**3**) where DPP = 2,9-di(pyrid-2'-yl)-1,10-phenanthroline. The chlorines can be replaced by a variety of other ligands.

References:

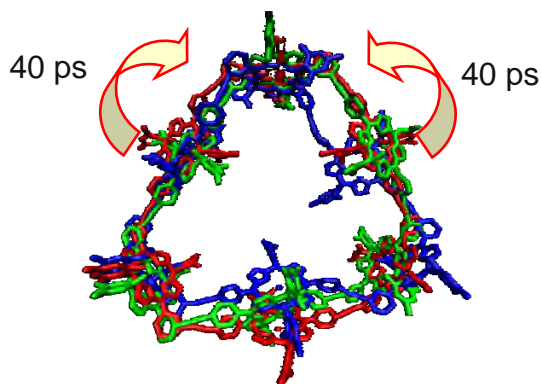
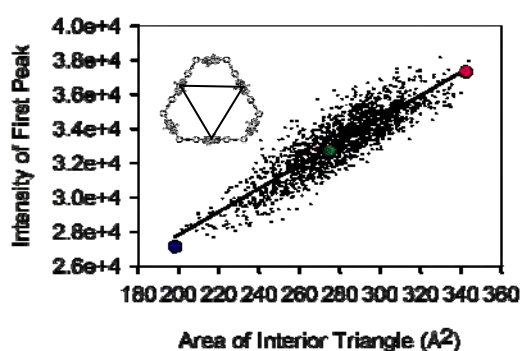
1. Deng, Z.; Tseng, H.-W.; Zong, R.; Thummel, R. *Inorg. Chem.* **2008**, *47*, 1835-1848.
2. Zhang, G.; Zong, R.; Tseng, H.-W.; Thummel, R. P. *Inorg. Chem.* **2008**, *47*, 990-998.

CONFORMATIONAL ANALYSIS OF A SUPRAMOLECULAR PORPHYRIN ARRAY USING MOLECULAR DYNAMICS MODELING AND X-RAY SCATTERING

David M. Tiede¹, Kristy L. Mardis², Xiaobing Zuo¹, Jonathan S. Lindsey³

Chemical and Engineering Sciences, Argonne National Laboratory, Argonne, IL 60439,
Department of Chemistry and Physics, Chicago, IL 60628, Department of Chemistry, North
Carolina State University, Raleigh, North Carolina, 27695

Wide-angle x-ray scattering measurements in combination with coordinate-based modeling offer new possibilities for gaining atomic-scale insight into the structure and conformational dynamics of supramolecular architectures in solution. A comparison has been made between the configurationally broadened x-ray scattering patterns measured at room temperature for dilute toluene solutions of a hexameric, diphenylethyne-linked porphyrin array with scattering patterns calculated from structural ensembles in constant pressure and temperature molecular dynamics simulations. The array serves as a cyclic host for assembly of light-harvesting arrays for solar energy conversion. Thermal fluctuations sampled at picosecond intervals within nanosecond time scale dynamic simulations show large amplitude motions that include porphyrin ring “tipping” around the porphyrin linkage axes and extended hexameric porphyrin array “breathing” motions involving torsional distortions collectively distributed along porphyrin and diphenylethyne groups. Each type of group motion is found to produce characteristic, angle-dependent dampening of wide-angle scattering features that are needed to reproduce dampening features in experimental x-ray scattering. However, mismatches in the magnitudes of experimental and simulated dampening of high-angle x-ray scattering patterns indicate that large amplitude, hexamer array breathing-type motions are significantly under-represented in the simulated ensembles. The comparison between experiment and simulation provides a means to interpret x-ray scattering data in terms of an explicit atomic model, and additionally suggests the opportunity to use wide-angle x-ray scattering as an experimental benchmark in the development of simulation methods that more accurately predict function-linked configurational dynamics of supramolecular assemblies.



- Large amplitude “breathing”, tipping motions under-populated in MD
- Distortions lower symmetry
- Non-equivalent porphyrin sites
- Uniform energy transfer
 - Role for linker σ -bond supporting conformation independent transfer

DISCOVERY OF NATIVE METAL ION SITES ON THE FERREDOXIN DOCKING SIDE OF PHOTOSYSTEM I

Lisa M. Utschig, Lin X. Chen, Jenny V. Lockard, David M. Tiede, and Oleg G. Poluektov
Chemical Sciences and Engineering Division
Argonne National Laboratory
Argonne, IL 60439

Photosynthetic reaction center (RC) proteins are highly efficient solar energy converters. Crystal structures of RCs from purple photosynthetic bacteria, and photosystems I and II (PSI, PSII) of cyanobacteria and higher plants reveal specifically tailored protein environments that act as “smart matrices”, dynamically adjusting to promote directional electron transfer, stabilize charge separation, and enable coupling to secondary reactions, i.e. proton transfer or electron transfer with mobile charge carriers. Our research is focused on understanding the role of localized environments in tuning light-driven electron transfer. Metal ion binding to RCs can affect primary photochemistry and provides a probe for investigation local protein environments.

Recently, we have discovered intrinsic Zn^{2+} and Cu^{2+} sites on PSI. PSI is a large, membrane protein complex composed of 12 protein subunits and 127 cofactors (Figure 1) that catalyzes light-driven electron transfer across the thylaloid membrane. In PSI, photoexcitation of the primary electron donor P700 initiates electron transfer through a series of acceptors, terminating in the electron transfer to F_A and F_B , two iron-sulfur clusters held within an extrinsic stromal protein subunit. The electron is then transferred to ferredoxin, a small [2Fe-2S] protein that shuttles the reducing equivalents from PSI to several metabolic pathways.

We have employed a combination of bioinorganic and spectroscopic techniques to

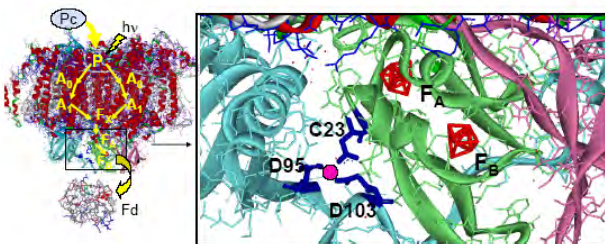


Figure 1 Left: Photosystem I reaction center (PDB 1JB0) showing the photo-initiated sequential electron transfer pathway from the primary donor P to the terminal electron acceptors, F_A and F_B . Ferredoxin (Fd) (PDB 1A70) accepts the light-generated electron from PSI; plastocyanin (Pc) reduces the oxidized donor, P^+ . Right: Enlargement of the stromal subunits showing the proposed Cu binding site ligands in PSI. A putative Cu atom is illustrated.

of the PSI crystal structure reveals a cluster of three highly conserved residues, His(D95), Glu(D103), and Asp(C23), as a likely Cu^{2+} binding site. (Figure 1) Future studies will focus on elucidating the Zn^{2+} site, differentiating the two Cu^{2+} sites, and investigating local metal site responses to light-driven electron transfer. The discovery of surface metal sites on the acceptor side of PSI provides a unique opportunity to probe the stromal region of PSI and the interactions of PSI with its reaction partner, the soluble electron carrier protein ferredoxin.

PLASMON RESONANCE IMAGING

Manuel J. Romero,² Garry Rumbles,¹ Mowafak Al-Jassim² and Jao van de Lagemaat¹

¹Chemical Sciences and Biosciences Center, ²National Center for Photovoltaics

National Renewable Energy Laboratory

Golden, Colorado 80004

In this paper, we demonstrate a new high spatial-resolution time-resolved imaging technique that enables the study of energy and charge transport in nanoscale systems. It also enables the study of energetic, surface chemical, and opto-electrical properties of individual quantum systems and superstructures of such, as well as the interaction with surface plasmons.

In order to better understand the nanoscale energy flow, two different plasmon modes that are active in the tip-substrate system in our microscope were identified as illustrated in Figure 1: A localized surface plasmon (LSP) and a propagating surface plasmon (PSP). The relative intensity of the two modes is shown to depend on the excitation energy and on the local morphology of the substrate. This observation allows for control of the size, symmetry and energy of the nanoscale lightsource that is generated beneath the tip. The ability to distinguish between the two also allows us to differentiate between localized electronic processes in the tip-substrate cavity and longer-range processes. This result, combined with earlier data where the quenching of the LSP modes by single quantum dots was demonstrated (Romero et al. *Nanolett.* **6**, 2833 (2006)), is essential to understanding the interaction between surface plasmons and nanoscale species present in the gap such as semiconductor quantum dots. Using the techniques presented here, we are currently studying energy transport in quantum dot superstructures, interaction of plasmonic states with excitonic states on nearby species and exciton dynamics in pi-conjugated polymers. We are also extending the capabilities of our microscope to include time-resolved data, further elucidating energy and charge flow in these systems.

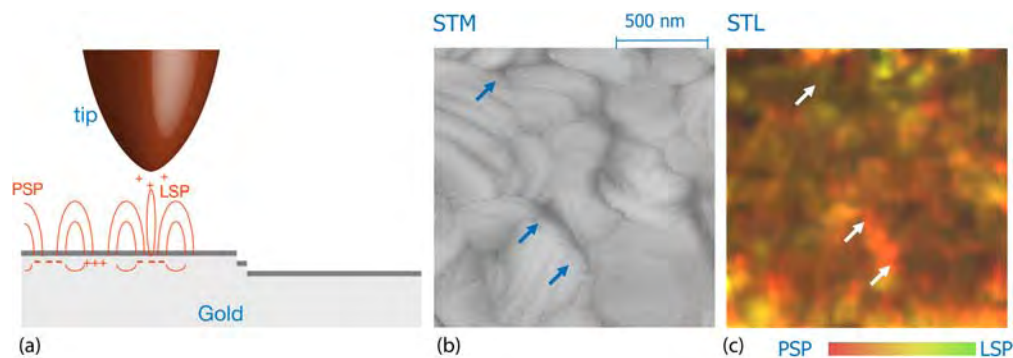


Figure 1. Plasmon resonance imaging of a Gold substrate covered with a 1,6-hexane-dithiol self-assembled monolayer. (a) Illustration of the two possible plasmon modes. (b) STM image of the imaged area (c) simultaneously collected tunnelling luminescence image. The colour indicates the active mode.

References:

M. J. Romero, J. van de Lagemaat, G. Rumbles, M. Al-Jassim, "Plasmon excitations in scanning tunneling microscopy: simultaneous imaging of modes with different localization coupled at the tip," *Appl. Phys. Lett.* **90**, 193109 (2007) (partial support by BES)



STRUCTURAL CHANGES IN THE OXYGEN EVOLVING COMPLEX OF PHOTOSYSTEM II DETECTED USING X-RAY SPECTROSCOPY

Junko Yano,¹ Yulia Pushkar,¹ Alain Boussac,³ Uwe Bergmann,⁴ Ken Sauer,^{1,2} Vittal Yachandra¹

¹Physical Biosciences Division, Lawrence Berkeley National Laboratory, Berkeley, CA, 94720.

²Department of Chemistry, University of California, Berkeley, CA, 94720. ³Service de Bioenergetique, CEA Saclay, 91191 Gif sur Yvette, France. ⁴Stanford Synchrotron Radiation Laboratory, Menlo Park, CA, 94025

The Mn₄Ca cluster of the oxygen evolving complex (OEC) of photosystem II (PS II), cycles through five oxidation states (S_i state, i=0-4) coupling the one electron photochemistry of the reaction center with the 4 electron redox chemistry of water oxidation. While the structure of the OEC in the S₁ state is emerging from X-ray diffraction and spectroscopy studies, much less is known about the structural changes in the Mn₄Ca cluster through the catalytic cycle, which are critical for understanding the mechanism of oxygen evolution.

We used X-ray absorption spectroscopy, in particular, range-extended EXAFS to study the changes in structure of the OEC during the catalytic cycle. The use of a high resolution crystal monochromator allows EXAFS collection beyond the Fe K-edge and improves the distance resolution. We show that there are three di-μ-oxo-bridged Mn-Mn distances and the higher resolution also allowed us to discriminate between the Mn-Mn and Mn-Ca (3.2 - 3.4 Å) vectors. The S₃ state spectra demonstrate a significant increase in Mn-Mn di-μ-oxo-bridged distances in the S₂ to S₃ transition (Fig. 1, left). Studies of oriented membranes in the S₃ state suggest a change in the orientation of the Mn-Mn vectors relative to that observed in the S₁ and S₂ states.

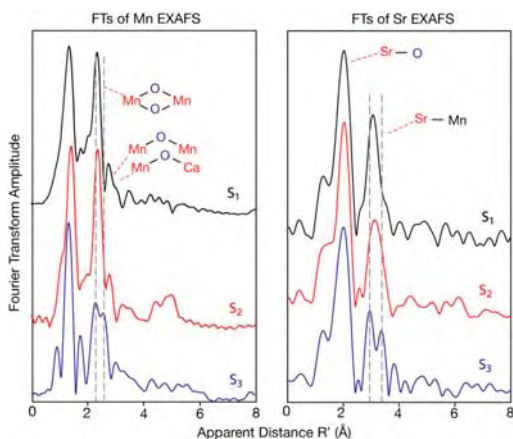
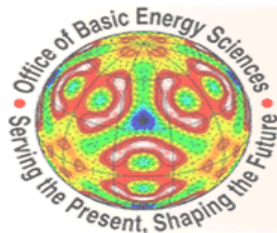


Fig. 1 Fourier transforms from Mn EXAFS (left), and Sr EXAFS (right). There are significant changes in the Mn-Mn and Sr-Mn distances (dashed lines) between the S₂ and S₃ states.

Using PS II from Sr-medium grown *Thermosynechococcus elongatus*, we detected considerable changes in the Sr-Mn distances, especially for the S₂ to S₃ transition (Fig. 1, right). These changes demonstrate that Ca(Sr) is not just a spectator atom involved in providing a framework but that it is actively involved in the mechanism of water oxidation. The Mn and the complimentary Sr EXAFS results implicate the involvement of at least one critical bridging oxygen atom between the Mn-Mn and Mn-Ca(Sr) atoms in the complex. Recently we have collected Mn X-ray emission spectra that show a distinct signature for a Mn-oxo bridge in the S₁ state; these studies will be extended to the higher S-states.

Theoretical analysis of the OEC from other groups indicate that the formation of a low-lying ligand oxygen radical precursor state may be required for forming the O-O bond. The changes that are detected by X-ray spectroscopy favor such a model, and we propose that to reach this state, a structural rearrangement is needed during the S₂ to S₃ transition. The implications of these results to the mechanism of water oxidation will be presented.

List of Participants



Announcing the
**2008 DOE Solar Photochemistry
Contractors' Meeting**

Sponsored by the U.S. Department of Energy, Office of Basic Energy Sciences
Chemical Sciences, Geosciences, and Biosciences Division

Neal Armstrong

University of Arizona
Department of Chemistry
1306 E. University Blvd.
Chemical Sciences Building 218
Tucson, Arizona 85721
520-621-8242
nra@email.arizona.edu

Paul Barbara

The University of Texas at Austin
1 University Station, A5500
Austin, Texas 78712
512-471-2356
p.barbara@mail.utexas.edu

Greg Barber

Penn State
104 Chemistry Building
University Park, PA 16802
814-863-9791
gdb102@psu.edu

Victor Batista

Yale University
Chemistry Department
225 Prospect Street
New Haven, CT 06520-8107
203 432 6672
victor.batista@yale.edu

Matt Beard

National Renewable Energy Laboratory
1617 Cole Blvd.
Golden, CO 80401
303-384-6781
matt_beard@nrel.gov

Jeffrey Blackburn

National Renewable Energy Laboratory
1617 Cole Boulevard
Golden, CO 80401-3393
303-384-6649
jeffrey_blackburn@nrel.gov

David Blank

University of Minnesota
207 Pleasant St SE
Minneapolis, MN 55455
612-624-0571
blank@umn.edu

Robert Blankenship

Washington University in St. Louis
Department of Biology and Chemistry
Laboratory Sciences 401B
St. Louis, MO 63130
314 935-7971
blankenship@wustl.edu

David Bocian

University of California, Riverside
Department of Chemistry
CHEM SCI 230
Riverside, CA 92521
951-827-3660
David.Bocian@ucr.edu

James Brainard

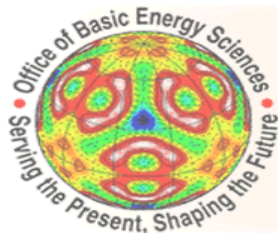
National Renewable Energy Laboratory
1617 Cole Boulevard
Golden, CO 80401-3393
303-384-6462
james_brainard@nrel.gov

Karen Brewer

Virginia Tech
1405 Karr Lane
Blacksburg, VA 24061
540-231-6579
kbrewer@vt.edu

Gary Brudvig

Yale University
Department of Chemistry
P.O. Box 208107
New Haven, CT 06520-8107
203-432-5202
gary.brudvig@yale.edu



Announcing the
**2008 DOE Solar Photochemistry
Contractors' Meeting**

Sponsored by the U.S. Department of Energy, Office of Basic Energy Sciences
Chemical Sciences, Geosciences, and Biosciences Division

Louis Brus

Columbia University
3000 Broadway
New York, NY 10027
212 854 4041

leb26@columbia.edu

Donald Bryant

The Pennsylvania State University
S-235 Frear Building
University Park, PA 16802
814-865-1992

dab14@psu.edu

Ian Carmichael

University of Notre Dame
321 Radiation Research Building
Notre Dame, IN 46556
574 6314502

carmichael.1@nd.edu

Lin Chen

Argonne National Laboratory
Northwestern University
9700 S. Cass Ave.
Building 200
Argonne, IL 60439
630-252-3533

lchen@anl.gov

Kyoung-Shin Choi

Purdue University
Department of Chemistry
560 Oval Drive
West Lafayette, IN 47907
765-494-0049

kchoi1@purdue.edu

Philip Coppens

University at Buffalo, SUNY
732 NSM Complex, Amherst Campus, UB
Buffalo, NY 14260-3000
716-645-6800 X2217

coppens@buffalo.edu

Bob Crabtree

Yale University
225 Prospect St
New Haven, CT 06520-8107
203 432-3925

robert.Crabtree@yale.edu

Carol Creutz

Brookhaven Nation Laboratory
Chemistry
P. O. Box 5000
Building 555
Upton, NY 11973
614-292-4532

ccreutz@bnl.gov

Niels Damrauer

University of Colorado at Boulder
Campus Box 215
Boulder, CO 80309
303-735-1280

niels.damrauer@colorado.edu

Prabir Dutta

The Ohio State University
120 W 18th Avenue
Columbus, OH 43210
614 292 4532

dutta.1@osu.edu

Richard Eisenberg

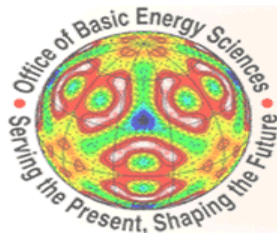
University of Rochester
Department of Chemistry
Hutchinson Hall, Rm B14
Rochester, NY 14627
585-275-5573

eisenberg@chem.rochester.edu

Randy Ellingson

National Renewable Energy Laboratory
1617 Cole Blvd.
Golden, CO 80401
303-384-6464

randy_ellingson@nrel.gov



Announcing the
**2008 DOE Solar Photochemistry
Contractors' Meeting**

Sponsored by the U.S. Department of Energy, Office of Basic Energy Sciences
Chemical Sciences, Geosciences, and Biosciences Division

C. Michael Elliott

Colorado State University
Department of Chemistry
1301 Center Ave.
Fort Collins, CO 80523
970-491-5204

ELLIOTT@LAMAR.COLOSTATE.EDU

Gregory Fiechtner

U.S. Department of Energy
19901 Germantown Road
Germantown, MD 20874-1290
301-903-5809

Gregory.Fiechtner@science.doe.gov

Graham Fleming

University of California, Berkeley
221 Hildebrand Hall
Berkeley, CA 94720
510-643-2735

grfleming@lbl.gov

Marye Anne Fox

University of California, San Diego
1530 Soledad Ave.
La Jolla, CA 92037
858-349-3182

mafox@ucsd.edu

Arthur Frank

National Renewable Energy Laboratory
1617 Cole Blvd.
Golden, CO 80401-3393
303-384-6262

afrank@nrel.gov

Heinz Frei

Lawrence Berkeley National Laboratory
1 Cyclotron Road
Physical Biosciences Division
Berkeley, CA 94720
510 486 4325

HMFrei@lbl.gov

Richard Friesner

Columbia University
Dept of Chemistry
3000 Broadway, MC 3110
New York, NY 10027
(212) 854-7606

rich@chem.columbia.edu

Etsuko Fujita

Brookhaven National Laboratory
Chemistry Department
P.O. Box 5000 / Building 555
Upton, NY 11973-5000
631-344-4356

fujita@bnl.gov

Elena Galoppini

Rutgers University
73 Warren Street
Newark, NJ 7041
973-353-5317

galoppin@rutgers.edu

Wayne Gladfelter

University of Minnesota
Department of Chemistry
207 Pleasant St. SE
A-15, 139 Smith Hall
Minneapolis, MN 55455
612-624-4391

wlg@umn.edu

John Golbeck

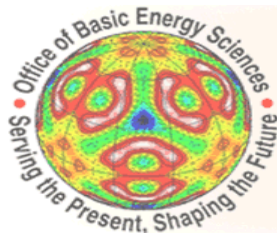
The Pennsylvania State University
310 South Frear Building
University Park, PA 16801
814 865 1163

jhg5@psu.edu

Ian Gould

Arizona State University
Department of Chemistry and Biochemistry
Office: D-109 Lab: D-126
Temp, AZ 85287
480-965-7278

igould@asu.edu



Announcing the
**2008 DOE Solar Photochemistry
Contractors' Meeting**

Sponsored by the U.S. Department of Energy, Office of Basic Energy Sciences
Chemical Sciences, Geosciences, and Biosciences Division

Richard Greene

U.S. Department of Energy
19901 Germantown Road
Germantown, MD 20874-1290
(301) 903-6190

Richard.Greene@science.doe.gov

Brian Gregg

National Renewable Energy Laboratory
1617 Cole Blvd.
Golden, CO 80401
303-384-6635

brian_gregg@nrel.gov

David Grills

Brookhaven National Laboratory
Chemistry Department
P.O. Box 5000 / Building 555
Upton, NY 11973
631-344-4332

dcgrills@bnl.gov

Craig Grimes

Penn State
217 Materials Research Lab
University Park, PA 16802
814.865.9142

cag14@psu.edu

Devens Gust

Arizona State University
Department of Chemistry and Biochemistry
Box 871604
Tempe, AZ 85287-1604
480-965-4547

gust@asu.edu

Alex Harris

Brookhaven National Laboratory
P.O. Box 5000 / Building 555
Upton, NY 11973
631-344-4301

alexh@bnl.gov

Michael Heben

National Renewable Energy Laboratory
1617 Cole Blvd
Golden, CO 80401
303.384.6641

michael_heben@nrel.gov

Michael Henderson

Pacific Northwest National Laboratory
PO Box 999, MS K8-87
Richland, WA 99352
509-371-6527

ma.henderson@pnl.gov

Craig Hill

Emory University
1515 Dickey Dr.
Atlanta, GA 30322
404-727-6611

chill@emory.edu

Dewey Holten

Washington University
Department of Chemistry
Louderman 336
St. Louis, MO 63130
314-935-6502

holten@wustl.edu

Michael Hopkins

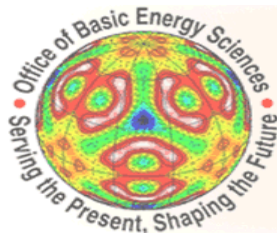
The University of Chicago
Department of Chemistry
5735 S Ellis Avenue
GHJ 111
Chicago, IL 60637
773-702-6490

mhopkins@uchicago.edu

Joseph Hupp

Northwestern University
2145 Sheridan Road
Evanston, IL 60208
847-491-3504

j-hupp@northwestern.edu



Announcing the
**2008 DOE Solar Photochemistry
Contractors' Meeting**

Sponsored by the U.S. Department of Energy, Office of Basic Energy Sciences
Chemical Sciences, Geosciences, and Biosciences Division

James Hurst

Washington State University
Department of Chemistry
PO Box 644630
Fulmer 170
Pullman, WA 99164-4630
509-335-7848
hurst@wsu.edu

Justin Johnson

National Renewable Energy Lab
1617 Cole Blvd
Golden, CO 80401
303-384-6190
justin_johnson@nrel.gov

David Jonas

University of Colorado
215 UCB
Boulder, CO 80309-0215
303-492-3818
david.jonas@colorado.edu

Prashant Kamat

University of Notre Dame
235 Radiation Laboratory
Notre Dame, IN 46556
574-631-5411
pkamat@nd.edu

David Kelley

University of California, Merced
5200 N. Lake Rd
Merced, CA 95344
209 228 4354
dfkelley@ucmerced.edu

Lowell Kispert

The University of Alabama
Department of Chemistry
Box 870336
250 Hackberry Lane
Shelby Hall Room 113 D
Tuscaloosa, AL 35487-0336
(205) 348-7134
lkispert@bama.ua.edu

Valeria Kleiman

University of Florida
PO BOX 117200
Gainesville, FL 32611
352 392 4656
kleiman@chem.ufl.edu

Bern Kohler

The Ohio State University
Dept. of Chemistry
100 W 18th Ave
Columbus, OH 43210
614-688-3944
kohler@chemistry.ohio-state.edu

Todd Krauss

University of Rochester
120 Trustee Road
Rocheste, NY 14627-0216
585-275-5093
krauss@chem.rochester.edu

KV Lakshmi

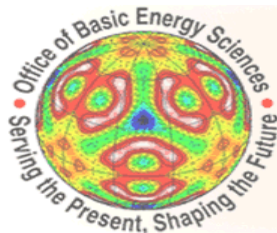
Rensselaer Polytechnic Institute
Department of Chemistry and Chemical Biology
110 8th Street
Troy, NY 12180
(518) 276 3271
lakshk@rpi.edu

Frederick Lewis

Northwestern University
Department of Chemistry
2145 Sheridan Road
Tech K348
Evanston, IL 60208
847-491-3441
fdl@northwestern.edu

Nathan Lewis

California Institute of Technology
1200 E. California Blvd.
MC 127-72
Pasadena, CA 91125
626-395-6335
nslewis@caltech.edu



Announcing the
**2008 DOE Solar Photochemistry
Contractors' Meeting**

Sponsored by the U.S. Department of Energy, Office of Basic Energy Sciences
Chemical Sciences, Geosciences, and Biosciences Division

Tianquan Lian

Emory University
1515 Dickey Drive
Atwood Hall 408
Atlanta, GA 30322
404-727-6649
tlian@emory.edu

Jonathan Lindsey

North Carolina State University
2620 Yarbrough Drive
CB 8204
Raleigh, NC 27695-8204
919-515-6406
jlindsey@ncsu.edu

Mark Lonergan

University of Oregon
1253 Department of Chemistry
Eugene, OR 97403
(541) 346-4748
lonergan@uoregon.edu

Paul Maggard

North Carolina State University
Department of Chemistry
2620 Yarbrough Drive,
740 Dabney Hall
Raleigh, NC 27695-8204
919-515-3616
Paul.Maggard@ncsu.edu

Thomas Mallouk

Penn State University
104 Chemistry Building
University Park, PA 16802
814-863-9637
tom@chem.psu.edu

Kent Mann

University of Minnesota
Department of Chemistry
668B Kolthoff Hall
Minneapolis, MN 55455
651-206-9865
krmann@umn.edu

Diane Marceau

U.S. Department of Energy
19901 Germantown Road
Germantown, MD 20874-1290
301-903-0235

diane.marceau@science.doe.gov

Mark Maroncelli

Penn State
104 Chemistry Building
University Park, PA 16802
814-865-0898
maroncelli@psu.edu

Dmitry Matyushov

Arizona State University
PO Box 871504
Tempe, AZ 85287-1504
480-9650057
Dmitrym@asu.edu

James McCusker

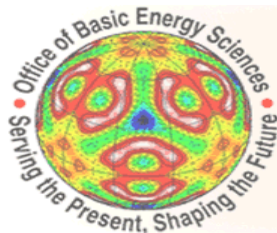
Michigan State University
Department of Chemistry
437 Chemistry
East Lansing, MI 48824
517-355-9715 x.106
jkm@chemistry.msu.edu

Dan Meisel

University of Notre Dame
Radiation Laboratory, Chemistry & Biochemistry
251 Nieuwland Science Hall
RL218
Notre Dame, IN 46556
(574) 631-5457
dani@nd.edu

Gerald Meyer

Johns Hopkins University
Dept of Chemistry
3400 N Charles Street
Baltimore, MD 21209
410-516-7319
meyer@jhu.edu



Announcing the
**2008 DOE Solar Photochemistry
Contractors' Meeting**

Sponsored by the U.S. Department of Energy, Office of Basic Energy Sciences
Chemical Sciences, Geosciences, and Biosciences Division

Thomas Meyer

University of North Carolina
Department of Chemistry
Campus Box 3290
Caudill and Kenan Laboratories
Chapel Hill, NC 27599-3290
919-843-8312
tjmeyer@unc.edu

John Miller

Brookhaven National Laboratory
Chemistry
P.O. Box 5000 / Building 555
Upton, NY 11973
631-344-4354
jmiller@bnl.gov

Ana Moore

Arizona State University
Center for Bioenergy and Photosynthesis
Department of Chemistry and Biochemistry
PS C212 / Mail Code: 1604
Tempe, AZ 85287
480 965 2953
amoore@asu.edu

Thomas Moore

Arizona State University
Center for Bioenergy and Photosynthesis
Department of Chemistry and Biochemistry
Box 871604 / PS C-214
Tempe, AZ 85287
480 947 2389
tmoore@asu.edu

James Muckerman

Brookhaven National Laboratory
P.O. Box 5000 / Building 555
Chemistry Department
Upton, NY 11973-5000
631-344-4368
muckerma@bnl.gov

Djamaladdin Musaev

Emory University
Department of Chemistry
1515 Dickey Dr.,
Atlanta, GA 30345
404-727-2382
DMUSAEV@EMORY.EDU

Marshall Newton

Brookhaven National Laboratory
Chemistry Department
P.O. Box 5000 / Building 555
Upton, NY 11973
631 344 4366
newton@bnl.gov

Daniel Nocera

Massachusetts Institute of Technology
77 Massachusetts Avenue
Building 6-335
Cambridge, MA 02139
617-253-5537
nocera@mit.edu

James Norris

University of Chicago
5735 S. Ellis Ave
Chicago, IL 60637
773-702-7864
jnorriss@uchicago.edu

Arthur Nozik

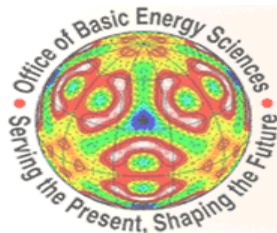
National Renewable Energy Laboratory
1617 Cole Blvd
Golden, CO 80401
303 384 6603
anozik@nrel.gov

Jennifer Ogilvie

University of Michigan
450 Church St
Ann Arbor, MI 48109
734-615-0485
jogilvie@umich.edu

John Papanikolas

University of North Carolina at Chapel Hill
Department of Chemistry
Campus Box 3290
Caudill and Kenan Laboratories
Chapel Hill, NC 27599
919 962-1619
john_papanikolas@unc.edu



Announcing the
**2008 DOE Solar Photochemistry
Contractors' Meeting**

Sponsored by the U.S. Department of Energy, Office of Basic Energy Sciences
Chemical Sciences, Geosciences, and Biosciences Division

Bruce Parkinson

Colorado State
Department of Chemistry
C117 Chemistry
Fort Collins, CO 80523
970-491-0504

Bruce.Parkinson@colostate.edu

Piotr Piotrowiak

Rutgers University
73 Warren Street
Newark, New Jersey 7102
973-353-5318

piotr@andromeda.rutgers.edu

Oleg Poluektov

Argonne National Laboratory
9700 S. Cass Ave.
Argonne, IL 60439
630 2523546

Oleg@anl.gov

Oleg Prezhdo

University of Washington
Department of Chemistry
Box 351700
Seattle, WA 98195
206 221-3931

prezhdo@u.washington.edu

Jeffrey Pyun

University of Arizona
1306 E University Blvd
Tucson, AZ 85721
520-626-1834

jpyun@email.arizona.edu

Krishnan Rajeshwar

University of Texas at Arlington
Dept of Chemistry and Biochemistry
700 Planetarium Place, Room 114 CPB
Arlington, TX 76019-0065
817 272 3491

rajeshwar@uta.edu

John Reynolds

University of Florida
Leigh Hall 318
Box 117200
Gainesville, FL 32611
352-392-9151

reynolds@chem.ufl.edu

Garry Rumbles

National Renewable Energy Laboratory
1617 Cole Boulevard
MS 3216
Golden, CO 80401-3393
303 384 6502

garry_rumbles@nrel.gov

Kirk Schanze

University of Florida
Chemistry Department
PO Box 117200
Gainesville, FL 32611
352-392-9133

kschanze@chem.ufl.edu

Russell Schmehl

Tulane University
Department of Chemistry
5059 Percival Stern Building
New Orleans, LA 70118
504-862-3566

russ@tulane.edu

Charles Schmuttenmaer

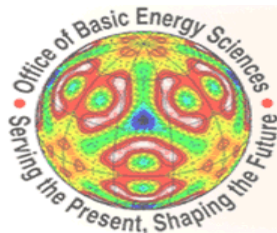
Yale University
Chemistry Department
225 Prospect St., PO Box 208107
New Haven, CT 06520-8107
203-432-5049

charles.schmuttenmaer@yale.edu

Wade Sisk

U.S. Department of Energy- BES/CGBS
1000 Independence Ave., SW
Washington, DC 20585
301-903-5692

wade.sisk@science.doe.gov



Announcing the
**2008 DOE Solar Photochemistry
Contractors' Meeting**

Sponsored by the U.S. Department of Energy, Office of Basic Energy Sciences
Chemical Sciences, Geosciences, and Biosciences Division

Mark Spitler

U.S. Department of Energy, BES
1000 Independence Ave., SW
Washington, D.C. 20585
301 903 4568

mark.spitler@science.doe.gov

Robert Stack

U.S. Department of Energy
19901 Germantown Road
Germantown, MD 20874
(301) 903-5652

robert.stack@science.doe.gov

Michael Therien

Duke University
Department of Chemistry
2213 FFSC
Durham, NC 27708-0354
215-898-0087

therien@sas.upenn.edu

Randolph Thummel

University of Houston
Dept. of Chemistry
136 Fleming
Houston, TX 77204-5003
713 743-2734

thummel@uh.edu

David Tiede

Argonne National Laboratory
9700 South Cass Ave
Argonne, IL 60439
630-252-3539

tiiede@anl.gov

Lisa Utschig

Argonne National Laboratory
9700 S. Cass Ave.
Argonne, IL 60439
630-983-2203

utschig@anl.gov

Jao van de Lagemaat

National Renewable Energy Laboratory
1617 Cole Blvd
Golden, CO 80401
303-3846143

jao_vandelagemaat@nrel.gov

Hendrik Verweij

The Ohio State University
2041 N College Road
Columbus, OH 43210-1178
614-247-6987

Verweij.1@osu.edu

Albert Wagner

Argonne National Laboratory
9700 S. Cass Ave.
Bldg. 205
Argonne, IL 60439
630-252-4383

wagner@tcg.anl.gov

Michael Wasielewski

Northwestern University
Department of Chemistry
2145 Sheridan Rd.
Evanston, IL 60208-3113
847-467-1423

m-wasielewski@northwestern.edu

James Whitesell

University of California, San Diego
1530 Soledad Ave.
La Jolla, CA 92037
858-349-3182

jkwhitesell@mac.com

Vittal Yachandra

Lawrence Berkeley National Laboratory
1 Cyclotron Road
MS: 66R0200
Berkeley, CA 94720
510 486 4330

vkyachandra@lbl.gov

Author Index

Achord, P.	165	Cho, B.	151
Ahn, T.	77	Choi, D-j.	61
Ai, X.	141	Choi, K-S.	131
Akdag, A.	150	Choi, S.	125
Al-Jassim, M.	177	Cohen, B. W.	148
Amick, T. J.	135	Collins, A. M.	1
Anfuso, C.	155	Cook, A.	90
Arachchige, S.	128	Coppens, P.	45
Armstrong, N. R.	121	Costas, A. M. G.	130
Asaoka, S.	90	Crabtree, R. H.	124, 132, 173
Attenkofer, K.	41	Cramer, D. L.	156
Barbara, P. F.	122	Creutz, C.	8
Barber, G. D.	123	Damrauer, N. H.	133
Barnes, T. M.	144	Das, S.	5
Bassi, R.	77	de Tacconi, N.	169
Batista, V. S.	124, 132, 173	Deason, B.	140
Beard, M. C.	108, 125, 134 144	Deli, J.	73
Bergmann, U.	178	Deng, Z.	174
Bhise, A. D.	156	Diers, J. R.	127, 147
Biswas, P.	1	Dixon, D. A.	73
Blackburn, J. L.	144, 170	Doherty, M. D.	142
Blank, D.	126, 160	Du, P.	20
Blankenship, R. E.	1	Dutta, P.	36
Block, A.	99	Eisenberg, R.	20
Bocian, D. F.	127, 147, 156	Ellingson, R. J.	108, 125, 134
Bolinger, J.	122	Elliott, C. M.	135
Boussac, A.	178	Engel, G. S.	1
Bowman, M. K.	73	Ferguson, A.	170
Brewer, K. J.	128	Fleming, G. R.	1, 77
Brown, A.	163	Focsan, A. L.	73, 129
Brown, J.	128	Fox, M. A.	136
Brown, P.	27	Fradkin, L.	122
Brudvig, G. W.	124, 129, 132, 173	Frank, A. J.	67
Brus, L.	115	Frei, H.	137
Bryant, D. A.	130	Friesner, R. A.	23
Cady, C. W.	132, 173	Fujita, E.	138, 142, 165
Calhoun, T.	77	Galoppini, E.	64
Cape, J. L.	5	Gao, Y.	129
Carlson, L. J.	112	Gasyna, E.	99
Cass, L. C.	164	Gasyna, Z.	99
Chambers, S. A.	145	Gay, L.	1
Chand, S.	153	Geletii, Y. V.	146
Chen, L. X.	41, 176	Gembicky, M.	45
Chen, X.	150	Gerth, K. A.	134
Cheung, S. H.	145	Gervaldo, M.	143
Chew, A. G. M.	130	Ginsberg, N.	77
Chipman, D. M.	164	Gladfelter, W. L.	126, 160
Chitta, R.	160	Golbeck, J. H.	139

Gould, I. R.	140	Kodis, G.	143
Gregg, B. A.	141	Kohler, B.	36
Grills, D. C.	142	Kongkanand, A.	27
Grimes, C. A.	32	Konovalova, T. A.	73
Gross, M.	1	Kopidakis, N.	67, 141, 170
Grumstrup, E. M.	133	Krauss, T. D.	112
Gundlach, L.	105	Kumaresan, D.	172
Gust, D.	143, 159	Kuznetsov, A.	146
Hambourger, M.	143	Lakshmi, K. V.	153
Han, H.	137	Law, M.	108, 125, 134
Hanna, M. C.	108, 125	Lawrence, J.	73
Hasjim, P.	99	Lazarides, T.	20
Hata, H.	159	LeBard, D. N.	162
Heben, M. J.	144, 170	Lebkowski, K.	172
Henderson, M. A.	145	Lee, A.	123
Herrick, R.	61	Lee, K-J.	122
Hester, H.	172	Lee, S.	153
Hill, C. L.	146	Lee, S-H. A.	159
Hill, R. J.	151	Lentz, D.	159
Hoertz, P. G.	159	Lewis, F. D.	17
Holten, D.	127, 147, 156	Lewis, K. L. M.	167
Hopkins, M. D.	148	Lewis, N. S.	154
Hou, Y.	146	Li, G.	173
Huang, J.	155	Li, X.	161
Huang, L.	112	Lian, T.	146, 155
Huang, Z.	146	Lin, F.	157
Hughes, B.	134	Lindsey, J. S. ...	41, 127, 147, 156, 175
Hupp, J. T.	149	Liu, H.	115
Hurst, J. K.	5	Liu, Z.	130
Huss, A.	126	Lockard, J. V.	41, 176
Jäckel, B.	61	Lonergan, M.	157
Jamula, L.	163	Lovaasen, B.	148
Jarosz, P.	20	Lu, Y.	61
Jennings, G.	41	Luther, J. M.	108, 125, 134
Jiang, H.	171	Ma, R.	159
Johnson, J. C.	108, 134, 150	Maggard, P. A.	158
Jonas, D. M.	151	Mallouk, T. E.	123, 159
Kamat, P. V.	27	Mann, K. R.	126, 160
Kee, H. L.	156	Mardis, K. L.	175
Keirstead, A.	143	Maresca, J. A.	130
Keller, J. M.	90	Marino, A.	99
Kelley, D. F.	152	Maroncelli, M.	161
Kimball, G. M.	154	Matyushov, D. V.	140, 162
King, P. W.	144	McCusker, J. K.	163
Kirmaier, C.	147	McIlroy, S.	90
Kispert, L. D.	73, 129	McNamara, W. R.	132, 173
Kleiman, V. D.	55	Meisel, D.	164
Knowles, K.	20	Merga, G.	164

Messerschmidt, M.	45	Redmond, P.	115
Meyer, G. J.	49	Reese, M. O.	141
Meyer, T. J.	52	Reynolds, J. R.	55
Miao, R.	128	Robel, I.	27
Michl, J.	150	Romero, M. J.	177
Midgett, A.	134	Rumbles, G.	170, 177
Miller, J. R.	90, 171	Saavedra, S. S.	121
Modesto-Lopez, L.	1	Sauer, K.	178
Molnar, P.	73	Schanze, K. S.	55, 90, 171
Montgomery, M. A.	133	Schlau-Cohen, G.	77
Moore, A. L.	143, 159	Schleicher, J. M.	173
Moore, G. F.	143	Schmehl, R.	172
Moore, T. A.	143, 159	Schmittenmaer, C. A. ...	124, 132, 173
Morales, W.	169	Schneemeyer, L.	105
Morris, A.	49	Schneider, J.	20
Muckerman, J. T.	138, 165	Schwartz, K.	160
Muresan, A. Z.	41, 127	Semonin, O.	134
Murphy, J. E.	108	Shankar, K.	172
Musaev, J.	146	Shen, F.	130
Myahkostupov, M.	105	Shinopoulos, K.	129
Myers, J. A.	167	Snoeberger, R. C.	124, 132, 173
Neale, N. R.	67	Song, H-e.	147
Nelson, J. J.	135	Song, Q.	108, 125, 134
Newsom, M. I.	148	Spitler, M.	61
Newton, M. D.	166	Sreearunothai, P.	90
Niyogi, K. K.	77	Staniscewski, A.	49
Nocera, D. G.	11	Stay, D.	157
Norris, J.	99	Stockwell, D.	155
Nozik, A. J.	108, 125, 134, 150	Svedruzic, D.	144
Ogilvie, J. P.	167	Takeda, N.	90
Ohsawa, T.	145	Tanaka, K.	138, 165
Palacios, R. E.	122	Taniguchi, M.	127, 147, 156
Papanikolas, J. M.	52	Tekavec, P. F.	167
Parkinson, B.	61	Thall, J.	20
Pedrosa, H.	112	Thamyongkit, P.	127
Peters, W. K.	151	Therien, M. J.	87
Piotrowiak, P.	105	Thimsen, E.	1
Pitak, M.	45	Thummel, R.	174
Poluektov, O. G. 95, 99, 143, 153, 176		Tiede, D. M.	95, 175, 176
Polyansky, D. E.	138, 165	Tracewell, C. A.	129
Ponomarenko, N.	99	Traub, M. C.	154
Postier, B. L.	1	Tronrud, D. E.	1
Prezhdo, O. V.	168	Tsai, M-K.	138
Pushkar, Y.	178	Tseng, H-W.	174
Pyun, J.	121	Tvrdy, K.	27
Rajeshwar, K.	169	Utschig, L. M.	95, 176
Rajh, T.	143	van de Lagemaat, J.	67, 177
Read, E.	1, 77	Verweij, H.	36

Wada, T.	138
Wagner, A.	153
Walker, E.	157
Wang, A.	99
Wang, B.	174
Wang, D.	141, 174
Wang, Y.	157
Wasielewski, M. R.	83
Wasinger, E. C.	41
Wells, N.	126
Wen, J.	1
Whitesell, J. K.	136
Wu, B.	155
Wu, X.	115
Yachandra, V.	178
Yano, J.	178
Youngblood, W. J.	159
Zhang, H.	1
Zhang, J.	20, 41
Zhang, X.	41
Zheng, S-L.	45
Zhu, K.	67
Zhu, L.	136
Zigler, D.	128
Zong, R.	174
Zou, X.	175